UNIVERSITY OF NOVI SAD
Technical faculty "Mihajlo Pupin"
Zrenjanin, Republic of Serbia

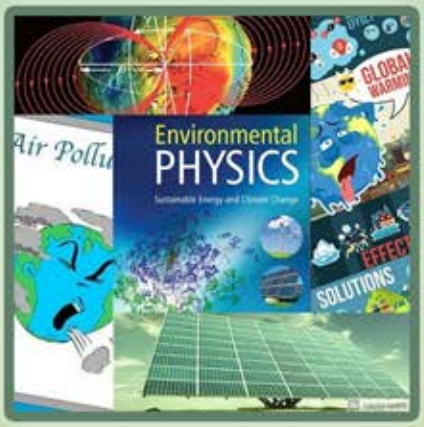

II International Conference on Physical Aspects of Environment ICPAE 2023

PROCEEDINGS

Zrenjanin, Serbia, August 24-26, 2023.

University of Novi Sad
Technical Faculty
“Mihajlo Pupin”
Zrenjanin, Republic of Serbia

II International Conference on Physical Aspects of Environment ICPAE2023

Proceedings

Zrenjanin, 24 – 26th, August 2023.

Proceedings of the II International Conference on Physical Aspects of Environment ICPAE2023

Conference Organizer:
Technical Faculty "Mihajlo Pupin", Zrenjanin, University of Novi Sad, Serbia

Publisher:
Technical Faculty "Mihajlo Pupin", Zrenjanin, University of Novi Sad, Djure Djakovića bb, Zrenjanin, Serbia

For Publisher:
Milan Nikolić, Dean of Technical Faculty "Mihajlo Pupin", Zrenjanin, Serbia

Editor:
Darko Radovančević, Technical Faculty "Mihajlo Pupin", Zrenjanin, Serbia

Co-Editor:
Saša Jovanović, University of Novi Sad, Technical Faculty "Mihajlo Pupin", Zrenjanin, Serbia
Ljubiša Nešić, Faculty of Sciences and Mathematics, Nis, Serbia

Technical preparation:
Luka Djordjević, Technical Faculty "Mihajlo Pupin", Zrenjanin, Serbia
Milan Marković, Technical Faculty "Mihajlo Pupin", Zrenjanin, Serbia

CIP Classification:

CIP - Каталогизација у публикацији
Библиотеке Матице српске, Нови Сад

502(082)(03.034.4)

INTERNATIONAL Conference on Physical Aspects of Environment (2 ; 2023 ; Zrenjanin)
Proceedings [Elektronski izvor] / II International Conference on Physical Aspects of Environment ICPAE2023, Zrenjanin, 24-26th August 2023 ; [editor Darko Radovančević]. - Zrenjanin : Technical Faculty "Mihajlo Pupin", 2023. - 1 elektronski optički disk (CD-ROM)

Elektronska publikacija u formatu pdf opsega 232 str. - Nasl. sa naslovnog ekrana. - Bibliografija uz svaki rad.

ISBN 978-86-7672-366-9

а) Животна средина -- Заштита -- Зборници

COBISS.SR-ID 124144649

SCIENTIFIC PROGRAM COMMITTEE

- Darko Radovančević, University of Novi Sad, Technical Faculty "Mihajlo Pupin", Zrenjanin, Serbia – President of the Scientific Program Committee
- Ljubiša Nešić, University of Nis, Faculty of Sciences and Mathematics, Nis, Serbia - Vice President of the Scientific Program Committee
- Saša Jovanović, University of Novi Sad, Technical Faculty "Mihajlo Pupin", Zrenjanin, Serbia
- Đorđe Vučković, University of Novi Sad, Technical Faculty "Mihajlo Pupin", Zrenjanin, Serbia
- Bogdana Vujić, University of Novi Sad, Technical Faculty "Mihajlo Pupin", Zrenjanin, Serbia
- Višnja Mihajlović, University of Novi Sad, Technical Faculty "Mihajlo Pupin", Zrenjanin, Serbia
- Ljiljana Radovanović, University of Novi Sad, Technical Faculty "Mihajlo Pupin", Zrenjanin, Serbia
- Jelena Stojanov, University of Novi Sad, Technical Faculty "Mihajlo Pupin", Zrenjanin, Serbia
- Jasna Tolmač, University of Novi Sad, Technical Faculty "Mihajlo Pupin", Zrenjanin, Serbia
- Ljubiša Đorđević, University of Nis, Faculty of Sciences and Mathematics, Nis, Serbia
- Vesna Nikolić, University of Nis, Faculty of Occupational Safety, Nis, Serbia
- Tatjana Jovanović, University of Nis, Faculty of Medicine, Nis, Serbia
- Milan Pantić, University of Novi Sad, Faculty of Sciences, Novi Sad, Serbia
- Miodrag Krmar, University of Novi Sad, Faculty of Sciences, Novi Sad, Serbia
- Nataša Todorović, University of Novi Sad, Faculty of Sciences, Novi Sad, Serbia
- Jovana Nikolov, University of Novi Sad, Faculty of Sciences, Novi Sad, Serbia
- Nikola Jovančević, University of Novi Sad, Faculty of Sciences, Novi Sad, Serbia
- Dragan Markušev, Institute of Physics, Belgrade, Serbia
- Zoran Mijić, Institute of Physics, Belgrade, Serbia
- Robert Repnik, University of Maribor, Faculty of Natural Sciences and Mathematics, Maribor, Slovenia
- Vanja Radolić, Josip Juraj Strossmayer University of Osijek, Department of Physics, Osijek, Croatia
- Diana Mance, University of Rijeka, Department of Physics, Rijeka, Croatia
- Slavoljub Mijović, University of Montenegro, Faculty of Science and Mathematics, Podgorica, Montenegro
- Lambe Barandovski, Ss. Cyril and Methodius University, Faculty of Natural Sciences and Mathematics, Skopje, North Macedonia
- Snježana Dupljanin, University of Banja Luka, Faculty of Natural Sciences and Mathematics, Banja Luka, Bosnia and Herzegovina
- Senad Odžak, University of Sarajevo, Faculty of Science, Sarajevo, Bosnia and Herzegovina

ADVISORY COMMITTEE

- Vjekoslav Sajfert, University of Novi Sad, Technical Faculty "Mihajlo Pupin", Zrenjanin, Serbia – President of the Advisory Committee
- Goran Đorđević, University of Nis, Faculty of Sciences and Mathematics, Nis, Serbia – Vice President of the Advisory Committee
- Milan Pantić, University of Novi Sad, Faculty of Sciences, Novi Sad, Serbia

ORGANIZING COMMITTEE:

- Dragica Radosav, University of Novi Sad, Technical Faculty "Mihajlo Pupin", Zrenjanin, Serbia – President of the Organizing Committee
- Darko Radovančević, University of Novi Sad, Technical Faculty "Mihajlo Pupin", Zrenjanin, Serbia – Vice President of the Organizing Committee
- Ljubiša Nešić, University of Nis, Faculty of Sciences and Mathematics, Nis – Vice President of the Organizing Committee
- Milan Marković, University of Novi Sad, Technical Faculty "Mihajlo Pupin", Zrenjanin, Serbia – Secretary of the Organizing Committee
- Luka Đorđević - University of Novi Sad, Technical Faculty "Mihajlo Pupin", Zrenjanin, Serbia – Secretary of the Organizing Committee
- Katarina Ivanović, University of Novi Sad, Technical Faculty "Mihajlo Pupin", Zrenjanin, Serbia
- Marija Pešić, University of Novi Sad, Technical Faculty "Mihajlo Pupin", Zrenjanin, Serbia
- Jasna Tolmač, University of Novi Sad, Technical Faculty "Mihajlo Pupin", Zrenjanin, Serbia
- Lana Pantić Ranđelović, University of Nis, Faculty of Sciences and Mathematics, Nis, Serbia
- Teodora Crvenkov, University Clinical Centre of Serbia, Belgrade, Serbia
- Ognjen Popović, Mining institute, Belgrade, Serbia

INTRODUCTION

II International Conference on Physical Aspects of Environment ICPAE2023, 24-26th August 2023, was organized by the Technical Faculty "Mihajlo Pupin" from Zrenjanin. The members of the scientific program, advisory and organizational committee of the conference were distinguished professors and researchers from the University of Novi Sad, the University of Niš, the Institute of Physics in Zemun, the University of Maribor, the University of Josip Juraj Štrosmajer in Osijek, the University of Montenegro, the University of St. Cyril and Methodius" from Skopje, the University of Banja Luka and the University of Sarajevo.

The conference was opened by Prof. Dr Milan Nikolić, dean of the Technical Faculty, "Mihajlo Pupin", in the presence of conference participants, members of the conference board and guests from abroad. After the ceremonial opening of the presentation of papers, the conference was led by: Marija Pešić, Ph.D., Slavoljub Mijović, Ph.D., Lambe Barandovski, Ph.D., Đorđe Vučković, Ph.D., Saša Jovanović, Ph.D.

36 papers were presented at the conference: 15 papers from abroad, 21 from Serbia. Invited lectures were given by:

- **Irena Zlatanovska**, Faculty of Science, University of St. Cyril and Methodius, North Macedonia;
- **Slavoljub Mijović**, Faculty of Science, University of Montenegro, Montenegro;
- **Diana Mance**, Faculty of Physics, University of Rijeka, Croatia;
- **Abdullah Akšamović**, Faculty of Electrical Engineering, University of Sarajevo, Bosnia and Herzegovina;

Other papers were submitted for shorter oral presentations.

The conference brought together eminent participants who shared the results of their research, ideas and achievements related to the most current topics in the fields of: geophysics, environmental modeling, air pollution, the greenhouse effect, global warming and climate change, radiation and the environment, energy efficiency and sustainable development, environmental physics and education.

President of the Scientific Program Committee

Assistant Professor Darko Radovančević, Ph.D.

Zrenjanin, 24 - 26th August 2023.

Conference participants are from the following countries:

Spain

Bosnia and Herzegovina

Hungary

North Macedonia

Serbia

Croatia

Iran

Australia

Ethiopia

Montenegro

China

Slovenia

CONTENTS

INVITED LECTURES

LECTURES

II International Conference on Physical Aspects of Environment ICPAE2023
August 24-26th, 2023, Zrenjanin, Serbia

INVITED LECTURES

Conference Proceedings
ICPAE 2023, 24th August – 26th August, Zrenjanin, Serbia
University of Novi Sad, Technical Faculty "Mihajlo Pupin", Zrenjanin

Terrestrial Radioactivity in the City of Bitola and Its Environs

Irena Zlatanovska[1*], Trajče Stafilov[2], Robert Šajn[3], Bojana Dimovska Gonovska[4], Snežana Dimovska[5], Jovan Janusheski[5], Lambe Barandovski[1]

[1]Institute of Physics, Faculty of Natural Sciences and Mathematics, Ss Cyril and Methodius University in Skopje, POB 162, 1000 Skopje, Republic of Macedonia
[2]Institute of Chemistry, Faculty of Natural Sciences and Mathematics, Ss Cyril and Methodius University in Skopje, POB 162, 1000 Skopje, Macedonia
[3] Geological Survey of Slovenia, Dimičeva ul. 14, 1000 Ljubljana, Slovenia
[4] Scientific Tobacco Institute, St. Kliment Ohridski University, Kičevska bb, 7500 Prilep, Macedonia
[5]Republic Institute for Health Protection, 50 Divizija 6, 1000 Skopje, Macedonia
zlatanovskairena@gmail.com

Abstract. For the purpose of a comprehensive investigation of soil radioactivity in the Bitola region, Republic of Macedonia, topsoil samples were collected from 58 locations within a 5x5 km grid. The radioactivity level was measured using a gas-flow proportional counter, resulting in data that shows the gross alpha and beta activities. In order to obtain information regarding the type and activity concentrations of radionuclides present in the studied area, gamma spectrometry analysis was conducted. The obtained data revealed significant variability in activity concentrations. The median values of activity concentrations for ^{40}K, ^{226}Ra, and ^{232}Th were found to be higher than the global medians. The absorbed dose rate in the air and the annual effective dose rate calculations were used to evaluate the radiological health effects of the observed soil radioactivity. Colored maps were prepared to show the spatial distribution of radionuclides and the annual dose rate for the investigated area.

Keywords: soil, radioactivity, activity concentration, proportional counting, gamma spectrometry

INTRODUCTION

Whether predetermined by geology or by human activity, the presence of radionuclides in soil and their radiological impact on the population should be investigated. In Macedonia, the Institute for Health Protection maintains regular monitoring of the radioactivity level in soils from several locations. A detailed investigation based on a large number of soil samples collected from a regular grid exists only for Kavadarci, Veles, and their environs, but such an investigation has not been conducted for the entire territory. The results derived from such a comprehensive investigation will establish a reference for future comparisons of soil radioactivity levels, while also providing insights into potential rises in industrial, nuclear, and other human activities [1,2].

EXPERIMENTAL

Study area

The region investigated in this study is located in the southwest part of Macedonia, and it covers an area of 1400 km^2 (Fig. 1a). Located in the middle part of the Pelagonia Valley and surrounded by mountains and hills, the town of Bitola is the main urban center of the examined area. The existence of coal-lignite deposits throughout the studied area enabled the establishment and operation of the Thermoelectric power plant "REK Bitola", located 12 km east of Bitola. With a capacity of 700 MW, it satisfies 70% of the electricity demand in Macedonia. The geological map of the studied area (Fig. 1b) reveals various types of rocks that belong to two distinct geological units. Granites, gneisses (predominantly muscovite gneiss), and schists are part of the Pelagonian massif. The West-Macedonian zone consists of rocks formed during the Paleozoic era, including low metamorphic schists and granite rocks. Along Crna Reka, which is the border between the two geological units, there are quaternary alluvial and diluvial sediments [3,4].

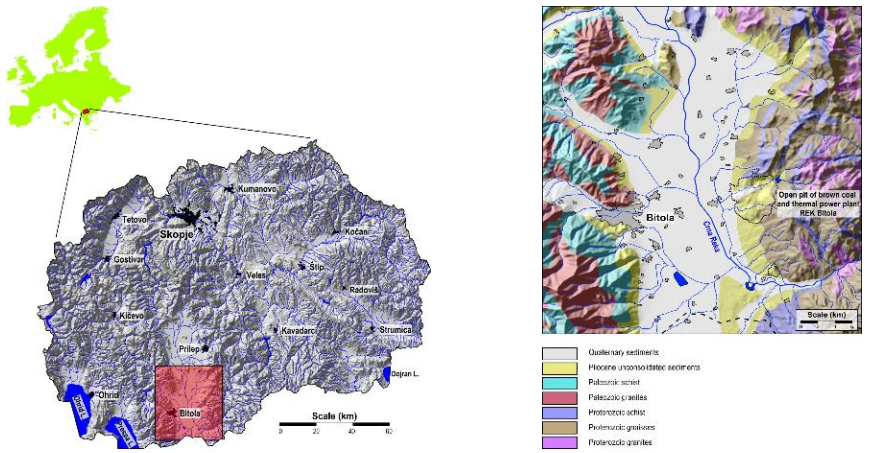

a b

Figure 1. Location (a) and geological map of the study area (b).

Sampling and analyses

For this study, a total of 58 soil samples were collected from locations within a dense grid of 5x5 km. Each sample is a mixture of five subsamples collected from the upper 5 cm in uncultivable areas or from the 0-30 cm depth range in cultivable areas. Following adequate soil processing, samples were prepared for the measurement of gross alpha and beta activity, each containing 100 mg of soil, spread in an aluminum planchette, fixed with acetone, and dried under an infrared lamp. Gamma spectrometry samples comprise 150 g of soil packed into cylindrical containers, tightly sealed, and kept for 30 days before measurement to achieve secular equilibrium between ^{226}Ra and its short-lived progeny [5].

WPC 1050 gas-flow proportional detector manufactured by Ortec was used to determine the gross alpha and beta activity. The counting time was 100 min. Gamma spectrometry

samples were measured with a P-coaxial, high-purity germanium detector (Canberra Packard). The counting time for each sample was 60 000 s. The three most important natural radionuclides, ^{40}K, ^{226}Ra, and ^{232}Th, as well as the artificial ^{137}Cs, were identified in the soil samples. ^{40}K and ^{137}Cs activity concentrations were calculated using their single gamma-ray lines. The weighted mean of its progeny activity concentrations with multiple gamma-ray lines of ^{214}Pb and ^{214}Bi were used to determine the activity concentration of ^{226}Ra. Separate gamma-ray lines of ^{228}Ac, ^{212}Pb, and ^{208}Tl were used to determine the activity concentration of ^{232}Th.

For an assessment of radiological health effects, from the obtained activity concentrations of all identified isotopes, the gamma dose rate in the air 1 m above the ground and the annual effective dose rate were calculated.

RESULTS AND DISCUSSION

Descriptive statistics for activity concentrations of ^{40}K, ^{226}Ra, ^{232}Th, and ^{137}Cs, gamma dose (*D*), and effective dose rates (*H*), including arithmetic mean, median, minimum, and maximum, arithmetic standard deviation, and mean absolute deviation, are presented in Table 1.

Gross alpha activity ranges from 120 Bq/kg to 710 Bq/kg, while gross beta activity varies between 580 Bq/kg and 1550 Bq/kg. The obtained values for the median of gross alpha and gross beta activities are 420 Bq/kg and 1030 Bq/kg, respectively. The presence of naturally occurring alpha and beta emitters in the uranium (^{226}Ra) and thorium (^{232}Th) series predetermined the spatial distribution of gross alpha and beta activities (Figs. 2a and 2b). The spatial distribution of beta activity is also influenced by ^{40}K and ^{137}Cs.

The minimum activity concentration of ^{40}K is 290 Bq/kg, and the maximum activity concentration is 1200 Bq/kg. The obtained median value is 640 Bq/kg. Higher activity concentrations of ^{40}K are related to igneous rocks, especially granite. The application of fertilisers containing the essential nutrient potassium to enhance plant growth may contribute to the observed higher concentrations of ^{40}K in the cultivable area (Fig. 2c).

The activity concentration of ^{226}Ra increases with the age of the rocks [6]. Pelagonian massif, with rocks dating from the Proterozoic eon, has the highest activity concentration of ^{226}Ra (Fig. 3a). The median value for the activity concentration of ^{226}Ra is 43 Bq/kg and it ranges from 21 Bq/kg to 87 Bq/kg. Fly ash from the burned lignite enriched with radioactive material and concentrated at the surface of the soils may be the reason for increased concentrations of ^{226}Ra in the valley, but further investigations of multilayer soil samples from different distances from REK Bitola can provide a better insight [7].

The minimum and maximum activity concentrations of ^{232}Th are 21 Bq/kg and 78 Bq/kg, with a median value of 49 Bq/kg. Comparing Fig. 3a and Fig. 3b, consistency in the spatial distribution of ^{226}Ra and ^{232}Th can be found. ^{232}Th activity concentration is greater in regions with acid igneous rocks and sediments along Crna Reka formed by erosion, where the clay content leads to enhanced adsorption of thorium [8].

All of the natural isotope activity concentrations found in this study are higher than the global median values of 400 Bq/kg, 35 Bq/kg, and 30 Bq/kg for ^{40}K, ^{226}Ra, and ^{232}Th, respectively [9].

Table 1. Descriptive statistics of the obtained data.

	Unit	X	Md	Min	Max	S
α	Bq/kg	440	420	120	710	140
β	Bq/kg	1040	1030	580	1550	230
^{40}K	Bq/kg	650	640	290	1200	160
^{226}Ra	Bq/kg	46	43	21	87	13
^{232}Th	Bq/kg	51	49	21	78	13
^{137}Cs	Bq/kg	72	36	1,7	330	71
D	nGy/h	88	87	44	131	18
H	mSv/a	0,11	0,11	0,054	0,16	0,022

X–arithmetic mean, Md-median, Min-minimum, Max-maximum, S-arithmetic standard deviation

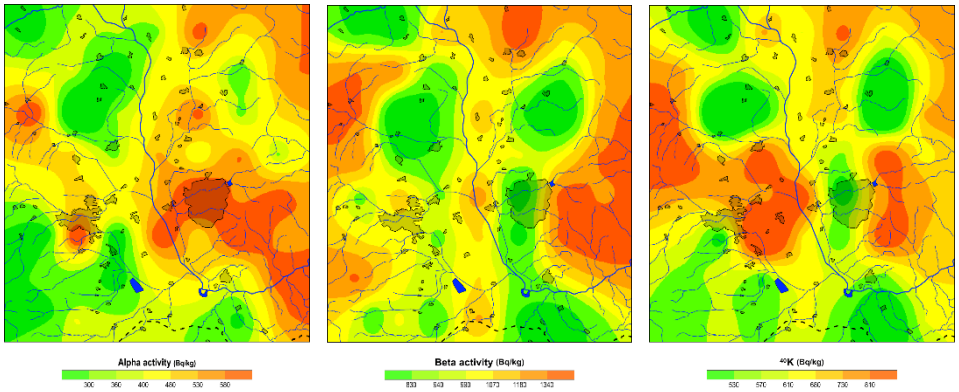

a b c

Figure 2. Spatial distribution of the gross alpha activity (a), gross beta activity (b), and the specific activity of ^{40}K in the soils from the investigated area (c).

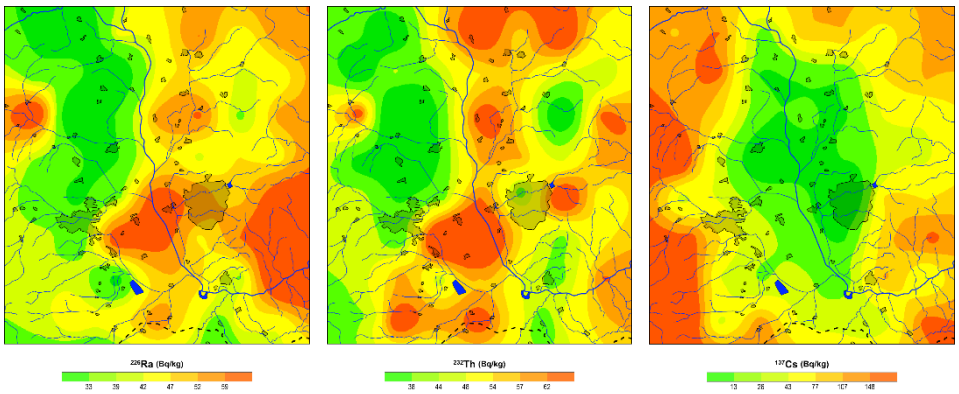

a b c

Figure 3. Spatial distribution of the activity concentration of isotopes: ^{226}Ra (a), ^{232}Th (b), and ^{137}Cs in the soils from the investigated area (c).

The activity concentration of ^{137}Cs varies widely (1,7 Bq/kg-330 Bq/kg), with a median value of 36 Bq/kg. This radionuclide, originating from the nuclear accident in Chernobyl, was accumulated in soils by wet deposition. Fig. 3c clearly shows that ^{137}Cs activity concentration is minimal in the Pelagonian valley, while soils from the surrounding mountains, which usually record higher amounts of precipitation, despite years of washing out and redistribution, still have the highest activity concentration [10].

The obtained gamma dose rate varies in the range from 44 nGy/h to 131 nGy/h with a median of 87 nGy/h. In comparison to the results from the Kavadarci region study, the obtained median is slightly greater than the Kavadarci region's median (61 nGy/h), and the maximum value for gamma dose rate is slightly lower (gamma dose rates for Kavadarci varies between 42 nGy/h and 168 nGy/h). The region of granite rocks in both geological units is characterized by the highest values of annual effective dose which ranged between 0,054 mSv/a to 0,16 mSv/a with the median value of 0,11 mSv/a.

CONCLUSION

The results from this study show that the activity concentration of all the natural radionuclides is strongly influenced by the geology of the area and the highest concentration is related to igneous rocks, especially granite. The annual effective dose rate is within normal limits, and there is no significant radiological risk to the population.

REFERENCES

1. S. Dimovska, T. Stafilov and R. Sajn, 2012, Radioactivity in soil from the city of Kavadarci (Republic of Macedonia) and its environs, *Radiat Prot Dosimetry*, vol. 148, pp 107-120
2. S. Dimovska, T. Stafilov, R. Sajn and M. Frontasyeva, 2010, Distribution of some natural and man-made radionuclides in soil from the city of Veles (Republic of Macedonia) and its environs. *Radiat Prot Dosimetry*, vol. 138, pp 144-157
3. B. Dimovska, T. Stafilov and R. Sajn, 2014, Distribution of lead and zinc in soil over the Bitola region, Republic of Macedonia, *GeolMac*, vol. 28, pp 87-91
4. T. Stafilov, R. Šajn, A. Puteska and B. Dimovska, 2015, Geochemical atlas of Pelagonia, Faculty of Natural Sciences and Mathematics, Skopje
5. S. P. Theocharopoulos, G. Wagner, J. Sprengart, M. E. Mohr, A. Desaules, H. Muntau, M. Christou and P. Quevauviller, 2001, European soil sampling guidelines for soil pollution studies, *Sci Total Environ*, vol. 264, pp 51-62
6. F. J. Dahlkamp, 1993, Uranium Ore Deposits, Springer-Verlag Berlin Heidelberg, New York.
7. Z. Papp, Z. Dezso and S. Daróczy, 2002, Significant radioactive contamination of soil around a coal-fired thermal power plant. *J Environ Radioact* vol. 59, pp 191-205
8. David A. Atwood, 2010, Radionuclides in the Environment. John Wiley & Sons, Chichester, England
9. United Nations Scientific Committee on the Effects of Atomic Radiation (UNSCEAR), 2000, *Sources and effects of ionizing radiation*, UN, New York
10. N. Movsisyan, G. Demirtchyan, K. Pyuskyulyan and O. Belyaeva, 2021, Identification of radionuclides' altitudinal distribution in soil and mosses in highlands of Armenia, *J Environ Radioact.* vol. 231

Conference Proceedings
ICPAE 2023, 24th August – 26th August, Zrenjanin, Serbia
University of Novi Sad, Technical Faculty "Mihajlo Pupin", Zrenjanin

The Global Mean Temperature

Slavoljub Mijovic[1*]

[1]*University of Montenegro, Faculty of Natural Sciences and Mathematics, Podgorica, Montenegro*
slavom@ucg.ac.me

Abstract. Global climate change is one of major concern of modern society. To estimate this change usually one estimates the global mean temperature. Measuring and calculating the Earth's average temperature are multi-steps complex processes which combine data from various sources and use statistical techniques. Nowadays, the dataset containing the space-time data about Earth's temperature is readily to use. Although scientists claim that to be able to achieve an accuracy of a few tenths of a degree, the main question is, does the global mean temperature make sense at all? It is shown that existing methodology of determining the global mean temperature is quite inappropriate for the estimation of climate change and in long term creating wrong science. A new methodology is introduced, concerning energy budget of heating and cooling of the Earth. The total influence of the atmosphere can be easily estimate by comparison with the Moon's temperature as a bare body. The 'potential temperature for cooling' is introduced as a right parameter to estimate global warming trend and climate change.

Keywords: Tte Earth's temperature, climate change, global warming, methodology, energy budget

INTRODUCTION

By climate system we primarily mean the land, ocean, ice on the surface of the Earth together with the atmosphere that overlies it and the radiation from the Sun that provides energy. All of these interact, to produce the conditions on and around the surface of our planet that we call the climate [1]. Averaging physical quantities which characterize these conditions in space and time defines the climate. Typically these statistics are calculated over a period of 30 years [2]. The physical quantities taken into account are the surface temperature but also precipitation, cloud cover, wind field, etc.

The major task as Klaus Hasselmann, Nobel Laureate for physics in 2021, said is the detection problem, often viewed as a task of identifying the most sensitive climate index, from a large set of potentially available indices, for which the anticipated climate change signal can be most readily distinguished from the natural climate noise. Global or regional mean surface temperature, vertical temperature differences, sea ice extent, sea level change, and integrated deep ocean temperatures are examples of indices [3]. Anyway, measuring and reconstructing the global mean temperatures remain the main task of many world's prominent organizations, like NASA *Goddard Institute for Space Science*, *National Oceanic and Atmospheric Administration* (NOAA) and *the Hadley Centre of the UK Met-*

Office [4]. These organizations analyze the data to determine the average temperature of the Earth's surface over a specific period, usually on an annual basis or over longer time spans.

Measuring and calculating the global mean temperature involves collecting temperature data from various locations around the world and then averaging these values to get the overall temperature. Basically, the globe is divided in many space cells and for each grid cell the anomaly-the difference of the measured and the usual temperature on that day, is calculated. Finally, the average of all anomalies is calculated and compared with other years. It's important to note that this process can be complex and requires sophisticated methods to handle issues like data quality, spatial and temporal gaps, and biases. Further, it's worth mentioning that the calculation of the global mean temperature is an ongoing scientific endeavor, and various organizations might use slightly different methodologies and datasets, leading to some variations in the reported global mean temperature values. Although scientists claim that to be able to achieve an accuracy of a few tenths of a degree [1,5] the general public concern and scientific debate still continue.

The focus of this paper is to analyze and answer a simple question: Does the global mean temperature make sense?

THE CURRENT METHOD

By summing and thereafter averaging the temperatures in different regions of the Earth's surface, we get a quantity which has no direct physical meaning. To say in another way, the given quantity is a pure statistical indicator insensitive to climate change and so far is interpreted in a wrong way. Below are listed examples (thoughtful experiments) that support this claim.

Thoughtful Experiments

A Simple Proof about Inadequacy of the Current Methodology

Imagine that the Earth is heated in a such way that has uniformly distributed moderate temperature, $t_{Earth} = 15$ ℃. Now, if the Earth experiences severe climate change so, that one half has the mean temperature, $t_1 = 0$℃, and the other, $t_2 = 30$ ℃, we still have the same mean temperatures , $t_{Earth} = \frac{(t_1+t_2)}{2} = 15$ ℃. We can conclude that there are infinity number of temperature distributions, which actually reflects climate change, although we calculate the same mean temperature. Insensitivity the mean global temperature to climate change is obvious.

A Spatial Temperature Distribution is Important

To calculate the Earth's temperature one can use different models but all models are based on energy balance budget between heating the Earth with solar shortwave radiation and the Earth's cooling with long-wave infra-red (IR) radiation. In the simplest way for the Earth without atmosphere and in equilibrium of incoming and outgoing fluxes, one can easily calculate the mean temperature of Earth surface as:

$$T_{Earth} = \sqrt[4]{\frac{(1-\alpha)S}{4\sigma}} \approx 255K = -18℃, \quad (1)$$

where are $S = 1.361\ \mathrm{kW/m^2}$ −solar constant, $\sigma = 5.67 \cdot 10^{-8}\ \mathrm{Wm^{-2}K^{-4}}$ − Stefan-Boltzmann constant, and $\alpha \approx 0.3$ − the Earth's albedo. This temperature, usually named as effective or sometimes radiometric, is of course far away from the real Earth's temperature (13.9 ℃), emphasizing the role of the atmosphere [6]. Two problems immediately arise here that make these comparisons pointless. First, the albedo is different for a bare planet and planet with atmosphere. Second, such calculated temperature as in formula (1), implicitly implies uniformly heated planet that actually never happened in reality.

To underline the importance of spatial temperature distribution, let's consider one such drastic case. Imagine, for the sake of simplicity, that only one side of the planet is uniformly heated and the other side remains cold $T_2 \approx 0$ K. The temperature of the first side is easily calculated by the equation (1), only four in the denominator is replaced by two, $T_1 \approx 303$ K. So, the global mean temperature, with the same source of heating, is now, $T_{Earth} = \frac{(T_1+T_2)}{2} \approx 152$ K!!!

A Temporal Temperature Distribution is Important

Imagine that the planet heated uniformly half of the time with two Suns, $2S$, and half of the time without heating i.e averaging in time, we have one Sun. If we further suppose that the body has small heating capacity and immediately cooling without the heating source, we get again the same results as in the previous example. Thus, one can conclude that any spatial and temporal temperature distribution lead to decreasing the global mean temperature. It does not mean the mandatory cooling of the planet.

THE PROPOSED METHOD

The basic idea is a finding link between energy balance and global temperature. Due to complexity of the atmosphere influence, let us firstly analize a 'bare' planet like the Moon. It is at the same distance from the Sun as the Earth, so solar constant is the same. Its albedo is 0.12, thus the average temperature can be easily calculated using the zeroth order model [6]: $T_{Moon} = 270$ K. Since the temperature distribution is very inhomogeneous and the cooling of each point on the surface is proportional to the fourth degree of temperature, it is necessary to have these values at every moment of time and at every point on the surface to calculate the outgoing energy flux. So, theoreticaly one can calculate the outgoing energy flux of cooling by integrating in a certain period of time the flux from all point of the surface. At the balance point the total incoming energy flux in a certain period of time is equal to the outgoing energy. The same method is analogously applicable to the Earth.

Fortunately, for the Earth we have the dataset of the surface temperatures with some spatial and temporal steps, readily to use. Because of presence of the atmosphere, the cooling is mainly by convection, but one can introduce 'the potential cooling' by radiation

i.e simulate the case of absence the atmosphere. Thus, the formula of the energy equilibrium is:

$$\sum_{i=1}^{N} \Delta S_i \left(\sum_{j=1}^{M} \sigma T_j^4 \Delta t_j \right) = F_{in} S_{Earth} \tau, \quad (2)$$

Where are $\Delta S_i -$ the area of i cell, $N -$total number of the grid cells, $\Delta t_j - j$ time step, $M -$total number of time steps in the chosen time period, $\tau = \sum_{j=1}^{M} \Delta t_j$, $F_{in}[\mathrm{W/m^2}] -$incoming energy flux to the Earth's surface, $S_{Earth} = \sum_{i=1}^{N} \Delta S_i -$the area of the Earth's surface.

Now, the total influence of the atmosphere, like greenhouse effect, can be easily calculated as the difference between 'the potential cooling energy', given by the term on the left side of the equation (2), and total incoming energy that the Earth would receive in that period of time without atmosphere. In this case the value for albedo is changed to the value of albedo of the Earth surface, $\alpha_{Earh\ surface} \approx 0.2$ [7]. For the constant 'potential cooling energy', the global mean temperature can serve as a measure for redistribution temperature field around the globe.

So, the proper way to calculate the Earth's temperature in a certain period of time, to estimate climate change (warming or cooling), is

$$\sum_{i=1}^{N} \Delta S_i \left(\sum_{j=1}^{M} \sigma T_j^4 \Delta t_j \right) = S_{Earth}\ \sigma T_{P.C}^4 \tau. \quad (3)$$

This temperature, $T_{P.C}$, one can call the 'effective temperature for potential cooling'. Previous parameter-the global mean temperature could serve as an indicator for spatial and temporal temperature redistribution.

CONCLUSION

Here comes the conclusion that current methodology for estimating global warming and climate change by calculating the global mean temperature is not adequate. The main reason is that there is not direct conection with the energy balance. Mathematicaly, this inconsistency is the consequence that the global mean temperature is linear combination of other temperatures and energy budget is higly non-linear and depends on the forth power of temperatures. The proper method is introduced and its testing would give a new insight to climate change with the existing datasets. The reference point could be chosen in the pre-industrial time (1850), i.e. establishing carfully the'natural' greenhouse effect and evolution of climate change and global worming could be folowed by the change of the 'effective temperature for potential cooling'.

ACKNOWLEDGEMENTS

I am grateful to the organizers of ICPAE2023, who invites me and thus initiated this work.

REFERENCES

1. F. W. Taylor, 2005, Elementary Climate Physics, Oxford University Press
2. IPCC Global Warming of 1.5 ºC, Special Report, 2018 https://www.ipcc.ch/sr15/
3. Scientific Background on the Nobel Prize in Physics 2021 “FOR GROUNDBREAKING CONTRIBUTIONS TO OUR UNDERSTANDING OF COMPLEX PHYSICAL SYSTEMS” https://www.nobelprize.org/uploads/2021/10/sciback_fy_en_21.pdf
4. PLANTON Serge (July 29, 2020), The average temperature of the earth, Encyclopedia of the Environment, Accessed August 15, 2023 [online ISSN 2555-0950] url : https://www.encyclopedie-environnement.org/en/climate/average-temperature-earth/
5. Lenssen, N. J. L., Schmidt, G. A., Hansen, J. E., Menne, M. J., Persin, A., Ruedy, R., & Zyss, D. (2019). Improvements in the GISTEMP uncertainty model. Journal of Geophysical Research: Atmospheres, 124, 6307–6326. https://doi.org/10. 1029/2018JD029522
6. Slavoljub Mijovic Greenhouse effect: Background, Experiments and Modelling; Conference Proceedings ICPAE 2022, March 31st – 2nd April, Zrenjanin, SerbiaTechnical faculty "Mihajlo Pupin", Zrenjanin & Faculty of Sciences and Mathematics, Nis pp. 2-9 http://147.91.177.109/icpae/conference%20program/ICPAE2022.pdf
7. R. T. Pieerehumbert, 2010, Principles of Planetary Climates, Cambridge University Press, New York

Conference Proceedings
ICPAE 2023, 24th August – 26th August, Zrenjanin, Serbia
University of Novi Sad, Technical Faculty "Mihajlo Pupin", Zrenjanin

Estimation of Groundwater Mean Residence Time in Karst Aquifers

Diana Mance[1*], Andrea Makjanić[1]

[1]*University of Rijeka, Faculty of Physics, Radmile Matejčić 2, Rijeka, Croatia*
diana.mance@uniri.hr

Abstract. Karst relief is formed by the dissolution of soluble rocks such as limestone, dolomite, and gypsum. This type of dissolution process results in highly permeable and complex aquifer systems that are recognized as important sources of fresh water in many parts of the world. Due to the heterogeneity and anisotropy of subsurface networks, the study and description of karst aquifers is extremely difficult. We provide an overview of the groundwater age problem and methods for estimating mean residence time (MRT). MRT is one of the most important pieces of information about karst aquifers and is critical for assessing the risks of groundwater contamination.

Keywords: karst, isotopic techniques, groundwater, mean residence time

INTRODUCTION

Karst is a particular area consisting of a surface relief and a complex subsurface network of fissures, cavities, cracks, and channels formed and expanded by the movement of water and its powerful chemical and physical action on soluble carbonate rocks (e.g., limestone, chalk, dolomite, gypsum, and salt) [1]. It is estimated that karst accounts for up to 20% of the earth's ice-free land and that about 25% of the world's population relies on drinking water from karst systems [2]. In many countries on the European continent, the entire population living in karst areas obtains drinking water from karst water resources, and in some cases (e.g., Austria, Slovenia, Bosnia and Herzegovina, Montenegro) the share of karst water in the total water supply exceeds the share of carbonate deposits in the total area of the country [3].

An aquifer is a rock (or sediment) formation that contains significant amounts of water. Typical of the karst aquifer is the so-called dual porosity, which refers to a rock matrix with numerous small fissures in which a network of wide channels is laid out. Consequently, the karst aquifer is also characterized by dual flow: slow and laminar in the rock matrix and fast and turbulent through wide conduits.

The process of "self-purification" in karst aquifers is poor because the surface of the karst is usually covered with a thin layer of soil and there are often completely bare rocks. Therefore, potential contaminants can easily enter the groundwater and then quickly travel long distances to karst springs. The high sensitivity to anthropogenic activities and potential pollution requires a good knowledge of karst aquifers, and the residence time of water in the subterrain is a good indicator of this sensitivity.

HOW OLD IS GROUNDWATER?

We cannot give a simple answer to the question of the age of groundwater. In fact, there is already a problem with the term "age of groundwater" itself. When we talk about the "age", we intuitively think of human age, which refers to the time from birth to the moment we ask the question. In the case of groundwater, the sample taken at the spring represents a mixture of waters from different precipitation events that have spent different amounts of time in the subsurface. Therefore, the age of groundwater cannot have a definite unique value, and we should distinguish between “idealized water age”," “tracer age,” and “residence time” [4].

The idealized water age is close to what we intuitively perceive as age. It is defined as the time difference between the time the parcel of water (an infinitesimally small volume of water) passed the groundwater table and the time of sampling, assuming that no mixing, diffusion, or dispersion occurred during the parcel's journey through the underground [4]. Since mixing of water occurs in all parts of the hydrologic cycle, and even the water molecule itself changes during the cycle, the above assumption is highly problematic.

At the moment there is no way to determine the age of the water itself, but for that we resort to tracers (either isotopes of the water or certain substances that are transported in a similar way as the water). But we must be aware that this is essentially how we determine the age of the tracer. It is also important to keep in mind that a particular tracer can only be used for a certain time range. For example, CFC/SF_6 can be used for modern groundwater with an expected time span of 10–40 years, tritium for an expected time span of 1–50 years, and stable water isotopes for recently recharged water with an expected time span of 0.1–3 years [4]. Since karst springs can respond very quickly to rain events, it can be assumed that the water at the springs is young and stable water isotopes are suitable tracers for karst water dating. The age of water and tracer is comparable only if both water and tracer exhibit the same behavior. When converting a measured value to a tracer age, numerous interpretations of the age can be made. This problem can only be solved by using multiple tracers.

The residence time is the time the substance spends in the volume:

$$t = \frac{V}{J}, \tag{1}$$

where:
V – a control volume (m^3); and
J – the flux through the control volume (m^3/y).

In groundwater systems, the position of the control volume and the flow field within the control volume have a significant impact on residence time.

From the above, it is clear that there is a discrepancy between the ages of the real water samples, which are actually a mixture of idealized ages, the concept of age as a time difference attributed to a water parcel, and the concept of residence time. This discrepancy can be overcome through the use of models. The models most commonly used in water dating are the so-called "lumped parameter models".

The stable isotopes of water and the aforementioned models will be discussed in more detail in the next two subsections.

Stable isotopes of water

Hydrogen has two stable isotopes: ^{1}H and ^{2}H (deuterium). ^{1}H accounts for 99.98% and ^{2}H for 0.02% of the total stable hydrogen in nature. Oxygen has three stable isotopes, but we will deal only with ^{16}O (99.76% of the total stable oxygen in nature) and ^{18}O (0.2% of the total stable oxygen in nature). The most common stable configurations of water molecules in nature are: $^{1}H^{1}H^{16}O$, $^{1}H^{2}H^{16}O$ and $^{1}H^{1}H^{18}O$.

The stable isotopic composition of water is expressed by $\delta^{2}H$ and $\delta^{18}O$ values. The δ-value is defined as:

$$\delta(‰) = \frac{R_{\text{sample}} - R_{\text{standard}}}{R_{\text{standard}}}, \tag{2}$$

where:
R_{sample} – ratio of the heavier and lighter isotopes ($^{18}O/^{16}O$; $^{2}H/^{1}H$) in the sample; and
R_{standard} – ratio of the heavier and lighter isotopes ($^{18}O/^{16}O$; $^{2}H/^{1}H$) in the standard.

Isotope ratio mass spectrometry (IRMS) and laser absorption spectroscopy are commonly used for the accurate measurement of small differences in the abundances of hydrogen and oxygen isotopes in water samples, i.e., for the determination of their δ-values.

In addition to dating karst water, $\delta^{2}H$ and $\delta^{18}O$ are also used in isotope hydrology to study karst recharge processes and reservoir mixing [5–9], to study vadose water mixing and storage in non-conduit parts of karst systems [10], for estimating average elevation of the recharge area [11,12], but also in more unconventional ways as a basis for managing water commons [13], and as a possible predictor of marine microbial pollution and differentiation [14,15].

Lumped parameter models

The water of a karst spring contains an immense number of water molecules from many different precipitation events. The karst groundwater flows rapidly through channels and slowly through the porous matrix where most of the recharged water can be stored for a long time. As a result, the spring water may contain water with different residence times. The mean residence time (MRT) of groundwater is the mass-weighted average residence time of all water discharged to a spring at a given time.

Mathematical models help us to describe an average value for a mathematically specified combination of different ages. In lumped parameter models, the convolution integral relates the output tracer to the input tracer [16]:

$$C_{out}(t) = \int_{-\infty}^{t} C_{in}(t') \cdot g(t - t') \cdot e^{-\lambda(t-t')} dt', \tag{3}$$

where:
$C_{out}(t)$ – the time series of tracer values in spring water (the output tracer signature);
$C_{in}(t')$ – the time series of tracer values in precipitation (the input function);
t' – time of tracer entry;

$t - t'$ – the residence time;
$g(t-t')$ – the residence time distribution (the response function); and
$e^{-\lambda(t-t')}$ – related to radioactive decay ($\lambda = 0$ for stable isotopes).

By the response function the convolution integral assigns a weight to each individual age. The assigned weight represents the proportion to which an individual age contributes to the overall mean. Mean Residence Time (MRT) corresponds to the weighted average value of all idealized ages. MRT can be calculated from the convolution integral of the tracer [16]:

$$\tau = \frac{\int_{-\infty}^{t}(t-t')C_i(t-t')dt'}{\int_{-\infty}^{t}C_i(t-t')dt'}, \tag{4}$$

where:
τ– the mean residence time;
C_i – the tracer concentration observed at the measuring point as the result of an instantaneous injection at the injection point at $t = 0$.

However, in practice, the formula (4) is not often used because the practical modeling approach is to vary until an optimal fit to the measured data is obtained [4].

The response function defining a pre-factor for each age in the convolution integral dominates the modeling process. There are several lumped parameter tools available as public domain software [4,16,17]. This paper presents the results obtained using LUMPY [18]. LUMPY contains several different models: the piston flow model (PM); the exponential model (EM); the exponential piston flow model (EPM); the linear model (LM); the linear piston flow model (LPM); the dispersion model (DM); and the gamma model (GM). Each of the above models has a corresponding response function. In the following, we will describe in more detail only the models whose results we have presented in this paper.

The exponential piston flow model and the exponential model

There are two different residence time distributions in the EPM: the exponential distribution and the distribution modeled by the piston flow which is represented by an age distribution corresponding to the Dirac delta distribution [19]. The PM assumes that there is no mixing in the aquifer system, i.e., that the sample is represented by water of a single age. Response function for EPM is:

$$g(t-t')\begin{cases}\frac{1}{\eta\tau}\exp\left(\frac{-(t-t')}{\eta\tau}+\frac{1}{\eta}-1\right) & \text{for } (t-t') \geq \tau\ln(1-\eta), \\ 0 & \text{for } (t-t') \geq \tau\ln(1-\eta), \end{cases} \tag{5}$$

where:
η – indication for the time the water spends in the exponential and the piston flow part of the mode i.e. the ratio of the total volume (V_{EM}+V_{PM}) to the volume with exponential distribution of ages (V_{EM}): $\eta = V_{EM}/(V_{EM}+V_{PM})$. V_{PM} – the volume with an age distribution corresponding to the Dirac delta distribution i.e. piston flow.

η can take values from 0 to 1, and for η=1 the EPM converts to the EM with the age distribution:

$$g(t-t') = \frac{1}{\tau}\exp\left(\frac{-(t-t')}{\tau}\right). \quad (6)$$

Note: The EM should only be used if the water sample contains recent rain [19].

Dispersion Model

For the DM, the corresponding response function is:

$$g(t-t') = \sqrt{\frac{Pe\cdot\tau}{4\pi(t-t')}}\cdot\frac{1}{t-t'}\exp\left(-\left(1-\frac{t-t'}{\tau}\right)^2\frac{P_e\cdot\tau}{4(t-t')}\right), \quad (7)$$

where:
Pe – Peclet number.

The Peclet number shows relative significance of the advective and dispersive fluxes in the system [20]. The Peclet number is defined by:

$$Pe = \frac{l\cdot v}{D}, \quad (8)$$

where:
l –the characteristic length of the system;
v – the advective velocity average, and
D – the coefficient of molecular diffusion.

AN EXAMPLE OF GROUNDWATER MEAN RESIDENCE TIME ESTIMATION

We chose a karst well at the Martinšćica pumping station near Rijeka, Croatia, as an example of an MRT estimate. There are 5 wells at the Martinšćica pumping site, of which well 2 (MW2) is the most frequently connected to the water supply network of Rijeka and the surrounding settlements. All wells were sampled to characterize the karst aquifer, which includes the most important springs of the Kvarner Bay [21].

Isotopic values were determined in the IRMS laboratory at the University of Rijeka. The precision of measurements was better than 0.1‰ for δ^{18}O‰ and better than 1‰ for δ^{2}H.

The regression equation between δ^{2}H and δ^{18}O for the wells is (Figure 1):

$$\delta^{2}\mathrm{H} = 8.12\cdot\delta^{18}\mathrm{O} + 15.41 \quad (\mathrm{R}^2 = 0.974). \quad (9)$$

Because of the strong correlation and better precision, only δ^{18}O was used for MRT assessment. The equation (9) is comparable to the LMWL equation for the study area [7]:

$$\delta^2H = 8.2 \cdot \delta^{18}O + 14\,. \tag{10}$$

This indicates that the wells are recharged by local, recently recharged precipitation, and confirms stable water isotopes as the method of choice for MRT estimation.

The input function (Figure 2) was determined using isotopic values of monthly rainwater samples collected at 3 rain totalizators distributed at different locations within the assumed area of aquifer recharge [8]. Wells were sampled weekly and rainwater was collected at the end of the month. The average (median) of weekly groundwater values for each month were used to obtain the corresponding output function (Figure 2). For the flow model calculations, we used the exponential model (EM), the combined exponential-piston model (EPM), and the dispersion model (DM).

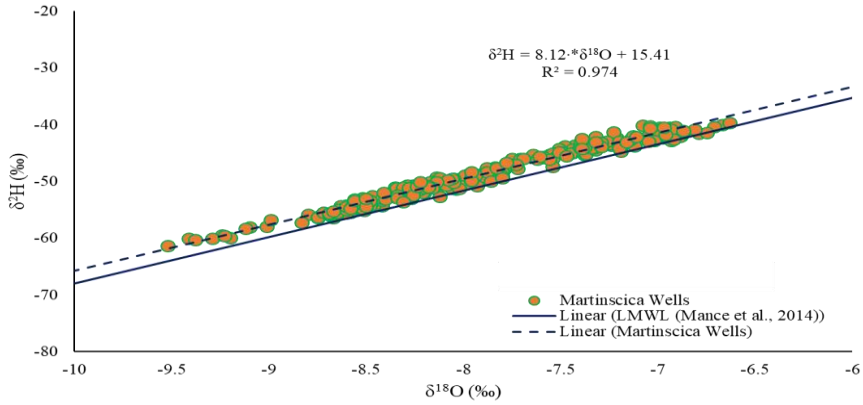

Figure 1. Correlation diagram of δ^2H and $\delta^{18}O$ values for Martinšćica wells. LMWL – local meteoric water line based on equation (10)

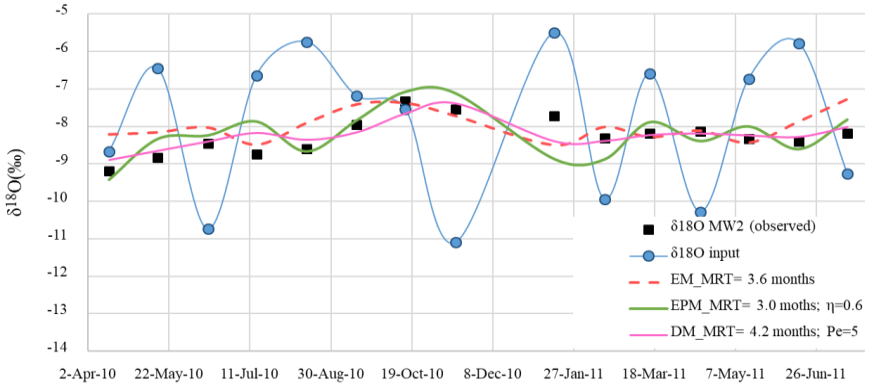

Figure 2. $\delta^{18}O$ content for input (rain), measured output (groundwater collected at Martinšćica well 2 – MW2) and fitted output calculated by the exponential model (EM), the combined exponential-piston model (EPM) and the dispersion model (DM)

The best agreement between observed and modeled data was obtained with DM (R^2=0.66) and the corresponding MRT is 4.2 moths (Table 1). The estimated fraction of

water younger than 1/2 MRT is 19.1%. The estimated fraction of water younger than 1 MRT is 61.6% and the fraction of water younger than 2 MRT is 92.7%. We can assume that 99.9% of the water in MW2 is younger than 2.25 years.

Table 1. Results of flow model calculations for mean residence times (MRTs)

Flow model	MRT (months)	% of water younger than			99.9% younger than (years)
		0.5 MRT	1 MRT	2 MRT	
Exponential model R^2=0.22	3.6	39.3	63.2	86.5	2.7
Dispersion model P_e=5; R^2=0.66	4.2	19.1	61.6	92.7	2.25
Exponential piston model η= 0.6; R^2=0.43	3	39.4	63.2	86.5	2.3

Since 99.9% of the water is younger than 3 years according to all three models used (Table 1), we can say that the water in the well was recently recharged i.e., is young water.

According to [20], a Peclet number in the range of 0.4 to 6 indicates that there is a transition zone in which the effects of diffusion and longitudinal mechanical dispersion are comparable. Therefore, for recharge zone of MW2, we can say that there is a deep, well-integrated network of broad channels connected by less karstified pathways. The existence of dual flow conditions for the MW2 has already been confirmed by Gaussian mixture modeling [8].

CONCLUSION

Karst aquifers are important water resources worldwide. Stable water isotopes are used to supplement conventional hydrologic methods in the study of karst aquifers. One such application is the estimation of MRT. Among other, MRT is used to predict potential contamination trends. Knowledge of the travel times of contaminants through an aquifer is necessary for early warning of groundwater quality degradation and effective groundwater protection.

Using the lumped parameter model, we estimated that the MRT of the water in the MW2 is about 4 months and that 99.9% of the water in the well was recently recharged. This shows that the water in this well is very sensitive to pollution and its quality must be constantly monitored.

ACKNOWLEDGEMENTS

This work was partially supported by project uniri-pr-prirod-19-24 and UNIRI INOVA project “Mikroplastika u različitim sastavnicama okoliša”.

REFERENCES

1. O. Bonacci, 1987, Karst Hydrology, Springer Series in Physical Environment, vol 2. Springer: Berlin, Heidelberg, pp 1–3
2. D.C. Ford and P. Williams, 2007, Karst Hydrogeology and Geomorphology, John Wiley: Chichester
3. Z. Stevanović, 2019, Karst waters in potable water supply: A global scale overview, *Environ. Earth Sci.* **78** 662 doi: 10.1007/s12665-019-8670-9
4. A. Suckow, 2014, The Age of Groundwater – definitions, models and why we do not need this term, *App. Geochem.* **50** 222–230 doi: 10.1016/j.apgeochem.2014.04.016
5. A.J. Long and L.D. Putnam, 2004, Linear model describing three components of flow in karst aquifers using ^{18}O data, *J. Hydrol*. **296** 254–270 doi: 10.1016/j.jhydrol.2004.03.023
6. P. Maloszewski, W. Stichler, A. Zuber and D. Rank, 2002, Identifying the flow systems in a karstic-fissured-porous aquifer, the Schneealpe, Austria, modeling of environmental 18O and 3H isotopes, *J. Hydrol*. **256** 48–59 doi: 10.1016/S0022-1694(01)00526-1
7. D. Mance, T. Hunjak, D. Lenac, J. Rubinić and Z. Roller-Lutz, 2014, Stable isotope analysis of the karst hydrological systems in the Bay of Kvarner (Croatia), *App. Radiat. Isotopes* **90** 23–34 doi:10.1016/j.apradiso.2014.03.001
8. D. Mance, M. Radišić, D. Lenac and J. Rubinić, 2022, Hydrological Behavior of Karst Systems Identified by Statistical Analyses of Stable Isotope Monitoring Results, *Hydrology*, **9** 82 doi: 10.3390/hydrology9050082
9. D. Mance D. Lenac, M. Radišić, D. Mance and J, Rubinić, 2022, The use of ^{2}H and ^{18}O isotopes in the study of coastal karstic aquifers, *Proc. of 9th Int. Symp. Monitoring of Mediterranean coastal areas: problems and measurement techniques*, pp 525–534
10. D. Paar, D. Mance, A. Stroj and M. Pavić, 2019, Northern Velebit (Croatia) karst hydrological system: results of a preliminary ^{2}H and ^{18}O stable isotope study, *Geologia Croatica*, **72** (3), 205–213 doi: 10.4154/gc.2019.15
11. M. Barbieri, T. Boschetti, M. Pettita and M. Tallini, 2005, Stable isotope (^{2}H, ^{18}O and $^{87}Sr/^{86}Sr$) and hydrochemistry monitoring for groundwater hydrodynamics analysis in a karst aquifer (Gran Sasso, Central Italy), *Appl. Geochem*. **20** 2063–2081 doi: 10.1016/j.apgeochem.2005.07.008
12. A. Charideh and A. Rahman, 2007, Environmental isotopic and hydrochemical study of water in the karst aquifer and submarine springs of the Syrian coast, *Hydrogeol. J.* **15/2** 351–364 doi: 10.1007/s10040-006-0072-xbyjhydrol.2004.03.023
13. D. Mance, D. Mance and D. Vukić Lušić, 2022, Managing water commons using mediator variables to bridge the gap between environmental factors and anthropogenic pollution indicators, *Proc. of 9th Int. Symp. Monitoring of Mediterranean coastal areas: problems and measurement techniques*, pp 515–524
14. D. Mance, D. Mance and D. Vukić Lušić, 2018, Environmental isotope ^{18}O in coastal karst spring waters as a possible predictor of marine microbial pollution, *Acta Adriatica*, **59/1** 3–16 doi: 10.32582/aa.59.1.1
15. D. Mance, D. Mance and D. Vukić Lušić, 2018, Marine Pollution Differentiation with Stable Isotopes of Groundwater, *Pomorstvo*, **32** 80–87 doi: 10.31217/p.32.1.10
16. P. Maloszewski and A. Zuber, 1996, Lumped parameter models for the interpretation of environmental tracer data, *IAEA-TECDOC-910*, International Atomic Energy Agency, Technical-Report 9–58 (available online: osti.gov/etdeweb/biblio/439998)
17. N.N. Ozyurt, H.O. Lutz, T. Hunjak, D. Mance and Z. Roller-Lutz, 2014, Characterization of the Gacka River basin karst aquifer (Croatia): Hydrochemistry, stable isotopes and tritium-based mean residence times, *Science of The Total Environment*, **487** 245–254 doi: 10.1016/j.scitotenv.2014.04.018
18. A. Suckow, 2012, Lumpy - an interactive lumped parameter modeling code based on MS Access and MS Excel, *Geophisical Research Abstracts*, **14** EGU2012-2763
19. A. Suckow, 2014, Lumped Parameter Modelling of Age Distributions using up to two Parallel Black Boxes, Manual for Lumpy Version 2.9
20. C. W. Fetter, 1993, Contaminant Hydrogeology, 1st ed., Macmillan Publishing Company, p. 54

21. D. Mance, 2014, Karakterizacija Krškog Vodonosnika Temeljena na Prostornim i Vremenskim Promjenama Stabilnih Izotopa Vodika i Kisika. *Ph.D. Thesis*, University of Zagreb, Croatia (in croatian)

Conference Proceedings
ICPAE 2023, 24thAugust– 26thAugust, Zrenjanin, Serbia
University of Novi Sad, Technical Faculty "Mihajlo Pupin", Zrenjanin

Measurement of the Diffuse Component of Solar Radiation

Abdulah Akšamović[1*], Senad Odžak[2], Ajdin Fejzić[1]

[1]University of Sarajevo - Faculty of Electrical Engineering, Zmaja od Bosne bb, 71000 Sarajevo, Bosnia and Herzegovina*
[2]University of Sarajevo - Faculty of Science, Zmaja od Bosne 33-35, 71000 Sarajevo, Bosnia and Herzegovina
aaksamovic@etf.unsa.ba

Abstract. Photovoltaic technology offers a promising solution for transitioning from environmentally harmful energy sources to sustainable green energy. The main challenge lies in the unpredictability of renewable energy sources based on photovoltaic. To ensure a stable energy supply, power companies need efficient planning methods for energy exchange between producers and consumers. This planning relies on an accurate models of both consumers and producers. While consumer models are well-established, modeling the production of photovoltaic plants poses an ongoing research challenge due to their inherent uncontrollability. Existing models use various parameters, but to effectively plan production, reliable predictions of solar insolation intensity, temperature, and wind speed are essential. While weather forecasts can provide temperature and wind speed data, estimating the diffuse and reflective components of solar radiation, which depend on the photovoltaic plant microclimate, requires additional measurements at the specific microlocation. This study proposes a method for directly measuring the diffuse component of solar radiation on panels, similar to those used in photovoltaic plants. Through a series of measurements at a test microlocation, we obtained valuable insights and discuss their potential application in accurate photovoltaic production models.

Keywords: green energy, photovoltaic plants, diffuse component of solar radiation, modeling

INTRODUCTION

Photovoltaic technology is becoming the most serious candidate for the energy transition from environmentally unacceptable sources of electrical energy to new sources of green energy [1,2]. The fundamental issue with renewable energy sources based on photovoltaic technology is their uncontrollability. Electric power companies engaged in energy exchange between production units and consumers are seeking new ways to plan this exchange in order to ensure economically acceptable continuity in supply. For effective planning, consumer models and producer models are of a crucial importance. Consumer models are well known and validated based on the consumption measurements over extended periods of operation [3,4]. Photovoltaic installations (PV) belong to the category of new energy sources and are generally uncontrollable (production cannot be increased or decreased according to demand). Hence, the issue of modeling the production

of photovoltaic installations is a pressing research problem. Existing models of photovoltaic installations [5], use input parameters such as the geographic location, panel tilt angle, installed capacity of the system, and panel efficiency. Based on these parameters, the models provide expected daily, monthly, and yearly production. These outputs are useful in the process of designing installations for feasibility studies, but not for production planning. Production planning requires predictions of a solar insolation intensity, temperature, and wind speed. Temperature and wind speed can be obtained from weather forecasts to the extent of these forecasts accurate. Solar insolation is estimated from the weather forecast, considering the geographic location of the installation and the tilt angle of the panels. This estimation provides information about the expected global insolation, consisting of three components: direct, diffuse, and reflected [6]. Direct solar radiation can be predicted based on geographical coordinates and weather forecasts with the same degree of reliability as weather predictions. The diffuse and reflected components are significantly dependent on microclimate specific to the installation location. Existing weather forecast software and photovoltaic modeling software do not possess microclimate parameters due to their high variability. Therefore, it is necessary to develop efficient methods for measuring the diffuse and reflected components of solar radiation, from which microclimate parameters suitable for modeling PV production prediction can be estimated. This paper proposes a method for estimating the diffuse component directly on the same type of panel as those used in the photovoltaic plants. A series of measurements of the diffuse component were conducted at a test microlocation under various weather conditions. The results of these measurements are presented, and their use in models is discussed.

Model of Solar Radiation Components

We will observe the panel tilt at a fixed angle α, the angle of incidence of direct solar radiation G_{DIR} onto the horizontal plane during the measurement period at an angle β, and we will divide the diffuse component into the horizontal G_{DIFH} and the normal G_{DIFN} components (Figure 1). Now, the total insolation G that falls on the panel can be expressed as:

$$G(\alpha) = G_{\mathrm{DIR}} \cos(90° - \alpha - \beta) + G_{\mathrm{DIFN}} \cos\alpha + G_{\mathrm{DIFH}} \sin\alpha + G_{\mathrm{REF}} \sin(\alpha - \beta)\, w, \qquad (1)$$

where $w = \begin{cases} 1, \alpha \geq \beta \\ 0, \alpha < \beta \end{cases}$.

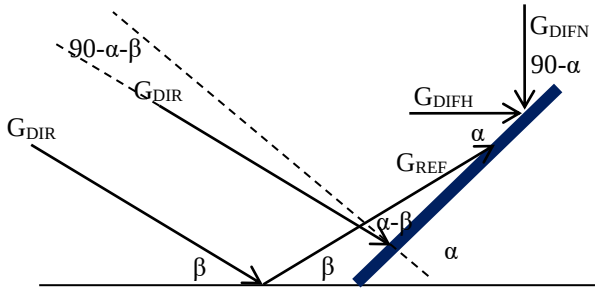

Figure 1. Components of solar insolation according to the model.

In the method, we will use measurements of the generated electrical power by the panel at the points of maximum at the angles of 0°, 30°, 60°, and 90°. By substituting these angles into equation (1), we obtain the following system of equations:

$$\begin{aligned} G(0°) &= G_{\mathrm{DIR}}\cos(90° - \beta) + G_{\mathrm{DIFN}}, \\ G(30°) &= G_{\mathrm{DIR}}\cos(60° - \beta) + G_{\mathrm{DIFN}}\cos 30° + G_{\mathrm{DIFH}}\sin 30°, \\ G(60°) &= G_{\mathrm{DIR}}\cos(30° - \beta) + G_{\mathrm{DIFN}}\cos 60° + G_{\mathrm{DIFH}}\sin 60°, \\ G(90°) &= G_{\mathrm{DIR}}\cos\beta + G_{\mathrm{DIFH}} + G_{\mathrm{REF}}\sin(90° - \beta). \end{aligned} \quad (2)$$

By solving the system (2) G_{DIFN}, G_{DIFH}, G_{DIR} and G_{REF} can be determined.

Dependency of Panel Electrical Power on the Insolation and Temperature

The electrical power generated at the maximum point on the panel is a function of solar insolation and ambient temperature and can be determined for G>125 W/m^2 according to [7-9]:

$$P(G,T) = P_{\mathrm{M}}\left(1 + k_{\mathrm{p}}\frac{T_{\mathrm{c}} - T_{\mathrm{r}}}{100}\right)\frac{G}{1000}, \quad (3)$$

where P_M is the nominal panel power, k_{p} is the temperature coefficient of power, T_{C} is the cell temperature, and T_{r} is the reference cell temperature at which the nominal power is determined (25 °C). T_{C} is calculated according to [9,10]:

$$T_{\mathrm{C}} = T_{\mathrm{a}} + \frac{\mathrm{NOCT} - 20°\mathrm{C}}{800}G, \quad (4)$$

where T_{a} is the ambient temperature, NOCT is the cell temperature at standard test conditions (STC).

The solution to the previous two equations for G is a quadratic equation with coefficients:

$$a = \frac{k_{\mathrm{p}}(\mathrm{NOCT} - 20)}{80000},\ \ b = 1 + \frac{k_{\mathrm{p}}}{100}(T_{\mathrm{a}} - T_{\mathrm{r}}),\ \ c = -\frac{1000P}{P_{\mathrm{M}}}. \quad (5)$$

We take the solution with the smaller value, as the second solution gives a significantly larger value of G than the maximum insolation.

For G<125 W/m^2, the cell temperature differs slightly from the ambient temperature (3.6°C for G=125 W/m^2 and NOCT=43 °C). Therefore, for experiments where G<125W/m^2, we will neglect the influence of temperature and consider P only as a function of G:

$$P(G) = P_M\frac{G}{1000}. \quad (6)$$

EXPERIMENTAL RESULTS

The University of Sarajevo Campus was chosen as the testing location with coordinates: 43.856811°, 18.397636°. The measurements were conducted on the ground

with an asphalt surface, and the immediate surroundings were covered with tall grass. In the close vicinity of the testing location (20-100 m), there are trees as well as low and tall buildings. The location is not sufficiently structured to be classified into any typical category. For testing, a polycrystalline panel of type CHSM661OP-250 was used, with the following catalog characteristics [11]: warranted power output STC (P_{Mmin})=250 W, Module efficiency=15.2%, temperature coefficient k_p (P_{mpp})= −0.469%/K, temperature coefficient k_i (I_{sc})=+0.052%/K, temperature coefficient k_u (V_{oc})=−0.344%/K, NOCT=43 °C. Multiple experiments were conducted: measurement before sunrise, measurement after sunset, measurement in the shade, and measurement on a cloudy day.

Experiment 1: Sunset

The experiment was conducted after sunset on a clear day from 18:43 to 20:10, on July 12th, 2023. The panel was oriented towards the west (facing the direction of sunset). The ambient temperature was 30°C and remained constant throughout the duration of the experiment. Two sets of measurements were taken for panel tilt angles of 0, 30, 60, and 90 degrees. The measurement setup for Experiment 1 is shown in Figure 2 (left).

Figure 2. Measurement setup for Experiment 1 (left) and Experiment 2 (right).

For the conditions of Experiment 1, the direct and reflective components are zero (as the sun has set), leaving us with only the diffuse normal and diffuse horizontal components. The equation describing the system is:

$$G(\alpha) = G_{\mathrm{DIFN}}\cos\alpha + G_{\mathrm{DIFH}}\sin\alpha. \tag{7}$$

To estimate the two unknown values, we need two measurements. Since four measurements were taken, we will determine solutions for all six combinations.

Processing of measurement results for the Experiment 1.1 are given in the Table 1. From the analyzed 6 combinations based on the measurements taken at 4 different angles (0, 30, 60, and 90 degrees), the average values obtained are G_{DIFN}=33.91W/m^2 and G_{DIFH}=38.25 W/m^2.

Table 1. Processing of measurement results for the Experiment 1.1

T_a[°C]	Angle	P_m [W]	Measurements	G_{DIFN} [W/m^2]	G_{DIFH} [W/m^2]	Δ_N[%]	Δ_H[%]
30	0	9.89	0-30	39.56	21.16	16.65	-28.98
30	30	11.96	0-60	39.56	33.37	16.65	-12.75
30	60	12.17	0-90	39.56	44.16	16.65	15.45
30	90	11.04	30-60	34.18	36.47	0.79	-4.63
			30-90	39.74	44.16	-12.29	15.45
			60-90	20.87	44.16	-38.45	15.45

The percentage errors relative to the obtained mean values are provided in the columns 7 and 8 of Table 1. If we consider the values at 0 and 90 degrees as reliable since they correspond to the definition upon which the model was formed, then the measurements at 30-60 degrees yield better results than 0-30, 0-60, 30-90, and 60-90. The percentage error of the 30-60 measurements compared to the 0-90 measurements is −13.59% and −17.41%. The conditions under which the measurements were conducted need to be taken into account, primarily concerning the duration of the measurement process, which took 37 minutes during which the angle of incidence of sunlight into the atmosphere changed, and the diffuse component of radiation varied. Despite the mentioned factors, we believe that measurements at 0-90 and 30-60 can provide a good estimation of both components of diffuse solar radiation. The electrical power values obtained from the panel range from 3.95% to 4.86% of the nominal power of the used panel.

Processing of measurement results for the Experiment 1.2 are given in the Table 2.

Table 2. Processing of measurement results for the Experiment 1.2

T_a[°C]	Angle	P_m [W]	Measurements	G_{DIFN} [W/m^2]	G_{DIFH} [W/m^2]	Δ_N[%]	Δ_H[%]
30	0	3.30	0-30	13.20	8.57	5.44	-19.41
30	30	3.93	0-60	13.20	10.53	5.44	-1.05
30	60	3.93	0-90	13.20	11.08	5.44	4.11
30	90	2.77	30-60	11.51	11.51	-8.07	8.12
			30-90	11.75	11.08	-6.10	4.11
			60-90	12.24	11.08	-2.15	4.11

From the analyzed 6 combinations, the average values obtained are G_{DIFN}=12.52 W/m^2 and G_{DIFH}=10.64 W/m^2. The percentage errors relative to the obtained mean values are provided in columns 7 and 8 of Table 2. If we consider the values at angles 0 and 90 degrees as reliable since they correspond to the definition upon which the model was formed, then measurements at 0-30 degrees yield a slightly poorer estimation. We believe that the mentioned measurements can provide a good estimation of both components of diffuse solar radiation. The electrical power values obtained from the panel range from 1.1% to 1.57% of the nominal power of the used panel.

Experiment 2: Sunrise

Experiment 2 was conducted before sunrise under variable cloudy conditions from 6:03 to 6:50 on July 13th, 2023. The panel was oriented towards the east (facing the direction of sunrise). The ambient temperature was 22 °C and remained constant throughout the duration of the experiment. Two sets of measurements were taken for panel tilt angles of 0, 30, 60, and 90 degrees. The measurement setup for Experiment 2 is shown in Figure 1 (right).

For the conditions of Experiment 2, similar to Experiment 1, the direct and reflective components are zero (since the sun has not yet risen), leaving us with only the diffuse normal and diffuse horizontal components. Thus, we will use the same equation as in Experiment 1 (equation 7).

Processing of measurement results for the Experiment 2.1 are given in the Table 3.

Table 3. Processing of measurement results for the Experiment 2.1

T_a[°C]	Angle	P_m[W]	Measurements	G_{DIFN} [W/m^2]	G_{DIFH} [W/m^2]	Δ_N[%]	Δ_H[%]
22	0	4.45	0-30	17.8	5.49	6.60	-43.42
22	30	4.54	0-60	17.8	10.02	6.60	4.01
22	60	4.41	0-90	17.8	10.08	6.60	3.89
22	90	2.52	30-60	13.81	12.39	-17.27	27.73
			30-90	15.15	10.08	-9.27	3.89
			60-90	17.82	10.08	6.72	3.89

From the analyzed 6 combinations, the average values obtained are G_{DIFN}=16.69 W/m^2 and G_{DIFH}=9.7 W/m^2. The percentage errors relative to the obtained mean values are provided in columns 7 and 8 of Table 3. If we consider the values at angles 0 and 90 degrees as reliable since they correspond to the definition upon which the model was formed, then measurements at 0-60 and 60-90 degrees yield better results than 0-30, 30-60, and 30-90. The percentage error of the 0-60 (60-90) measurements compared to the 0-90 measurements is 0% (0.09%) and −0.11% (0%). We believe that measurements at 0-90, 0-60, and 60-90 degrees can provide a good estimation of both components of diffuse solar radiation. The electrical power values obtained from the panel range from 1.0% to 1.8% of the nominal power of the used panel.

Processing of measurement results for the Experiment 2.2 are given in the Table 4. From the analyzed 6 combinations based on the measurements taken at 4 different angles (0, 30, 60, and 90 degrees), the average values obtained are G_{DIFN}=32.7W/m^2 and G_{DIFH}=19.01W/m^2. The percentage errors relative to the obtained mean values are provided in columns 7 and 8 of Table 4. If we consider the values at angles 0 and 90 degrees as reliable since they correspond to the definition upon which the model was formed, then measurements at 30-60 and 60-90 degrees yield worse results than 0-30, 0-60, and 30-90.

Table 4. Processing of measurement results for the Experiment 2.2

T_a[°C]	Angle	P_m[W]	Measurements	G_{DIFN}[W/m^2]	G_{DIFH} [W/m^2]	Δ_N[%]	Δ_H[%]
22	0	8.14	0-30	32.56	17.84	-0.43	-6.17
22	30	9.28	0-60	32.56	20.09	-0.43	5.64
22	60	8.42	0-90	32.56	18.32	-0.43	-3.67
22	90	4.58	30-60	30.61	21.21	-6.38	11.55
			30-90	32.28	18.32	-1.27	-3.67
			60-90	35.62	18.32	8.95	-3.67

The percentage error of the better measurements compared to the 0-90 measurements ranges from -0.85% to 9.6%. The duration of the process was 29 minutes, during which conditions changed less compared to Experiment 2.1, resulting in smaller deviations from the mean values. We believe that the mentioned measurements can provide a good estimation of both components of diffuse solar radiation. The electrical power values obtained from the panel range from 1.8% to 3.7% of the nominal power of the used panel.

Experiment 3: Full shade

Experiment 3 was conducted during the day under clear weather conditions from 14:03 to 14:50 on July 18th, 2023. The panel was oriented towards the northeast (opposite to the direction of the sun) and was placed in complete shade of surrounding objects. The ambient temperature was 27 °C and remained constant throughout the duration of the experiment. Measurements were taken for panel tilt angles of 0, 30, 60, and 90 degrees.

For the conditions of Experiment 3, similar to the Experiment 1, the direct and reflective components are zero (since the panel is in complete shade), leaving us with only diffuse normal and diffuse horizontal components. Thus, we will use the same equation as in the Experiment 1 (Equation 7).

Processing of measurement results for the Experiment 3 are given in the Table 5.

Table 5. Processing of measurement results for the Experiment 3

T_a[°C]	Angle	P_m [W]	Measurements	G_{DIFN} [W/m^2]	G_{DIFH} [W/m^2]	Δ_N[%]	Δ_H[%]
27	0	20.97	0-30	83.88	6.07	5.21	-55.96
27	30	18.92	0-60	83.88	9.91	5.21	-28.17
27	60	12.63	0-90	83.88	18.32	5.21	32.81
27	90	6.57	30-60	80.56	11.82	1.05	-14.28
			30-90	76.81	18.32	-3.64	32.81
			60-90	69.31	18.32	-13.06	32.81

From the analyzed 6 combinations, the average values obtained are G_{DIFN}=79.72 W/m^2 and G_{DIFH}=13.79 W/m^2. The percentage errors relative to the obtained mean values are provided in columns 7 and 8 of Table 5. The horizontal component shows significant variations in values due to the different influence of surrounding objects for different

panel tilt angles. The normal component can be considered well-estimated. The electrical power values obtained from the panel range from 2.6% (at a 90° angle) to 8.3% (at a 0° angle) of the nominal power of the used panel.

Experiment 4: Cloud shadow

Experiment 4 was conducted under variable cloudy weather conditions from 13:00 to 14:10 on July 25th, 2023. The panel was oriented towards the south (facing the direction of the sun). The ambient temperature varied between 32 °C and 35 °C during the experiment. Measurements were taken for panel tilt angles of 0, 30, 60, and 90 degrees. The measurement setup for the Experiment 4 is shown in Figure 3.

Figure 3. Measurement setup for the Experiment 4, the right and left images depict the sky conditions during measurements at different moments.

For the conditions of Experiment 4, we have all four components of solar radiation, and we will use equations (2). The angle of incidence of the direct component, β=65.48°.

Processing of measurement results for the Experiment 4 are given in the Table 6.

Table 6. Processing of measurement results for the Experiment 4

Time	T_a[°C]	Angle	U_m[V]	I_m[A]	P_m[W]	Estimated components of solar radiation [W/m^2]	
13:00	35	0	28	1.78	49.84	G_{DIR}	67.15
13.:17	34	30	28.23	1.76	60.41	G_{DIFN}	85.65
13:37	33	60	27.73	1.89	52.41	G_{DIFH}	10.39
13:52	32	90	27	1.23	33.21	G_{REF}	3.38

Considering the conditions under which the portion of a direct solar radiation passed through the clouds, we estimated all four components. The estimated values indicate a significant contribution from the diffuse component as well as the presence of the direct component. For these values of the direct and reflective components, a reflection

coefficient of 0.15 is obtained. The electrical power values obtained from the panel range from 13.28% to 24.16% of the nominal power of the used panel.

CONCLUSION

A series of measurements of the output electrical power of the solar panel were conducted under various conditions. Measurements were taken at four different panel tilt angles (0, 30, 60, and 90 degrees), enabling the estimation of all four components of solar insolation. The percentage of generated output power relative to the nominal power ranged from 1% to 25%. The variations in the measurement results and relatively high errors for some measurements are attributed to the changing conditions during the procedures. To reduce these errors, simultaneous measurements on four panels of the same type can be used, each placed at a different angle. For drawing more generalized conclusions, additional measurements under different conditions should be conducted, such as rainy weather, clear sunny days, sunny days with snow, foggy weather, etc.

In the market, there are instruments used for measuring the direct and diffuse components of solar insolation. Here, a method is employed to estimate the components of solar insolation by measuring the generated electrical power on the panel. The idea is to use the same type of panel as used for the PV system and to incorporate the spectral characteristics of the panel into the method.

REFERENCES

1. International Energy Agency (IEA), "Renewables 2022. Analysis and forecast to 2027." [Online]. Available: https://www.iea.org/reports/renewables-2022.
2. IRENA, "World Energy Transitions Outlook 2023: 1.5°C Pathway, Volume 1," International Renewable Energy Agency, Abu Dhabi, 2023.
3. T. Mutanen, T. Sorasalmi, and R. Weiss, "Electricity usage type selection and model validation based on electricity usage measurements," in Proceedings of the 12th Industrial Conference on Advances in Data Mining (ICDM 2012), Berlin, Germany, 2012.
4. Nelson Fumo, M.A. Rafe Biswas, Regression analysis for prediction of residential energy consumption, Renewable and Sustainable Energy Reviews, Volume 47, 2015.
5. Solargis Prospect, [Online]. Available: https://solargis.com.
6. Global Solar Atlas, "Frequently Asked Questions," [Online]. Available: https://globalsolaratlas.info/support/faq.
7. A. P. Dobos, "PVWatts Version 5 Manual," 2014.
8. A. Hadj Arab et al., "Maximum power output performance modeling of solar photovoltaic modules," Energy Reports, vol. 6, no. 1, pp. 680-686, 2020.
9. D. L. King, J. A. Kratochvil, and W. E. Boyson, "Photovoltaic array performance model," Sandia Tech. Rep., 2004.
10. R. Bharti, J. Kuitche, and M. G. Tamizhmani, "Nominal Operating Cell Temperature (NOCT): Effects of module size, loading and solar spectrum," in Proceedings of the 34th IEEE Photovoltaic Specialists Conference (PVSC), 2009, pp. 001657-001662.
11. M. G. I. Distribución, "Datasheet: CHSM661OP-250 Polycrystalline PV Module," 2015. [Online]. Available:https://www.mgi.com.uy/images/pdf/paneles-poly-cristalin/20151014_CHSM6610P_3BB_40mm_frame.pdf.

II International Conference on Physical Aspects of Environment ICPAE2023

August 24-26th, 2023, Zrenjanin, Serbia

LECTURES

Conference Proceedings
ICPAE 2023, 24th August – 26th August, Zrenjanin, Serbia
University of Novi Sad, Technical Faculty "Mihajlo Pupin", Zrenjanin

Measuring Solar Irradiance with Vernier Pyranometer

Robert Repnik[1*], Robert Sterkuš[1]

[1]*Faculty of Natural Sciences and Mathematics, University of Maribor, Koroška cesta 160, 2000 Maribor, Slovenia*
robert.repnik@um.si

Abstract. A pyranometer is a measure device used for measuring solar irradiance on a planar surface. It is designed to measure the solar radiation flux density (W/m^2) from the sky above within a wavelength range typically from 300 nm to 3000 nm, which corresponds the wavelength of the solar radiation spectrum that reaches earth's surface. In our case, we used Vernier pyranometer. In the measurement of the irradiance, the response of the sensor of radiation varies with the cosine of the angle of incidence. The experiment is appropriate for the secondary schools, since includes theoretical background, experimental setup, analysis of experimental results, computer simulations, and application. The radiation flux density varies during the day (and year) at any populated location on the Earth and is additionally dependent of the weather. All this plays important role in setup of the solar panels in order to use the energy of the sun in an effective way.

Keywords: pyranometer, solar irradiance, physics teaching, environmental awareness

INTRODUCTION

The needs and demand of humanity for energy are constantly growing. In recent years, concepts such as green energy and renewable energy sources have been integrated into the ecological equation. When converting energy from one form to another, electrical energy is the widely usable form that powers all electrical devices. Discussing heat makes sense because heat represents energy that is also necessary – for heating and also for driving turbines, which transform this energy into electrical energy through generators. Eurostat statistics indicate that households use 63.5% of the total energy for heating. A significant portion of this heat comes from electrical devices (heating elements). The EU countries primarily obtain electrical energy from gas and petroleum derivatives (Eurostat, 2023).

In addressing the issues of electricity and heat supply, alternatives such as solar, wind, water, and nuclear energy are used. Solar panel production technology has advanced, leading to modern panels with higher efficiency. The research question is: what can the output of a solar panel be? Can we rely on claims from traders that the output of a solar module is, for example, 1000 W/m^2 under normal illumination?

In this contribution, our focus is mainly on measuring the light flux density using the Vernier sensor - pyranometer and the Vernier interface. This research approach broadens our perspective on atmospheric phenomena, atmospheric pollution, and energy behavior during transitions.

Experimental work becomes more engaging and mobilizes students to explore. In exploring (existing) elementary and secondary school curricula, teachers have the autonomy to incorporate modern scientific approaches and meteorology, which is undoubtedly the study of atmospheric phenomena. Before delving into the research, I introduce the concept of solar constant (energy source), the atmosphere (as a "filter"), and Earth as an absorber (albedo), global irradiance (direct, reflected, diffuse). The experiment's design is problem-based and stems from real-life contexts (social, economic).

During the experimental phase, we adhere to pedagogical methodology and explore various ways and paths in investigating the issue - both with students (in the field of physics) and with the teacher (in the pedagogical domain). Through quantitative methods, we seek to understand and predict atmospheric phenomena. The question could be expanded to the impact of CO_2 on atmospheric processes.

THEORY OF ENERGY TRANSFER THROUGH THE ATMOSPHERE

The Sun, in all its magnificence, represents the most crucial source of energy for Earth. Earth is also "heated" from within (geothermal flux), but this contribution is thousands of times smaller than the energy Earth receives from the Sun.

The Sun emits electromagnetic radiation and various particles (protons, electrons). The majority of emitted electromagnetic radiation consists of waves in electric and magnetic fields that propagate through space, carrying energy. Electromagnetic radiation is categorized into different parts of the spectrum - different types of radiation. UV radiation, visible light, and IR radiation have the most impact on the atmosphere.

Radiation intensity is expressed through energy flux density, denoted as j. The Sun can be described as a black body. The Stefan-Boltzmann law describes the energy flux density of radiation emitted by the surface of a black body. Bodies that are not black emit slightly less, a factor accounted for by the substance's emissivity (ε). The radiation equation is as follows:

$$j = \varepsilon \cdot \sigma \cdot T^4 \tag{1}$$

where $\sigma = 5{,}67 * 10^{-8} \frac{\mathrm{W}}{\mathrm{m^2 K^4}}$. The emissivity (ε) of the Sun's surface is 1. For the atmosphere, the emissivity is around 0.7.

At higher temperatures of an object, the spectrum of emitted radiation shifts towards shorter wavelengths. The Sun emits about 10% of its energy in the UV part of the spectrum, around 40% in visible light, and the remainder in the IR part of the spectrum. Planck's law describes the radiation of an object at a specific wavelength. This radiation is a function of wavelength.. (B., 2021)

Solar radiation propagates into the surrounding space, and the energy flux density decreases with the square of the distance from the Sun. At the distance of Earth, it has a value of around 1366 W/m^2. This value is called the solar constant (denoted as j_0). The constant's value isn't constant itself but represents an average, as we know Earth orbits the Sun in an almost circular path – the eccentricity is small, and Earth's distance from the Sun varies by ±2%. Consequently, the energy flux density (solar constant) realistically fluctuates by around ±4%.

The assumption about the solar cycle is also important; within an 11-year solar cycle, the energy flux (density) changes by about 0.1%. In reality, the Sun illuminates half of Earth at any given moment. Earth is inclined to the plane around the Sun by a declination angle of 23.5°. Due to this inclination and distance, we experience seasons and a slightly different pattern of solar energy flux.

The Sun emits radiation similar to a black body. The surface temperature of the Sun is around 5800 K. The diameter of the Sun is 1392000 km. The solar photosphere has a thickness of 300 – 400 km. The distance (r_0) between the Sun and Earth is 150 million km. With the data and the help of Stefan's law, we arrive at the value of the solar constant.

Energy flux density depends on the amount of energy that an object (the Sun) emits per second through a certain area.

$$j = \frac{P}{S} = \frac{W}{t * S}. \tag{2}$$

Stefan's law of radiation for a black body is:

$$j = \varepsilon \cdot \sigma \cdot T^4. \tag{3}$$

From equation (3), we calculate the energy flux density of the Sun. In doing so, we utilize the value of the Stefan-Boltzmann constant ($\sigma = 5{,}67 \cdot 10^{-8} \frac{\mathrm{W}}{\mathrm{m^2 K^4}}$), with the emissivity of the Sun being 1 (emitting as a black body).

In this case, we do not consider scattering and absorption because the space between the photosphere and the top of the atmosphere is "empty," and there is no substance to weaken the energy radiation. Provides the value of the solar constant as 1397 W/m².

In this task, we assume that the solar constant doesn't change, and we take its value as 1366 W/m². (J.Strnad, 1998)

Radiation through the atmosphere – passage of radiation through the atmosphere

The quantity and spectral composition of solar radiation on Earth change because various interactions occur during its passage. This means that a portion of the radiation is absorbed (substance absorption), and some of it is reflected back in the direction of radiation (reflectivity or albedo). Albedo depends on the wavelength of incident radiation.

During its passage through the atmosphere, which is composed of diverse layers at various altitudes, the radiation value depends on the current composition of the atmosphere. Different gases have distinct line absorption spectra. (Skok, 2020).

The Sun emits most of its energy at shorter wavelengths compared to Earth. Sunlight scatters on air molecules, particularly solar radiation. Blue and violet light have the shortest wavelengths in the visible spectrum.

In the scattering of sunlight, the violet component is weaker than the blue, and even the cells in the eyes (cones) are less sensitive to violet light, resulting in a blue sky. Light with longer wavelengths generally passes through the atmosphere with little obstruction. (Skok, 2020).

Solar radiation reaching the top of the atmosphere has the most energy in the visible spectrum (0.4 to 0.75 μm) around 46%, approximately the same in the IR range (between 0.75 and 24 μm), and around 7% in the UV part of the spectrum (between 0.2 and 0.4 μm). (Jože Rakovec, 2017). Gases present in the atmosphere absorb specific spectra of light with different wavelengths. In the upper parts of the atmosphere, all UV radiation is absorbed, and there are significant absorbers in the IR range such as CO_2, water vapor, and ozone.

Substances absorb electromagnetic radiation most strongly at frequencies that match their own resonant frequencies. (J.Strnad, 1998). The absorption of radiation flux density at a specific wavelength depends on the density of the absorbing gas and the path length that light travels through the substance. The decrease in radiation flux density is described by Beer's law, defining the reduction in energy flux in a layer of thickness ds.

$$dj' = -j' \cdot k \cdot \rho \cdot ds. \tag{5}$$

Equation (5) gives the change in light flux density (j'), which depends on density (ρ) and the absorption coefficient of the substance (k). The equation is valid when radiation falls on the substance from only one direction and doesn't consider scattering and emission within the substance. Equation (6) is a differential equation, and if we divide both sides by j' and integrate:

$$\int_{j0}^{j} \frac{dj'}{j'} = -\int_{0}^{s} k \cdot \rho \cdot ds'. \tag{6}$$

The integral on the right side represents the optical thickness (τ). Integrating the equation yields the solution to the differential equation:

$$\ln\left(\frac{j}{j_0}\right) = -\tau, \tag{7}$$

which results in the Lambert-Beer law:

$$j = j_0 \cdot e^{-\tau}. \tag{8}$$

Since the Earth rotates around its axis, the solar zenith angle (β) is important for the passage of radiation, elongating the light path through the atmosphere by an angle of $1/cos\beta$, where β represents the angle of deviation of the incident light from the zenith.

In this case, considering the angle β and replacing ds with dz, equation (8) takes the form:

$$j = j_0 \cdot e^{-\frac{\tau zen}{cos\beta}}. \tag{9}$$

Modeling the problem and fieldwork – experiment design

Assuming the presence of CO_2, O_2, H_2O (water vapor), and ozone (O_3) in the atmosphere. Carbon dioxide is uniformly distributed throughout the atmospheric thickness,

while this cannot be said for ozone. Water vapor is more prevalent in lower layers. Gas distribution is changing, non-uniform, and complicated.

Calculating the radiation reaching the ground is extremely complex – we need to know the gas distribution in a narrow region.

Modeling the issue emphasizes that the atmosphere is homogeneous everywhere, the Earth moves around the Sun in a circular orbit, and the year has 365 days.

Modeling is easily performed using the Python programming language, correlating physics, computing, mathematics, and experimentation. The experiment becomes more complex and interesting. The changing solar altitude (declination) is explained as follows:

The Earth's axis is inclined by $\delta_0 = 23{,}44°$ with respect to the normal of the plane of Earth's orbit around the Sun, causing the solar declination (δ) to change over the year. Notably, it reaches its maximum value on June 21st during the summer solstice $\delta = \delta_0 = 23{,}44°$ (the Sun then crosses the local celestial meridian at its highest point in the sky), and its lowest value on December 21st during the winter solstice, $\delta = -\delta_0 = -23{,}44°$ (the Sun then crosses the local celestial meridian at its lowest point in the sky).

The changing declination over the year can be approximately estimated for any day of the year (N) with the equation:

$$\delta = \delta_0 sin\left(\frac{360°}{365\ day}(N - 81\ day)\right) \tag{10}$$

Considering that the year has 365 days and that January 1st is N = 1. This equation fairly accurately determines the maximum ($\delta = \delta_0,\ 21.\ junij\ N = 172$) and minimum ($\delta = -\delta_0,\ 21.\ december\ N = 355$) declination. However, due to the eccentricity of Earth's orbit around the Sun, deviations occur during the spring and autumn equinoxes. Additional corrections could enhance the equation, but it's sufficiently accurate for estimating declination. (Grubelnik, 2013)

The equation for calculating the Sun's height above the horizon also includes the solar hour angle Ω due to the Earth's rotation around its axis. If we consider that the Earth rotates around its axis in 24 hours, we can write the solar hour angle.

$$\Omega = \frac{360°}{24h}(T - 12h) \tag{11}$$

where T = local time (for our region, this is Central European Winter Time). It's worth mentioning that this equation only roughly provides the solar hour angle since the Sun doesn't cross the local celestial meridian at 12 h throughout the year. For a more accurate calculation, equation 13 should also consider the changing speed of Earth on its orbit around the Sun and the influence of Earth's axial tilt toward the plane of the ecliptic, which we know as the equation of time (T_ε).

If we also consider the influence of time zones, we can write:

$$T = T_L + \left(\Delta T_G - \frac{24\ h}{360°}\lambda\right) + T_\varepsilon \tag{12}$$

where λ is the longitude of the observation location, and ΔT_G is the difference between local time and time at the prime (Greenwich) meridian, which is 1 hour in winter and 2 hours in summer. (Grubelnik, 2013).

The Sun's position in the sky can thus be determined using the equations:

$$sin\gamma = sin\delta sin\varphi + cos\delta cos\varphi cos\Omega \tag{13}$$

$$sin\vartheta = \cos\delta \, sin\Omega \, / cos\gamma \tag{14}$$

where γ is the solar altitude angle above the horizon, and ϑ is the solar azimuth angle relative to the south. (Grubelnik, 2013)

Modeling in Python is based on equations 13 and 14, along with the source code in Python (Fig.1).

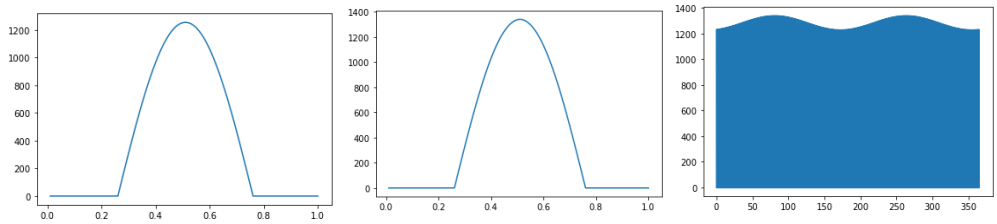

Figure 1. Variation of j at the top of the atmosphere on the 121st day of the year and on January 1st. Variation of j throughout the year (from January 1st to December 31st).

This represents Earth's energy output at the top of the atmosphere. The fluctuation in illumination and the changing energy flux throughout the year are depicted in diagram 2.

During the equinoxes, the day and night are of equal length. The spring equinox occurs around March 20th, and the autumn equinox around September 20th. In the upper graph, the value of the solar constant is highest at these times. This occurs around the 81st day of the year and around the 260th day of the year.

Conversely, during the winter solstice, when the day is shortest on December 21st (the 355th day of the year), and during the summer solstice (when the day is longest) around June 21st (around the 170th day), the value of the solar constant is lowest.

The cause is Earth's axial tilt of 23.27°. The northern hemisphere is tilted away from the Sun during winter. Then Earth is closer to the Sun, and conversely, during summer, Earth is tilted towards the Sun and is on the other side of the Sun – resulting in summer in the northern hemisphere.

In modeling, we base our approach on Earth's motion along an ideal circle.
The model considers:

- Variation of the declination angle throughout the year (variable β)
- Variation of j throughout the year
- Variation of j throughout the day

EXPERIMENTAL DETERMINATION OF J USING THE INTERFACE AND PIRANOMETER FROM VERNIER

Every teacher is an autonomous practitioner who, according to their beliefs and abilities, teaches. The methods they use in the educational process and the extent to which they use them is a matter of their judgment.

The purpose of the experiment is to prove laws, explain relationships between quantities, and inspire students to engage in research activities. Through a simple experiment measuring the solar energy flux, we encounter multiple layers of problem-solving in entirely different fields of science. Natural sciences knowledge, as a fundamental discipline (ranging from astronomy, mathematics, physics, chemistry, biology, and more), interweaves here, and the role of the teacher, the practitioner, is crucial.

Before conducting the experiment, it's essential to clarify concepts: solar declination, Earth's rotation around its axis (rotation), Earth's motion around the Sun (revolution), time definition, absorption, diffusion, energy, light flux, etc.

Experimental tools (Fig.2).

- Pyranometer (Vernier) – a sensor for measuring surface radiation
- Vernier LabQuest interface
- Pyranometer stand

Measurements were conducted using a specialized sensor for measuring solar radiation and the Vernier interface. The sensor measures the quantity and transmits it to the interface, which stores the data. The data is processed using the LoggerPro software (Fig.3).

Figure 2. Vernier Interface and Pyranometer

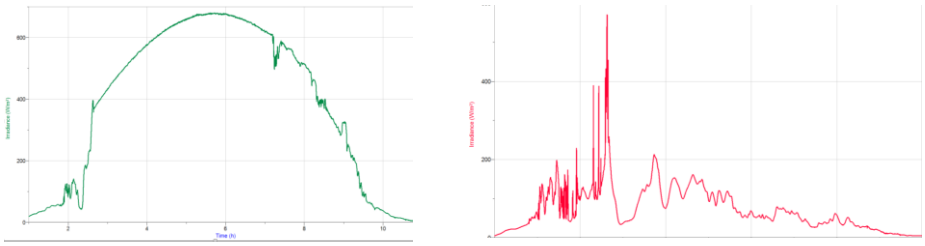

Figure 3. Comparison of Energy Input to the Surface (Sunny, Rainy Day)

The comparison of two measurements illustrates a sunny and rainy day and their energy output. It's also necessary to define energy loss in the atmosphere. The graphs clearly show that there are energy-related processes occurring within the atmospheric layers. The experiment is supported by visual material.

Measuring the composition of the atmosphere (which gases are currently present) is extremely challenging, as it requires a meteorological balloon to measure the atmospheric composition, winds, and air pressure at a specific altitude. These measurements are conducted locally and are limited by time.

Before the balloon reaches higher altitudes, parameters in the lower layers can quickly change. This demonstrates that weather phenomena influence the flow of energy through the atmosphere. When observing the weather, we often rely on qualitative observations - if there are many clouds, it indicates higher humidity, and consequently, the influx of energy through the atmosphere due to water vapor is hindered.

CONCLUSION

Physics and natural science education must cater to the upcoming generations. Currently, the Generation Z is departing from our elementary school system. The characteristics of this generation are well-known (Sterkuš, 2021). The teacher plays a vital role in fostering interaction with the students during experimental work. They explain the importance and purpose of the experiment, citing examples from everyday life, describing them, and encouraging students to recognize their own experiences. This approach stimulates student activity and curiosity. By attaching other content to the experiment, the teacher creates a mosaic of knowledge synthesis that students must process and internalize. The teacher guides and directs students toward the goals.

The use of sensors transforms the significance of experimental work for students. Through formative monitoring, we can observe their progress. Their achievements are more easily evaluated, leading to assessment. By involving students in the process, they become co-creators of learning, able to assess their achievements in comparison to others. The teacher adjusts the dynamics of teaching based on feedback and insights gained from students during the teaching process (Sterkuš, 2021).

REFERENCES

1. Klemen, B. Obtined from: https://slideplayer.com/slide/14111410/.
   Eurostat. Electricity sector analysis. Obtined from: https://ec.europa.eu/eurostat/statistics-explained/index.php?title=Electric_vehicles_and_energy_generation_statistics#Electricity_sector_analysis [Online, accessed 14. 8. 2023]
2. Grubelnik, V. (2013). Višina Sonca nad obzorjem. Astronomi v Krnici, 6-7.
3. Strnad, J. (1998). Fizika 1.
4. Rakovec, J. and Vrhovec, T. (2017). Osnove meteorologije. Ljubljana: DMFA.
5. Skok, G. (2020). Uvod v meteorologijo. DMFA.
6. Sterkuš, R. (2021). Vrednotenje fizikalnih vsebin v osnovni šoli za generacijo-Z. EDUVISION.
7. Gimnazija Šentvid. Astronomija. Obtined from Sevanje Sonca: http://www2.arnes.si/~gljsentvid10/spekter.html [Online, accessed 14. 2. 2019]

8. Zaplotnik, Ž. Razumeti podnebne spremembe. Pridobljeno iz: https://www.alternator.science/sl/daljse/razumeti-podnebne-spremembe/ [Online, accessed 15. 2. 2021]

Conference Proceedings
ICPAE 2023, 24th August – 26th August, Zrenjanin, Serbia
University of Novi Sad, Technical Faculty "Mihajlo Pupin", Zrenjanin

Assessment of Experimental Skills and Physics Knowledge of Students at Measuring Albedo

Robert Sterkuš[1], Robert Repnik[1*]

[1]*Faculty of Natural Sciences and Mathematics, University of Maribor, Koroška cesta 160, 2000 Maribor, Slovenia*
robert.repnik@um.si

Abstract. Physics is experimental science; consequently, also the physics teaching in schools should include experimental work. It develops skills and attitudes, not only physics knowledge. It is great challenge for the teacher, how to assess student's results at experimental work. In this contribution we present an example, how this could be done. We prepared experiment, where we measured reflected light with light intensity sensor and calculated albedo. In addition, we measured energy absorption with temperature sensor in different samples. The absorbed energy of the sun light on earth depends among other factors also of albedo of different surfaces on the planet and can implicate the temperature changes in different areas and globally. This experiment is adequate for physics courses on different levels of education and helps the students understand the influence of light irradiance, light reflection due to albedo and other factors in the process of climate changes.

Keywords: albedo, energy absorption, exploratory experiments, physics teaching

INTRODUCTION

Experimental work with interfaces and sensors opens new chapters in teaching and learning natural laws. Wireless sensors are available on the market today, enabling even higher-quality experimentation. Software applications are on phones and tablets. The experiment becomes interesting, modern, and attracts students to independent work. The experiment should be exploratory. Students are creative in experimental work, using and learning scientific methods, discovering, being curious, focused, precise, and doubt about the success of the experiment must always be present.

- Evaluation or assessment of experimental work involves the following phases:
- Readiness for the experiment,
- Measurement execution: handling equipment and measuring instruments,
- Data work: precision and systematic handling of measurements,
- Interpretation of results.

Example experiment: Measuring reflectance and experimentally determining albedo. In the example, the evaluation method is also described.

PHYSICS THEORY

Solar energy is electromagnetic radiation emitted by the Sun into space. This energy travels through a vacuum and reaches the Earth in the form of sunlight. When solar rays reach the Earth, they encounter various interactions and processes that influence the passage of energy through the atmosphere. Some key concepts related to energy transfer include albedo, Earth's temperature, absorption, and physical laws.

Albedo is a measure of surface reflectance. It represents the ratio of reflected solar light to incident solar light on a specific surface. High-albedo surfaces reflect more solar light back into space, while low-albedo surfaces absorb more solar light. For example, a snowy landscape has high albedo, while a dark asphalt road has low albedo.

When solar rays reach the Earth, some of the energy is absorbed in surface layers such as soil, oceans, and plants. This absorbed energy is converted into heat, causing a rise in Earth's temperature. The heat is then emitted back into the atmosphere in the form of infrared radiation.

The atmosphere plays a crucial role in energy transfer through Earth's atmosphere. Some solar energy is scattered from particles in the atmosphere, a phenomenon known as scattering. The atmosphere also contains various gas molecules such as carbon dioxide, methane, and water vapor, which absorb some of the infrared radiation emitted by the Earth. This process is called absorption. Absorption of infrared radiation contributes to atmospheric warming.

Physical laws influencing energy transfer through the atmosphere include laws of reflection, refraction of light, and laws of radiation. The law of reflection states that solar rays are reflected from surfaces at specific angles, depending on the surface properties. The law of refraction describes how light bends when passing through different media, such as air or water.

Laws of radiation include Planck's law of radiation, which describes the spectral distribution of electromagnetic radiation energy based on the source's temperature, and Stefan-Boltzmann's law, which describes the amount of energy emitted by an object based on its temperature. The proportion of energy reflected and absorbed by a surface (material) depends on albedo.

In accordance with the principles of thermodynamics, energy is conserved during passage through the atmosphere. Solar energy reaching the Earth can be reflected, scattered, absorbed, and re-emitted as heat. Interactions between the Sun, atmosphere, and Earth are complex, involving multiple processes and factors influencing energy transfer through the system.

In the wave spectrum of electromagnetic waves (which is what light is), light from 290 nm to 4000 nm is ecologically very important. The area of the visible part of the light spectrum (400 nm – 800 nm) is especially important.

Experimental Approach

Texture and color of the Earth's surface affect albedo, determining how much solar radiation is reflected, which in turn affects how much radiative energy or heat is absorbed at a given location. A high-albedo surface reflects a lot of solar radiation, while a low-albedo surface reflects very little.

As the Earth's surface is composed of various colors and textures, it heats unevenly. Snow, ice, and clouds reflect a lot of solar radiation back into space, while green forests, plants, and exposed soil absorb solar radiation. You can experience the albedo effect yourself on a sunny day by wearing light or dark clothing. Would you feel cooler if you wore a light or dark shirt on a hot, sunny day?

In this experiment, we will explore the relationship between the albedo of different surfaces and the change in temperature due to energy absorption. Using a light sensor, we will measure the amount of light reflected from paper of various colors and calculate the percentage of reflectance. We will also measure the change in air temperature beneath the surface due to energy absorption using a temperature sensor.

Objectives

Using a light sensor, measure the amount of light reflected from different color pieces of paper.
Calculate the albedo of different surfaces.
Using a temperature sensor, measure the amount of absorbed energy for each sample.

Tools for Experimental Work:

- Vernier - light intensity meter
- Vernier - temperature sensor (surface)
- LabQuest interface
- LabPro program and computer
- Blank A4 paper

Stand and 100 W lamp, plastic container with white interior (e.g., ice cream container).
Different samples: colored sheets, grass, sand, soil, clean water, dirty water, etc.
Course of work:

1. Assemble the apparatus as shown in Figure 1.
2. The sensor for measuring reflected light should be no more than 10 cm above the samples.
3. Connect the sensors to the application.
4. Set the measurement time to 3 minutes.
5. Turn on the light and begin the measurement.
6. After completing the measurement, save the data and turn off the light.
7. Place leaves of different colors on the thermometer and measure the amount of light that is reflected.
8. Also measure the temperature.
9. Place sand, soil, ... on the thermometer, making sure the thickness is the same (Fig.2).

Figure 1. Experiment – albedo, senzors (Vernier, 2023)

Enter the data into the table (Tab. 1.):

Table 1. Different substances

Sample	Initial T(°C)	Final T(°C)	ΔT(°C)	Total radiation (lux)	Reflected light (lux)	Percentage of absorbed light
Sand						
Soil						
Grass						
Pure						

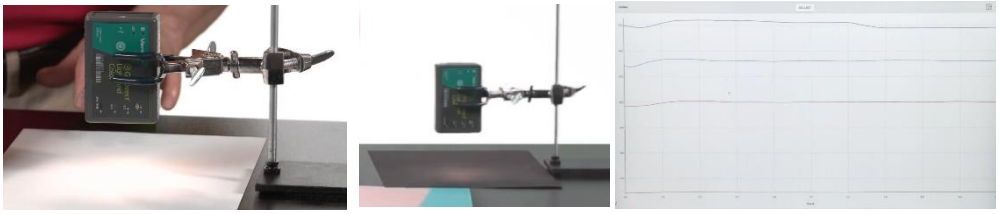

Figure 2. Measurement of illumination and different values of reflection (Vernier, 2023)

Discussion

Why does dirty water heat up more than clean water? How about the sea? Influence of algae and organisms in water on temperature, ocean currents. Urban heating, Earth's warming? – possibilities for broader discussion with students and differentiation, formative monitoring.

Evaluation of Experimental Work

Experimental work begins long before entering the classroom, laboratory, or selected natural location. Preliminary preparation for the work partly takes place during physics classes, while the majority is done by students at home through careful study of prepared instructions. At the start of the experimental work, we evaluate the student's readiness for the experiment by reviewing notebooks and asking questions to verify:

- Whether the student has written a summary of the experiment and created a work plan in the notebook
- Whether the student knows the theoretical foundations of the subject matter related to the experiment,
- Whether the student understands the instructions for conducting the experiment and measurements.

When evaluating the skills of experimental work, the most demanding phase is the execution of measurements. In the data analysis phase, students need a calculator and geometric tools. Without these tools, high-quality data analysis is not possible.

When scoring, we take into account:

- Systematic and clear collection of data and measurement results
- Drawing graphs and graphical procedures,
- Accuracy of measurements and calculation of errors,
- Form and organization of the laboratory report,
- Accuracy of results and answers to simpler questions.

In the final phase of interpreting the results, students are expected to:

- Identify the relationship between the quantities measured in the experiment,
- Relate observed quantities to appropriate physical laws,
- Provide appropriate comments on the results of the experiment,

The teacher writes the student's name in the right column of the table. The criteria are written in the left column. The critera are: Theoretical foundations, Understanding of instructions, Experiment execution, Assembly of the experiment, Choice of sensors and measurement range, Reading measurements, Use and handling of elements (safety), Working with data, Clarity and systematic collection of data, Graphical procedures, graph drawing, Observance of measurement accuracy, Form and organization of experiment notes, Accuracy of results and answers, Interpretation of results, Evaluation of results and measurement procedures, Discussion, argumentation, connection with theory, Grade.

Evaluation scale and criteria are presented in Table 2.

Table 2. Evaluation scale and criteria – measurement execution

Evaluation category	Evaluation		
	0 points	3 points	5 points
Plan for work	He or she didn't prepare for the exercise.	He or she prepared properly for the exercise.	He or she prepared perfectly for the exercise.
Theoretical foundations	Does not know the theoretical foundations of the learning topic with which the exercise is connected.	He or she knows the theoretical basics, but he does not understand some of the work.	Knows and understands well all the theory with which the exercise is connected.
Comprehension of instructions	Does not understand work instructions. He only completes the exercise if the instructions are fully explained to him.	He needs additional instructions for individual parts of the exercise.	Understands all instructions well.
Assembling tripod accessories	He cannot assemble accessories without help. He does not know the terms for individual parts of the accessory.	He only needs help with some tasks, he does most of the work himself.	He does not need help when assembling the gadgets
Selection of meter and measurement range	He does not know how to choose the appropriate meter and the appropriate range.	Selects the appropriate meter, but has difficulty selecting the appropriate range.	Selects the appropriate meter and the appropriate measuring range.

Reading measurements	On a meter with several scales, he cannot choose the right one, he cannot read decimal places from the scale.	It selects the appropriate scale, but the reading of decimal places is defective.	He chooses the appropriate rock and takes the correct reading from it.
Using sources of voltage, heat...	When using sources, he does not follow the safety and technical instructions for working with the source. He does not know how to handle the origin independently, comprehensive and permanent supervision is necessary.	When using the sources, it takes into account most of the safety and technical instructions. Can handle selection but needs advice or supervision.	It fully complies with the safety and technical instructions for working with sources. He handles them completely independently and does not need supervision.
Systematicity and transparency of sample collection	He is unable to write down samples in an orderly manner. He can't find his way from the notes, he needs additional information from classmates or the teacher. He lacks data for further work.	The measurements are arranged, but there is no visible system. Less important data about the experiment is incompletely collected, prefixes or units are missing from the data.	The measurements are systematically arranged, e.g. in descending or ascending order, prefixes and units are written.
Graphic procedures, working with graphs	When drawing graphs, he does not follow the rules about proportions and axis marking, the scale of the graphs is untidy, he does not mark measurements with visible marks, he cannot comment on or read graphs.	The graph is drawn in accordance with the rules, takes into account the proportions when drawing graphs, indicates scales on the axis and correctly writes the values of individual measurements. Has trouble reading intermediate values from graphs.	He has no problem drawing and analyzing graphs. Follows all instructions for transparent drawing of graphs and for their analysis.
Taking into account the accuracy of measurements	Measurements cannot be recorded with an accuracy rating. It is wrong in determining the characteristic places and in calculating the absolute and relative error. He does not know the rules for calculating with imprecise quantities	Records the measurements with an accuracy rating. Needs advice on writing characteristic places, knows how to estimate absolute and relative error, but has trouble with imprecise quantities.	He writes down the measurements with an accuracy assessment, follows everywhere the rules for determining characteristic places, writing with exponents and determines the absolute and relative error of the measurement. Follows the rules for calculating

			with imprecise quantities.
Format and organization of the report	The exercise is processed superficially, it is opaque and illegible. Graphs are of inappropriate dimensions.	The exercise has the required systematics and content. It has been corrected and deleted in some places. The tables are not equipped with units, the graphs do not have a marked axis...	The exercise is flawlessly processed. Tables and graphs are complementary and are correctly labeled and completed.
Correctness of results and answers	Most of the results are not correct, the answers to the questions are incorrect or incomplete.	Most of the results and answers are correct.	The answers and results are correct.
Evaluation of results and measurement procedures	The exercise does not contain comments on the results and measurement procedures, or the comments are incomplete or without content.	The commentary is poor in content and only covers the main points of the exercise superficially.	The commentary is rich in content, discusses the goals and procedures of the exercise, and compares individual results with predictions.rezultate z napovedmi.
Connection with theory	From the exercise and comments, there is no sense of knowledge and connection with theory.	In the commentary, he only superficially compares results and procedures with theory. He is content with commenting on individual graphs and equations.	The commentary provides a comprehensive analytical overview of the theoretical background and predictions. He looks for the causes of unusual results, comparing them with predictions.

CONCLUSION

Physics and natural sciences education must cater to the upcoming generations. Currently, Generation Z is departing from our elementary school system. The characteristics of this generation are known (Sterkuš, 2021). The teacher guides interaction with students during experimental work. The significance and purpose of the experiment are explained. Everyday life examples are listed, described, and students are encouraged to recognize their own experiences. This stimulates students' learning activity and curiosity. The teacher

guides interaction with students during experimental work. The significance and purpose of the experiment are explained. Everyday life examples are listed, described, and students are encouraged to recognize their own experiences. This stimulates students' learning activity and curiosity. Additional content is tied to the experiment, which the student must process and acquire to piece together a mosaic of knowledge (synthesis). The teacher should guide and lead students towards achieving goals.

By using sensors, the meaning of experimental work is transformed for students, and with the help of formative monitoring, we can see how they progress. Their achievements can be assessed more easily and consequently graded. Students are included in the process, allowing them to co-create the learning process and evaluate their achievements compared to others. The teacher adjusts the dynamics of teaching based on feedback and insights gained from the teaching process with students.

REFERENCES

1. Sterkuš, R. (2021). Vrednotenje fizikalnih vsebin v osnovni šoli za generacijo-Z. *EDUVISION*.
2. Toman, I. Zavod Republike Slovenije za šolstvo. https://www.zrss.si/digitalnaknjiznica/izzivi-razv-vred-znanja-gimn-FIZIKA-CD/vsebina_gim2/G2_1_poglavje/G2_1_03/ocenjevanjevescineksperimentalnegadela.pdf, [Online, accessed 14. 7. 2023]
3. Vernier. *Vernier*. Pridobljeno iz Vernier: https://www.vernier.com/experiment/hsb-cm-e-2_investigating-albedo/ [Online, accessed 14. 7. 2023]

Conference Proceedings
ICPAE 2023, 24th August – 26th August, Zrenjanin, Serbia
University of Novi Sad, Technical Faculty "Mihajlo Pupin", Zrenjanin

Recent Progress and New Approach in Numerical Modelling of Airborne Sub-pollen Particles

Zoran Mijić[1*], Slobodan Ničković[1,2], Luka Ilić[1,3], Slavko Petković[2], Goran Pejanović[2], Alfredo Huete[4]

[1]Institute of Physics Belgrade, Pregrevica 118, Belgrade, Serbia*
[2]Republic Hydrometeorological Service of Serbia, Kneza Višeslava 66, Belgrade, Serbia
[3]now at Barcelona Supercomputing Center, Plaça Eusebi Güell, 1–3, Barcelona, Spain
[4]A School of Life Sciences, University of Technology Sydney, Sydney, Australia
zoran.mijic@ipb.ac.rs

Abstract. Thunderstorm asthma (TA) events refer to the outbreak of severe asthma attacks caused by favorable environmental conditions producing a high concentration of pollen ruptured fragments. Intact pollen grains entrained by updrafts into a thunderstorm might be ruptured releasing many sub-pollen particles (SPPs). These SPPs remain suspended in the air for several hours after the storm and can be transported to the ground level triggering TA outbreaks. Predicting of TA occurrences has priority for the regions with frequent thunderstorms and should involve the pollen forecasting systems with included SPPs production and dispersion. In this paper recent progress in developing a new numerical model DREAM-POLL introducing novel parameterization scheme for production of sub-pollen particles is presented. The model is tested for two pollen seasons when four largest decadal TAs occurred in Melbourne. The proposed modelling approach has potential to provide effective early warnings forecasting system for TAs applicable to different pollen types.

Keywords: particle rupturing, sub-pollen particles, extreme pollen episodes, asthma epidemic, early warning system

INTRODUCTION

Thunderstorm asthma (TA) episodes are an epidemic of acute asthma attacks caused by environmental conditions that might result in a high concentration of pollen fragmented particles staying in the air for several hours after a storm has passed [1]. It is hypothesized that intact pollen grains entrained by updrafts into a thunderstorm are ruptured, thus releasing sub-pollen particles (SPPs) with up to a thousand allergenic particles released from a single intact grain. High humidity, lightning, and extreme upwind streams are thought to produce pollen rupturing within convective clouds [2]. Thunderstorm downdrafts and outflows can transport these SPPs' respirable allergens to ground level, raising the danger of TA outbreaks. The medical evidence shows strong link between of the arrival of thunderstorm outflow and large increase in concentrations of ruptured pollen grains [3]. In regions with frequent thunderstorms, there can be increases of the attacks that put a strain in local hospitals and if not managed properly these attacks can be fatal. Obviously, there is a strong need for developing a forecasting system capable to issue early warnings for

such TA events, but accurate predicting of TA occurrences has been extremely challenging task over the last decade. To address the missing SPPs in most existing pollen forecasting systems, we developed DREAM-POLL, a numerical model that forecasts not only the airborne intact pollen process but also the production and dispersion of allergenic SPPs released from ruptured pollen grains [4]. In this paper we explain the progress made in pollen modeling related to parameterization scheme for production of SPPs and present the results of model tests on pollens seasons during TAs occurred in Melbourne, Australia.

METHODOLOGY

DREAM-POLL is an Euler-type model in which prognostic pollen concentration equation is embedded on-line into a high-resolution non-hydrostatic weather prediction model. It represents a modified version of the DREAM regional dust aerosol atmospheric model [5], to mathematically describe the major phases of the atmospheric pollen cycle, including the emission of pollen, vertical and horizontal transport, and pollen turbulent mixing and deposition. The model domain in this study covers the southwestern region of Australia, and there are 28 model vertical levels spanning from the surface to 50 hPa with the horizontal grid resolution of approximately 5 km. The model was run over the pollen season periods of 15 October - 15 December 2010 and 2016. The initial and boundary conditions for the atmospheric model component were specified using weather prediction parameters of the European Centre for Medium-range Weather Forecast (ECMWF) global model. The major pollen-related input to the model is geographical distribution of grass pollen sources specified using the Australian Land Use and Management (ALUM) 50 m gridded data [6]. The pollen fraction in the model grid box is calculated as a mean value of ALUM fractions belonging to this grid box and the intensity of the emission is made depended on near surface turbulent conditions. According to the Taylor-Jonsson hypothesis [2], intact pollen grains are lifted by convective updrafts and ruptured due to high humidity, wind force and electric charge effects in a thunderstorm cloud. After rupturing, a fraction of SPPs is released to the air after which the intact, the ruptured shells and SPPs continue their independent dispersion (Figure 1).

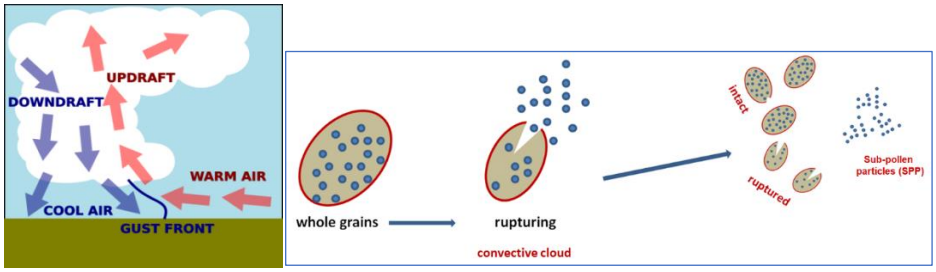

Figure 1. Conceptual scheme of convective circulation (left) and schematic description of the pollen rupturing process in convective clouds, as parameterized in DREAM-POLL (right).

The initial version of the rupturing process parameterization in the model was associated with the lower threshold of relative humidity (RH) of 60% when rupturing began [7], where SPP concentrations vary from ~1.000 to 10.000 grains m^{-3} for RH>60%. After strong link between convective instability and TA occurrence has been recently demonstrated [8], we

introduced a new parameterization for sub-pollen particles (SPP) production dependent on the convection instability parameter CAPE - convective available potential energy [4]. CAPE [Jkg^{-1}] is the parameter describing the overall convective features of thunderstorms and it is defined as the vertically-integrated air buoyancy

$$CAPE = \int_{LCL}^{EL} g \frac{T - T'}{T} dz \quad (1)$$

Here, g is the gravity acceleration; T and T' are temperature of the air parcel and temperature of the surrounding air, respectively; *LCL* is the lifting condensation level (the bottom of the convection cloud) at which an unsaturated air parcel reaches its relative humidity 100%; EL is the level at which the air parcel becomes as cool as the environment. The percentage of the intact pollen mass converted by convection to SPPs is defined by a function of CAPE with tunable parameters [4].

RESULTS

Although the event on 7 November 2016 was accompanied with a grass pollen intrusion over Melbourne there were no observed thunderstorm conditions. In contrast, 7 November 2010, declared as TA, was accompanying with a thunderstorm. Obviously, presence of intact pollen is necessary but not sufficient condition to trigger TA. Despite a relatively low observed number of intact pollens, convective conditions increased SPPs and triggered TA. There were two peaks of intact pollen concentrations observed in Melbourne during the 20-21 November 2016 period. During 20 November there were no significant ruptured pollen numbers recorded, which indicates that particle fragmentation did not occur under the prevailing stable synoptic conditions. However, on the 21 November both observations and model results show increased numbers of intact and ruptured pollen particles linked with the passage of the wind gust front. Significant increase in the observed ruptured-to-intact grain ratio after the front passage [9], was reproduced by the model as well (Table 1).

Table 1. 1 h and 4 h averages of observed and predicted ruptured/intact grain ratios before and after the squall-line front passage on 21 November 2016 at the Burwood observation site.

	Observed 1 h average ruptured/intact grain ratio	Predicted 1 h average ruptured/intact grain ratio	Observed 4 h average ruptured/intact grain ratio	Predicted 4 h average ruptured/intact grain ratio
Before front passage	0,55	0,73	0,56	0,32
After front passage	1,06	0,98	1,02	1,4

In order to further improve the model accuracy a new parameterization for SPPs production dependent on the CAPE was introduced and tested [4]. In Figure 2 vertical cross sections of pollen concentrations along the normal to the gust front obtained using different parameterization is presented. Overall, reliability of the intact pollen concentration prediction for the selected periods is reasonable but more importantly is that the model correctly reproduces the temporal dynamics of the observed intact pollen concentrations (for selected periods correlation coefficient reaches about R=0,8). In addition, since there are no routine daily observations of the respirable SPPs in Melbourne and elsewhere, the

available Melbourne hospital admission records for two pollen seasons 2010 and 2016 were used for model prediction evaluation. The results obtained for 2010 pollens season is presented in Figure 3.

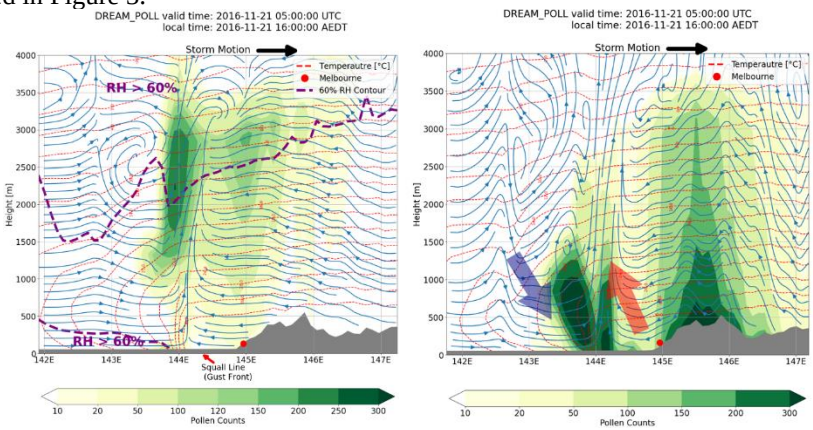

Figure 2. Predicted intact pollen concentration at 16:00 AEDT on 21 November 2016. Vertical cross sections along the normal to the front, with pollen concentration of 60% relative humidity (left) and CAPE used for SPPs parameterization (right).

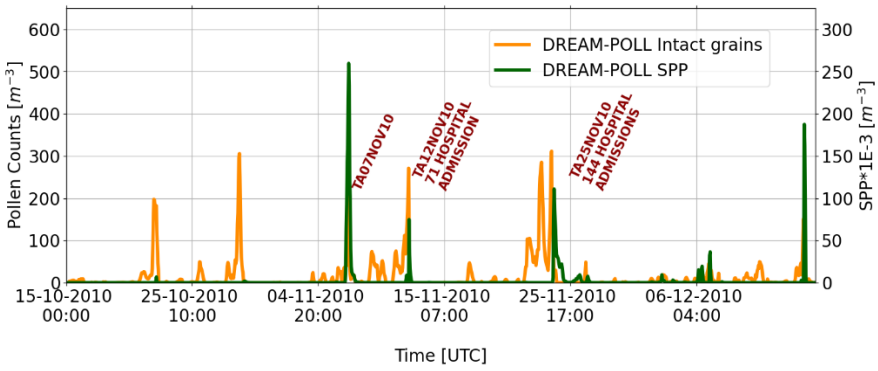

Figure 3. Temporal variation of predicted hourly intact and SPPs pollen concentrations for Melbourne during 2010 grass pollen season.

Numerous modelled intact pollen intrusions were not related to TA events, as evidenced by the data. For each of the four main Melbourne TAs, SPP increases are consistently anticipated at the same time. There is just one SPP maximum on December 14, 2010, which may be seen as a false alarm but not confirmed since we were unable to locate any medical documentation for this specific incident. The obtained results demonstrate that the new modelling approach has a very high potential for TAs events predictions.

CONCLUSION

Chronical asthma can be triggered under prolonged exposure of patient to pollen concentratios. However TA is related to acute asthma attacks occurring soon after a storm has passed. Many high pollen intrusions happening during the pollen season did not trigger TAs since no thuderstorms occured. Under favorable thunderstorm conditions even relatively low number of intact pollens can produce SPPs sufficiently high to provoke hospital admissions in short time. With its high success rate and adaptability to different geographical areas and pollen types the presented modeling approach, tested on major TA events happend in Melbourne, has potential to provide effective forecasting system for TAs early warnings. Developement a new measurement technique for routine respirable SPPs observations and addition systematic validation of the model results are needed.

ACKNOWLEDGEMENTS

The authors acknowledge Prof. Ed Newbigin and Jeremy Silver (the University of Melbourne, Australia) for supplying the pollen observation data and Dr. Elizabeth E. Ebert (Weather and Environmental Prediction, Bureau of Meteorology Melbourne, Australia) for useful discussions. L. Ilic and Z. Mijic acknowledge funding provided by the Institute of Physics Belgrade, through a grant by the Ministry of Science, Technological Development, and Innovation of the Republic of Serbia. Partial support has also been provided by the Republic Hydrometeorological Service of Serbia.

REFERENCES

1. Hughes D. D, Mampage C. B. A, Jones L. M, Liu ., Stone E. A, 2020, Characterization of Atmospheric Pollen Fragments during Springtime Thunderstorms, *Environ. Sci. Technol. Lett.* 7 409-414
2. Taylor P. E, Jonsson H, 2004, Thunderstorm asthma. *Curr. Allergy Asthma Rep.* 4 409-413.
3. D'Amato G, Vitale C, D'Amato M, Cecchi L, Liccardi G, Molino A, Vatrella A, Sanduzzi A, Maesano C, Annesi-Maesano I, 2016, Thunderstorm-related asthma: what happens and why, *Clin. Exp. Allergy* 46 390-396
4. Nickovic S, Petković S, Ilić L, Pejanović G, Mijić Z, Huete A, Marks G, 2023, Prediction of airborne pollen and sub-pollen particles for thunderstorm asthma outbreaks assessment, *Sci. Total Environ.*, 864, 160879
5. Nickovic S, Kallos G, Papadopoulos A, Kakaliagou O, 2001, A model for prediction of desert dust cycle in the atmosphere, J. Geophys. Res. Atmos., 106 18113-18129
6. ABARES, 2017, Catchment Scale Land Use of Australia http://data.daff.gov.au/anrdl/metadata_files/pb_luausg9abll20171114_11a.xml
7. Wozniak, M.C., F. Solmon, and A.L. Steiner, 2018, Pollen rupture and its impact on precipitation in clean continental conditions. Geophys. Res. Lett. 45 (14), 7156-7164.
8. Bannister T, Csutoros D, Arnold A.-L., Black J, Feren G, Russell R, Watson A, Williams S, Silver J. D, Hughes N, 2020, Are convergence lines associated with high asthma presentation days? A case-control study in Melbourne, Australia, *Sci. Tot. Environ*. 737 140263.
9. The Chief Health Officer's Report, 2017, The November 2016 Victorian epidemic thunderstorm asthma event: an assessment of the health impacts. Available at https://www.health.vic.gov.au/publications/the-november-2016-victorian-epidemic-thunderstorm-asthma-event-an-assessment-of-the

Conference Proceedings
ICPAE 2023, 24th August – 26th August, Zrenjanin, Serbia
University of Novi Sad, Technical Faculty "Mihajlo Pupin", Zrenjanin

Impact of Textile Industry on the Environment

Roohollah Bagherzadeh[1], Vasilije Petrovic[2*], Dragan Djordjic[3], Anita Milosavljevic[4], Marija Petrovic[5], Predrag Pecev[6]

[1]Institute for Advanced Textile Materials and Technology (ATMT), Textile Engineering Department, Amirkabir University of Technology, Tehran, Iran
[2,4] University of Novi Sad, Technical faculty „Mihajlo Pupin", Đure Đakovića BB, 23000 Zrenjanin, Serbia
[3]The Institute of General and Physical Chemistry, Studentski trg 12/V, Belgrade, Serbia
[5] University of Travnik, Faculty of Technical Studies, Aleja konzula br. 5, 72270 Travnik, Bosnia and Herzegovina
[6]Preschool Teacher Training and Business Informatics College of Applied Studies "Sirmium", Zmaj Jovina 29, 22000 Sremska Mitrovica, Serbia

bagherzadeh_r@aut.ac.ir,vasilije.petrovic1962@gmail.com

Abstract. The paper describes that today's social development guides an increasing focus on environmental protection as well as the causes that leave consequences on the environment. When talking about harm to the environment, the textile and clothing industry is usually not mentioned. That term is not as popular as, for example, the state impact of plastic, plastic bags, etc. However, the reality is different, as waste from the textile industry adversely affects the environment. Therefore, the paper analyzes the life cycle of textile products starting from design, development, production, distribution, use, maintenance, and up to its recycling or disposal. According to presented facts, the textile sector is the third largest source of water pollution and land use in 2020. On average, nine cubic meters of water, 400 square meters of land and 391 kilograms of raw materials are needed for the production of clothing and footwear per EU resident. It is estimated that dyeing and finishing processes in textile production are responsible for 20% of global water pollution. It is a fact that 2,700 liters of drinking water are needed to produce one cotton T-shirt. That is the amount that one person drinks in two and a half years. Synthetic clothing that is washed in household machines is responsible for 35% of primary microplastics released into the environment. One wash of polyester clothing can release 700,000 microplastic fibers that can end up in the food chain. The paper states that almost 26 kg of textiles are consumed annually and about 11 kg of textiles are thrown away per EU resident. Strategies to address these issues are also highlighted, including developing new business models for clothing rentals, designing products to facilitate reuse and recycling (a circular approach), persuading consumers to buy less and better quality clothing, and generally directing consumer behavior towards more sustainable options.

Keywords: textile, industry, ecology, product life cycle, recycling

INTRODUCTION

The textile industry anually generates 40 million tons of textile waste on the global level. Most of this waste is sent to landfills or is incinerated. On the other hand, the technological process of textile production consumes huge amounts of water, land and raw materials. Therefore, serious efforts are being made to move from the linear economy to closed-loop recycling. In this direction, special emphasis is placed on high-quality recycling, which would ensure that primary raw materials are reduced with recycled raw materials to a greater extent. This would, on the one hand, reduce waste as well as the production of primary raw materials, which has a large negative impact on the environment. Closed-loop systems tend to recycle materials constantly, after each technological process of production, i.e. discarding old clothes, so that textile materials theoretically remain in constant circulation. Textile production, if all activities in the value chain are considered, consumes more resources than many other sectors. Thus, in the countries of the European Union, the textile sector is the fourth largest consumer of primary raw materials and water (after food, housing and transport). All this considered, the reliance of the textile industry on synthetic fibers, which are based on fossil fuels in their raw material composition, also contributes to the unfavorable impact on the environment. This includes polyester, which is one of the most common textile fibers in the fashion industry today. Therefore, the negative impact of the textile industry on the environment is recognized at the global level, which has recently contributed to obtaining more quality proposals for solving these problems. This contributes to the significant development of closed-loop recycling processes that have the potential to limit textile waste and partially reverse the impact of fast fashion. Material recycling in the textile industry is not seriously represented. Today, less than 10% of recycled materials make up the global textile market. In that 10%, open-loop recycling products using PET (polyethylene terephthalate) bottle waste prevail. However, this is not a solution to make textile material from recycled bottles, because by recycling plastic bottles, new plastic bottles can be made in that area. Therefore, the textile industry must develop quality closed-loop recycling systems for its materials. For that reason, the Action Plan for the circular economy was adopted in the EU countries. This plan aims to ensure the application of circular economy principles to textile production, products, consumption and waste management. The EU Waste Directive Framework was also adopted, requiring countries to separate all textile waste by 2025. Several European countries have already implemented extended producer responsibility schemes, making brands and retailers responsible for post-consumer waste and requiring financial contributions from producers to collect, recycle and reuse products [1,2].

NEGATIVE IMPACT OF THE TEXTILE INDUSTRY ON THE ENVIRONMENT

The textile sector was the third largest source of water and land degradation in 2020. Textile products are diverse, and for this reason it is difficult to accurately determine their impact on the environment. Some estimates put it at 2% to 10% globally. It is estimated that this impact in the EU, caused by the consumption of textiles, ranges from 4 to 6%. Some reports for 2015 indicate that the global textile and clothing industry was responsible for the consumption of 79 billion cubic meters of water and produced 92 million tons of waste.

The same estimates say that by 2030, under a business-as-usual scenario, these numbers will increase by at least 50%.

In 2020, on average, the production of clothing and footwear per EU citizen required [2]:

- 9 cubic meters of water,
- 400 square meters of land and
- 391 kilograms of raw materials.

From these data, it can be seen that the textile industry is a large consumer of water. It is estimated that the global textile industry used 79 billion cubic meters of water in 2015, while the total consumption of the entire EU economy in 2017 was 266 billion cubic meters. For example, the production of 1 cotton T-shirt requires 2.700 liters of drinking water. That is the amount that 1 person drinks in 2,5 years [2].

It is estimated that textile finishing processes, mostly dyeing and finishing in production, are responsible for 20% of global water pollution.

Figure 1. Waste water as the result of the dyeing and finishing processes of textile [4]

In the textile industry, large amounts of water are used for various processes and stages. Therefore, we should expect different amounts and types of waste water, which is an important and significant burdening factor of negative impact on the environment. In the process of pre-treatment, i.e. preparation of raw fabrics and knitwear, various impurities are removed from textiles, starchy agents, various soaps and other auxiliary agents, which later end up in waste water. In the textile industry, the presence of large concentrations of salt and various surfactants is noted. You can also find various inks, solid varnishes based on water or latex that do not contain organic solvents, heavy metals, various detergents, softeners, etc. means that pollute the human environment to a greater extent. In the washing process, a washing solution is used that contains: soaps, surfactants, phosphates, various complex compounds, etc. During the preparation process for washing, the most common and largest part of waste water consists of fibers, oils, fats, waxes, mineral oils, starch-based scum, polyvinyl alcohol (PVA), polyacrylate, etc. The waste water that was created after the processing of textile material is characterized by the presence of dyes and optical bleaching agents, then washing agents, thickeners, phenols, aromatic compounds, etc. So, for example, in the processing of wool, the most significant water pollution occurs in the first stages of the process, i.e. while washing, boiling and rolling the wool. The biggest problem of these wastewaters are related to the disruption of the photosynthesis of aquatic

plants. This causes a significant increase of bacteria to the level of insufficient biological degradation, which has the effect of disrupting the ecological balance. In that area, the most problems are caused by waste water that carries with it large amounts of dye, used for dyeing textile materials [2].

Figure 2. Production plant for textile refining [2]

Clothes made of synthetic materials, which are washed in washing machines, are responsible for 35% of primary microplastics released into the environment. A single wash of PES clothing in washing machines can release 700.000 microfibers that can end up in the human food chain. Most microplastics from textiles are released during the first few washes, and fast fashion, due to its mass production, low prices and high volume sales, is responsible for many first washes [2].

NEGATIVE IMPACT OF PRODUCTION OF RAW TEXTILE MATERIALS

The cultivation of natural fibers as well as the technological procedures for obtaining chemical fibers have a significant negative impact on the environment. Cotton, whose use at the global level is around 43% of the total mass of all fibers, is considered particularly problematic. This is because growing cotton requires huge amounts of land, water, fertilizers and pesticides. It is a fact that natural fibers have a significant impact on the environment, with silk having a particularly harmful effect in terms of depleting natural resources. Cotton is a major contributor to water scarcity. Less commonly used natural fibers, such as hemp and flax, require less water, fertilizers and pesticides.

Polyester, according to its raw material composition, is a product of fossil fuels. It is therefore not biodegradable. Today, it is represented by about 16% in the total mass of all fibers used in the production of clothing. Its main advantages are that it consumes less water, it can be washed at lower temperatures, it dries quickly, and it hardly needs to be ironed. Its biggest advantage is that it can be easily recycled into new fibers of good quality. What is disadvantageous is that the clothes are not made from recycled textile materials, but from materials recycled from plastic bottles. [2]

Fibers from regenerated cellulose are represented in amounts of about 9% compared to the total amount of all fibers. Viscose, also known as rayon, is used most often. These fibers are made from wood. Therefore, they are also biodegradable, but the big problem is a sustainable source of cellulose, because it has doubled its consumption from 1990 to 2017. Otherwise, the production of all fibers is increasing, as can be seen from Picture 3.

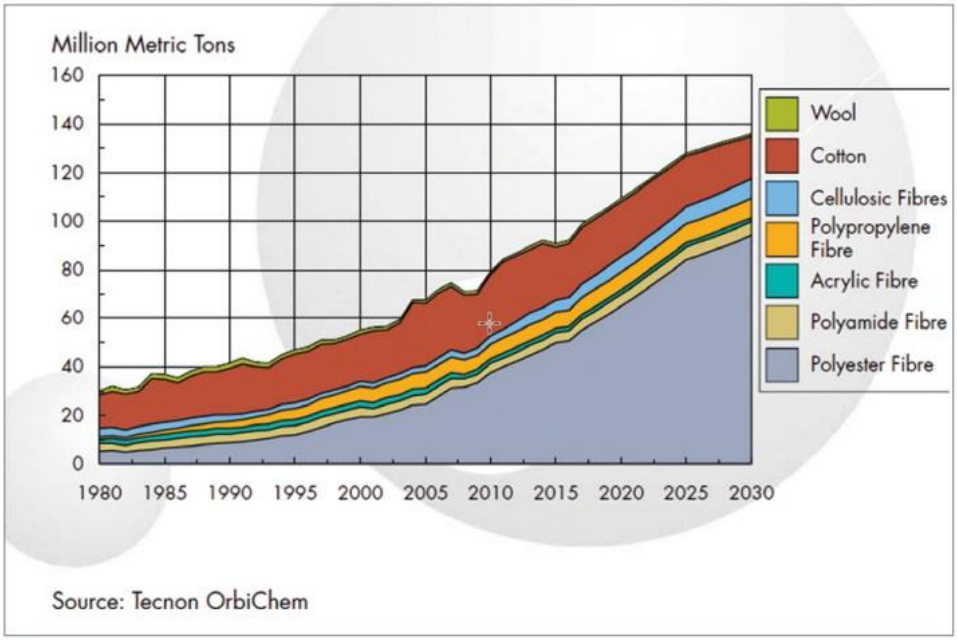

Figure 3. The global production of fibers in the period between 1980-2030 [2]

SUGGESTIONS FOR SOLVING THE PROBLEM

The textile industry is increasing its production to a large extent, and thus creating large amounts of waste and a negative impact on the environment. To solve these problems, new ways are recommended to reduce the impact on the environment in the processing and production phase, including reducing the consumption of chemicals, replacing them with enzymes, using color controllers and dyeing machines that require less water, and water recycling. Integral knitting is also recommended, where the entire garment is produced in one piece without the need for cutting and sewing. Some companies are experimenting with

new dyeing processes, such as using CO_2 as a dyeing medium instead of water. Others are experimenting with different material savings in tailoring, new cuts, computer-controlled pattern making tools to reduce fabric consumption, and so on [3-9].

We are also working on finding new raw materials. Emphasis is placed on organic cotton because it uses less water and causes less pollution. The share of organic cotton increased from 6% in the period from 2012 to 2013 to 19% in the period from 2016 to 2017.

Some proposals also go in the direction of bio based polyester (also known as biosynthetics). It is partly made from renewable resources such as starch and lipids from corn, sugar cane, beet or vegetable oils.

Further development is focused on lyocell fiber made from eucalyptus pulp, which grows quickly and requires no irrigation or pesticides. Bemberg fiber (cupro) is developed, which is made from waste cotton fibers.

One of the innovative processes was developed by the Technical Research Center of Finland and the Infinite Fiber Company. The environmental advantages compared to viscose production are: 98% less water is used and harmful chemicals such as carbon disulphide can be avoided [10].

Figure 4. Technical Research Center of Finland and Infinite Fiber Company [10]

The Textile and Clothing Research Institute from Hong Kong is working on solutions for textile recycling from fiber mixtures of different raw material compositions into new fibers and yarns through the hydrothermal process and biological methods [11].

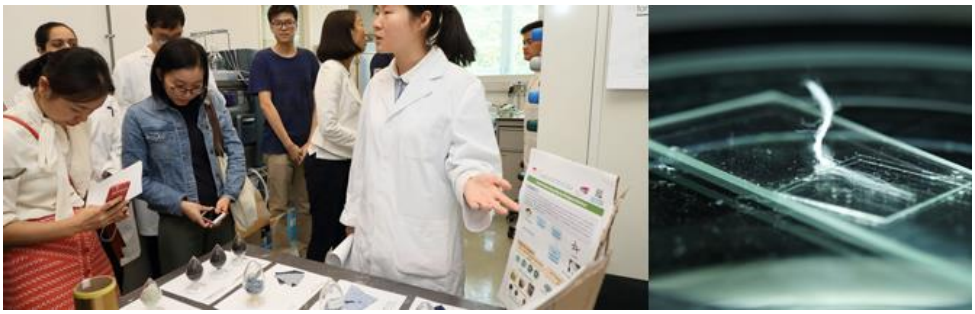

Figure 5. The Textile and Clothing Research Institute from Hong Kong [11]

Different strategies of dealing with the problem of textile waste usually include the following:

- development of new technologies for making clothes with less waste in production,
- designing products in a way to facilitate reuse and recycling (circular way),
- persuading consumers to buy less clothing, but of better quality (slow fashion),
- constant direction of consumer behavior towards more sustainable options
- development of new business models for clothing rental.

Strategies to tackle textile waste in the EU include:

- In 2022, a new strategy was launched to fight against fast fashion,
- supporting innovations for the production of textiles that will be more sustainable, with easy maintenance and easier recycling possibilities,
- new requirements of ecodesign for textiles,
- clearer product information – digital product passport
- encouraging companies to take responsibility for environmental protection.

Existing EU measures on textile waste are:

- Waste Directive - member states must obtain textiles separately by 2025.
- New measures to address the problem of the presence of hazardous chemicals and help consumers choose sustainable fabrics.
- Manufacturers who respect ecological criteria are allowed to mark their products with the EU Ecolabel, which guarantees the limited use of harmful substances and the reduction of water and air pollution,
- The Obzor 2020 program finances RESYNTEX, a project using chemical recycling, which could serve as a circular economy business model for the textile industry.

All these measures are necessary because less than 50% of clothes are reused for recycled, and only 1% is recycled (returned) into new clothes. In the period from 2000 to 2015, the production of clothing doubled, while the average use of clothing decreased. Europeans annually consume almost 26 kg and throw away about 11 kg of textiles.

Figure 6. Products made from recycled materials [2]

CONCLUSION

The textile industry generates 40 million tons of textile waste a year on a global level. Most of this waste is sent to landfills or is incinerated. On the other hand, the technological process of textile production consumes huge amounts of water, land and raw materials. Therefore, the textile sector is the third largest source of water degradation and land use in 2020. Today, less than 50% of used clothing is recycled or reused, and only 1% is recycled (returned) into new clothes.

New ideas are recommended to reduce the impact on the environment in the processing and production phase, including reducing the consumption of chemicals, replacing them with enzymes, using color controllers and dyeing machines that require less water, and water recycling. Closed processes of textile recycling into new textile products are still in development and have not reached the commercial stage, but they are intensively studied and work is being done on their application.

REFERENCES

1. V.Petrović, J.Stepanović, M.Stamenković, I.Skoko, S.Stefanović: „Životni ciklus i reciklaža tekstilija“, časopis Tekstilna industrija, 2011, vol.59, br. 3, str. 34-39.
2. https://www.eea.europa.eu/publications/eea-signals-2023, accessed 25.07.2023.
3. https://textile-platform.eu/ accessed 15.07.2023.

4. https://www.iamrenew.com/environment/bangladeshs-polluted-waters-rivers-dying-due-to-dyeing/, accessed 20.07.2023.
5. Vasilije Petrovic, Dragan Djordjic, Anita Milosavljevic, Marija Petrovic, Jelena Djukic: 4.0 Industrial Revolution in Clothing Production, Trends in Textile & fashion Design 5(4)-2023. LTTFD.MS.ID.000216. DOI: 10.32474/ LTTFD. 2023.05.000216.
6. V.Petrović, M.Gašović: Modna kolekcija, Tehnički fakultet „Mihajlo Pupin“, Zrenjanin, 2016., ISBN 978-86-7672-257-0, COBISS.SR-ID 299045383
7. V. M. Petrović, Tehnologija pletenja I deo, Univerzitet u Novom Sadu, Tehnički fakultet »Mihajlo Pupin«, Zrenjanin, Zrenjanin 2000.
8. Junyi Xu, Guoxiang Yuan, Vasilije Petrovic, John Wilson: Laser Engraved Batik Pattern in Garment Design, Symposium on the futures of sustainability: Tackling sustainability through academic and practitioner collaboration, 17 and 18 september 2022., Shanghai, China.
9. Yiran Feng, Guoxiang Yuan, Vasilije Petrovic, John Wilson: Gothic clothing design by using Laser engraving, Symposium on the futures of sustainability: Tackling sustainability through academic and practitioner collaboration, 17 and 18 september 2022., Shanghai, China.
10. https://infinitedfiber.com/ accessed 10.08.2023.
11. https://www.hkrita.com/ accessed 15.08.2023.

Conference Proceedings
ICPAE 2023, 24th August – 26th August, Zrenjanin, Serbia
University of Novi Sad, Technical Faculty "Mihajlo Pupin", Zrenjanin

Methods of Textile Waste Recycling

Xu Ming[1], Dragan Djordjic[2*], Vasilije Petrovic[3], Anita Milosavljevic[4], Marija Petrovic[5], Samir Pačavar[6]

[1] Glorious Sun School of Business and Management, Donghua University, Shanghai, China
[2]The Institute of General and Physical Chemistry, Studentski trg 12/V, Belgrade, Serbia
[3,4] University of Novi Sad, Technical faculty „Mihajlo Pupin“, Đure Đakovića BB, 23000 Zrenjanin, Serbia
[2,5,6] University of Travnik, Faculty of Technical Studies, Aleja konzula br. 5, 72270 Travnik, Bosnia and Herzegovina
xuming@dhu.edu.cn, ddjordjic@yahoo.com

Abstract. The paper discusses textile waste, which is most often classified as biodegradable nowadays. However, the paper points out that this classification is not appropriate. A large part of textile waste is biologically poorly degradable, such as: synthetic fibers, wool, surface-treated textile materials, fibers supplemented with composites, etc. The fact is that today the disposal of textile waste in landfills is increasingly limited. On the other hand, the burning of textile waste produces harmful gases for the environment. Therefore, the paper recommends the use of different methods of textile waste recycling. The paper analyzes the recycling of textile waste by two methods, mechanical and chemical. The current state of mechanical recycling, which represents the basic process for recycling textile materials, is described. It implies the mechanical deconstruction of textile materials in order to obtain multipurpose fibers and materials. The paper also shows some procedures of chemical recycling, which are not widespread, because the procedures are mostly in the stage of development of industrial application. The good quality of chemically recycled materials is also emphasized. At the end, possibilities for the use of recycled textile products in construction, automotive industry, agriculture, etc. are listed.

Keywords: textile waste, recycling, insulation, recycled products

INTRODUCTION

The textile and clothing industry is one of the world's largest and fastest-growing industrial sectors, thanks to the increase in population, the increase in consumption, the diverse application of textiles and greater productivity in mass production processes. With annual revenue of 1.3 trillion USD in 2016 [1]. In many industrialised countries however, clothing is now subject to fashion and style, which greatly reduces the time the clothing is used before disposal. While this rapid turnover is one of the key drivers for growth in the textile industry, this behaviour results in an overconsumption of clothing and an excessive use of resources and energy and is also significantly responsible for the generation of textile waste [2].

Annual production has nearly doubled since 2000, surpassing 100 billion units in 2015 with apparel consumption expected to rise 63% by 2030. This increase is partly due to the burgeoning fast fashion industry, which relies on shorter production cycles and style turnaround, often at lower prices, enabling a larger selection and choice for consumers [3].

Textiles mainly consist of fibres. The term fibre is a morphological term for materials characterised by their fineness, flexibility and high length to cross-sectional area [4]. While fibres can consist of a wide range of materials, they are usually classified as either man-made fibres or natural fibre, as seen in Figure 1. Natural fibres are both the hairs and wools of animals, and fibres from planted crops, such as cotton and hemp. The term man-made fibres refers to the process of manufacture and not the chemical composition of the material. For example, while cotton and viscose both are fibres consisting of cellulose, cotton is a crop fibre and therefore classified as a natural fibre, and viscose is a man-made fibre produced by the viscose process [5].

Figure 1. Categorisation of fibre types [4].

As a resource and energy intensive industry, the apparel sector's presence is far-reaching with associated environmental, economic, and social impacts across the value chain. Total fiber production in the global textile industry had increased by nearly 20% to 103 million tons between 2011 and 2017 [6].

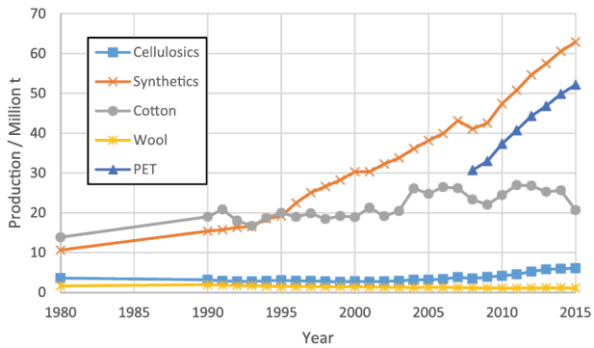

Figure 2. Global fibre production from 1980 to 2015 [7].

Global fiber production in 2016 was estimated to be 94,5 million tons, dominated by synthetic fibers (68,3%) –predominantly polyester (64%) estimated at 64,8 million tons, followed by cotton (22%), man-made cellulosic (6%), and animal-based fibers (1,5%- 80% wool, 20% down) Picture 3 [8].

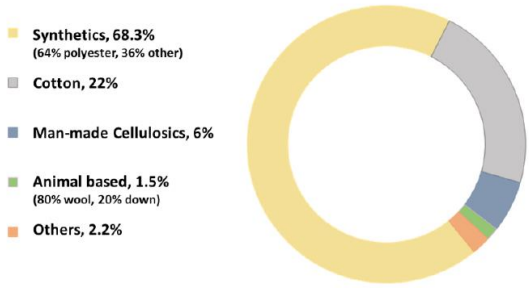

Figure 3. Global fiber production in 2016 [9].

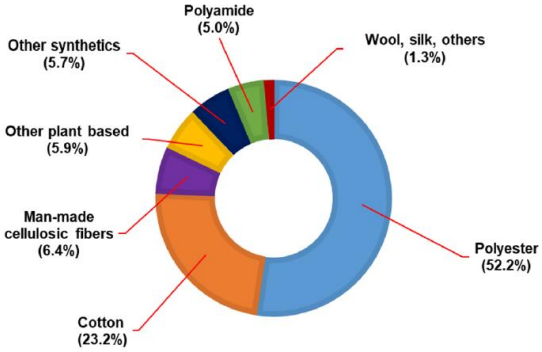

Figure 4. Global fiber production share in 2019 [10].

The textile and apparel industry is expected to increase its CO2 emissions by more than 60% (roughly 2.5 billion tons per year) by 2030 while also experiencing a 50% increase in freshwater consumption from 79 million cubic meters in 2017 [1].

Clothing and textiles contributed 6% to the world exports of manufactured goods in 2017; China and the European Union (EU) are the two leading regions for clothing and textile exports [11].

THE IMPORTANCE OF TEXTILE RECYCLING AND REUSE

The global trend of "fast fashion" leads to the mass production of cheap clothing in order to meet the needs of the market. From 2000 to 2015, the production of clothing almost doubled on a global level. The vast majority of clothing that reaches the market consists of cheap clothing products whose value ranges from 5 to 10 dollars on average and whose quality corresponds to the price at which it is sold.

Most often, these are products made from synthetic fibers and with a small percentage of natural fibers. The trend in Western countries is to throw away the wardrobe after only two or three uses. America is the largest exporter of textile waste, which consists of slightly used clothing. The clothes they export are bought by poor countries in order to resell them to second-hand shops for a few tens of cents.

The large amount of clothing that remains is of poor quality and is not even wanted by charities that supply poor and vulnerable populations with clothing. It is estimated that over 13 million items of clothing are thrown away in just one week in Great Britain, which is the second largest exporter of used textiles after the US. Most of the textile waste from Western countries ends up in the Atacama Desert of Chile. Every year, 39,000 tons of textile waste are throw away in this desert. On average, the amount of textile waste dumped in this desert is equivalent to one full truckload of waste every second and takes at least 200 years to decompose [12].

According to current European EU regulations, all textile waste is classified as biodegradable, but such classification is only partially justified. In most cases, only cellulose fibers (cotton, jute, ramie, flax, hemp...) are easily biodegradable, but in order for them to be completely biodegradable, they must not be excessively processed with various surface polymers [13].

Almost all polymer fibers are poorly biodegradable (polyamide, polyester, polyurethane, polypropylene, PVC, elastane, ...). Considering a large percentage of clothing products that are "fast fashion" products are made of synthetic fibers and cellulose fibers are represented in a much smaller percentage, it would be more objective to classify all textile waste as poorly biodegradable. Considering that polyester, which is the cheapest fiber and also the most represented in "fast fashion", is obtained on the basis of oil, like plastic, by mixing ethylene glycol with dimethyl terephthalate and after their reaction at high temperatures and air formed a polymer who needs at least 200 years to decompose. That is why it is necessary to recycle textile waste in order to prevent the disastrous impact of textile waste on the ecosystem.

Generally, textile reuse and recycling could reduce environmental impact because it could potentially reduce virgin textile fiber production and avoid processes further downstream in the textile product life cycle. Moreover, textile reuse and recycling are more sustainable when compared to incineration and landfilling. However, reuse is considered more beneficial than recycling, mainly when sufficiently prolonging the reusing phase [14].

Recycling provides alternatives to both the diversion of waste from landfill, and raw material production utilizing agricultural land. The mechanical recycling of cotton from is well established and is applied to both pre- and post-consumer waste, an generally entails the respinning of recycled combined with virgin material, without additional chemicals [3].

When the recycling routes are not well designed, the pollution effects, for example, global warming, become stronger [15].

Reuse and recycling of textile waste offers environmental sustainability. Upcycling and closed-loop recycling are the potential recycling routes that maximize conservation of resources such as raw materials, water, and energy, with minimal environmental impact [16].

While the separated collection of textiles requires energy for transport sorting and packing, every kilogram of virgin cotton replaced by a second hand product saves 65 kWh of energy and for polyester every virgin material replaced by second-hand clothing saves even more energy with 90 kWh (Woolridge et al., 2006). Therefore, a big supply of second-hand clothing can have a positive impact on the environment [17].

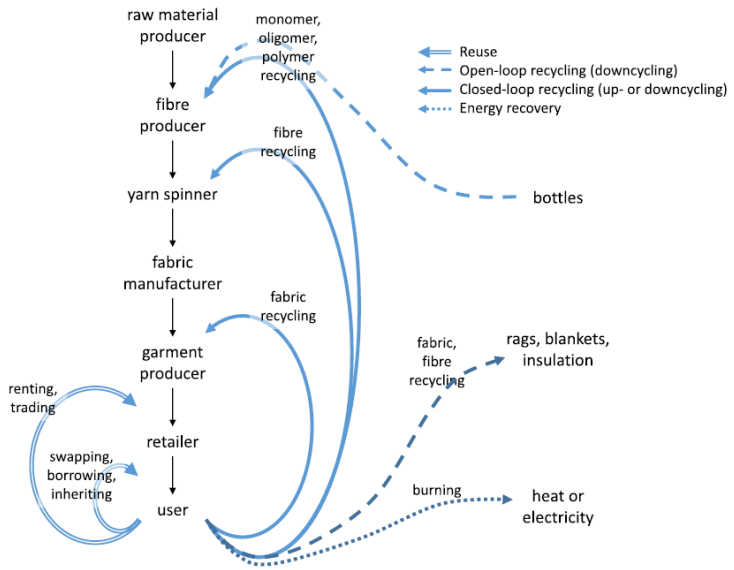

Figure 5. A classification of textile reuse and recycling routes [18].

METHODS OF TEXTILE WASTE RECYCLING

There are a many of ways to recycle textile waste. One of the newer ways is patented technology by company "Infinited Fiber Technology's" that involves mechanical and chemical processes to obtain high-quality recycled fibers.

Infinited Fiber Technology Company Oy's patented technology can turn textile, cardboard and agricultural waste into new natural fiber without any decrease in the quality of the fiber. Regardless of the raw material's origin (virgin or already recycled), the process may be performed not just once, or a limited number of times, but infinitely, while obtaining the same results in terms of output quality [19].

This technology includes 6 steps: 1. SHREDDING: Clothes are shredded and non-textile materials like buttons and zippers removed; 2. FIBER SEPARATION: Cellulose based fibres are separated from other fibres like polyester and elastane. Colours and finishing chemicals are removed; 3. CONTACT WITH UREA: Urea is compressed into cellulose and heated. The cellulose carbamate is formed. Cellulose carbamate is a stabile powder that can be easily stored; 4. DISSOLVING: Cellulose carbamate is dissolved into honey like liquid in alkali solution. Dissolved dope is then filtered; 5. WET SPINNING: In wet spinning the filtered dope is pumped into acid bath through very small holes. Cellulose is crystallizing and orientated and a new fibre is born. Fibres form a tow called filament. Filament is then cut to needed length and fibres are washed, dried and baled; 6. PRODUCTS MANUFACTURED: Yarns, textiles and non-woven fabrics produced in different facilities [19].

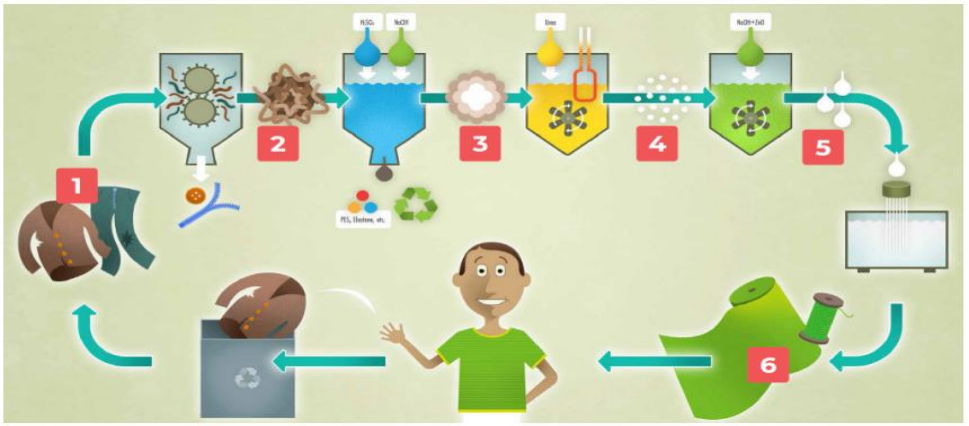

Figure 6. Patented technology of recycling by company "Infinited Fiber Technology's" [19].

CHEMICAL RECYCLING

Carbios Biorecycling is an enzyme-based recycling process based on the use of enzymes, which can be considered "highly specific biological tools". This innovative approach enables the specific de-polymerization of a single polymer (e.g., PET) contained in the various plastics to be recycled. This de-polymerization process results in monomers that are purified in order to be re-polymerized, thus enabling a perpetual recycling process. If plastic residues occur that are not degraded during the first stage, they are de-polymerized in a second stage by means of the same process, but by applying a different enzyme that will de-polymerize other polymers in the same way as in the first stage [19].

These polymers feature monomers chains that are easily identifiable by the enzymes, and are therefore easier to de-polymerize. In addition to textile waste, this technology is suitable for plastic bottles and containers (water, milk, sodas, cosmetics, etc.), packaging and films.

At the beginning of 2020 the company announced its new step forward in the development of its enzymatic depolymerization process in order to make it suitable for PET polyester fibers from textile waste [19].

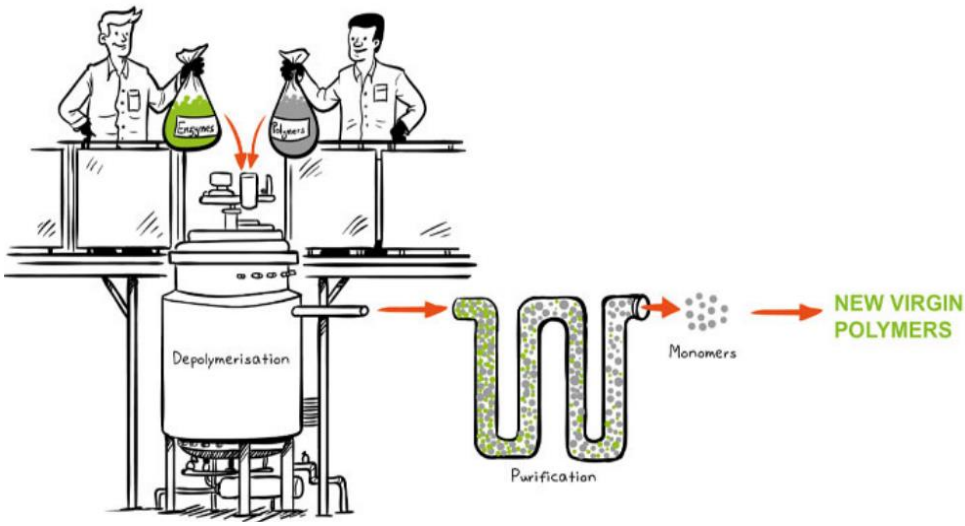

Figure 7. Chemical recycling technology [19].

MECHANICAL RECYCLING TECHNOLOGY

Mechanical recycling is the basic and most common process for recycling textile materials and consists of mechanical deconstruction to obtain reusable fibers in an efficient way. In the case where natural fibers are recycled, the obtained recycled fibers are ready for the production of new yarn or new textile products, but show reduced quality characteristics due to the fact that the fibers are shortened and damaged during the shredding process and may require mixing with additional fibers in order to obtain a higher quality yarn. and finally the finished product [13].

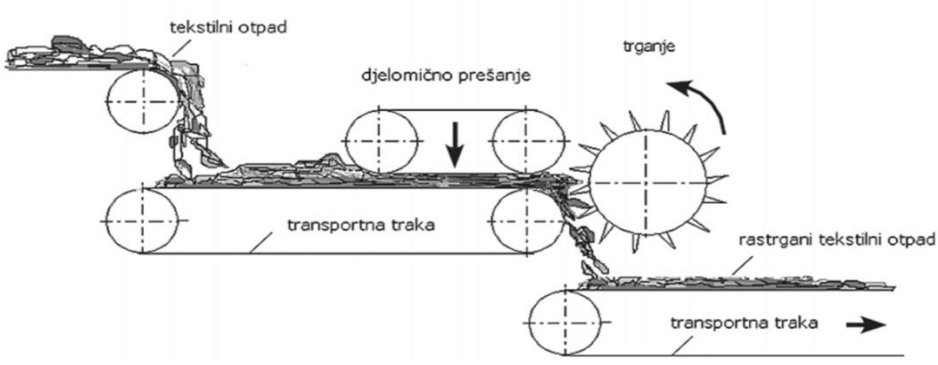

Figure 8. Mechanical recycling technology [13].

CONCLUSION

The mass production of textiles leads to an ever-increasing amount of textile waste. There are fewer and fewer areas left on our planet that have not been contaminated by man with his waste. When we no longer need a clothing product and if it is not possible to sell it in second-hand shops and enable it to be reused, then that clothing item is most often placed in a landfill where it is left to long-term biodegradation that will last for the next 200 years. Another option is to recycle the garment and make new textile products from it, and the third option is to burn it with other textile waste, which leads to additional pollution of our planet. Of all the three possibilities, only recycling is environmentally acceptable if we want to enable the new generations to come to have an ecosystem that is not destroyed and contaminated by waste that is a direct consequence of excessive production and little interest of responsible government of big countries to deal with this very important problem. It is necessary for us to understand that until the consciousness of every inhabitant of our planet changes and we do not understand the importance of preserving our ecosystem and our environment, be it in our immediate vicinity or thousands of kilometers away, neither will the global policy change regarding the importance of preserving a healthy ecosystem of our planet.

REFERENCES

1. Euromonitor International Apparel & Footwear, "Global fashion industry statistics - International apparel," Fashion United, 2016. Available: https://fashionunited.com/global-fashion-industry-statistics/
2. Benjamin Piribauer, Andreas Bartl, Textile recycling processes, state of the art and current developments: A mini review, *Waste Management & Research* 2019, Vol. 37(2) 112– 119.
3. Oakdene Hollins, Apparel and Footwear Recycling Innovation," Sustainable Apparel Coalition, 2014.
4. Krieger A, Prezzavento F, Edel MK, et al. Terminology of man-made fibres. Brussels, Belgium: BISFA, 2009
5. Woodings C Regenerated Cellulose Fibres. Manchester, UK: Woodland Publishing, 2001
6. K Storry and A McKenzie, "Unravelling the Problem of Apparel Waste in the Greater Vancouver Area," 2018.
7. CIRFS Information on man-made fibres, Brussels, Belgium: European Man-Made Fibre Organisation, 2016
8. Kotiba Hamad, Mosab Kaseem, Fawaz Deri Polymer Degradation and Stability, 2013; 98, p. 2801-2812
9. Tetra Tech EBA Inc., "2016 Waste Composition Monitoring Program," Metro Vancouver, Burnaby, 2016.
10. Textile Exchange. Preferred Fiber & Materials, Market Report. 2020. Available online: https://textileexchange.org/wp-content/uploads/2020/06/Textile-Exchange_Preferred-Fiber-Material-Market-Report_2020.pdf (accessed on 10 January 2021).
11. WTO (World Trade Organization). World Trade Statistical Review. 2018. Available online: https://www.wto.org/english/res_e/statis_e/wts2018_e/wts2018_e.pdf (accessed on 6 December 2019).
12. https://www.dailymail.co.uk/news/article-10450221/Dumped-Atacama-desert-mountain-discarded-cheap-clothes-West.html
13. Mario Krzyk, Jože Panjan, Darko Drev, Postupci recikliranja tekstilnog otpada, Sveučilište u Ljubljani, Fakultet građevinarstva i geodezije, Institut za zdravstvenu hidrotehniku 1Institut za vode Republike Slovenije, Tekstil 63 (9-10) 306-313 (2014.)

14. Sandin, G.; Peters, G.M. Environmental impact of textile reuse and recycling—A review. J. Clean. Prod. **2018**, 184, 353–365. [CrossRef]
15. Wang, X.-C.; Klemeš, J.J.; Wang, Y.; Foley, A.; Huisingh, D.; Guan, D.; Dong, X.; Varbanov, P.S. Unsustainable Imbalances and Inequities in Carbon-Water-Energy Flows across the EU27. Renew. Sustain. Energy Rev. **2021**, 138, 110550. [CrossRef]
16. Chavan, R.B. Environmental sustainability through textile recycling. *J. Text. Sci. Eng.* 2014. [CrossRef]
17. Woolridge AC, Ward GD, Phillips PS, et al. (2006) Life cycle assessment for reuse/recycling of donated waste textiles compared to use of virgin material: An UK energy saving perspective. *Resources, Conservation and Recycling* 46: 94–103.
18. G.Sandin, G.Peters, Environmental impact of textile reuse and recycling - A review, Journal of Cleaner Production, 2018, 354-366.
19. https://infinitedfiber.com/, Textile recycling technologies

Conference Proceedings
ICPAE 2023, 24th August – 26th August, Zrenjanin, Serbia
University of Novi Sad, Technical Faculty "Mihajlo Pupin", Zrenjanin

Eco-Textile and Redesign

Guoxiang Yuan[1], Marija Petrovic[2*], Vasilije Petrovic[3], Dragan Djordjic[4], Anita Milosavljevic[5], Predrag Pecev[6]

[1]World Textile University Alliance, Donghua University, Shanghai, 201620, China
[2] University of Travnik, Faculty of Technical Studies, Aleja konzula br. 5, 72270 Travnik, Bosnia and Herzegovina
[3,5] University of Novi Sad, Technical faculty „Mihajlo Pupin", Đure Đakovića BB, 23000 Zrenjanin, Serbia
[4]The Institute of General and Physical Chemistry, Studentski trg 12/V, Belgrade, Serbia
[6] Preschool Teacher Training and Business Informatics College of Applied Studies "Sirmium", Zmaj Jovina 29, 22000 Sremska Mitrovica, Serbia

e-mail: yuanguoxiang@gmail.com, petrovic.marija.0808@gmail.com

Abstract. The paper highlights that the design and production of clothing are increasingly influenced by modern trends, wherein ecology plays a significant role in human creation and life in general. Eco-friendly clothing refers to items that cause minimal or no harm to the environment. The paper explains that any textile product produced in an environmentally friendly way and processed within ecological limits is known as an environmentally friendly textile. Textile materials are primarily considered ecological based on factors such as product renewability, the ecological footprint of resources (i.e., the amount of land required for full product growth), and the environmental acceptability of the product (including the use of chemicals during production). The fashion industry has recognized the importance of ecological principles, and designers worldwide are consciously making efforts to preserve natural resources. This movement is commonly known as sustainable fashion or eco-fashion. The redesign of textiles and clothing is a component of eco-fashion. The paper particularly emphasizes redesign as an activity that shapes our reality. Through ecological awareness, redesign embodies an approach that could be described as a love for nature. The paper argues that redesign, as a creative form of transforming seemingly unusable items, results in unique creations characterized by originality, standing out from everyday uniformity. Redesign, through waste reduction, directly contributes to environmental preservation. Consequently, this approach also helps reduce pollution in the natural environment caused by the processing of raw materials and the production of final products in the textile industry.

Keywords: ecology, eco-fashion, redesign, ecological textiles

INTRODUCTION

Shopping for clothes used to be considered an event. Consumers saved up to buy new clothes at certain times of the year and were informed about fashion styles through fashion shows several months in advance before they reached the stores. All this started to change at the end of the nineties, when shopping became a form of entertainment, and the consumption of clothes increased. The media began to invite customers to enter fast fashion

because it is fashionable clothing, mass-produced at low prices, that allows consumers to feel as if they are wearing the same models that "walk the runway" or that are worn by movie stars. Today, the goal is to quickly produce economically viable garments as a response to changing customer demands. It must be taken into account that consumers decide to buy clothes that are often poorly made because they do not intend to wear them for years or even more than once.

The current state of the market can be described as fast fashion. What is fast fashion? Fast fashion is a term used to describe clothing designs that move quickly from runway to the stores, using the advantages of the trends. Fast fashion allows consumers to purchase a fashionable new product that is currently trending or will be trending at an affordable price. All this has led to a sharp increase in clothing sales. Research by the Center for Environmental Improvement in Belgrade shows that 82,000 tons of clothing are sold in Serbia in one year. This means that each resident buys almost 12 kilograms of clothes. There are similar trends in EU countries, where about 5% of money is spent on buying clothes and shoes. From that, about 80% is spent on clothes and 20% on shoes. It is estimated that EU citizens bought 6.4 million tons of new clothes in 2015 (12.66 kg per person). Data show that in the period between 1996 and 2012, the amount of clothing purchased per person in the EU increased by 40%. At the same time, more than 30% of clothes in the wardrobes of Europeans have not been used for at least a year. When discarded, more than half of clothing items are not recycled, but instead end up in mixed household waste and then sent to incinerators or landfills.

The rise of fast fashion contributed the most to this increase in consumption. Fast fashion, the epitome of multinational retail chains, relies on mass production, low prices and high volume sales. The business model is based on plucking styles from high-end fashion shows and delivering them in a short amount of time at low prices, usually using lower quality materials. Fast fashion is constantly offering new styles to shop. The average number of annual collections launched by European clothing companies is constantly increasing. This has led to consumers increasingly seeing cheap clothing as perishable goods that are "almost disposable" and are thrown away after only being worn a few times [1-7].

ECO TEXTILE

Ecological textile products are made from organic fibers that are produced according to organic standards, in all stages of production. Ecological textiles (Eco-Tex) consist of the main lines related to human health and environmental effects such as chemicals, waste water, workplace conditions, fuel gases, noise level, from raw material to final product. When Ecological Textile is considered only as a marketing tool, it cannot ensure competitive advantages in the market.

Eco textiles emerged as one of the solutions for reducing textile waste that has a negative impact on the environment. Raw materials are a key element on the way to greater biodegradability of textile waste. Therefore, we are working on finding new biodegradable raw materials. Some proposals also go in the direction of biobased polyester (also known as biosynthetics). It is partly made from renewable resources such as starch and lipids from

corn, sugar cane, beet or vegetable oils. Further development is lyocell fiber made from eucalyptus pulp, which grows quickly and requires no irrigation or pesticides. Bemberg fiber (cupro), which is made from waste cotton fibers, is also being developed.

The emphasis is still on organic cotton because it uses less water and pollutes less. The share of organic cotton increased from 6% in the period from 2012 to 2013 to 19% in the period from 2016 to 2017.

Figure 1. Organic cotton [5]

Organic cotton is cotton produced from a plant that has not been genetically modified, and that has been grown without the use of chemicals such as synthetic fertilizers and pesticides. A prerequisite for the production of organic cotton is organic land that has undergone a three-year cleanup of artificial substances. Organic cottonseed is also used as animal feed, and organic cottonseed oil is an integral part of many human food products. Apart from the fact that this kind of production reduces the harmful impact on the environment, it encourages biological cycles. This cultivation method increases the price of cotton. Therefore, producers are very cautious in expanding the scope of organic cotton production due to the unstable market and more expensive production [5,6].

Figure 2. Ecological textile products [6]

The world production of organic cotton is constantly increasing in the past years. The production of organic cotton is spread all over the world: the biggest producers are Turkey, India and China, Tanzania, USA, Uganda, Peru and Egypt.

Finished products made of organic cotton do not contain any substances harmful to health. The base material is colored with vegetable and mineral dyes and does not contain heavy metals or formaldehyde, which is particularly allergenic. Garments must contain 95% organic cotton in order to be accepted as products with an organic composition. It is allowed that 5% of the composition is made of dyes of natural origin, lace, elastin and other materials [5-7].

EXTENSION OF THE LIFETIME OF CLOTHES

In order to reduce the amount of waste generated by the disposal of textile products and clothing, there are some recommendations that stand out: finding a more sustainable raw material mix of fabrics to reduce the use of conventional cotton, improving sorting and recycling technologies, more efficient washing and drying, increasing energy efficiency and using renewable energy in technological processes, extending the life of clothes and improving sorting and recycling. Extending the life of clothes implies that the number of times the clothes are worn increases. Therefore, several solutions have been developed in this direction:

Slow fashion. Unlike fast fashion, slow fashion is an attempt to persuade consumers to buy fewer, better quality clothes and keep them longer. The philosophy behind slow fashion includes relying on reliable supply chains, small-scale production, traditional artisanal techniques, using local materials and garments that last through the season. It calls for a change in the economic model that leads to a decrease in clothing sales. However, this could threaten the economic survival of clothing manufacturers unless consumers are willing to pay higher prices.

Fashion as a service. New business models could increase the number of wearables of certain items using the principles of the sharing economy. Some brands are already offering clothes as a service – renting out clothes instead of selling them – taking cues from already established wedding and special occasion wear, protective clothing and newer maternity and baby wear. Other companies have clothing subscription services, where consumers pay a monthly fee to rent a fixed number of items at a time, allowing them to change their wardrobe frequently without buying new clothes (this already works well with handbags and high-end fashion, but increasingly for everyday wear).

Improved collection for repair, redesign and reuse of clothing. Brands like Filippa K. are taking pioneering steps by selling their second-hand clothes in their stores to make buying second-hand clothes easier. Others offer long-term warranties that include free product repair or replacement, a repair offer or repair instructions, or instructions for reuse.

Smart and current fashion. It is predicted that in the future, smart fashion could be designed - clothing that would tremendously reduce waste. Smart fashion could bring clothes of the future that can use smart technology to instantly adapt to consumer preferences, for example by changing colors, which would also reduce the need to produce multiple versions of the same garment. Instant fashion could enable on-demand production

at the point of sale, with the help of, for example, future and improved 3D printing. Consumers could get what they want locally produced. Some smaller brands already avoid overproduction by producing only what consumers order [7].

SOME OF THE PROPOSALS FOR REDUCING THE NEGATIVE IMPACT OF THE CLOTHING INDUSTRY ON THE ENVIRONMENT

The current linear economic model in the textile sector has put a lot of negative pressure on the environment. There is strong pressure within the textile industry to make every stage of production more environmentally sustainable. In this direction, large sportswear companies and large fashion brands are leading the way in investing in new technologies and ways of doing business. However, this task is difficult because efforts to reduce environmental impacts can result in increased product prices for consumers. Persuading consumers to buy less clothing could reduce the company's profits.

The current way of recycling by shredding largely does not meet the requirements. In order to enable the recycling of different textile fibers on the market, innovative solutions are needed. For textile materials that do not consist of fiber mixtures of different raw material composition, numerous industrial-scale solutions are beginning to enter the market. Renewcell has partnered with multiple brands including H&M and Levi's and has a deal with their parent company Beyond Retro Bank & Vogue, which supplies Renewcell with post-use textile waste.

One of the technical challenges which the industry faces is the high proportion of garments made from fiber blends such as cotton and polyester, which makes them difficult to separate. Pilot solutions that are expected to reach industrial maturity have appeared in that sector [7].

Figure 3. Linear economic model [7]

In accordance with sustainable development - treating waste as raw material - the amount of waste is reduced. This reduces the volume of production of raw materials and semi-finished products, because production, in addition to financial costs, has a very large harmful impact on the environment. Thus, cotton production destroys agricultural land and pollutes watercourses. About 22,5% of all insecticides and 10% of all pesticides consumed annually in the world are used to grow cotton. The production of just one cotton T-shirt requires 150 grams of pesticides. Pesticides are a danger to the environment because they seep into groundwater, poison birds, bees and other animals, as well as farmers. After cotton enters the production processes of the textile industry, its harmful impact on the

environment is even greater. The processes in the textile industry produce a lot of waste, including wastewater, as well as airborne and solid waste. In combating pollution, some of the solutions go towards the 4R model of the circular economy, namely:

- redesigning,
- reducing clothing consumption,
- reuse and
- recycling

REDESIGN

The redesign of textiles and clothing represents a segment of eco fashion and as such is present in the sphere of modern business management. By redesigning worn out and unusable textile products and clothing, they create new products acceptable by the market. By introducing redesign in the process of production and creation of textile products, which according to their use belong to clothing or ambient textiles, the entire reality is affected, which includes a humane and socially responsible attitude towards the future and refers to the preservation of all factors of the biosphere. Redesigning, apart from directly preserving the environment - through waste reduction, also saves the costs that would be required for the production of raw materials. Therefore, the pollution of the natural environment, which is inevitably caused by the processes of making and processing raw materials and the production of final products in the textile industry, is also reduced.

Textile material from existing clothing can be used in the production of clothing.

Figure 4. Redesign of clothing that uses the textile material of already existing clothing [12]

Redesign - an ecological approach to creativity in modern business and art which occupies an important place, globally accepted as an act of creativity, is an actuality whose importance is reflected daily in the presence of the personal example of the business of important designers, through education and numerous manifestations in the fashion world. It can be said that redesign is becoming a trend. Redesigning requires the deconstruction

and reconstruction of old clothes, a more complex process than the changes a tailor can make to improve the fit of a garment. Redesign can vary depending on the extent of changes to the garment, from adding minor design details such as decorative details, to changing the silhouette of the garment as well as completely transforming the original purpose of the garment.

The redesign of clothing and textiles is a design that transforms waste into a usable form, and thus represents a small segment of ecological - eco-fashion or fashion of sustainable development. Redesign includes three aspects [1-4]:

- Remake - (eng. Remake) and decoration (eng. Recraft)
- Repair
- Upcycle

Reshaping - is the creation of something new by transforming an unusable textile material into a product of greater value, with the characteristic of improving the useful and aesthetic function.

Figure 5. Reshaping done by redesign [12]

Alteration - means remaking some features or adding decorative elements in order to implement a new use that is in line with fashion trends.

Decorating - decorating the surface of clothing (e.g. with embroidery) or by adding pleats, etc.

Repair - mending of clothing, which can make the textile item different and aesthetically improved [7-11].

Clothes modified by redesign

Clothes decorated by redesign

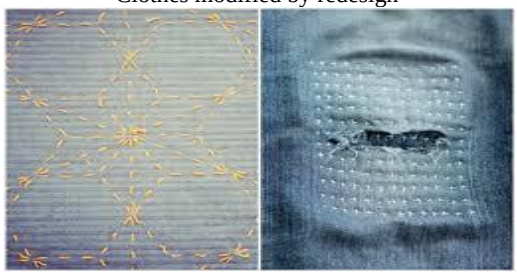

Clothes repaired by redesign

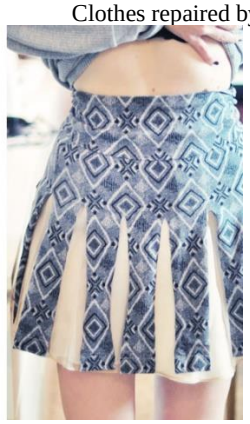

Transformation made by redesign – adding of constructive elements

Reformulation of element position made by redesign

Figure 6. Aspects of redesign [12]

In order to draw attention to the amount of textile waste that is created every day, an exhibition was organized in Hong Kong where the central place was occupied by a "mountain" of textile waste weighing 7,5 tons of textiles with a message of the justification and necessity of recycling.

Figure 7. „Mountain“ of textile waste weighing 7,5 tons of textile [13]

Figure 8. Poromotion of the textile waste recycling [13]

EXAMPLES FROM PRACTICE

The RECYCLING CENTER UŽICE was established from the funds of the IPA project entitled "Textile recycling to sustainable solutions". During the 10 years of its existence, the center has collected more than 125 tons of clothes. In their workshop, several women employees redesigned and distributed around 78.500 pieces of clothing for free.

CONCLUSION

The current linear economic model in the textile sector has put a lot of negative pressure on the environment. There is strong pressure within the textile industry to make every stage of production more environmentally sustainable. In order to reduce the amount of waste generated by the disposal of textile products and clothing, there are some recommendations that stand out: finding a more sustainable raw material mix of fabrics to reduce the use of conventional cotton, improving sorting and recycling technologies, more efficient washing and drying, increasing energy efficiency and using renewable energy in technological processes, extending the life of clothes and improving sorting and recycling.

The redesign of textiles and clothing represents a segment of eco fashion and as such is present in the sphere of modern business management. By redesigning worn out and unusable textile products and clothing, they create new products acceptable by the market.

REFERENCES

1. Junyi Xu, Guoxiang Yuan, Vasilije Petrovic, John Wilson: Laser Engraved Batik Pattern in Garment Design, Symposium on the futures of sustainability: Tackling sustainability through academic and practitioner collaboration, 17 and 18 september 2022., Shanghai, China.
2. Yiran Feng, Guoxiang Yuan, Vasilije Petrovic, John Wilson: Gothic clothing design by using Laser engraving, Symposium on the futures of sustainability: Tackling sustainability through academic and practitioner collaboration, 17 and 18 september 2022., Shanghai, China.
3. Qingyi Chai, Guoxiang Yuan, Vasilije Petrovic, John Wilson: Application of Laser Engraving on Acetate Fabric for Garment Design, Symposium on the futures of sustainability: Tackling sustainability through academic and practitioner collaboration, 17 and 18 september 2022., Shanghai, China.
4. V.Petrović, J.Stepanović, M.Stamenković, I.Skoko, S.Stefanović: „Životni ciklus i reciklaža tekstilija“, časopis Tekstilna industrija, 2011, vol.59, br. 3, str. 34-39.
5. https://www.alamy.com/a-farmer-carrying-a-basket-of-organic-cotton-on-their-farm-in-sendhwa-india-image212433979.html, accessed 24.06.2023.
6. https://environment.ec.europa.eu/topics/circular-economy/eu-ecolabel-home_en, accessed 24.07.2023.
7. https://www.eea.europa.eu/publications/eea-signals-2023, accessed 25.06.2023.
8. https://textile-platform.eu/, accessed 10.06.2023.
9. Vasilije Petrovic, Dragan Djordjic, Anita Milosavljevic, Marija Petrovic, Jelena Djukic: 4.0 Industrial Revolution in Clothing Production, Trends in Textile & fashion Design 5(4)-2023. LTTFD.MS.ID.000216. DOI: 10.32474/LTTFD. 2023.05.000216.
10. V.Petrović, M.Gašović: Modna kolekcija, Tehnički fakultet „Mihajlo Pupin“, Zrenjanin, 2016., ISBN 978-86-7672-257-0, COBISS.SR-ID 299045383
11. V. M. Petrović, Tehnologija pletenja I deo, Univerzitet u Novom Sadu, Tehnički fakultet »Mihajlo Pupin«, Zrenjanin, Zrenjanin 2000.
12. https://www.google.com/search?q=redesign+old+clothes+images, accessed 01.07.2023.
13. https://www.shutterstock.com/search/textile-recycling?, accessed 10.06.2023.

Conference Proceedings
ICPAE 2023, 24th August – 26th August, Zrenjanin, Serbia
University of Novi Sad, Technical Faculty "Mihajlo Pupin", Zrenjanin

Incorporating Li Brocade Patterns in Clothing Design: Exploring Creative and Sustainable Approaches

Guoxiang Yuan[1], Xiaoyu Xu[1], Danka Djurdjic[2], Marija Petrovic[3]*, Vasilije Petrovic[2], Dragan Djordjic[4], Anita Milosavljevic[2]

[1]World Textile University Alliance, Donghua University, Shanghai, 201620, China
[2]University of Novi Sad, Technical faculty „Mihajlo Pupin", Đure Đakovića BB, 23000 Zrenjanin, Serbia
[3]University of Travnik, Faculty of Technical Studies, Aleja konzula br. 5, 72270 Travnik, Bosnia and Herzegovina
[4]The Institute of General and Physical Chemistry, Studentski trg 12/V, Belgrade, Serbia
yuanguoxiang@gmail.com, petrovic.marija.0808@gmail.com

Abstract. In this research endeavor, a systematic analysis of Li brocade motifs will be undertaken, complemented by immersive field investigations. By intertwining the principles of circular economy and cultural heritage preservation, the study aims to explore how Hainan's Li brocade patterns could find renewed purpose in modern clothing design. Crucially, the rich history embedded in these patterns can inspire the revitalization of clothing design through the lens of the circular economy. By embracing the principles of reduce, reuse, and recycle, the Li brocade patterns could serve as a valuable source of inspiration for reimagining clothing, fostering a harmonious synergy between cultural heritage and sustainable fashion innovation. Through this transformative process, the study endeavors to contribute to the continued evolution of both the Li culture and the fashion industry within a circular economy framework.

Keywords: Li brocade, circular economy, cultural heritage, pattern classification, clothing design

INTRODUCTION

The intricate world of Li Brocade patterns serves as a canvas that intricately weaves the cultural heritage of the Li ethnic group, embodying diversity, ethnic allure, cultural practices, and spiritual symbolism. The fusion of masterful craftsmanship with innovative design concepts creates a unique aesthetic in Li Brocade, effortlessly balancing elegance and simplicity [1]. The chosen color palette, rooted in black, white, and blue, and enriched with vibrant shades like yellow, red, and green, imparts a dynamic chromatic symphony throughout the fabric. Li Brocade transcends mere visual appeal, acting as a repository of cultural narratives [2]. Originally symbolic representations of the Li ethnic group's written language, these patterns intricately carry the cultural legacy, visually narrating stories of the

Li people's profound connection with nature and the myriad facets of their daily existence. In the context of China's evolving economic landscape, Li Brocade emerges as a cultural gem, evolving from traditional materials to embrace modern synthetic fibers, carving its space in contemporary fashion. However, the advancement of mechanized weaving techniques casts a shadow on the preservation of traditional craftsmanship, raising pivotal questions about the equilibrium between evolution and heritage conservation.

In this juncture of tradition and innovation, a mission unfolds—to harmonize cultural legacy with sustainable advancement. This study embarks on a journey to guide the evolution of Li Brocade while upholding the flame of tradition. Guided by the principles of sustainable development and the circular economy, this exploration seeks to weave the threads of cultural continuity and progressive design into a cohesive narrative. By unraveling the synergy between heritage and advancement, this research contributes to preserving the Li ethnic group's cultural heritage while seamlessly embedding its resonance in the modern world. While a substantial body of research exists on Li Brocade, studies primarily emphasize its cultural, historical, and aesthetic dimensions [3-7]. The exploration of Li Brocade's integration in contemporary fashion design within the realms of sustainability remains a relatively untrodden path. Despite Li Brocade's rich historical and cultural significance [8-11], comprehensive analysis of its potential within the context of sustainable fashion is an existing gap in the scholarly discourse.

This paper recognizes the untapped potential of integrating Li Brocade patterns into modern clothing design, underscored by sustainability principles. The synthesis of Li Brocade's artistic legacy with contemporary fashion's demand for innovation and sustainability holds promise. Thus, this research seeks to bridge the existing gap by investigating the integration of Li Brocade patterns in modern clothing design while adhering to principles of sustainable development. By doing so, this study presents both academic and practical implications, nurturing a nuanced dialogue between heritage and modernity, and contributing to the preservation and evolution of cultural legacies in the ever-evolving world of fashion.

METHODOLOGY

Literature Review

The study employs a literature review approach to comprehensively explore existing research on Li Brocade patterns and Li ethnic culture. This method involves examining relevant materials related to Li ethnic culture to gain insights into the current state of research on Li Brocade patterns. Furthermore, the literature review aids in establishing a theoretical foundation for the present study.

Field Research

The author conducted on-site visits to various cultural and creative bases as part of the research process. These visits included locations such as Binglang Valley Scenic Area, Beishan Village in Haitang Bay, and Binglang Village in Sanya. Additionally, visits were made to ethnographic schools in Hainan, facilitating interactions with professionals in the field. These visits not only yielded relevant research data but also provided an immersive

experience of local customs and culture. The insights gained from these interactions deepened the understanding of the cultural significance represented by Li Brocade patterns.

Image Analysis

Given that the Li ethnic group lacks a written language and relies heavily on oral communication, particularly in their native dialect, the study relies on image analysis to decipher the cultural nuances embedded within Li Brocade patterns. As many of the remaining Li Brocade artisans are advanced in age and communicate solely in the Li dialect, comprehensive image analysis is essential to decode the intricate cultural details conveyed through the patterns. Despite Li Brocade patterns often depicting processed and refined representations of natural elements, variations in usage and customs among different lineages contribute to the complexity of interpreting these patterns.

Therefore, the study recognizes the paramount importance of investigating fabric patterns to attain a holistic understanding of Li Brocade, considering the intricate and multifaceted nature of these patterns.

CLASSIFICATION AND CHARACTERISTICS OF LI BROCADE PATTERNS

Classification of Li Brocade Patterns

Botanical Patterns

Within Li ethnic attire, botanical patterns typically serve as supplementary motifs. Among these, geometric floral patterns and branch-and-blossom motifs emerge with higher frequency. The forms of these botanical patterns tend to be relatively straightforward and are often employed in various knitted designs.

Animal Patterns

In the patterns adorning Li ethnic women's attire, a diverse array of animal motifs is prevalent. Examples include deer patterns, sheep patterns, parrot patterns, and dragon patterns. The dragon motif holds particular significance within Li culture, as it is regarded as an auspicious symbol denoting harmony and peace. By incorporating the dragon motif into their attire, the Li people not only signify their lineage as descendants of the dragon but also express a hopeful anticipation for happiness.

Humanoid Patterns

In Li culture, humanoid patterns are commonly referred to as "great strength deity patterns" or "ancestor patterns." Within Li society, there exists a profound veneration for ancestors, leading to the prevalent inclusion of humanoid motifs in attire patterns, regardless of the specific dialect. The category of "humanoid patterns" can be further divided into two

primary types: abstract and representational forms. This variety of patterns is characterized by its diverse designs, relatively refined depictions, and a color palette that tends toward earthy tones, reflecting a sense of antiquity.

Patterns Depicting Production and Life

Patterns depicting production and life often draw inspiration from daily experiences. Common motifs within this category include wedding scenes, hunting scenes, and harvest scenes. These patterns tend to be intricate and are frequently employed in textile printing and dyeing designs.

Geometric Patterns

Geometric patterns are typically constructed using points, lines, and shapes, often imbued with a certain level of abstraction. The composition of these patterns is characterized by a sense of generosity and simplicity, aligning with the design aesthetics of the modern era. In the realm of woven brocade, geometric patterns are frequently employed as border decorations, enhancing the overall aesthetic appeal.

Characteristics of Li Brocade Patterns

Diversity of Li Brocade Pattern Forms

(1) Color diversity

Li ethnic attire patterns are characterized by their pursuit of rich, vibrant colors, skillfully employing strong color contrasts to create a diverse spectrum. Embracing the concept of "five primary colors," namely black, red, cyan, yellow, and white, Li Brocade often combines these hues. Among these, black and blue are commonly used in daily Li clothing, often complemented by bright and vivid shades such as sky blue, grass green, and deep red. These colors are used in small accents or large color blocks to create contrast against the primary colors of Li Brocade.

(2) Variety in pattern styles

Different regions inhabited by the Li ethnic group exhibit distinct Li Brocade pattern styles. In the mountainous central and southern regions of Hainan Island, the predominant topography is hilly. This contrasts with the plains, resulting in varying weaving and embroidery patterns. Patterns frequently draw inspiration from natural scenery and surroundings. For women residing in mountainous areas, elements like colorful butterflies, water deer, reptiles, kapok flowers, birds, and dragon bone flowers are commonly depicted. On the other hand, women in flatland areas often feature motifs like frogs, shrimp, fish, and herons in their attire designs.

Uniformity in Hainan Li Brocade Pattern Forms

(1) Repetition of symmetrical patterns

Li Brocade designs primarily encompass abstract geometric shapes such as squares, parallel lines, straight lines, and zigzags.

(2) Repetition of similar form patterns

Due to variations in decorative item shapes, materials, and techniques, the forms of Li Brocade patterns are somewhat limited. To ensure both decorative quality and completeness, appropriate decorative patterns are chosen. Traditional patterns often employ continuous arrangements like two-sided or four-sided repeats, employing identical patterns to generate new designs through repeated arrangement.

APPLICATION

Pattern Analysis

Patterns employed in clothing often directly influence the style of the garments. In this clothing design collection, a sense of elegance and dignity is a primary objective, necessitating the selection of appropriate motifs. Presently, Li Brocade encompasses a variety of pattern categories including botanical, animal, humanoid, production and life, and geometric patterns. Upon analysis, it becomes evident that geometric patterns often consist of combinations of dots, lines, and shapes, aligning well with the requirement for a dignified and elegant design. Simultaneously, the use of patterned designs can enhance the aesthetic appeal of the clothing. Consequently, the current design integrates numerous geometric pattern motifs, incorporating representative patterns such as frog motifs, deer motifs, and great strength deity motifs, extracted from Li Brocade. These are then reimagined through a secondary design phase, serving as the primary motifs for the clothing, as illustrated in Figure 1.

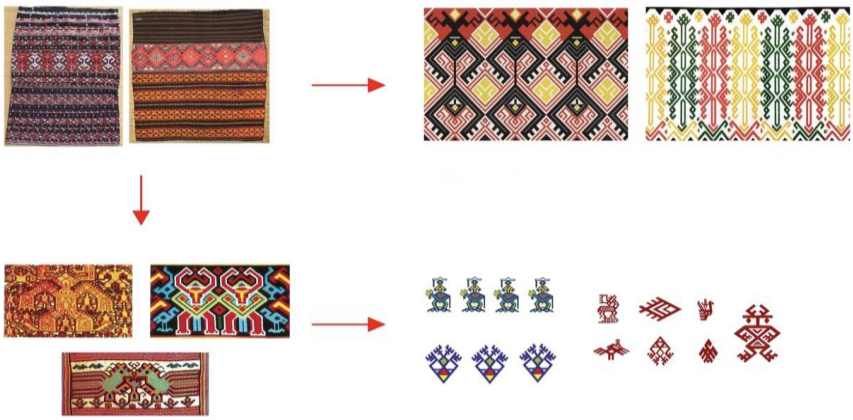

Figure 1. Redesign of Li brocade patterns [1]

Color Analysis

Within the context of Li Brocade, the selection of clothing colors varies based on distinct occasions. Generally, Li women tend to gravitate towards darker tones as the foundational color palette for their everyday attire. However, in ceremonial contexts, brown frequently assumes the role of the principal color, often accompanied by accents of gold and white. Fundamentally, the chosen color scheme plays a pivotal role in shaping the appropriateness of the attire for specific events. In the context of this clothing design collection, the central objective revolves around the seamless integration of Li Brocade patterns into contemporary garments, necessitating the harmonious convergence of traditional and modern aesthetics. As a result and shown in Figure 2, the design direction crystallized with the selection of black as the primary color for the clothing, complemented by the deliberate choice of red to underscore the patterns.

Figure 2. Extraction of Li brocade colours [2]

Clothing Design

This clothing series comprises a total of five sets, progressively translating inspiration into design elements applied to the finished garments in terms of color, silhouettes, fabric craftsmanship, and pattern extraction. The transition of inspiration into design elements is carefully orchestrated. The Li Brocade patterns and clothing silhouettes, presented with a slight exaggeration that carries a touch of theatricality, harmonize practical wearability and contemporary appeal.

Figure 3 illustrates the color rendering of the "Li" women's clothing series design, refined through continuous adjustments. Building upon the line drawings, it incorporates more Li Brocade pattern elements, thus epitomizing the representation of Li Brocade in the design. The overall clothing series features outer outlines predominantly in A-line and O-shapes, with a focus on autumn and winter coats.

Figure 3. Clothing design collection

As shown in Figure 3, the garment design collection comprises three main components: the top, skirt, and outerwear. For the blouse, an innovative DuPont paper fabric is utilized, adorned with a geometric pattern commonly found in Li Brocade. The skirt employs materials such as chiffon and satin, enhancing the garment's feminine grace. The outerwear features red leatherette fabric, mimicking the texture of silk satin. The distinctive erhe patterns from Li Brocade are achieved through collage techniques, enhancing the overall depth, contemporary flair, and cultural essence of the ensemble, while simultaneously reflecting the unique attributes of Li ethnic culture.

CONCLUSION

In conclusion, the convergence of sustainable principles, traditional cultural heritage, craftsmanship, transmission, fashion, and design unveils a transformative journey embedded with profound significance. The preceding discussions underscore the underlying harmony between Li Brocade patterns and the principles of the circular economy. From the intricate weavings of Li Brocade, a panorama of color dynamics emerges,

reflecting the Li ethnic group's distinctive sensibilities. While the influence of Han culture has left its mark, the Li people's unique perception of color manifests in the vibrant interplay of hues. Analysis elucidates the prevalent use of black, green, brown, yellow, and red hues in Li Brocade, aptly illustrating the spectrum of Li Brocade's color palette.

This study serves as a compass guiding the assimilation of Li Brocade patterns into modern clothing design, fostering a seamless dialogue between heritage and innovation. The discourse commences with a historical exposition of the cultural tapestry of the Li ethnic group and the contextual backdrop of Li Brocade patterns. These intricate patterns are meticulously categorized, encompassing botanical, animal, humanoid, and production and life motifs, each an embodiment of Li culture. As the journey progresses, contemporary clothing design emerges as a canvas that artfully intertwines Li Brocade patterns. Guided by innovative principles, the fusion of tradition and modernity gains momentum. Strategies unfold, delineating how to dismantle, extract, reshape, and meld Li Brocade patterns into modern garments, reinvigorating the legacy within a new context.

This exploration culminates with the unveiling of a self-crafted case, manifesting the very essence of the study's premise. The thematic genesis, inspiration, and meticulous rendering coalesce into a coherent design narrative. The culmination of this research presents both a creative endeavor and a practical solution—rekindling the flame of Li ethnic graphic language within contemporary design. By nurturing this harmonious synthesis, we embark on a journey that not only preserves but also enriches a cultural tapestry, underscoring the infinite potential when tradition converges with sustainable circular practices.

REFERENCES

1. Z. Hu and D. Xu, 2009. Analysis on External Factors of the Combination of Aesthetics and Functions of the Li Nationality. Asian Social Science.
2. F.Q. Chen, and Y.P. Zhou, 2015, December. Color feature extraction of Hainan Li brocade image based on RGB and HSV. In 2015 12th International Computer Conference on Wavelet Active Media Technology and Information Processing (ICCWAMTIP) (pp. 214-219). IEEE.
3. X. Deng, I.T. Kim and C. Shen, 2021. Research on convolutional neural network-based virtual reality platform framework for the intangible cultural heritage conservation of China hainan Li nationality: boat-shaped house as an example. Mathematical Problems in Engineering, 2021, pp.1-16.
4. S. Lyu, 2020. Research on the Culture of Frog Patterns in Li Brocade. International Journal of Frontiers in Sociology, 2(8).
5. L. Yue, L. Yang and M. Yuke, 2021. Culture Identity and Innovation Based on Hainan Li Brocade-Future Patch of Sustainability of ICH. CIVINEDU 2021, p.711.
6. Y. Zhou, F. Chen and Y. Zhou, 2017, March. Research on feature extraction techniques of Hainan Li brocade pattern. In Selected Papers of the Chinese Society for Optical Engineering Conferences held October and November 2016 (Vol. 10255, pp. 75-82). SPIE.
7. E.G. Davies and S.K. Wismer, 2007. Sustainable forestry and local people: the case of Hainan's Li minority. Human Ecology, 35, pp.415-426.
8. Z. Yuping, 2017, April. Development of information display software for Hainan Li brocade patterns. In 2017 3rd International Conference on Information Management (ICIM) (pp. 266-269). IEEE.
9. Q. Li and D.L. Ma, 2011. Creative Thinking on World Cultural and Natural Heritage Protection-Declaration on Silk Culture Protection. Advanced Materials Research, 175, pp.549-553.

10. G. Bo, W. Chen, 2017. The Traditional Handicraft Resources of Ethnic Minorities in the South of China and the Supposing of its Gene Mapping. Journal of South-Central University Nationalities (Humanities and Social Sciences), pp. 43-47.
11. M. Xiaoming, 2014. Study on basic patterns in Hainan Li nationality brocade. Popular culture and arts, 5, p.55.

Conference Proceedings
ICPAE 2023, 24th August – 26th August, Zrenjanin, Serbia
University of Novi Sad, Technical Faculty "Mihajlo Pupin", Zrenjanin

Environmental Aspects of Sustainable Fashion

Gebregziabher Kidus Tesfamariam [1], Anita Milosavljević[2*], Vasilije Petrović[3], Darko Radovančević[4], Dragan Đorđić[5], Predrag Pecev[6], Marija Petrović[7]

[1] Fitsum Etefa (B. Sc) Ethiopian Institute of Textile and Fashion Technology, EiTEX, Bahir Dar University, Ethiopia
[2,3,4] University of Novi Sad, Technical faculty „Mihajlo Pupin", Đure Đakovića BB, 23000 Zrenjanin, Serbia
[5] Institute of General and Physical Chemistry, Studentski trg 12/V, Belgrade, Serbia
[6] Preschool Teacher Training and Business Informatics College of Applied Studies „Sirmium", Zmaj Jovina 29, 22000 Sremska Mitrovica, Serbia
[7] University of Travnik, Faculty of Technical Studies, Aleja konzula br. 5, 72270 Travnik, Bosnia and Herzegovina
e-mail: oneday790@gmail.com, anita.milosavljevic@hotmail.com

Abstract. The paper presents sustainable fashion, which contributes to social stability and quality of life because it is a movement and a process of nurturing changes in fashion products and the fashion system towards greater environmental integrity and social justice. All the shortcomings and problems of unsustainable fashion are covered, due to which we have to change habits and turn to the circular economy in textiles, as well as how much consciousness is changing and that it is becoming a future and a trend or just an ecological necessity. The impact of manufacturing industries, sustainable development and development that meets the needs of the present, while not jeopardizing the future of generations in accordance with its definition of how much it includes survival from the aspect of technology, economy, ecology and society. The connection between fashion and sustainability, the influence of fast and the need for slow fashion in the world as well as in Serbia is presented on the basis of conducted research. Based on all the above, it can be concluded that sustainable fashion will provide a new market for additional employment opportunities, continuous cash flow in the economy, reduction of raw materials and export resources, attitudes towards consumption and use, change in attitudes and behavior of individuals, awareness of strategy for its production. Social networks play a significant role in all of this.

Keywords: fast fashion, slow fashion, recycling, ecology, circular economy, green strategy, sustainable clothing.

INTRODUCTION

A key area of the fashion industry is sustainable fashion, which contributes to social stability and quality of life in many ways. Sustainable fashion is a movement and process that drives change in fashion products and fashion systems towards better environmental protection and social justice. The downfall of unsustainable fashion is that cheap, affordable and trendy clothes have become available to the masses, thus creating the economic fashion concern that low-income people have the same opportunity to 'renew' their wardrobes as

high-income people. This leads people to buy a lot of cheap clothes instead of quality ones. The economics of fashion also mean that many sustainable fashion solutions, such as buying quality goods that last longer, are not available to those with limited resources.

THE ENVIRONMENTAL IMPACT OF THE TEXTILE AND CLOTHING INDUSTRY

The manufacturing industry does not have as great an impact on the environment as the textile and apparel industry. Because fashion places special and unique styles, personal tastes and designs at the center of its existence, primary functional purpose of clothing is equated, if not repressed. Only mass production can respond to environmental influences and rapid changes in trends, leading to global problems in the textile industry. Conflicting economic development, production and profit needs, and limited resources have led to the question of how we will meet the needs of future generations. Today's linear economic order makes it difficult to achieve a balance between development, production, profit and sustainability.

"Sustainable development is development that meets the needs of the present without compromising the ability of future generations to meet their needs." Sustainable development, according to its definition, includes minimal sustainability from the aspect of technology, economy, ecology and society.

Figure 1. Goal of the circular economy – 100% sustainable [7].

The concept of sustainable development may not be the first thing that comes to mind when talking about fashion, but there is a connection between fashion and sustainability. Sustainable fashion, which stands for slow fashion, is a relatively new movement in the fashion industry that is emerging in opposition to the currently growing aggressive fashion (fast fashion). Fast fashion leads to overconsumption of fashion products and is considered unsustainable. Uniqueness and low quality of fast fashion, and its business model causes many social problems such as the overuse of natural resources and the low quality of working conditions [3,4].

The term 'slow fashion' refers to a socially conscious movement that runs counter to the fast fashion cycle from production to disposal that is constantly accelerating. Sustainable awareness enables innovation in fashion solutions by protecting the environment, building a healthier economy and tackling social inequalities, first by easing the conflict between fashion and sustainability through sustainable fashion. Sustainable fashion will be achieved

when lead designers and other big players in the textile industry start to dictate trends and production while abandoning the high-traffic fashion industry in favor of flexible design with focus on the ecosystem.

FAST FASHION POLLUTES THE ENVIRONMENT

Fast fashion has led to the fact that today the textile industry is one of the biggest polluters of the environment, and is a source of water, air and soil pollution. In order to make the production process as cheap as possible, in addition to cheap and harmful raw materials, one of the key features of mass production is exploiting workers in labor-exploiting workshops where they work in inhumane conditions, as shown in Figure 2, and earn below average wages. According to the Serbian chamber, up to 50.000 tons of textile waste is generated annually in Serbia, which is about 12 kg of waste per citizen.

Figure 2. Production plant – inhumane working conditions [8].

Society needs to recognize the problem start to actively work on scientific research projects, where they monitor new smart technologies in the field of fashion and industrial design in order to organize and create sustainable collections, Instead of manufacturing, designers create their own creations and thus participate in the production from start to finish.

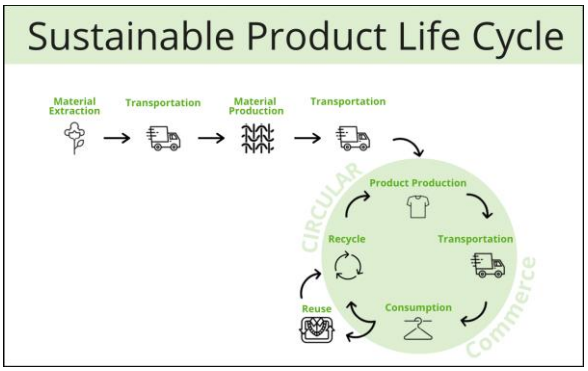

Figure 3. Sustainable product life cycle [5].

This production method is the key to slow fashion. Countries must prepare more actively for the transition to a circular economy because in the current global crisis and climate change, one of the key factors of surviving is benefits of a circular economy. According to various experts, sustainable fashion is definitely associated with the concept of circular economy or circular economy as shown in Figure 3 and Figure 4, which is almost unheard of Serbia.

CIRCULAR ECONOMY

One of the elements of the circular economy and a prerequisite for its implementation is sustainable waste management. The circular economy concept is a potential response to a global crisis. Sustainability in the fashion industry is realized through the idea of sustainable fashion and involves a responsible attitude towards textile waste as a useful raw material for the production of new clothes.

Sustainable fashion incorporates use of sustainable or organically grown materials and a responsible attitude towards all workers in the clothing production and distribution chain. The circular approach emphasizes getting used items back into productive operation. Estimates of circular economy adoption in the EU project productivity reaches growth of 30% by 2030 with GDP growth of 1% and the creation of over two million new jobs. It is estimated that circular economy generates €600 billion in savings per year in the European Union.

Figure 4. Circular economy as the future [6].

POSSIBILITY OF PROMOTING SUSTAINABLE FASHION COMMERCIALLY

As a result, in order for the concept of sustainable fashion to be commercially feasible, a market that will desire such an offer must first be formed. At the moment, it appears that

the trend of fast and inexpensive fashion will strengthen, while sustainable fashion will remain an alternative, rather than a financially viable trend that must be changed.

With an unsustainable, unconscious, and anti-ecological way of life, we will be forced to better set priorities and fight for our own life and health, as the current "produce - use - throw" economy exhausts all of our resources. It is critical that humanity recognizes its responsibilities. Any human can demonstrate their responsibility through everyday actions such as waste selection, saving water and energy, using more environmentally friendly modes of transportation, purchasing fewer clothes, etc.

The green strategy includes second-hand fashion, high-quality and timeless design fashion, textile collection and recycling systems, production of eco-labeled clothing according to eco-labels and fair trade; these are some of the strategies and activities that increase the company's sustainability and encourage more sustainable production and consumption patterns.

CONCLUSION

Because sustainable fashion is a requirement, some companies have linked up to tackle environmental and societal concerns together, helping to expedite change and limit the dangers of working on these difficulties alone.

It is necessary to develop standards and practices for clothing design that can be easily reused or recycled [2]. Next, invest in the development of new fibers that will reduce the impact of production and manufacture life-saving clothing, support the development of mechanical and chemical recycling technologies [1], and establish higher operational and environmental standards.

A more sustainable method of production may be more expensive, but it can drive innovation and shield businesses from supply chain shocks and reputational risks, resulting in better resilience and profitability.

REFERENCES

1. J. Stepanović, S. Janjić, Mechanical textile technology, University of Banja Luka, Faculty of Technology, 2015
2. D. Radivojević, M. Đorđević, D. Trajković, Textile testing, High School of Textile, Leskovac, Investigation of the influence of qualitative characteristics of fabrics on thermophysiological properties of clothes - doctoral dissertation – Mirjana Reljić – Leskovac 2016.
3. https://oradio.rs/sr/vesti/drustvo/odrziva-moda-buducnost-ili-trend-9621.html
4. https://www.movem.rs/vesti/odrziva-moda/84
5. https://greenbusinessbureau.com/industries/fashion/sustainable-fashion-identifying-fast-fashion-flaws-and-extending-the-life-cycle-of-clothing/
6. https://www.asyousow.org/blog/as-you-sow-heralds-a-zero-waste-future-with-rebranded-circular-economy-program
7. https://www.ecotextile.com/2019011623983/fashion-retail-news/report-yields-sustainable-fashion-advice-2.html
8. https://sukrittakerinnonta.wordpress.com/2013/10/09/examples-of-poor-working-conditions-from-fashion-history/

Conference Proceedings
ICPAE 2023, 24th August – 26th August, Zrenjanin, Serbia
University of Novi Sad, Technical Faculty "Mihajlo Pupin", Zrenjanin

Recycled Textile Fibers and Materials – Current State and Development Perspectives

Ana Gojic[1], Nadiia Bukhonka[1*]

[1]*University of Novi Sad, Technical faculty "Mihajlo Pupin" Zrenjanin, Djure Djakovica bb, 23000 Zrenjanin, Serbia*
nbukhonka@gmail.com

Abstract. The production, use, and disposal of fibers and textiles have a profound impact on people and the planet. As resources become scarcer and populations grow, the textile industry actively seeks to reduce these negative impacts and embrace sustainable fiber and material production. Recycling fibers and textiles play a crucial role in reducing the industry's overall environmental impact. By implementing recycling practices, the industry can minimize waste and conserve resources, fostering a more sustainable production system. This entails discovering innovative ways to repurpose fibers and textiles throughout their life cycle. Through comprehensive strategies, recycling initiatives, and addressing crucial areas, the textile industry can make significant strides towards a sustainable and eco-friendly future. This benefits not only the industry but also enhances the well-being of both people and the planet.

Keywords: recycling, recycled textile, textile fiber, textile materials

INTRODUCTION

The production, utilization, and disposal of fibers and textiles have far-reaching consequences for both the people and the planet. With resources becoming increasingly scarce and populations continuing to grow, the textile industry recognizes the pressing need to mitigate these negative impacts and embrace sustainable practices in fiber and material production [1]. Central to this effort is the adoption of recycling methods, which play a vital role in reducing the industry's overall environmental footprint.

Textiles are highly recyclable, with the potential for nearly 100% of them to be recycled [2]. However, despite this potential, a significant portion of textiles still end up in landfills for various reasons. In recent years, there has been a growing emphasis on the development of value-added products derived from recycled textile materials [3,4]. This shift in focus is driven by the increasing awareness and commitment of consumers, policy makers, engineers, and industry experts towards environmental stewardship.

By prioritizing recycling, stakeholders in the textile industry can avoid the punitive costs associated with landfill disposal. Recycling textiles not only reduces waste, but also contributes positively to employment opportunities, charitable contributions, and the overall environmental impact [1-4]. It is a holistic approach that encompasses strategic partnerships and collaborative efforts throughout the recycling process.

Overall, by embracing recycling and adopting a comprehensive approach to the recycling process, the textile industry can unlock numerous benefits. These include cost savings, job creation, support for charitable causes, and a positive environmental impact [2, 3].

Textile recycling is the process of recovering fibers, yarns, or fabrics and reprocessing them into new, useful products [5]. Textile waste can be categorized as pre-consumer waste and post-consumer waste [6].

Pre-consumer waste refers to a material that is discarded before it reaches the consumer. Previously used recycled materials can be further processed into similar or different materials, or they can be sold "as is" to third-party buyers who use them for consumer products. Pre-consumer textile waste typically includes waste by-products from the production of fibers, yarns, textiles, and clothing. These can be scraps or goods damaged during manufacturing, and the majority are returned and reused as raw materials in industries such as automotive, furniture, mattresses, coarse yarn, home furnishings, paper, and others [6].

Post-consumer textile waste usually refers to any product that an individual no longer needs and decides to dispose of due to wear or damage. It typically includes used or worn-out clothing, linens, towels, and other widely used textiles. Recoverable consumer waste includes garments, curtains, towels, bed linens, blankets, cleaning cloths, tablecloths, matching socks, and so on [6].

Additionally, recycled fibers offer several benefits [6]. Firstly, they conserve non-renewable resources by eliminating the need for virgin materials. Secondly, they divert waste from landfills by providing a second life to garments. Lastly, the recycling process requires less primary energy and generates less waste, resulting in a lower climate impact compared to virgin fibers.

Recycled materials are gaining increasing popularity not only in the advancement of recycling processes but also in the wider acceptance and use of products made from these materials. For instance, research conducted by Cotton Incorporated's Lifestyle Monitor™ [7] reveals a growing consumer interest in recycled materials. However, it is important to note that consumers do not always associate "recycled" with "sustainable." According to the study, while 24% of consumers are willing to pay a premium for clothing or home textiles labeled as "recycled," only 5% of consumers associate "sustainable" with "recycled."

Additionally, the research highlights that 32% of consumers who plan to purchase clothing or home textiles actively seek out "recycled" options. However, consumers tend to prioritize products labeled as "100% cotton," "natural," or "environmentally-friendly" over those solely labeled as "recycled."

RESULTS AND DISCUSSION

Global fiber production

Global fiber production reached an unprecedented milestone, surpassing all previous records and reaching 113 million tonnes in 2021, rebounding from a slight decline experienced in 2020 due to the COVID-19 pandemic [1]. Over the course of the past two decades, fiber production has nearly doubled, escalating from 58 million tonnes in 2000 to

the current 113 million tonnes in 2021 (Figure 1). If present trends continue, it is projected to further increase to 149 million tonnes by 2030. This surge in production is accompanied by a notable rise in per capita global fiber production, which has risen from 8,4 kilograms per person in 1975 to 14,3 kilograms per person in 2021, highlighting the growing demand and consumption of fibers on a global scale.

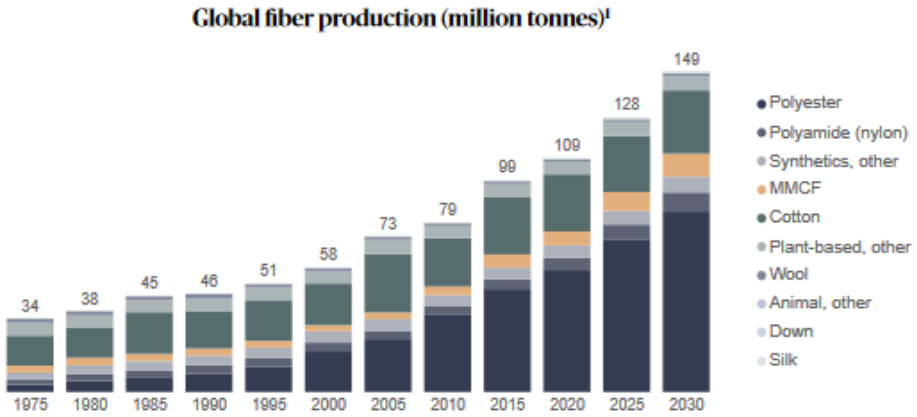

Figure 1. Global fiber production from 1975 to 2030 [1].

However, this escalating fiber production carries significant implications for both humanity and the planet. While there is an increasing awareness of the urgent need for responsible resource utilization and the decoupling of growth from resource consumption, the necessary changes have not yet been fully realized in terms of scale and speed. It is crucial to expedite the adoption of sustainable practices to effectively address these challenges.

Recognizing the imminent reality of dwindling resources and an ever-expanding population, the textile industry is taking proactive measures to obtain recycled fibers, transform discarded textiles into finished textile products, and develop end-of-life solutions [1]. These efforts are aimed at minimizing the overall impact of the industry. The production, utilization, and disposal of fibers and materials have significant consequences for the environment. Once collected, textiles are transported to recycling centers where they undergo sorting into three categories: reusable items, rags, and fibers. While this process is primarily manual, conveyor belts and bins may also be utilized to facilitate material separation. Garments that are suitable for reuse are often directed towards charitable organizations or sold in foreign markets.

Global fiber production and recycled fiber market in 2021

Since the mid-1990s, synthetic fibers have dominated the global fiber market, surpassing cotton in terms of production volumes. In 2021, synthetic fibers accounted for approximately 64% of the total global fiber production [1]. The global fiber production trends in 2021, as depicted in Figure 2, and the global recycled fiber production trends in

2021, as illustrated in Figure 3, showcase noticeable distinctions. These differences can be attributed to variations in the advancement of recycling processes for various fiber types.

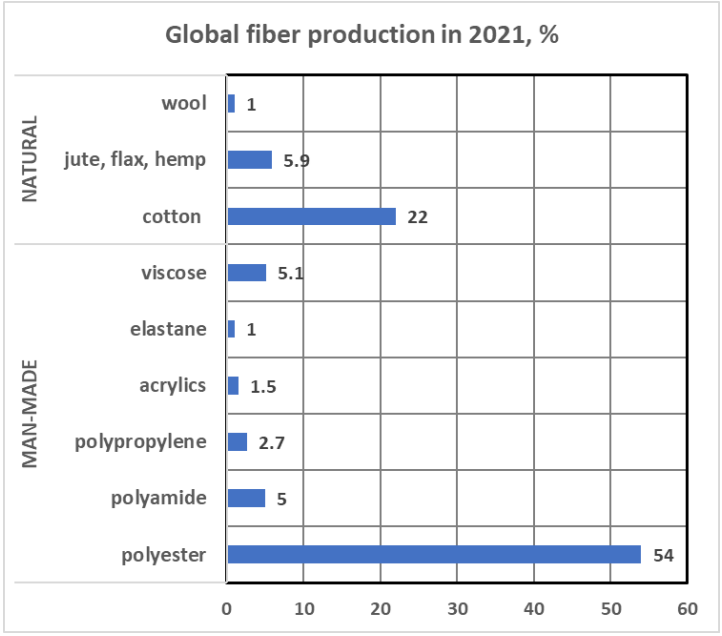

Figure 2. Global fiber production in 2021.

Polyester, the most widely utilized synthetic fiber, dominated the global fiber production market in 2021 with a significant market share of approximately 54% (Figure 2). Notably, around 15% of global polyester production consisted of recycled polyester (Figure 3). In contrast, polyamide, the second most commonly used synthetic fiber, accounted for roughly 5% of the global fiber market, with only 2% of the global polyamide fiber consisting of recycled polyamide. Other synthetic fibers, including polypropylene, acrylics, and elastane, collectively represented a market share of 5,2% in 2021. Polypropylene had a market share of approximately 2,7% of global fiber production, and only about 0,2% of all polypropylene fibers consisted of recycled fibers. Acrylic fibers accounted for 1,5% of the global fiber market in 2021, with the estimated market share of recycled acrylics at around 0,3% of total acrylic fiber production. Global elastane fiber production reached a market share of approximately 1% of the global fiber market in 2021, with an estimated 2,6% of the global elastane fiber production volume consisted of recycled elastane.

Manmade cellulosic fibers (MMCFs), which encompass materials like rayon, viscose, and modal, represented approximately 6,4% of global fiber production in 2021. Viscose fiber production alone accounted for roughly 5,1% of the global fiber market share in the same year, with an estimated 0,5% of the total viscose fiber production volume consisted of recycled fibers.

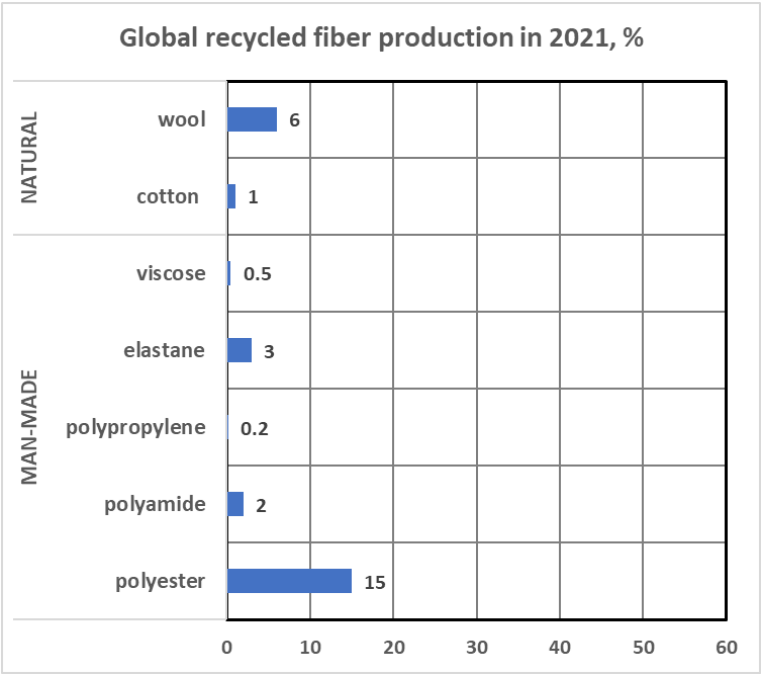

Figure 3. Global recycled fiber production in 2021.

In 2021, plant-based fibers, including cotton, jute, hemp, flax, and others, collectively held a market share of about 28% in the global fiber market. Cotton, as the second most significant fiber in terms of volume, contributed to approximately 22% of global fiber production. However, the recycling rate for cotton fibers remained relatively low at around 1% of the total cotton production in 2021 but is expected to grow significantly in the coming years [1]. Other plant-based fibers, such as jute, flax, hemp, and others, accounted for approximately 6% of the market share.

Animal fibers, specifically wool, constituted around 1,6% of global fiber production in 2021. Approximately 6% of all wool fibers were recycled.

Methods of recycling

There are two primary methods of recycling [6]:

1) mechanical,
2) chemical.

Mechanical recycling involves shredding the material to transform it into a nearly fibrous form. However, during this process, the fibers may lose their strength and, therefore, need to be mixed with virgin fibers, particularly in the case of cotton and wool. Mechanical recycling has been utilized for many years.

Chemical recycling employs a chemical process to extract the desired raw material. This method enables the recovery of more valuable products and currently demonstrates promising technological advancements. Although the industry is actively working on this type of recycling, it is not yet technologically or economically mature. Overall, both

mechanical and chemical recycling play crucial roles in the recycling industry, with each method having its own advantages and challenges.

CONCLUSION

Each year, a substantial quantity of textile waste is negligently dumped in landfills, resulting in significant negative impacts on both the economy and the environment. This careless practice not only squanders valuable resources but also exacerbates the challenges we currently face. Despite a noticeable increase in environmental awareness among the general public in recent years, their active participation in waste reduction through recycling still requires significant improvement.

One effective approach to address this issue is to advance recycling technologies, enhance the recycling rate of fibers, and explore the diverse applications and benefits of utilizing recycled fibers. These technological advancements provide us with the opportunity to convert waste into valuable products, rescuing items that were once deemed worthless and sold below their true value. By advocating for a more thoughtful and deliberate approach to rejuvenating waste fibers, individuals who previously disposed of waste hastily will come to recognize the potential for increased profits in their businesses. Moreover, this shift in mindset will enable them to contribute to a noble cause by actively reducing environmental contamination.

In conclusion, it is of utmost importance that we address the problem of textile waste disposal in landfills. This paper aims to emphasize the significance of fiber recycling technologies and encourage the broader adoption of recycling practices. By doing so, we can effectively convert waste into valuable resources, benefiting both our economy and the environment.

REFERENCES

1. https://textileexchange.org/app/uploads/2022/10/Textile-Exchange_PFMR_2022.pdf
2. J. M. Hawley, 2014, Chapter 15 - Textile Recycling, Handbook of Recycling, Elsevier, pp.211-217
3. S. Islam, G. Bhat, 2019, Environmentally-friendly thermal and acoustic insulation materials from recycled textiles, *Journal of Environmental Management*. Vol. 251, 109536, https://doi.org/10.1016/j.jenvman.2019.109536
4. Y. Arafat, A. J. Uddin, 2022, Recycled fibers from pre- and post-consumer textile waste as blend constituents in manufacturing 100% cotton yarns in ring spinning: A sustainable and eco-friendly approach, *Heliyon*, Vol. 8, Issue 11, e11275, https://doi.org/10.1016/j.heliyon.2022.e11275
5. U. Seval, 2019, A study on the suitability of which yarn number to use for recycle polyester fiber. The Journal of The Textile Institute. Vol.110. pp.1-20. 10.1080/00405000.2018.1550889.
6. A. Rengel, 2017, Recycled textile fibres and textile recycling. An overview of the Market and its possibilities for Public Procurers in Switzerland, Commissioned by the Federal Office for the Environment
7. https://cottonworks.com/en/topics/sustainability/cotton-sustainability/recycled-cotton/

Conference Proceedings
ICPAE 2023, 24thAugust– 26thAugust, Zrenjanin, Serbia
University of Novi Sad, Technical Faculty "Mihajlo Pupin", Zrenjanin

Laser Parameters to Ensure Qualitative and Saved for Environment Denim Garment Finishing Process

Ineta Nemeša[1*], Marija Pešić[1], Valentina Bozoki[1]

[1]University of Novi Sad, Technical faculty "Mihajlo Pupin",
Đure Đakovića bb, 23000 Zrenjanin, Serbia
inetavil@gmail.com

Abstract: Many traditional denim finishing methods are harmful to environment and workers performing them. To avoid these serious disadvantages denim garment producers use laser marking method. Right choice of process parameters is very important to ensure laser marking in high quality and speed. Light surface effects destroying indigo colour of the material are created by low-powered laser beam in lower speed. Different degree serious denim material degradations and holes are created by a high power laser beam. The higher the laser power, the higher should be the cutting speed. The focal length and with it a laser spot size is changed to change the degradation level of a material and its colour. The larger focal points are used to engrave mark denim materials. Smaller focal points are used cutting material fully. Process quality is also effected by cutting nozzle diameter, distance between a nozzle and cut material surface and a pressure of cutting gas. The right choice of process parameters is always very challenging, it depends on stated priorities and acceptable compromises between them.

Keywords: CO_2 laser, laser cutting, textiles, laser cutting parameters

DENIM LASER FINISHING

Many techniques, such as, sandblasting, stone washing, whiskering, damaging/destroying, bleaching, etc., are used for denim garment finishing to give a certain and unique look (a vintage effect) to the jeans. The most part of them are very much time, work and recourses consuming, harmful to environment and workers performing them [1,2]. To avoid these serious disadvantages, industry is developing new denim finishing methods. Laser finishing is one of them. Using it, the most part of desirable effects on the ready denim garments are created by help of a laser beam [3-10].

Performing the laser marking denim fabrics lose their indigo colour and the marks on the fabric surface appear in white colour. Changing processing parameters cotton material by itself can be damages to obtain effects of long time worn clothing (se Fig.1).

Figure 1. Jeans after finishing to obtain vintage effects
https://www.nytimes.com/wirecutter/reviews/best-jeans-for-men/

Figure 2. Mannequins fixed in horizontal or vertical position to perform denim marking by laser [14]

LASER MARKING PARAMETERS

Different finishing effects are obtained changing following laser treatment parameters: power and speed of the laser beam, the diameter of the focal point, focal position and focal length. Important are also cutting nozzle diameter and distance between it and cutting surface, as well as, cutting gas pressure. Right choice of process parameters is very important to ensure laser marking process in high quality and speed [11-14].

Laser power

Laser power is the total energy emitted in the form of laser light per second. The choice of laser power is dependent on the type and thickness of the cut material, complexity of cut shapes and desired laser processing effect. A higher wattage laser can cut faster and more dense material. Lower power laser beam is needed to process light textile materials, such as, silk and light cotton (10-30 W). To achieve high accuracy on

complex shapes, laser power also should be reduced. If too much heat is applied to the material, sides of the cut lines can burn out increasing a cut kerf (the groove made while cutting). The most part of textile materials may be processed 60-100 W lasers. However, there are some textiles, for example, Aramid (Kevlar) which is processed with 400 W lasers.

Performing the laser marking on denim garments detailed patterns and light surface effects, such us, honeycombs, whiskers, stacks, train tracks are created by low-powered laser beam (see Fig.3).

Figure 3. Creation of whiskers by laser beam
https://www.businessoffashion.com/articles/sustainability/levis-bets-on-lasers/

Different degree denim material degradations(for example,breaking of the warps of the fabric leaving weft untouched) and even holes (cutting both warp and weft of the fabric) are created by a high power laser beam. Sometimes cutting at high power can result in the material igniting. Small flashes of flame that don't hang around for a fraction of a second are acceptable (see Fig.4).

Figure 4. Small flashes of flame creating serious material damages and holes by high power laser beam https://www.cnbc.com/video/2018/03/02/levis-is-replacing-workers-with-lasers-to-distress-jeans.html

Cutting speed

The cutting speed must be matched to the laser power, the shape of the cut components, as well as, to thickness, absorption properties and micro-surface of the marked material. It also depends on processing requirements - the priority for high speed or high accuracy, desired effect of the cut edges.

The higher the laser power, the higher should be the cutting speed. Dense denim materials are processed in higher speed by a higher power laser and vice versa. The complex geometry lines have to be cut in reduced cutting speed to ensure high decoration accuracy. A speed which is too high or too low leads to increased roughness, burn formation and to large drag lines (left from fumes and other by-products).

Performing the laser marking on denim garments detailed patterns and light surface effects, such us, honeycombs, whiskers, stacks, train tracks have to be created by slowly moving laser beam (see Fig.5).

a b

Figure 5. Honeycombs on jeans (a) and fine patterns (b) created by laser [14]
https://denimhunters.com/denim-wiki/jeans-anatomy/honeycombs/

Focal/focus position

The beam focus is the point where the beam diameter is smallest. It provides highest *intensity of the laser beam* for material treatment. Above and below the focus the intensity of the laser beam drops. An acute angle with which the focus is set, keeps the focus very thin in longer distance and vice versa. It can be important processing thick materials. The laser beam focused in the acute angle creates thinner kerfs thus reducing vaporized material part on the cut edges.

The sensitivity to focal position is dependent on cut material properties. Smaller focal points are used cutting material fully to create holes and serious material damages on denim garments (see Fig.6). The larger focal points are used to engrave and mark denim materials creating honeycombs, whiskers, stacks, train tracks.

Figure 6. Serious material damages on jeans. https://www.etsy.com/listing/1408514427/mens-ripped-slim-fit-embroidery-stretch

Focal length

Focal length is the distance between the centre of the focusing lens and the focus of the laser beam (see Fig.7). A shorter focal length results in a smaller spot size and smaller depth focus. The focal length and with it a laser spot size can be changed raising or lowering the lense in the cutting head. It is done when the same laser equipment has to perform both material through cutting (with small spot size), and marking/engraving (with larger spot size).

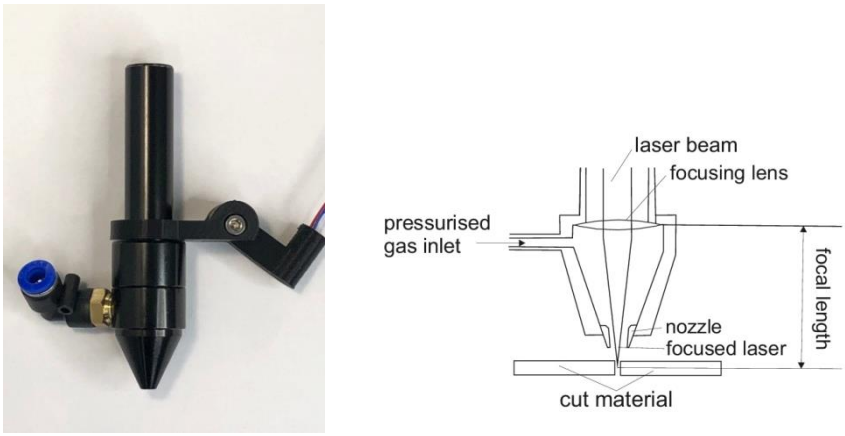

Figure 7. Cutting head of a laser cutter [12]

Cutting nozzle and its diameter

A cutting nozzle (see Fig.7) guides the stream of compressed air into the cutting gap and with it protects optical lenses from flying sparks, vapors and particles generated on the cut material surface. The use of the nozzle with correct diameter is very important. If the nozzle is too small, the cut edge is not cleanly cut and slag clings to the lower edge of the kerf. If the nozzle is too large, the gas pressure is lower, cutting gas consumption increases, but the cutting quality is not significantly affected.

Distance between the cutting nozzle and cut material

The distance between the cutting nozzle and the cut material surface can influence laser processing quality and speed. The smaller it is, the better cut quality is achieved. However, reducing it the risk of collision (when nozzle touches the material surface) increases. The stand-off distance for standard nozzles should be smaller than the diameter of the nozzle. Typical nozzle diameters are in the range of 0,8–3mm, so that the nozzle stand-off distance should be in the range of 0,5–1,5mm for best cutting results.

Cutting gas and its pressure

Compressed gas jet is used to keep focusing lens clean and to improve cutting quality. During the work process, the laser beam heats, melts and partially or completely vaporizes the cut material. The stream of compressed air is led to the material through a cutting nozzle to drive out the debris and molten material from the cut kerf (see Fig.8).

The cutting quality is very much dependent on the pressure of the cutting gas. If the pressure is too low, the fluid slag can remain adhered to the cut material, forming a permanent burr or closing the kerf again. If the pressure is too high, the lower edges of the cut can be burnt out and often make the cut unusable. Cutting gas pressure has to be increased increasing the material thickness. Fine jets of air ensure neat cut edges and material surfaces. Weak but wide air jets are beneficial to perform material engraving.

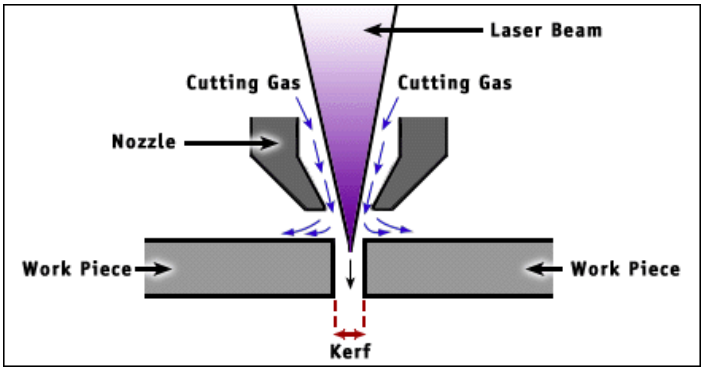

Figure 8. Cutting gas led through a cutting nozzle
http://engineeringdiys.blogspot.com/2016/03/kerf-of-welding.html

CONCLUSIONS

Decorations created on ready denim garments are unique and very different. Therefore the right choice of laser cutting parameters is always very challenging. It depends on desired designs, properties of treated textile materials, as well as, stated process priorities and acceptable compromises between them. Comparing with long time used manual denim decorating methods, laser finishing offers several important advantages:

- possibility to repeat absolutely the same design/image unlimited times,
- high processing speed and quality,

- water-free process using much less energy,
- no health risks to workers, harmless to environment.

The companies manufacturing laser equipment for denim finishing are: Macsa ID (Spain), Iber laser (Spain), Jeanologia (Spain), SEI laser (Italy), Golden Laser (china), Gbos (China),Ant laser systems (China), others (see Fig.2).

REFERENCES

1. *Roshan P. 2015,Denim. Manufacture, Finishing and Applications*. Woodhead Publishing, Elsevier, Cambridge
2. Joykrisna, Solaiman Saha 2015, Comparative analysis of manual fading and laser fading process on denim fabric, *Science Discovery*, Vol. 3(6), pp. 40-49
3. Yuan, G. X., Jiang, S. X., Newton, E., Fan, J. T., & Au, W. M. 2012, Application of laser treatment for fashion design, *Journal of the Textile Institute*, 103, str. 48–54
4. Juciene, M., Urbelis, V., Juchnevičienė, Ž., & Čepukonė, L. 2013, The effect of laser technological parameters on the color and structure of denim fabric, *Textile Research Journal*, Volume: 84 (6), pp: 662-670
5. Kan, C.-W. 2014, CO2 laser treatment as a clean process for treating denim fabric, *Journal of Cleaner Production*, Vol. 66, str. 624–631
6. Nayak, R. and R. Padhye 2016, The use of laser in garment manufacturing: an overview, *Fashion and Textiles*, Vol. 3(1): pp. 1-16
7. Khalil E. 2017, Sustainable and ecological finishing technology for denim jeans, available on: http://www.apparelviews.com/sustainable-ecological-finishing-technology-denim-jeans-2/
8. Brain M. 2018, Levi's will soon rely entirely on lasers to give its jeans that classic finish. available on: https://quartzy.qz.com/1215862/levis-jeans-will-be-broken-in-with-lasers/
9. Vilumsone-Nemes I. 2017, Automation in spreading and cutting, in R. Nayak, R. Padhye, *Automation in Garment Manufacturing*, Woodhead Publishing, Elsevier, Cambridge
10. Vilumsone-Nemes I. 2015, Fabric spreading and cutting, in R. Nayak, R. Padhye, *Garment Manufacturing Technology*, Woodhead Publishing, Elsevier, Cambridge.
11. Vilumsone-Nemes I. 2018,*Industrial Cutting of Textile Materials*, *2nd edition*, Woodhead Publishing, Elsevier, Cambridge
12. I. Nemeša. 2018, Automated laser cutting systems to process textiles, *Tekstilna Industrija*, br.4., 45-52
13. I. Nemeša,.2019, V. Kaplan, Textile finishing by laser, *Tekstilna Industrija*, vol. 67, iss. 1, pp. 33-38
14. I. Nemeša. 2019, E. Csanák, Laser finishing in manufacturing of denim garments, *Tekstilna Industrija*, vol. 67, iss. 4, pp. 20-25

Conference Proceedings
ICPAE 2023, 24th August – 26th August, Zrenjanin, Serbia
University of Novi Sad, Technical Faculty "Mihajlo Pupin", Zrenjanin

Laser Application in Textile and Apparel Industry

Marija Pešić[1*], Ineta Nemeša[1], Edit Csanak[2], Valentina Bozoki[1]

[1]*University of Novi Sad, Technical Faculty „Miahjlo Pupin“, Djure Djakovica nn, 23000 Zrenjanin, Serbia*
[2]*Óbuda Universit, Rejtő Sándor Faculty of Light Industry and Environmental Engineering, Doberdó út 6, Budapest, Hungary*
marija.pesic@tfzr.rs

Abstract. The textile and clothing industry has been facing major changes in recent years. Considering that it is one of the biggest polluter, transformations in this industry are largely directed towards sustainable development. It seeks to transform the clothing industry based on value propositions that integrate ethics, aesthetics and innovation. In order to respond to these changes, one of the ways is the application of lasers in various stages of textile and clothing production. The advantages of laser application are reflected in reduced manufacturing time, reduced material consumption and potential errors and damage, and there is no problem of toxic by-product disposal as is found in some non-laser processes. Laser application also increase productivity, product quality and reduced negative impact to the environment. The application of lasers in cutting, engraving, embossing, denim fading, body measuring, sewing and other applications as well as their advantages and disadvantages are discussed in this paper.

Keywords: laser, fabric, cutting, engraving, sewing

INTRODUCTION

In recent decades, the global interest in sustainability has been growing dramatically in the fashion world, so the textile and fashion industry is facing major changes and reforms that are planned to be implemented by 2030. The large consumption of clothing generates a large increase in the consumption of resources and the generation of waste, which places the fashion industry on the list of industries with the largest economy, but also with the big negative impact on society and the environment [1]. Consumers shape the fashion industry to a large extent, and lately their interest in sustainability has been increasing. Today's consumers are increasingly looking for information about who, where and how their clothes are made. These requirements increasingly encourage the brands themselves to develop new business models based on the integration of ethics, aesthetics and innovation [2].

One of the challenges is posed to the textile and fashion industries, which are expected to turn to ecological and innovative solutions for the production and manufacture of certain products. In order to meet these challenges, laser technologies are increasingly being used in various segments of the textile and clothing industry. There are several applications of laser technology in the apparel industry for cutting, engraving, embossing,

denim fading, body measuring, sewing and other applications, and they are disscused in this paper.

LASER TECHNOLOGY

Laser is being used in apparel industry from 19th century. Laser represents an energy source, whose intensity and power can be precisely controlled. It is an electromagnetic radiation, produced by the atoms due to energy states are changed in some materials. The atoms promoted to higher energy states emit laser in the form of light by the process known as "stimulated emission". Subsequently, this laser is being amplified in a suitable lasing medium with the help of mirrors. The final laser delivers from the equipment as a stream similar to light. The color of the laser depends on its wavelength [3,4].

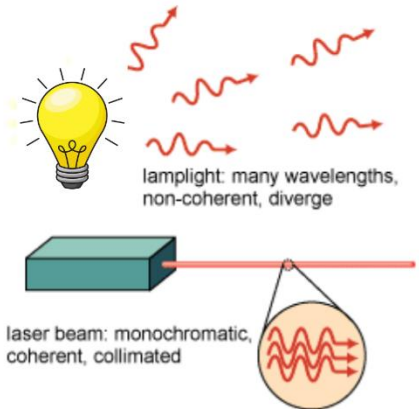

Figure 1. Comparision of laser and ordinary lamplight [5]

Laser light emitted from a laser has four fundamental characteristics: Intensity, coherency, monochromaticity and collimation, which distinguish it from natural light. A high energy concentration per unit area of the beam is present in the laser. A laser beam can be of very high intensity with 1–2 mm of beam diameter and an output power of some milliwatts (mW) [3,4].

Laser dyeing

Laser technology for textile and garment dyeing can offer digital design capabilities combined with the ability for short run production. Unlike the traditional dyeing method that uses a lot of water, dyeing with lasers is a dry technology, and has the potential to offer increased environmental sustainability through significant reduction in energy and wastewater [4].

A laser dyeing technique named peri-dyeing, developed during an Arts and Humanities Research Council, UK is the technique that allows the dye reaction and diffusion to take place at the point of laser material interaction. This technique allows intricate targeted surface design of textile substrates. Dye diffusion and reaction takes

place at the point of interaction between the laser and textile material. The non-contact laser set up allows precision detail to be achieved on three-dimensional textile surfaces, such as textured fabrics or finished garments [6].

Figure 2. Peri-dyeing laser dyeing texhnique [7]

The CAD aspect of the technology facilitates creativity development of the laser-dye process studied in the ability to combine textile engineering with textile design [7].

Laser surface modification – Irradiation

The irradiation of polymeric material by pulsed UV lasers generates characteristic modifications of the surface topography of the polymer beside other effects. The resulting surface properties may have an important impact in textile processing, as they can affect technical properties of the most common synthetic fibers but also with natural fibers such as wool or cotton [8].

In the case of synthetic fibers, irradiation provides better absorption of the dye and a reduction in temperature of the dyeing process. Color Fastness tests of laser irradiated and dyed synthetic fabrics showed that higher-intensity laser irradiation increased the wettability, light, rubbing and wash fastness of the test fabrics, however, properties such as bending rigidity and tensile strength were negatively affected by an increase in laser intensity [8].

Denim finishing

Denim is recognized and used across the globe for its vintage worn out effect, rough, and tough look along with comfort. Despite its popularity, durability and confort, denim manufacturing negatively impacts the environment as it is associated with the use of large amount of water, energy, chemicals, and emission of greenhouse gases. Whitening jeans and obtaining old faded look is more and more often achieved with new laser technologies instead of traditional sandblasting. Laser application in denim finishing is particularly attractive from a production system perspective because lasers can recreate the combined effect of several other chemical and mechanical processes in one single operation [4,9].

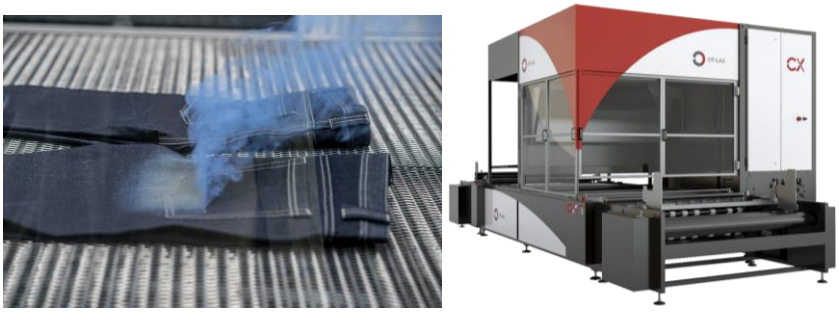

Figure 3. a) Denim laser bleaching, b) CX – T OT – LAS laser machine for bleaching, abrasion and decoration [10]

Laser marking and engraving

The terms laser engraving and laser marking are often used interchangeably, although there are differences between it. Textile fabrics are most often of a small thickness of 0.1 to 5.0 mm and It is more appropriate to apply laser marking for them while engraving is recommended for materials with thickness greater than 2.5 mm. Laser marking is a non-contact impact with a laser beam on the surface of the processed material and the aim is to obtain a lasting contrast image while laser engraving is used to engrave the printing screens, for hollowing, for creating pattern buttons, to engrave leather, denim etc. Pictures, flower patterns and even personalized signatures can be engraved on leather shoes, leather bag, wallet, leather belt, leather sofa and leather clothes, greatly increasing the added value of products [12].

Figure 4. Marking and Engraving textile materials [13,14]

Laser cutting

Laser cutting is a thermal, non-contact separating process for materials using a focused high-powered laser beam. The laser alone evaporates the material, removing layer by layer and creating a very thin cutting gap.The edges are carbonized for fibers of natural origin and melted for synthetic ones. In both cases, their unraveling is prevented. Laser cutting is possible on different materials such aslinen, cotton, silk, felt, as well as Kevlar® or other technical textiles. Advantages of laser cutting technology, compared to conventional methods by mechanical cutting with a knife or other devices are: no

mechanical contact with fabric, no stretching of the material, edges are smooth, without tears and sealed during cutting, laser works with stretch fabrics, loss of material is minimal, high accuracy for intricate designs, possibility to realize fine contours with arbitrary radius, excellent cut quality, high flexibility and individuality, high processing speeds, very narrow neat affected zones, no tool wear [12,15].

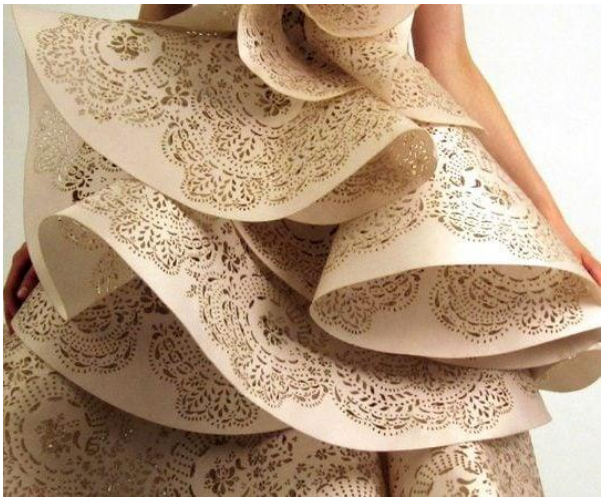

Figure 5. Laser cutting effect [16]

Laser welding

Laser welding is advanced manufacturing technique which is growing rapidly and it represent a welding of thermoplastic textile materials with a laser beam. Laser energy is focused on the point of connection, raising the temperature of the material until it melts and the individual parts connect. The main advantages of this technique over conventional polymeric joining methods and processes, include: ability to weld all thermoplastic textiles including nylon, PP and polyester, carbon fiber reinforced composites; it gives a weld strength capable of reaching strength of the parent material and a seam is clean and have aesthetically pleasing appearance; enables the joint and seam sealing process to be combined into one; high weld speeds up to 20 m/min; multiple layers may be welded simultaneously. The main difference between sewing with needles and welding of garments is the perforations caused by a conventional sewn seam which compromises the integrity and performance of the garment, while welding creates completely sealed seams [4,12].

Laser 3D body skanning

3D body scanners find their application in the textile and clothing industry for the construction of clothes, for making custom-made garments and for creating virtual fitting rooms where shoppers can use a 3D version of themselves to try on clothes no matter where they are [17,18].

There are several technologies that are used for 3D body measurement, one of them is laser technology. This type of 3D scanner uses harmless, invisible lasers to measure the body. They work on the principle of triangulation, projecting a single point, line, or multiple lines onto the subject, and using a video camera offset from the laser source to view the laser light on the subject being scanned. Cyberware, Hamamatsu Photonics, and Human Solutions all manufacture laser scanners. The measurements obtained using this technology are more precise and reproducible than those obtained through the traditional, physical measurement process [18].

Figure 6: The Vitus Smart LC3 is a 3D body scanner designed by Human Solutions, a global manufacturer based in Germany [19]

Laser application of seam pucker

Garment appearance greatly influences garment quality while seam pucker has a negative impact on garment appearance. The laser beam can measure the degree of puckering in garments by geometrical models. In this method a seam in the garment is scanned by a 3D laser scanner by putting the garment on a dummy. The laser head can be moved to any 3D space within a confined place by an operator. It is possible to scan the target object from different angles. A pucker profile of the scanned seam can be obtained by processing the image with a 2D digital filter [4].

CONCLUSION

In this paper, an overview of the possibility of using lasers in the textile and clothing industry is given. The laser technology is one of the technologies that recently has the increasing concern in the textile and garment industry. They are used widely in textile and clothing manufacturing, including cutting, marking, welding, dyeing, printing, measurement applications, bar code scanning, sewing.

The major reasons for wide application of laser in garment industries may be reflected in reduced manufacturing time, reduced material consumption and potential errors and damage, and there is no problem of toxic by-product disposal as is found in some non-laser processes. The benefits of using Laser technologies increase productivity, product quality and reduce negative impact on the environment.

Replacing traditional labor intensive operations with laser technologies offers new opportunities for innovative solutions and is a key issue for the economic success of each industry, inclusive of the textile industry, in the future.

REFERENCES

1. F. R. Rinaldi, 2019, Fashion Industry 2030: reshaping the future through sustainability and responsable innovation, *Bocconi University Press, Milano.*
2. Wen-Jie Yan, Shang-Chia Chiou, 2020, Dimensions of Customer Value for the Development of Digital Customization in the Clothing Industry, *Sustainability 2020,* No12.
3. P.Senthil Kumar, S. Suganya, 2018, Laser – Based Apparel Production, Part of the Textile Science and Clothing Technology book series.
4. Z.Jamal, N. Yadav, S.Rani, 2018, Application of laser technology in textiles, International Journal of home science, 4 (2): 269-274
5. https://collegedunia.com/exams/laser-light-physics-articleid-631
6. K.Akiwowo, F. E. Kane, J.R. Tyrer, G. Weaver, A. Filarowski, 2017, CO2 laser dye patterning for textile design and apparel manufacture, Journal of Textile Engineering and Fashion Technology, Vol.2, Issue 3
7. L. Morgan, J. Shen, J Matthew, J. Tyrer, 2018, Laser Peri-Dyeing for Agile Textile Design: Implementing Laser Processing Pesearch within the Textile Industry, 18th *AUTEX World Textile Conference, Istanbul, Turkey.*
8. https://www.dmu.ac.uk/
9. L. Morgan, Laser Textile Design: The Development of Laser Dyeing and Laser Moulding Processes to Support Sustainable Design and Manufacture, Loughborough University School of the Arts, English and Drama.
10. https://www.raylase.de/en/applications/laser-marking/jeans-bleaching.html
11. R. Nayak, M. George, L. Jajpura, A. Khandual, T. Panwar, 2022, Laser and ozone application for circularity journey in denim manufacturing – A developing country perspective, Current Opinion in Green and Sustainable Chemistry, Vol.38
12. Angelova YP. 2018, Factors influencing the laser treatment of textile materials: An overview. *Journal of Engineered Fibers and Fabrics*. No15.
13. https://www.alldotech.com/fabric-laser-engraving-machine/
14. https://www.mainemedia.edu/workshops/item/laser-engraving-photographs-on-book-cloth/
15. R. Nayak, R. Padhye, 2016, The use of laser in garment manufacturing: an overview, Fashion and Textiles a Springer Open Journal, 3:5, 2-16.
16. https://www.lasercuttingshapes.com/materials/textiles-fabric/
17. Philip Treleaven, Jonathan Wells, 2007, 3D Body Scanning and Healthcare applications, Computer, vol 2.
18. P.Yasotha, K.M.Pachiyappan, C.Sobithaa,G.Nivetha Kanmani,2018, An Elucidate study of laser technology in apparel industry, Jorunal of Emerging Technologies and Innovative Research
19. https://www.aniwaa.com/

Conference Proceedings
ICPAE 2023, 24th August – 26th August, Zrenjanin, Serbia
University of Novi Sad, Technical Faculty "Mihajlo Pupin", Zrenjanin

Modeling Impact of Pollution on the Concentration of Dissolved Oxygen in Moraca River

Slavoljub Mijovic[1], Vladimir Petrovic[2*]

[1]University of Montenegro, Faculty of Natural Science and Mathematics, George Washington 66, Podgorica, Montenegro
[2] Elementary school "Jovan Tomasevic", XVIII street number 6, Goricani, Golubovci, Montenegro*
mvladimir055@gmail.com

Abstract. Streeter - Phelps equation model implies that the concentration of dissolved oxygen in the Moraca river, after the discharge of municipal wastewater, decreases exponentially and at some distance (called the critical distance) reaches minimum. After reaching this minimum, the concentration of dissolved oxygen increases linearly up to the initial (saturation) level. The experimental part of the research showed that there is a minimum of dissolved oxygen concentration located at 1.5 km from the collector for municipal wastewater treatment, but dissolved oxygen doesn't decreases exponentially. The main limitation of this model is taking the same reaeration coefficient for the entire river.

Keywords: Streeter - Phelps equation model, dissolved oxygen, reaeration coefficient

INTRODUCTION

This work presents the results of modeling the impact of pollution on the concentration of dissolved oxygen in rivers using the example of the Moraca river. The theoretical part of the modeling began with the presentation of important factors that influence water quality in rivers in which the processes of respiration and decomposition were particularly highlighted. Solutions of differential equations lead to the Streeter - Phelps equations which implies that the concentration of dissolved oxygen in the river, after the discharge of municipal wastewater, decreases exponentially, until at some distance (called the critical distance) dissolved oxygen in the river reaches minimum [1]. After reaching this minimum, the concentration of dissolved oxygen increases linearly up to the initial (saturation) level.

STREETER-PHELPS EQUATIONS

The wastewater problem began with the organization of the first permanent human settlements. Unfortunately, this problem was solved by bulding cities near the rivers into which the municipal waste was directly discharged. When waste water is dropped into the river system, two processes are most often studied: one is chemical and the other is physical. In the first process, living beings belonging to the river system use dissolved

oxygen, while in the second process, the atmosphere replenishes the dissolved oxygen. Microorganisms living in the river not only rapidly consume dissolved oxygen, in the processes of oxidation of organic matter that is discharged into the river, but at the beginning of the process they consume more oxygen than the atmosphere manages to compensate in the process of reaeration.

Let's analyze the "imaginary" case in which untreated sewage wastewater is discharged into a river at a temperature of 15 °C. The maximum concentration of dissolved oxygen, in this case, is 10 mg O_2/l. At the moment of wastewater discharge, the concentration of dissolved oxygen in the river is close to the maximum. When wastewater is discharged, the concentration of dissolved oxygen approaches zero, and in some cases is equal to zero. As the organic matter is oxidized and the reaeration process is included as a mechanism for compensating dissolved oxygen in the river, the concentration of dissolved oxygen slowly increases. At a certain moment, at some distance from the place of discharge of wastewater, the concentration of dissolved oxygen reaches its original value. This "imaginary" case is shown in the following figure.

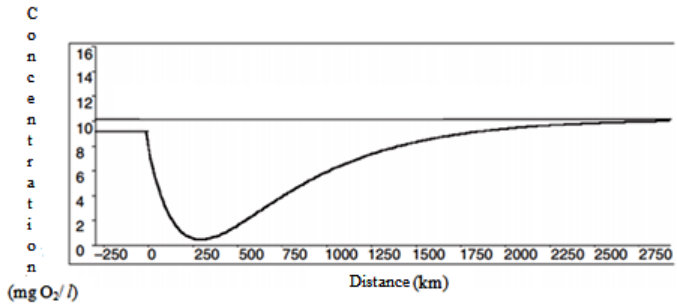

Figure 1. The influence of the discharge of sewage wastewater on the dissolved oxygen concentration of an "imaginary" river.

The minimum concentration of dissolved oxygen, in this "imaginary" case, is located 250 kilometers from the place of discharge of waste water. The initial value of dissolved oxygen concentration is reached 1750 kilometers from the place of discharge of waste water. In order to obtain the Streeter - Phelps equations, we can do the following thought experiment [2]. Put a sugar cube in the bottle. Then we fill this bottle with unpurified water. The bottle is open to the atmosphere. We can write the following balance equations:

$$V \cdot \frac{dL}{dt} = -k_d \cdot L \cdot V, \tag{1}$$

$$V \cdot \frac{do}{dt} = -k_d \cdot L \cdot V \; + \; k_a \cdot V \cdot (o_s - o)\,, \tag{2}$$

k_d – rate of loss of dissolved oxygen by consumption of micro-organisms (deoxidation coefficient);

$k_a -$ rate of replenishment of dissolved oxygen from the atmosphere (reaeration coefficient).

Before we proceed to solve the above system of differential equations, we will simplify the balance equation for oxygen by introducing a new variable representing the dissolved oxygen deficit:

$$D = o_s - o, \tag{3}$$

$$\frac{dD}{dt} = -\frac{do}{dt} \tag{4}$$

If previous expression is substituted into the balance equation for oxygen, the following equation can be written:

$$V \cdot \frac{dD}{dt} = k_d \cdot L \cdot V - k_a \cdot V \cdot D \tag{5}$$

If $L = L_0$ i $D = 0$, at the moment $t = 0$, the solution of the first differential equation in the previous system is obtained:

$$L = L_0 \cdot e^{-k_d \cdot t} \tag{6}$$

This is the first Streeter-Phelps equations. We put this solution in the equation (5) and we can get:

$$\frac{dD}{dt} + k_a \cdot D = k_d \cdot L_0 \cdot e^{-k_d \cdot t} \tag{7}$$

We can solve the previous differential equation by solving the homogeneous and inhomogeneous parts of the equations. We get the following expression:

$$D = \frac{L_0 \cdot k_d}{k_a - k_d}(e^{-k_d \cdot t} - e^{-k_a \cdot t}) \tag{8}$$

This previous expression represents the second Streeter-Phelps equation used in this paper under the assumption that the initial oxygen deficit is negligible. (upstream from the point of discharge of the pollutant is clean water saturated with oxygen) We can change Lo with biological oxygen demand BOD_l and this parametar we can measure by the experiment using this formula:

$$BOD_L = \frac{BOD_5}{1-e^{-k_a \cdot t}} \quad (9)$$

BOD_5 - biological oxygen demand for five day.

If we found first derivative of the dissolved oxygen deficit by time, and then this derivative equalized to zero, we can find following formula to determine critical time:

$$t_c = \frac{1}{k_a - k_d} \ln \frac{k_a}{k_d} \left[1 - \frac{D_0 \cdot (k_a - k_d)}{k_d \cdot BPK_L}\right] \quad (10)$$

Now we can measure critical parameters as: critical time, critical distance, critical deficit of dissolved oxygen and minimum concentration of dissolved oxygen at critical distance. For all this calculation we can use Fate simulation program putting initial parameters for the Moraca river.

THEORETICAL AND EXPERIMENTAL RESULTS

We should be careful when taking the flow of the river into calculation because it changes in different seasons, even during one month. We will model the impact of pollution on the concentration of dissolved oxygen for ten flows of the Moraca river characteristic for the month of May. [3] We will calculate the river velocities for the selected flows. We will determine the minimum concentrations of dissolved oxygen for two river temperatures 14°C and 15°C characteristic for the month of May. We will assume that the river is 110% saturated at the point of sewage discharge.

Table 1. Input parameters for the Moraca river

River flow (m^3/s)	Velocity of river (m/s)
68,34	0,34
398,39	1,99
191,20	0,95
75,62	0,38
84,53	0,42
79,81	0,39
97,23	0,49
152,76	0,76
248,63	1,24
321,57	1,60

The parameters of the model that are considered constant are:

- Waste water flow: 30 260 m^3/day
- BOD_5 of waste water: 104 mg O_2/l
- Waste water temperature: 18 °C
- deoxidation coefficient: $k_d = 0.30\ day^{-1}$
- concentration of dissolved oxygen in wastewater: 1 mg O_2/l
- BOD_5 of the river: 3.0 mg O_2/l

The mean value of the critical distance, for different river flows in the month of May, at a river temperature of 14 °C, is:

$$(2.03 \pm 0.69)\ km,$$

while the mean value of the minimum concentration of dissolved oxygen (DO) is:

$$(10.67 \pm 0.09)\ mg\ O_2/l.$$

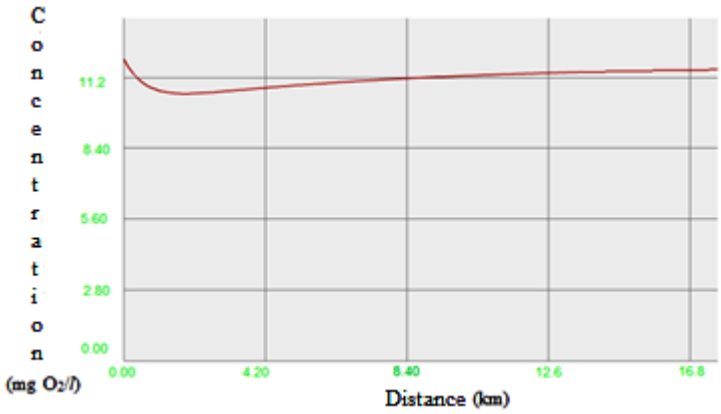

Figure 2. DO concentration curve at a 14°C river temperature.

The mean value of the critical distance, for different river flows in the month of May, at a river temperature of 15°C, is:

$$(1.8 \pm 0.68)\ km,$$

while the mean value of the minimum DO is:

$$(10.58 \pm 0.05)\ mg\ O_2/l$$

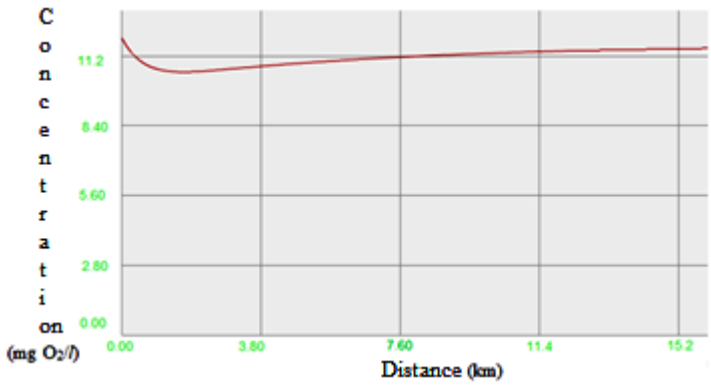

Figure 3. DO concentration curve at a 15°C river temperature.

Figure two and figure three show that when municipal waste water, which is partially or completely purified, is discharged into the Moraca river, there is an exponential drop in the concentration of dissolved oxygen, exactly as predicted by the Streeter-Phelps equation model.

Table 2. Results of experimental research

Distance (km)	Disolved oxygen concentration (mg O_2/l)	River temperature (°C)	Saturation (%)
0,5	11,15	14,4	109,6
1	11,73	14,4	115,3
1,5	10,21	14,6	100,1
2	11,54	14,6	114,2
3,1	11,04	14,4	103,4
3,7	11,18	14,4	106,5
4,4	11,27	14,6	110,7
5,1	11,69	14,6	113,1
6,4	11,37	14,4	110,5
7,3	11,42	14,6	118,7

The minimum concentration of DO was found 1.5 km from the point of discharge of sewage waste water and is 10,21 mg O_2/l. The saturation of the river at this location is the lowest and amounts to 100,1%.

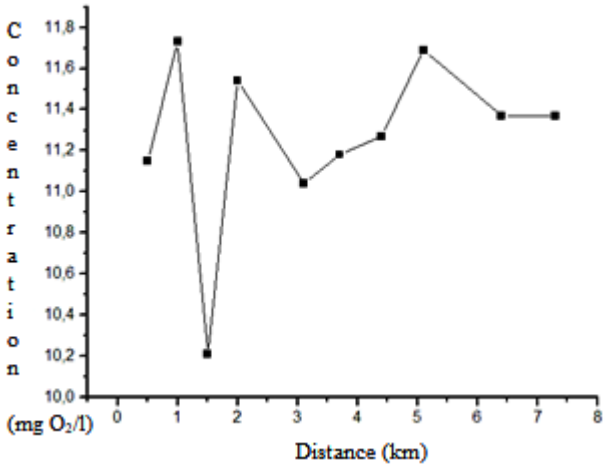

Figure 4. Dependence of DO concentration on distance (experimental results).

As can be seen from the previous picture, the concentration of DO varies from place to place. The experimentally obtained DO concentration values do not show an exponential decline, as predicted by the Streeter-Phelps equation model. The minimum concentration of DO is noticeable both in the theoretical and in the experimental part of the work.

MAIN LIMITATIONS OF THE MODEL

In the classic Streeter-Phelps model, it is assumed that the reareration coefficient is the same for the entire river. However, the speed of the river is not the same for different distances from the wastewater treatment collector.. Not taking into account the variation of the reaeration coefficient is one of the main limitations of this model. We could expect a higher level of agreement between the theoretical prediction and the experimental data during the summer months when the river velocity is uniform.

Another major limitation of the model is the assumption that oxygen is replenished only from the atmosphere. This cannot be true considering that plants, observed along the river, can produce oxygen through the processes of photosynthesis. The third major limitation of the model is that it doesn't take into account the sediment that is located at the bottom of the river. Microorganisms in the sediment, by consuming dissolved oxygen, can affect the concentration of dissolved oxygen in the river. It is also possible to point out here the assumptions that were made, which may affect to the theoretical and experimental results: the temperature of the river is the same during the day, the deoxidation coefficient doesn't change, the biological oxygen consumption of wastewater doesn't change, the amount of municipal wastewater discharge doesn't change.

CONCLUSION

In general, the self-purification ability of the river at the end of May is very high, especially due to the high speed of the river. The reaeration coefficient, which represents the rate of replenishment of dissolved oxygen in the river, is directly proportional to the river's speed. However, in the summer months, when the speed of the river decreases, the reaeration coefficient decreases, which leads to anaerobic conditions or spreading unpleasant smell near the wastewater treatment collector. The minimum concentration of dissolved oxygen is located at a greater distance compared to the month of May, and generally the concentration of dissolved oxygen in the river is lower. This indicates that it is necessary to build a new collector for the treatment of wastewater, remove silt from the bottom of the river and bild mechanisms of artificial reaeration along the river.

The theoretical part of the modeling continued using the Fate software program. River flows and temperatures were taken as input parameters of the Moraca river for May. After the theoretical part of the modeling, the analysis of the experimental part of this work completed at the end of May 2022. The experimental part of the research showed that, for the river temperature of 14.6 °C, minimum dissolved oxygen concentration of 10.21 mg O_2/l is located 1.5 km from the collector for municipal wastewater treatment, but concentration of dissolved oxygen doesn't decreases exponentially.

Analysis of the sensitivity [4], and limitations of the model indicated the necessity of taking into account other factors that influence on the concentration of dissolved oxygen in the Moraca river, of which the following factors must be highlighted:

- replenishment of dissolved oxygen is not only carried out through the atmosphere but also in the processes of photosynthesis;
- microorganisms that exist in the sediment of the river also consume dissolved oxygen and in this sense, we can analyze sediment oxygen demand.

Comparing experimental data on the concentration of dissolved oxygen in the Moraca river with the theoretically predicted values of the minimum concentration of dissolved oxygen, which with certain deviations correspond to the real situation, justified the use of the Streeter - Phelps equations model and indicated the validity of using this model for any river that is located in Montenegro or somewhere else in the world.

REFERENCES

1. F. M. Dunnivant, E. Anders. *A basic introduction to polutant fate and transport*. Wiley interscience, Canada, 2006.
2. S. Mijovic. *Modeling the dispersion of pollutants (material for students*). University of Montenegro, Faculty of Science, Podgorica, 2020.
3. M. Knezevic. *Study - water regime of Moraca river and Scadar lake*. Green home, Podgorica, 2009.
4. S. Rinaldi, R. Soncini-Sessa. *Sensitivity analiysis of Streeter-phelps models.* International institute for applied systems analysis, Austria, 1977.

Conference Proceedings
ICPAE 2023, 24th August – 26th August, Zrenjanin, Serbia
University of Novi Sad, Technical Faculty "Mihajlo Pupin", Zrenjanin

Impacts of Extreme Space Weather Events: Ionosphere and Primary Cosmic Rays

Mihailo Savić[1*], Aleksandra Kolarski[1], Nikola Veselinović[1], Vladimir Srećković[1], Zoran Mijić[1], Aleksandar Dragić[1]

[1]*Institute of Physics Belgrade, Pregrevica 118, Belgrade, Serbia*
msavic@ipb.ac.rs

Abstract. Extreme space weather events have potential severe impact on wide areas of human activities, from a direct radio wave interference effect on Global Navigation Satellite System (GNSS) transmission to high-frequency radio wave blackout and magnetic field variation. Ionospheric reactions to severe solar flares (SFs) and coronal mass ejections (CMEs) have been studied for several decades as an essential feature in space weather applications. In this study X-class SFs ionospheric impacts and the effects of accompanied heliospheric disturbances on primary cosmic rays (CR) occurred in September 2017 are investigated. The atmospheric D-region parameters are obtained and analyzed along with various heliospheric parameters associated with the accompanying interplanetary CME and flux of secondary cosmic ray muons. The results of both multi-instrumental observations and numerical simulations can be useful for application in space weather predictions.

Keywords: solar flares, sudden ionospheric disturbances, solar energetic particles, secondary cosmic ray flux

INTRODUCTION

Varying conditions in our Solar system, commonly known as space weather, are primarily driven by the dynamic processes on the Sun, especially in the case of extreme events induced by the Sun's magnetic activity, specifically solar flares (SFs) and coronal mass ejections (CMEs). Although the clear connection between these two effects is not easily established, SFs are often followed by CMEs, particularly in the case of more intense events [1].

Interest in studying such phenomena is currently as high as has ever been. Many methods and techniques can be effectively used to monitor space weather, some of them utilizing Earth-based detectors. Currently, when an increasing number of satellite instruments are available, such ground-based experiments remain relevant and have a potential comparative advantage because of their cost-effectiveness and specific location. The latter quality is of particular interest, as mentioned phenomena can have significant effect on Earth's immediate environment and man-made systems [2,3].

Two such ground-based detectors' systems are located at the Institute of Physics Belgrade and are effectively employed in the study of extreme space weather. These systems include the Belgrade very low frequency (VLF) receiver and the Belgrade Muon

station. We will illustrate the effectiveness and usability of these stations on the example of an extreme event that occurred on the Sun in early September 2017.

METHODOLOGY

September 2017 was a very active month in the descending phase of the 24th solar cycle, during which a number of significant solar flares were observed. Here we focus on the strongest one that occurred on September 6th. This was a very intense event classified as X9.3, and was followed by a CME directed toward Earth.

Absolute Phase and Amplitude Logger (AbsPAL) station, located in Belgrade (44.85°N; 20.38°E) was used for monitoring VLF signal emitted from military transmitter in Skelton (54.72°N; 2.88°W), UK on frequency 22.1 kHz, with code name GQD. Simultaneous monitoring of VLF signals' amplitude and phase in regular and perturbed ionospheric conditions allows retrieval of perturbation characteristic and modeling of ionospheric plasma properties [4-7]. The propagation parameters of sharpness and reflection height were retrieved using numerical simulations based on measured VLF signal perturbations related to the X9.3 SF, with electron density height profile variation obtained using Wait's empirical approach [8].

Belgrade CR Muon station is an integral part of the Low-background Laboratory for Nuclear Physics at the Institute of Physics Belgrade, effectively sharing the location with the Belgrade AbsPAL station. It comprises two identical detector setups: one on the ground level and another located 12 m underground. Both detectors are capable of measuring the flux of secondary cosmic ray muons with high efficiency [9]. The passage of a CME through interplanetary space (reffered to as interplanetary coronal mass ejection - ICME) modulates the flux of primary cosmic rays (CRs), leading to an effect known as a Forbush decrease (FD) [10]. This reduction in the primary CR flux is propagated and can be detected in the flux of secondary cosmic rays. A worldwide network of ground-based detectors, including the Belgrade Muon Station, performs routine measurements and is capable of detecting such events. Additionally, the passage of an Earth-directed ICME can lead to an increased proton flux, most likely due to particles being locally accelerated by the ICME shock [11]. Such an increase can be detected in relative vicinity of Earth by the ERNE instrument. This instrument is located at L1, on-board the SOHO satellite, and performs continuous measurements of proton flux in a number of energy channels [12]. A relationship between the shape of proton fluence spectra at L1 (more specifically, power exponents in the double-power law function used to model the spectra) and the magnitude of FD events has been established [13]. This dependence is especially significant in the case of FD magnitude corrected for magnetospheric effects. This fact allows us to predict FD magnitudes solely based on the fluence parameters derived from SOHO/ERNE measurements, as demontrated here for the FD associatted with the September 2017 X9.3 SF.

RESULTS AND DISCUSSION

Simultaneous variations of X-ray flux (measured by GOES-15 satellite [14]), phase and amplitude of GQD/22.10 kHz signal versus universal time UT during occurrence of

X2.2 and X9.3 class SFs of September 6th, 2017 is presented in Figure 1. Recorded amplitude and phase perturbation on monitored GQD signal increased several dB in amplitude (7.09 dB) and tens of degrees in phase (52.03°) compared to unperturbed values during September 3rd, 2017. In addition, following the incident soft X-ray radiation numerical simulations exhibited changes in electron density profiles, showing the increase of several orders of magnitude compared to their unperturbed values at the reference height of 74 km.

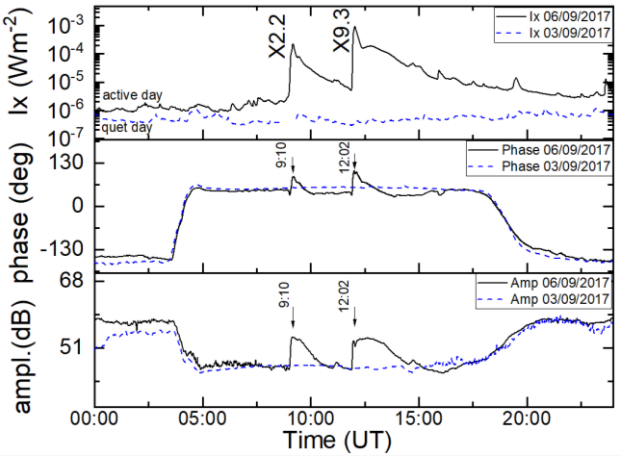

Figure 1. Simultaneous variations of X-ray flux, phase, and amplitude of GQD/22.10 kHz signal on September 6th, 2017.

The proton flux measured by SOHO/ERNE instrument during a period around September 6th 2017, for a selected energy channel is shown in Figure 2. Dashed red lines indicate the time interval for which the increased proton flux was determined to be a consequence of the passage of the ICME associated with the X9.3 SF. Proton flux within this interval was integrated (the respective area under the graph indicated by the red fill color) to determine the differential fluence for the selected energy channel for the event, with the green line marking the interval used for baseline determination.

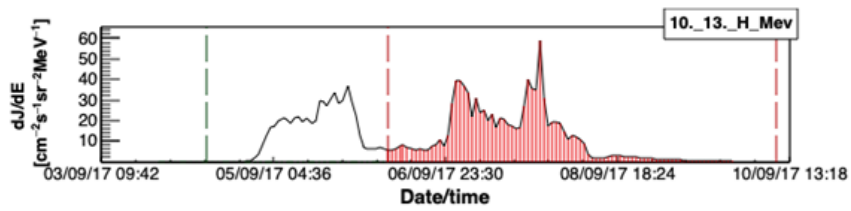

Figure 2. Proton flux in a selected SOHO/ERNE energy channel. Dashed red lines indicate the time period associated with the September 6th 2017 event and used to calculate the differential fluence value.

Based on thus calculated differential values, a fluence spectrum associated with the September 6th event was created, as shown in Figure 3. The blue line indicates the double-power law function used to fit the fluence spectrum.

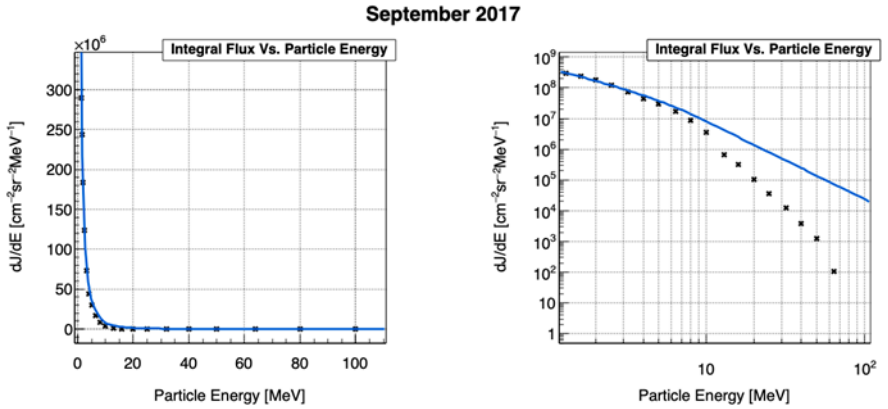

Figure 3. Proton fluence spectra for the September 6th 2017 event, shown in linear (left) and log-log scale (right). Double-power law function used to fit the spectra is indicated (solid blue line).

Using the first of the two power exponents (one related to lower energies and considered to be more reliably determined), FD magnitude (M) and FD magnitude corrected for the magnetospheric effects (M_M) were calculated. The obtained value for M_M of -8.3% was in reasonably good agreement with the value found in the IZMIRAN database [15], which reported a value of -7.7% (with relative difference between two values of 7%). For M (which is generally less reliably determined) we obtained the value of -8.1%, while value found in the IZMIRAN database is -6.9%, resulting in somewhat larger relative difference of 15%.

CONCLUSION

An complementary overview of the impact of the intense solar flare that occured on September 6th 2017, on Earth's immediate environment is presented. A substantial disturbance in Earth's ionosphere was detected, with the amplitude of the GQD signal increasing by several dB and tens of degrees in phase. Simulated electron density profiles showed similariliy drastic perturbation. The passage of the related ICME directed toward Earth led to a significant increase of proton flux measured at L1. It also significantly affected the flux of primary cosmic rays resulting in a Forbush decrease of considerable magnitude. Based on the analysis of fluence spectra of these energetic protons the estimated value for FD magnitude corrected for magnetospheric effects was calculated and was found to be in good agreement with the value found in the IZMIRAN FD data-base.

ACKNOWLEDGEMENTS

This work was funded by the Institute of Physics Belgrade, University of Belgrade, through a grant by the Ministry of Science, Technological Development, and Innovations of the Republic of Serbia.

REFERENCES

1. Yashiro S, Gopalswamy N, 2008, Statistical relationship between solar flares and coronal mass ejections. *Proc. of the International Astronomical Union*, *4* pp 233-243
2. Yasyukevich Y, Astafyeva E, Padokhin A, Ivanova V, Syrovatskii S, Podlesnyi A, 2018 The 6 September 2017 X-Class Solar Flares and Their Impacts on the Ionosphere, GNSS, and HF Radio Wave Propagation *Space Weather, 16* 1013-1027
3. Marov M.Y, Kuznetsov V.D, 2015, Solar Flares and Impact on Earth. In: Pelton, J., Allahdadi, F. (eds) Handbook of Cosmic Hazards and Planetary Defense. Springer, Cham.
4. Kolarski A, Veselinović N, Srećković V.A, Mijić Z, Savić M and Dragić, 2023, Impacts of Extreme Space Weather Events on September 6th, 2017 on Ionosphere and Primary Cosmic Ray, *Remote Sens*. 15 1403
5. Silber I, Price C, 2017, On the use of VLF narrowband measurements to study the lower ionosphere and the mesosphere–lower thermosphere, *Surv. Geophys*. 38 407–441
6. Kolarski A, Srećković V.A, Mijić Z, 2022, Response of the Earth's Lower Ionosphere to Solar Flares and Lightning-Induced Electron Precipitation Events by Analysis of VLF Signals: Similarities and Differences, *Appl. Sci.* 12 582.
7. Barta V, Natras R, Srećković V, Koronczay D, Schmidt M and Šulic D, 2022, Multi-instrumental investigation of the solar flares impact on the ionosphere on 05–06 December 2006, *Front. Environ. Sci.* 10:904335.
8. Wait J.R, Spies K.P., 1964, Characteristics of the Earth-Ionosphere Waveguide for VLF Radio Waves, US Department of Commerce, National Bureau of Standards, Gaithersburg MD, p.110.
9. Dragić A., Udovičić V, Banjanac R, Joković D, Maletić D, Veselinović N, Savić M, Puzović J, Anicin I, 2012, The New Setup in the Belgrade Low-Level and Cosmic-Ray Laboratory, *Nucl. Technol. Radiat. Prot.* 26. 10.2298/NTRP1101064N.
10. Cane H.V, 2000, Coronal Mass Ejections and Forbush Decreases, *Space Sci. Rev. 93*, 55-77
11. Desai M, Giacalone J, 2016, Large gradual solar energetic particle events. *Living Rev. Sol. Phys. 13*, 3
12. http://esdcdoi.esac.esa.int/doi/html/data/heliophysics/soho/ERNE.html
13. Savić M, Veselinović N, Dragić A, Maletić D, Joković D, Udovičić V, Banjanac R, Knežević D, 2022, New insights from cross-correlation studies between solar activity indices and cosmic-ray flux during Forbush decrease events, *Adv. Space Res. 71, 2006-2016*
14. NOAA National Centre's for Environmental Information. Available on the following link: https://satdat.ngdc.noaa.gov/sem/goes/data/avg/
15. http://spaceweather.izmiran.ru/eng/dbs.html

Conference Proceedings
ICPAE 2023, 24th August – 26th August, Zrenjanin, Serbia
University of Novi Sad, Technical Faculty "Mihajlo Pupin", Zrenjanin

Artificial Intelligence: Possible Application in Photoacoustics and Education

Mladena Lukić[1*], Dragana Markušev[2], Žarko Ćojbašić[3], Dragan Markušev[2]

[1*]*Faculty of Occupational Safety, Čarnojevića 10a, Niš, Serbia*
[2]*Institute of Physics, National Institute of the Republic of Serbia, University of Belgrade, Pregrevica 118, 11080 Beograd-Zemun, Serbia*
[3]*Faculty of Mechanical Engineering, Aleksandra Medvedeva 14, Niš, Serbia*
mladena.lukic@znrfak.ni.ac.rs

Abstract: In the past decades artificial intelligence (AI) has become an important tool for environmental research and applications. In this paper AI application within infrared photoacoustic spectroscopy (PAS) is discussed. Photoacoustic spectroscopy, as powerful techniques for trace gases monitoring achieves a high sensitivity and selectivity, primarily due to high-power lasers utilization. However, variations of the main parameters of high-power lasers can cause significant measurement errors. We applied a few AI techniques on a set of theoretical and experimental photoacoustic (PA) signals to simultaneous determination of parameters: the laser beam spatial profile $R(r_L)$, distance from the laser beam to the detector r^*, laser fluence Φ, and vibrational-to- translational relaxation time τ_{V-T}. Obtained results suggest that intelligent PA approach could fulfill requirement for developing modern, easy handling a trace gas monitoring devices with high accuracy, real time operation and self-correction capability. Also, we proposed AI as a promising tool for modeling new approaches to environmental physics issues using intermolecular potentials as an example. Employing AI tools can change the way students are taught, providing fast feedback to students, and deeper understanding of physical principles governing atmospheric phenomena.

Keywords: artificial intelligence, photoacoustic spectroscopy, spatial laser beam profile, vibrational-to-translational relaxation time, intermolecular potentials

INTRODUCTION

Trace gases play a significant role in various atmospheric phenomena leading to environmental pollution and consequently to acceleration of climate change. Also, they are important in industrial process control analysis, combustion processes, agriculture, food industry, and workplace safety. Negative impacts of trace gases could be studied more profoundly through development of more sensitive and selective detection techniques. Photoacoustic spectroscopy (PAS) is a powerful, sensitive, selective, and robust technique with wide dynamic range, simple setup, and easy calibration [1,2]. As a calorimetric, zero-background technique, PAS provides valuable data regarding IR absorption and relaxation of trace gases, which are useful for global warming and climate modeling. PA experimental setup has three main parts: laser (as radiation source), PA cell and detector (microphone, quartz tuning fork, cantilever, etc. [3]). Sensitivity and selectivity of PA detection are

determined primarily with the quality of radiation source and detector characteristics. High-power CO_2 laser is preferable radiation source in PAS of gases, allowing detection limits in the part-per-billion (ppb) and sub-parts-per-trillion (sub-ppt) levels of concentration [4]. Molecules in the gas sample absorb laser radiation (in the wavelength range from 9 to 11 μm, where majority of greenhouse gases have strong fundamental rovibrational transitions) and relax in mutual collisions, transferring energy mostly from vibrational to translational modes (V-T relaxation). V-T relaxation describes by vibrational-to-translational relaxation time τ_{V-T}. Absorbed energy release through nonradiative channel heating the sample. Local variations of temperature cause pressure variations and appearance of acoustic waves. Relaxation time τ_{V-T} as an important parameter takes part in electromagnetic radiation and matter interaction, in calculation of energy transfer collisional rate, energy transfer probability, collisional cross-section, and in theoretical models of energy transfer in the atmosphere.

Although high-power lasers provide various benefits for environment monitoring (sensitivity, selectivity, wide dynamic range, and good spatial and temporal resolution [1]), laser beam quality can be a critical issue in real-world applications. Intensity fluctuations between two successive pulses, and a varying intensity profile can affect sensitivity of trace gases detection [5]. The influence of the spatial laser beam profile on the relaxation time and correspondingly calibration, sensitivity and selectivity of PA detection have been discussed in detail in following papers [5,6]. The laser radiation profile can be measured by conventional devices, mostly for limited range of laser power and fluence Φ, due to harmful effect. Whereas progressive development of high-power lasers has not been followed by the adequate advancement of conventional devices for spatial laser profile measurements, we applied artificial intelligent (AI) methods for simultaneous determination of PA signal parameters (profile shape class $R(r_L)$, radius of the spatial profile of laser beam r_L, laser fluence Φ, distance from lasers to detector r^*, and relaxation time τ_{V-T}) [7]. PAS field measurements could be improved by AI because of its unique characteristics such as: real-time operation, adaptability to environment, possibility to deal with uncertainty, subjectivity, and indeterminacy. In this paper we will review implementation of Multilayer Perceptron (MLP), Generalized Regression Neural Network (GRNN) and the Adaptive Neuro-Fuzzy Inference System - ANFIS) within PAS [7-10]. Evaluation of AI techniques was accomplished on a set of simulated/experimental signals generated in two gas mixtures containing absorber (SF_6 and C_2H_4) and buffer gas (Ar).

In recent years, the application of AI in traditional education systems has attracted the attention of many educators and researches. AI offers new learning experience through different opportunities to teach, learn, and evaluate students [11]. In this paper we proposed the application of neural networks for molecule type determination (monoatomic, diatomic, or polyatomic), based on the potential curve shape. Based on our experience with AI implementation we believe that this approach could clarify and enable deeper understanding of different concepts within the physics curriculum.

METHODOLOGY

Photoacoustics – theoretical background

The sound and heat waves generated in the sample can be described by the classical laws of fluid mechanics and thermodynamics. In PAS, sound waves can be considered independently of thermal ones due to their different properties and spatial separation. Pressure variations ($\Delta p < 10\%$) can be represented by a linearized wave equation (1) [12]:

$$\frac{\partial^2 \delta p(r,t)}{\partial t^2} - c^2 \Delta \delta p(r,t) = S(r,t). \quad (1)$$

The quantity $\delta p(r,t)$ is the pressure variation from the equilibrium value, c is the speed of sound in the sample, and $S(r,t)$ is the source function, determined by the spatial and temporal characteristics of the sound source. Spatial characteristics are defined by spatial distribution of excited molecules after absorption, while time characteristics provide information about energy release (i.e., of the relaxation rate). To solve wave equation (1) for a certain source function and defined initial and boundary conditions, the commonly used methods are: Fourier transform method and Green's function method. For simple spatial laser beam profiles (top hat, Gauss, Lorentz, etc.) and the exponential decay of excitation energy, the solutions of the wave equation (1) calculated by the Fourier transform method, have a form [12]:

$$\delta p(r^*, t^*) = \frac{RE_0}{C_v V} \int_0^\infty (l^2 + \varepsilon^2)^{-1} (-\varepsilon \exp(-\varepsilon t^*) + l \sin l t^* + \varepsilon \cos l t^*) J_0(l r^*) h(l) l dl. \quad (2)$$

Quantities r^* and t^* are dimensionless - reduced coordinate and the reduced time. They are the function of radius of laser beam ($r^* = r/r_L$, and $t^* = tc/r_L$), R is the universal gas constant, E_0 is absorbed energy, V is the irradiated volume, C_V is the molar heat capacity at constant volume, $l = kr$, is a dimensionless quantity (k is the wave vector). J_0 and J_1 are the first-kind Bessel functions of orders 0 and 1. Dimensionless parameter $\varepsilon = r_L/c\tau_{V-T}$ is the most important in this study, because the shape and intensity of PA signals is a function of ε and relaxation time τ_{V-T}. The wave equation (1) could be solved for complex spatial profile of laser beam and nonexponential decay by the Green's functions method. The general solution has a form [13]:

$$\delta P(\boldsymbol{r}, t) = \int d^3\boldsymbol{r}' \int dt' g(\boldsymbol{r}, t|\boldsymbol{r}', t') S(\boldsymbol{r}', t') = -\frac{\partial T(0)}{\partial t} G(r,t) - \int_0^t \frac{\partial^2}{\partial t^2} G(r, t-t')\, dt' \quad (3)$$

where $g(\boldsymbol{r}, t|\boldsymbol{r}', t')$ is the Green's function for a 3D wave equation, $S(\boldsymbol{r}', t')$ is the source function and $G(r, t - t')$ is the Green's function averaged in cylindrical geometry. It allows to calculate PA signal for an arbitrary laser beam profile and excitation energy decay.

Theoretical computations are based on the characteristics of used PA setup: TEA CO_2 laser with a 45ns FWHM pulse, stainless-steel photoacoustic cell (18.5 cm long), and microphone (Knowles Electronics Co., Model 2832) placed in the cell. The experimental settings contained optical (beam splitter, lenses) and additional instruments (joulemeter, photon-drag detector, oscilloscopes), a vacuum system and a system for introducing gases.

We examined PA signal generated in two gas mixtures SF_6+Ar and C_2H_4+Ar. Measurements were performed in the mixture pressure range of 10–100 mbar and fluence range of 0.2–1.5 Jcm^{-2}. Absorbers pressure (SF_6 and C_2H_4) was kept constant at 0.47 mbar [5].

Artificial intelligence techniques

For simultaneous determination of PA signal parameters, we have employed MLP, GRNN and ANFIS [14].

MLP is a feed-forward neural network consisting of an input layer, hidden layers, and output layer. MLP architecture represents a tradeoff between complexity, execution time, and available data. Optimal network topology is selected through many trial-and-error processes. MLP used in this research is trained in an offline batch training regime, with standard backpropagation (BP) algorithm. For network training pairs of input–output data are used. To achieve good generalization capability data set was divided into training, validation, and test set.

GRNN is a viable alternative to MLP. The trial-and-error processes for getting optimal MLP architectures might be a very time demanding process, inconvenient for insitu measurements. GRNN network has a fixed structure, fast training process and it is suitable for dealing with experimental, noisy data. The number of neurons in hidden layer is equal to the number of training data. The data set divides into training and test data.

ANFIS has numerous advanced characteristics such as adaptability, robustness, and insensitivity to variations. It is an adaptive feedforward network consisting of several adaptive interconnected nodes. Fundamental issues in fuzzy logic implementation are fuzzy set, membership function, linguistic variables, and linguistic rule. Elements of a fuzzy set belong to set with different degrees. The most important fuzzy logic issue is the concept of linguistic variables and linguistic if-then rules. Fuzzy sets and fuzzy rules form the knowledge base as a crucial decision-making element in a fuzzy inference system (FIS). ANFIS uses Takagi–Sugeno fuzzy inference system.

RESULTS AND DISCUSSION

For fast and effective atmospheric pollutant detection the possibility to detect different molecules with the same instrument is an advantage. We applied a few AI techniques to assess whether sensitivity and selectivity (as inherent PAS features) could be supported by intelligent PAS.

Simultaneous determination of vibrational to translational relaxation time and spatial profile of laser beam in SF_6+Ar and C_2H_4+Ar gas mixtures

Molecule SF_6 is one of the most harmful greenhouse gasses. It has extremely high global warming potential (23,900 over 100 year time horizon) and a long lifetime of about 3,200 years. As a great IR absorber, and efficient collisional energy transfer partner under atmospheric pressure, SF_6 has an immense potential to affect climate in the future. Values of V-T relaxation time indicate his ability to absorb and transfer a large amount of energy for a wide range of radiation source energies and frequencies [15].

Unlike SF_6, molecule C_2H_4 is an atmospheric pollutant created primarily by exhaust emission. Molecule C_2H_4 is important for ozone formation, and tropospheric chemistry as a participant in ozone-alkene reactions. These two molecules are suitable for AI performance test due to very dissimilar absorption potentials, and consequently intensity and shape of the PA signals (Fig 1).

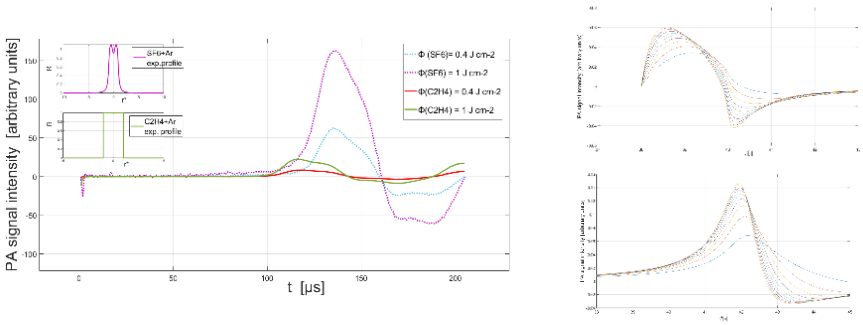

a) b)

Figure 1. a) PA signals generated in SF_6+Ar (dotted line) and C_2H_4+Ar (solid line) for low and high laser fluence ($\Phi = 0.4\ \mathrm{J/cm^2}$ and $\Phi = 1.0\ \mathrm{J/cm^2}$). b) PA signals used for MLP and GRNN training (figures show 10 theoretical signals for both mixtures for clarity).

MLP is used for estimation of parameters of PA signals generated in SF_6+Ar mixture. Different networks topologies with 21-28 input neurons, two hidden layers with 7-15 neurons each, and 3 output neurons are created for estimation of r^*, ε, and the profile shape class (Gauss, top hat, and Lorentz profile). According to our experimental setup and conditions values of r^* were taken from interval [39-42], for each profile shape, and ε values were in the range [0.5-5] [8,9]. In this paper, Artificial Neural Networks (ANNs) were trained on theoretical data and tested with simulated/experimental data. For example, network topology 28-7-7-3 estimated parameters r^* and ε of unknown (simulated PA signal) with precision of 0.1 % and 3 % respectively [8]). Obtained results sugest that if sufficient amount of simulations and/or experimental data are provided, ANNs are capable to estimate PA signal parameters efficiently. It confirms that the set of theoretical PA signals (2) and (3) contain relevant informations for a complete representation of the problem to be solved. To test the capability of the MLP for unknown parameters estimation, more realistic Lorentz with the hole laser beam profile, was used to train network. Theoretical PA signal which is calculated based on network outputs ($r^*$and ε) fitted the experimental PA signal with satisfactory accuracy (errors for the parameter $r^*$and ε were 2.5%, and 9% respectively) [9]. Slightly higher errors are caused by differences between theoretical and experimental laser beam profile and presence of noise in experimental signals.

We used GRNN for simultaneous determination of unknown parameters of the PA signals generated in C_2H_4+Ar mixture. GRNN was trained with theoretical PA signals calculated by Fourier method (2). Theoretical signals were calculated for parameters $\varepsilon \in$ [0.5-4] and $r^* \in$ (39, 39.5, 40, 40.5). Photoacoustic signals are sampled at 21 points [16]. GRNN topology had 21 input neurons, as well as an MLP network. The number of neurons in the hidden layer was 284. Outputs neurons estimate parameters r^* and ε. The most accurate results obtained by GRNN for simultaneous determination of unknown parameters

of experimental PA signal generated in C_2H_4+Ar mixture, were 1.57% for ε and 0.08 % for r^* (the value of r^* is more accurately determined in all cases, because PA signals with different r^* values are clearly separated [8,9]).

Neuro-fuzzy determination of absorption efficiency by PA signal intensity analysis

Spatial and temporal laser beam characteristics, relaxation time, and PA signal intensity and shape are laser fluence Φ dependent quantities. Laser fluence is an important experimental parameter which variations could affect the ratio between the absorption efficiency of the different trace gases. We used ANFIS to predict Φ values based on PA signal intensity [10]. ANFIS inputs were maximum, and minimum of PA signal intensity, while output was corresponding Φ value. Theoretical PA signals for ANFIS training were calculated for the laser profiles which provide the best match with the experimental signals (for both gas mixtures). ANFIS is estimated Φ values from experimental signals generated in SF_6+Ar and C_2H_4+Ar mixtures for $\Phi \in (0.2 - 1.4)\,\mathrm{J/cm^2}$ [10]. Several obtained results are shown in Table 1.

Table 1. ANFIS estimation of **Φ** from PA signals generated in SF_6+Ar and C_2H_4+Ar mixtures

Experimental **Φ** values ($\mathbf{J/cm^2}$)						
SF6+Ar	0.4	0.6	0.8	1.0	max error (%)	average error (%)
SF_6+Ar gas mixture						
ANFIS estimation	0.33	0.47	0.81	0.99	22.05	9.32
ANFIS error (%)	17.20	22.05	1.36	0.67		
C_2H_4+Ar gas mixture						
ANFIS estimation	0.43	0.64	0.79	1.07	26.05	9.80
ANFIS error (%)	7.62	7.12	1.08	7.14		

In both cases for higher Φ values ANFIS achieves better precision. Discrepancy is more obvious for low Φ values due to more pronounced noise influence (low S/N ratio). Average error is slightly higher for C_2H_4 (9.80 %) than for SF_6 (9.32 %), reflecting the vast difference in the absorption characteristics, and PA signal intensity. Despite that facts it does not affect ANFIS performances significantly.

Neural networks application in physics - molecule type determination

One of the critical issues within environmental physics teaching is to study, analyze and simplify complex physical and chemical processes that constantly occur in the atmosphere. The first step in clarifying those phenomena might be to define intermolecular potentials that can match real ones. To help students to assess and identify gaps in their knowledge, and to be able to improve their understanding of connection between molecule type and intermolecular potential, we proposed MLP application. Unlike previously used MLP (as a function approximator), for determination of molecule type (monoatomic, diatomic, or polyatomic) based on Lennard-Jones 12-6 potential, we utilized MLP as a classifier. We analyzed potential curves of six molecules: He, Ar, H_2, Cl_2, CO_2, C_6H_6. Potential curves shape calculated using Lennard-Jones 12-6 potential [17].

$$U(r) = 4\varepsilon\left[\left(\frac{\sigma}{r}\right)^{12} - \left(\frac{\sigma}{r}\right)^{6}\right], \tag{4}$$

where ε represents depth of the potential well, and σ is a molecular distance at zero energy.

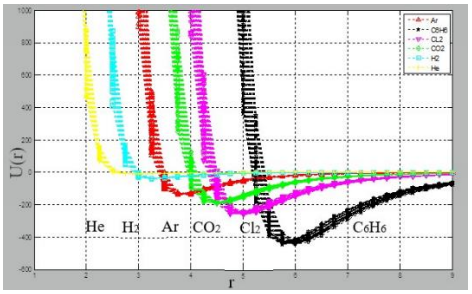

Figure 2. The data set for network training consists of 300 potential curves for six different molecules He, Ar, H_2, Cl_2, CO_2, C_6H_6.

The data set for network training (300) obtained by varying the corresponding parameters ε and σ of the potential curves of each molecule in the range of ±2.5% (Figure 2). Each potential curve is sampled in 33 points which are used as network inputs. MLP for molecular type classification consisted of 33 input neurons, one hidden layer with 35 neurons and outputs with 6 neurons (one neuron for each molecules class He, Ar, H_2, Cl_2, CO_2 или C_6H_6). Output classifies the certain potential curve according to criteria – belong to a given class (1) or not (0). The data set was divided into a training set (210 curves), validation set (45 curves) and test set (45 curves). Obtained results indicate that if potential curves define unequivocally, then MLP can associate the appropriate type of molecule (output) to corresponding potential curve (input).

CONCLUSION

We presented application of several AI techniques for simultaneous determination of radius of the laser beam spatial profile, τ_{V-T} relaxation time, and laser fluence, based on PA signal temporal shape analysis. In PAS experiments variations of these parameters can affect accuracy of measurements significantly. Also, different methods for τ_{V-T} could give quite different results, depending on laser beam spatial profile which is used. Implementation of AI could improve accuracy, provide real time operation allowing correction of laser beam profile between two successive laser pulses during the experiment. Also, simultaneous determination of PA parameters in real time might be adjust calibration procedures to field measurement. Results for two examined gas mixtures with quite different absorption characteristics are comparable, so it can be concluded that AI implementation supports well known PAS characteristics: sensitivity, selectivity, and wide dynamic range. A few limitations should be mentioned regarding the collection of available and representative data sets, which are usually obtain during numerous experiments.

Further, the training process in some cases can be very demanding and slow. Fortunately, the problem might be solved by choosing other AI methods or different network training.

Employing AI in education could be change the way students are taught, and in example of molecular type detection by ANNs, could enable deeper understanding and answer the question; what defines depth of the potential well, strength of the interaction; what determines existence of different aggregate state; why molecular collisions are important, and finally how molecule type can be distinguish based on the shape of the potential curve.

REFERENCES

1. P. L. Meyer and M. W. Sigrist, 1990, Atmospheric pollution monitoring using CO_2 laser photoacoustic spectroscopy and other techniques, *Rev. Sci. Instrum.* vol. 61, 1779.
2. M.W. Sigrist, R. Bartlome, D. Marinov, J. M. Rey, D. E. Vogler, and H. Wachter, 2008, Trace gas monitoring with infrared laser-based detection schemes, *Appl. Phys. B* vol. 90, pp 289–300.
3. J. Li, W. Chen, and B. Yu, 2011, Recent progress on infrared photoacoustic spectroscopy techniques. *Appl. Spectrosc. Rev.* vol. 46, pp 440–471.
4. T. Tomberg, M. Vainio, T. Hieta, and L. Halonen, 2018, Sub-parts-per-trillion level sensitivity in trace gas detection by cantilever-enhanced photo-acoustic spectroscopy, *Sci. Rep.* vol. 8, 1848.
5. M. D. Rabasović, D. D. Markushev, and J. Jovanovic-Kurepa, 2006, Pulsed photoacoustic system calibration for highly excited molecules, *Meas. Sci. Technol.* vol. 17 1826–1837.
6. M. D. Rabasović, J. D. Nikolić, and D. D. Markushev, 2007, Simultaneous determination of the spatial profle of the laser beam and vibrational-to-translational relaxation time by pulsed photoacoustics. *Appl. Phys. B* vol. 88, pp 309–315.
7. M. Lukić, Ž, Ćojbašić, M. D. Rabasović, D. D. Markushev, and D. M. Todorović, 2017, Laser fluence recognition using computationally intelligent pulsed photoacoustics within the trace gases analysis, *Int. J. Thermophys.* vol. 38, 165.
8. M. Lukić, Ž. Ćojbašić, M. D. Rabasović, D. D. Markushev, and D. M. Todorović, 2013, Neural networks-based real-time determination of the laser beam spatial profile and vibrational-to-translational relaxation time within pulsed photoacoustics, *Int. J. Thermophys.* vol. 34, pp 1795.
9. M. Lukić, Ž, Ćojbašić, M. D. Rabasović, and D. D. Markushev, 2014, Computationally intelligent pulsed photoacoustics, *Meas. Sci. Technol.* vol. 25, 125203.
10. M. Lukić, Ž, Ćojbašić, D. D. Markushev, 2023, Neuro fuzzy prediction of laser fluence based on photoacoustic signal analysis in different gas mixtures, Measurement, vol. 210, 112533.
11. O. Zawacki-Richter, V. I. Marín, M. Bond, and F. Gouverneur, 2019, Systematic review of research on artificial intelligence applications in higher education – where are the educators?, *Int. J. Educ. Technol. High. Educ.* vol.16, 39.
12. K. Beck, A. Ringwelski, and R. J. Gordon, 1985, Time-resolved optoacoustic measurements of vibrational relaxation rates*Chem. Phys. Lett.* vol.121, pp 529-534.
13. K. M. Beck and R. J. Gordon, 1988, Theory and application of time-resolved optoacoustics in gases *J. Chem. Phys*. vol. 89, pp 5560–5567.
14. A.P. Engelbrecht, 2007, Computational Intelligence, 2nd edition. John Wiley and Sons
15. J. Gajević, M. Stević, J. Nikolić, M. Rabasović, and D. Markushev, 2006, Global warming and SF_6 molecule, *FU Phys. Chem. Tech.* vol. 4 pp 57–69.
16. M. Lukić, Ž. Ćojbašić, and D. Markushev, 2022, Machine learning based determination of photoacoustic signal parameters for different gas mixtures, *Book of Abstracts, ICPPP21 - International Conference on Photoacoustic and Photothermal Phenomena*, pp 365-366 Bled, Slovenia.
17. J. B. Adams, 2001, Bonding Energy Models, ed.(s): K.H. J. Buschow, R. W. Cahn, M. C. Flemings, B. Ilschner, E. J. Kramer, S. Mahajan, P. Veyssière, *Encyclopedia of Materials: Science and Technology*, Elsevier, pp 763-767.

Conference Proceedings
ICPAE 2023, 24th August – 26th August, Zrenjanin, Serbia
University of Novi Sad, Technical Faculty "Mihajlo Pupin", Zrenjanin

A Simple School Experimental Assessment to Get Familiarized with Air Pollution

Vera Zoroska[1], Ljubcho Jovanov[2], Katerina Drogreshka[2*]

[1]Primary school Hristo Uzunov, Pitu Guli 127, Ohrid, Republic of North Macedonia
[2]Seismological Observatory at Faculty of Natural Sciences and Mathematics, Mariovska-3 65, Skopje, Republic of North Macedonia
katerinadrogreska@yahoo.com

Abstract. Air pollution is quickly becoming one of the biggest modern societal problems thus raising awareness of the danger of the problem is essential. Natural sciences aim to explain natural phenomena and processes and as such aid in the creation of a precise perception of global problems, the risks they carry, as well as the need for prevention. This paper aims to describe a simple experiment that can be performed in the classrooms or the student's home, showing different pollutants, the degree of pollution and the possible causes of air pollution in several different locations with different environmental conditions

Keywords: air pollution, experiment, students, quality of air, pollution sources

INTRODUCTION

Massive industrialization, the enormous daily level of emitted CO_2 gas by industry and cars, the massive deforestation etc., are the main factors causing irreversible environmental pollution - a global problem and one of the biggest challenges of the society nowadays. The fundamental civil right to a pure and healthy environment obligates the population to take over activities to protect, preserve and improve the ecosystem [1]. Plenty of the activities aimed to raise awareness of the people for the environmental problems, especially for air pollution as a most dangerous problem that affects the biggest part of the Earth's population, starting even in primary schools, with continuous upgrading of the knowledge during the later education.

Based on the key competencies for lifelong learning given by the European Reference Framework, as well as the framework of individual competencies developed by the European Commission [2], Macedonian national standards for the skills and attitudes that need to be acquired by the student especially in primary school are divided into eight groups [2]. The most important group is mathematics and natural sciences, the base of everyday living.

The implementation of the STEM programs in the recent curriculums for natural sciences, speeds up the whole process resulting in better results. The aim of this research is to design a class curriculum that will ease up the explanation and understanding of the process of air pollution as the most common environmental problem, and what can we do to prevent it.

EXPERIMENTAL SETUP

The experimental activities planned with this class curriculum are divided into two parts: the first class when the students will get familiar with the objectives, opportunities and disadvantages of the problem of air pollution and will setup the experiment, and the second class when the main activity will be analyzing the results of the experiment. All of the activities need to be supervised by a teacher.

The first class should be organized as a group discussion connected to the problem of air pollution and the objects in the nearest neighborhood that can cause it. Additionally, an explanation of the main air pollutant (PM2.5, PM10, SO_2, NO_2) can be presented [3], as well as the process of how their concentration in air can be measured. At the end of the discussion the students should be divided into groups and to be asked to forecast one place where air pollution will surpass the maximum permitted level and one place where the pollution will be in the acceptable interval of values. Each group's identified places should be taken as experiment laboratories where the students will place the experimental setup.

For the experimental setup each group will need: two plastic plates, some Vaseline (petroleum jelly), two zip bags for transportation, a marker and wet wipes. Firstly, each group is asked to place a thin layer of Vaseline on each plate, to set a group mark and carefully place it in a zip bag. Secondly, one plate (without a zip bag) needs to be placed at each of the two previously peaked places (Fig. 1). Finally, this way prepared setup should stay in the same place for at least 5-7 days.

Figure 1. Experimental plate set at the measuring place.

After a week, each group is asked to take the plates back to the classroom and analyze the surface in detail. For this purpose, students can use a magnifier, school microscope or even camera on their mobile phones. The main result should be a comparison of the determined level of concentration of the particles collected from the atmosphere and do the results correspond to the previously made forecasts. Furthermore, each group can make a comparison with the data for the air pollution level available at the national application for air quality measurements “AirCare” [4], or on the official website of the Ministry of

environment and physical planning [3], in order to get familiar with the app and how to use it, and to conclude if their results for the concentration agree with the average daily levels of air quality given in the app. Additionally, an analysis of the trapped particle's size, form and frequency can be done to identify if there is one main pollutant that emits the particles.

For the purposes of this study, experimental setups as explained above, were placed in three different locations, in three different cities – Skopje, Veles and Ohrid. The results are explained in the next section.

RESULTS AND DISCUSSION

After a week exposure of the "pollutant traps" in the selected places, they were collected and analyzed in detail. Throughout the exposure days, we continuously monitored the AirQualityIndex (AQI) values. The visual results for each place are given in Fig. 2-4.

Figure 2. Macroresults from the experiment placed in Skopje (left), microanalysis of the air pollutants using mobile phone's camera (right).

Figure 3. Macroresults from the experiment placed in Veles (left), microanalysis of the air pollutants using mobile phone's camera (right).

Figure 4. Macroresults from the experiment placed in Ohrid (left), microanalysis of the air pollutants using a magnifier (right).

The analysis of the concentration of the trapped particles showed that the number of the particles corresponds to the AQI values for the measurement period shown in Fig. 5 (low values) which means that the air pollution in the measurement period was low resulting in a low number of trapped particles.

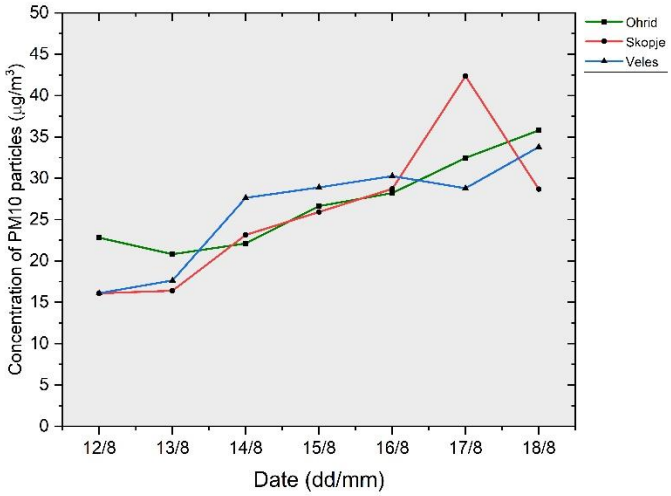

Figure 5. Daily average concentration of PM10 particles during the measurement period (12/8/2023-18/8/2023).

Comparing the results this way, students can easily get familiar with the meaning of the values for air pollution and why different medical alerts are issued during the high level of air pollution periods of the year.

Furthermore, the analysis of the size and form of the particles was done using an optical magnifier and a camera lens on mobile phones. As the results show, the concentration of

the particles is higher in the places located near frequent roads (Fig. 3), and the size of the particles is smaller compared to the concentrations at quiet places, farther from roads and factories (Fig. 2 and 4) where the particles are mostly bigger and come from the local trees and soil. The conclusions connected to the results should be made by a deep discussion while the students should be asked to classify the pollutant particles by size and potential source.

This way, students will gain their ability for practical use of mobile phones as well as an optical magnifier as a piece of ordinary laboratory equipment and because of the interdisciplinarity of the experiment it is expected that the student's curiosity and interest in natural sciences will increase as a key for creation of scientific thought at the student's mindset.

CONCLUSION

Each of us needs to contribute to the preservation and sustainability of the environment. In that direction, practical experiments like the presented one are of great importance, with which students awareness of the actual problem of the quality of the surrounding air and the dangers arising from it will gain, but the most important is that the students can try to identify and find solutions that lead to positive changes for better air quality, using their knowledge gained during the natural sciences classes.

Air pollution is changing the world and threats our everyday living and existence. These consequences are equally felt by developed and underdeveloped countries, but not all of them have enough economic power to deal with the damages and losses. That is why the student's mindsets should be set to look for innovative practices and methods to reduce the consequences of the problem.

REFERENCES

1. Challenges - Journal of Social Issues, We and the environment, number 53, 2020, pp. 18-28. (in Macedonian). https://library.fes.de/pdf-files/bueros/skopje/15369/05-2020-03.pdf (19.8.2023)
2. National standards for student achievements at the end of primary school, Ministry of education and sciences of the Republic of N. Macedonia, 2021
3. Air Quality Portal, Ministry of environment and physical planning of the Republic of N. Macedonia, https://air.moepp.gov.mk/?page_id=1351 (19.8.2023)
4. AirCare app, https://getaircare.com/. (19.8.2023)

Conference Proceedings
ICPAE 2023, 24th August – 26th August, Zrenjanin, Serbia
University of Novi Sad, Technical Faculty "Mihajlo Pupin", Zrenjanin

Building a Sustainable Future: Promoting Health and Resilience Through Sustainable Health Systems

Teodora Crvenkov[1]*, Milan Marković[2], Darko Radovančević[2]

[1]*University Clinical Centre of Serbia, Pasterova 2, Belgrade, Serbia*
[2]*University of Novi Sad, Technical Faculty "Mihajlo Pupin", Djure Djakovića bb, Zrenjanin, Serbia*
teodoracrvenkov@gmail.com

Abstract. This review article explores the promotion of health and resilience through sustainable health systems as a means to build a sustainable future. It emphasizes the need for transitioning to sustainable health system in regards to challenges such as the epidemic of non-communicable diseases, multidrug resistant microbes, food safety, unsustainable practices, malnutrition, environmental pollution, medical waste and others. The health benefits of building a more sustainable healthcare and strengthening the healthcare systems are highlighted, along with the importance of policy frameworks, education, prevention and community engagement. This article emphasizes the urgency of collective action for a more sustainable and equitable future.

Keywords: sustainable development, health promotion, health effects, public health, health systems

INTRODUCTION

Healthcare is facing two serious challenges that appear to be inter-related [1]. The first is the significant rise in prevalence of multiple non-communicable diseases and conditions (NCDs) (e.g., asthma, food allergies, obesity, celiac disease, type 1 diabetes, type 2 diabetes, inflammatory bowel disease, autism, Alzheimer's disease, Parkinson's disease, heart disease and cancer) not just in developed countries but globally. These diseases already account for a majority of deaths worldwide and are expected to continue to increase in impact in the coming decades [2]. This is paired with a second challenge: the emergence of multi-drug resistant bacterial pathogens that are outpacing the discovery and production of new antibiotics [3]. Multi-drug resistant bacteria are thought to have arisen in part due to the overuse of antibiotics [4]. Antimicrobial resistance (AMR) and persistence are associated with an elevated risk of treatment failure and relapsing infections [5]. They are thus important drivers of increased morbidity and mortality rates resulting in growing healthcare costs [5].

Malnutrition in all forms, ranging from undernourishment to obesity and associated diet-related diseases, is one of the leading causes of death worldwide, while food systems often have major environmental impacts. Rapid global population growth and increases in demands for food and changes in dietary habits create challenges to provide universal

access to healthy food without creating negative environmental, economic, and social impacts [6].

Food safety in the food market is one of the key areas of focus in public health, because it affects people of every age, race, gender, and income level around the world. The local and international food marketing continues to have significant impacts on food safety and health of the public. Food supply chains now cross multiple national borders which increase the internationalization of health risks [7].

One of our era's greatest scourges is air pollution, on account not only of its impact on climate change but also its impact on public and individual health due to increasing morbidity and mortality. There are many pollutants that are major factors in disease in humans. Among them, Particulate Matter (PM), particles of variable but very small diameter, penetrate the respiratory system via inhalation, causing respiratory and cardiovascular diseases, reproductive and central nervous system dysfunctions, and cancer. Despite the fact that ozone in the stratosphere plays a protective role against ultraviolet irradiation, it is harmful when in high concentration at ground level, also affecting the respiratory and cardiovascular system. Furthermore, nitrogen oxide, sulfur dioxide, Volatile Organic Compounds (VOCs), dioxins, and polycyclic aromatic hydrocarbons (PAHs) are all considered air pollutants that are harmful to humans. Carbon monoxide can even provoke direct poisoning when breathed in at high levels. Heavy metals such as lead, when absorbed into the human body, can lead to direct poisoning or chronic intoxication, depending on exposure [8].

Healthcare structures are supposed to protect and improve public health, but in the meanwhile they are socially and environmentally impactful structures which can cause negative side effects on the people’s health and on the context. A hospital which is sustainable both in its structure and management is the only possibility to promote wellbeing and healthiness for people attending it. This has to be taken into account both as a main requirement and a quality issue, since healthcare structures must be capable to deliver high standards also in changing circumstances. A sustainable structure is a structure that can be easily maintained and that can be functional from the environmental, social and economic point of view, in order to comply with the diverse interests and needs of all the stakeholders [9].

MATERIAL AND METHODS

To comprehensively address the topic of building sustainable health systems to promote health and resilience, a systematic search was conducted on major academic databases, including Google Scholar and PubMed. The search terms were carefully selected to capture relevant literature related to sustainable health systems, their impact on health promotion and resilience, and their implications for the future. The following search terms were used:
"Sustainable health systems", "Health system resilience", "Health promotion", "Sustainability in healthcare", "Future of healthcare", "Resilient healthcare infrastructure" and etc. The inclusion criteria for selecting papers were as follows:

1. Relevance to the theme of sustainable health systems and their impact on health promotion and resilience.
2. Published in peer-reviewed journals or reputable conference proceedings.

3. Covered the period from [2010] to [2023].
4. Articles written in English.

Papers were excluded if they were:

1. Not directly related to the theme of sustainable health systems and their impact on health promotion and resilience.
2. Published in languages other than English.
3. Not available in full text.
4. Duplicates or redundant publications.

Articles that passed the initial screening were subjected to full-text review. The reviewers assessed the articles for their alignment with the inclusion criteria. Data were extracted from the selected articles using a standardized form, including information on study objectives, methodologies, key findings, and implications for sustainable health systems.

AIM OF PAPER

The aim of this review article is to critically assess the current challenges encountered by contemporary health systems and explore the pivotal role of health promotion and education in shaping a sustainable future. Drawing from a comprehensive examination of literature sourced from reputable databases such as Google Scholar, PubMed, and others, this study seeks to illuminate the intricate web of challenges that modern health systems confront. By emphasizing the imperatives of sustainability, resilience, and adaptability, the review aims to underscore the urgency of integrating robust health promotion strategies and education initiatives into healthcare frameworks.

DISCUSSION

Sustainability is a broad and debated subject, often difficult to be defined and applied into real projects, especially when dealing with a complex scenario as the one of healthcare. Many research studies and evaluation systems have handled this topic from different perspectives, but many limits and criticalities still have to be overcome to properly cope with actual needs [9]. The newly developed evaluation system takes into consideration all the three pillars of sustainability, analyzing social, environmental and economic sustainability through a set of criteria, specified by measurable indicators [9].

Sustainability is an important point of attention for the public at large, for governments, and for the healthcare system [10-12]. Previously, the term sustainability has been mostly related to environmental degradation [13]. Nowadays, the significance of sustainability has evolved and is related to other aspects, such as the well-being of patients, healthcare employees, and the community. Hence, a sustainable structure should be defined as a one that ensures preservation of resources, is practical from ecological, social, and economical perspectives, and meets the interests of different stakeholders. There is sufficient literature suggesting methods for improving sustainability in healthcare systems; however, there is no consensus on feasible strategies for implementing the proposed sustainability measures in clinical laboratories despite several opportunities [10-12].

The meaning of sustainability is constantly evolving in this rapidly changing world. One of the very first official articulations of sustainable development was made in the Burtland Report, published by the United Nations in 1987, in which sustainable development was defined as "development that meets the needs of the present without compromising the ability of future generations to meet their personal needs" [11,13]. However, this definition is largely open to interpretation, which has made it difficult to build a consensus on the topic of sustainability. The Swedish scientist Karl-Henrik Robert proposed a more practical definition [13]. According to him, an ideal society would strive to reduce the consumption of mineral and other natural resources.

The definition of sustainable development proposed by the European Union (EU) is broader and more holistic and considers the multiple facets of all sustainability policies, including economical, human, and environmental facets [13].

Healthcare structures serve to preserve and improve public health; however, their environmental impact can negatively affect wellbeing of humans and other organisms [9]. Therefore, sustainability of hospitals and healthcare structures is also key to promoting human well-being and health. However, the sustainability measures implemented in healthcare structures need to ensure that the quality of service provided by healthcare structures and access to and affordability of healthcare are not compromised, so that both businesses and customers benefit [11,14,15]. Another important issue to be tackled regarding sustainability in the healthcare sector is the management of waste disposal and air pollution [16]. Klangsin & Harding [17], showed how medical waste has become one of the top pollutant sources worldwide and is a major factor affecting disease spread and air, water, and soil quality in and around healthcare structures [18]. Thus, it has become imperative for healthcare organizations to have a multidisciplinary team addressing various aspects of sustainability in healthcare.

The global environmental crisis will only worsen unless all societal implementors are held accountable for the true cost and risk of polluting nature and its consequences to the public and the environment. Too much responsibility for reducing environmental footprints is currently focused on citizens and waste management, and efforts made by individuals will remain insufficient unless action is taken across the entire value chain.. Acting too late in reducing our environmental footprint will pose major public health and environmental risks. Solutions, ranging from waste reduction to collection and recycling, to avoid the impending environmental crisis can be implemented only if all stakeholders are held accountable for their actions and the impact of these on the environment [19]. Several actions are envisioned in the pursuit of sustainability [20, 21]:

1. Recognition and promotion of the value of sustainable approaches by policymakers.
2. Publication of action plans, guidelines, and policy documents regarding sustainable practices.
3. Promulgation of novel policies for achieving sustainability goals and implementation of procurement and environment policies related to sustainability.
4. Encouragement of laboratory medicine professionals to implement sustainability measures and communicate new insights and outcomes.
5. Implementation of a sustainable procurement system that aligns suppliers and contractors in the healthcare system with the sustainability plan.

6. Provision of economical support to sustainable initiatives and research and development through indirect fiscal incentives, such as tax credits, or direct grants and loans.
7. Engagement of investors to build sustainable financial markets.
8. Catalyzation of innovation, emerging technologies, and experimentation for addressing social, environmental, and economic challenges.
9. Facilitation of transparent, standardized, and interoperable data sharing.
10. Ensuring of funding of data infrastructure.

The European Green Deal (EGD) Investment Plan, also known as the Sustainable Europe Investment Plan, will mobilize at least €1 trillion for sustainable investments over the next decade to achieve its objectives, which aim at making Europe the world's first climate-neutral continent by 2050 [22]. To achieve this goal, renewable power sources should become the main sources of energy in the EU. However, the effectiveness of the EGD depends on the involvement of all EU stakeholders. The European Commission has already taken some initiatives focusing on hospitals and healthcare stakeholders, such as "Towards Zero Carbon Hospitals with Renewable Energy Systems" [23], which aim to reduce CO_2 emissions from the 15,000 hospitals in Europe by providing them suitable tools to achieve greater sustainability. Their relatively high energy requirements make hospitals an ideal subject for exploring non-technical barriers to energy efficiency measures and renewable energy systems. However, in contrast to new hospitals, which can be designed to be energy-efficient, existing EU hospitals will need to focus on reducing energy consumption and exploiting renewable energy sources to achieve the long-term CO_2-reduction targets set by the European Commission. Further, a high-quality "Guide for European Hospitals on Renewable Energy" targeting decision-makers and based on good practices and lessons learned from regional hospitals has been developed and widely distributed [24]. This initiative incentivizes the pursuit of sustainability in healthcare structures and promotion of environment-friendly attitudes among all healthcare stakeholders, which can benefit the whole system [19].

CONCLUSION

In the journey toward a sustainable and resilient healthcare future, this review has illuminated the intricate interplay between sustainable health systems, health promotion, and the cultivation of resilience. The synthesis of diverse research findings underscores the urgency of adopting sustainable practices within healthcare systems to address the multifaceted challenges of our time. As we navigate the complexities of resource scarcity, demographic shifts, and evolving health threats, the imperative for sustainability becomes increasingly apparent.

The reviewed literature has showcased the indispensable role of health promotion and education in shaping healthier communities and enhancing the adaptive capacity of healthcare systems. From preventive measures and community engagement to empowering individuals with health literacy, these strategies are pivotal in promoting individual well-being and collective resilience. The integration of health promotion into the core fabric of healthcare practices fosters proactive healthcare delivery, ultimately

reducing the burden on healthcare systems and improving overall population health outcomes.

Moreover, the adoption of sustainability principles is not only an ethical choice but a practical necessity. Sustainable healthcare systems, encompassing energy-efficient infrastructure, responsible waste management, and equitable resource allocation, offer a blueprint for a more resource-conscious and efficient healthcare landscape.

In conclusion, this review articulates the call for action to shape a healthcare landscape that is not only responsive to current needs but also poised to meet the challenges of an ever-changing world. By integrating sustainability, health promotion, and resilience-building strategies into the fabric of healthcare systems, we can forge a path toward improved health outcomes, equitable access to care, and a more harmonious relationship with our planet. The future of healthcare lies in our ability to learn from the past, adapt to the present, and invest in a healthier and more sustainable world for generations to come.

REFERENCES

1. Dietert, R.R.; Dietert, J.M. The Microbiome and Sustainable Healthcare. Healthcare 2015, 3, 100-129. https://doi.org/10.3390/healthcare3010100
2. Bloom, D.E.; Cafiero, E.T.; Jané-Llopis, E.; Abrahams-Gessel, S.; Bloom, L.R.; Fathima, S.; Feigel, A.B.; Gaziano, T.; Mowafi, M.; Pandya, A.; et al. The Global Economic Burden of Noncommunicable Diseases; World Economic Forum: Geneva, Switzerland, 2011. [Google Scholar]
3. Cantón, R.; Horcajada, J.P.; Oliver, A.; Garbajosa, P.R.; Vila, J. Inappropriate use of antibiotics in hospitals: The complex relationship between antibiotic use and antimicrobial resistance. Enferm. Infecc. Microbiol. Clin. 2013, 4, 3–11. [Google Scholar] [CrossRef]
4. Cantón, R.; Horcajada, J.P.; Oliver, A.; Garbajosa, P.R.; Vila, J. Inappropriate use of antibiotics in hospitals: The complex relationship between antibiotic use and antimicrobial resistance. Enferm. Infecc. Microbiol. Clin. 2013, 4, 3–11. [Google Scholar] [CrossRef]
5. Huemer M, Mairpady Shambat S, Brugger SD, Zinkernagel AS. Antibiotic resistance and persistence-Implications for human health and treatment perspectives. EMBO Rep. 2020 Dec 3;21(12):e51034. doi: 10.15252/embr.202051034. Epub 2020 Dec 8. PMID: 33400359; PMCID: PMC7726816.
6. Lindgren, E., Harris, F., Dangour, A.D. et al. Sustainable food systems—a health perspective. Sustain Sci 13, 1505–1517 (2018). https://doi.org/10.1007/s11625-018-0586-x
7. Gizaw Z. Public health risks related to food safety issues in the food market: a systematic literature review. Environ Health Prev Med. 2019 Nov 30;24(1):68. doi: 10.1186/s12199-019-0825-5. PMID: 31785611; PMCID: PMC6885314.
8. Manisalidis I, Stavropoulou E, Stavropoulos A, Bezirtzoglou E. Environmental and Health Impacts of Air Pollution: A Review. Front Public Health. 2020 Feb 20;8:14. doi: 10.3389/fpubh.2020.00014. PMID: 32154200; PMCID: PMC7044178.
9. Buffoli M, Capolongo S, Bottero M, Cavagliato E, Speranza S, Volpatti L. Sustainable healthcare: how to assess and improve healthcare structures' sustainability. Ann Ig. 2013 Sep-Oct;25(5):411-8. doi: 10.7416/ai.2013.1942. PMID: 24048179.
10. Mosca I, van der Wees PJ, Mot ES, Wammes JJG, Jeurissen PPT. Sustainability of long-term care: puzzling tasks ahead for policy-makers. Int J Health Policy Manag. 2017;6:195–205. doi: 10.15171/ijhpm.2016.109. [PMC free article] [PubMed] [CrossRef] [Google Scholar]
11. Biason KM, Dahl P. [Updated on Oct 2016];Strategic steps to sustainability in healthcare - Sustainable Operations. https://healthcarefacilitiestoday.com/posts/Strategic-steps-to-sustainability-in-healthcare--13629 .
12. World Health Organization Regional Office for Europe, author. Environmentally sustainable health systems: a strategic document 2017. http://www.euro.who.int/en/health-topics/Health-

systems/public-health-services/publications/2017/environmentally-sustainable-health-systems-a-strategic-document-2017 .

13. Marimuthu M, Paulose H. Emergence of sustainability-based approaches in healthcare: expanding research and practice. Procedia Soc Behav Sci. 2016;224:554–61. doi: 10.1016/j.sbspro.2016.05.437. [CrossRef] [Google Scholar]
14. Marimuthu M, Paulose H. Emergence of sustainability-based approaches in healthcare: expanding research and practice. Procedia Soc Behav Sci. 2016;224:554–61. doi: 10.1016/j.sbspro.2016.05.437. [CrossRef] [Google Scholar] [Ref list]
15. Price R, Sergelen O, Unursaikhan C. Improving surgical care in Mongolia: a model for sustainable development. World J Surg. 2013;37:1492–9. doi: 10.1007/s00268-012-1763-1. [PubMed] [CrossRef] [Google Scholar] [Ref list]
16. Berwick DM, Hackbarth AD. Eliminating waste in US health care. JAMA. 2012;307:1513–6. doi: 10.1001/jama.2012.362. [PubMed] [CrossRef] [Google Scholar]
17. Klangsin P, Harding AK. Medical waste treatment and disposal methods used by hospitals in Oregon, Washington, and Idaho. J Air Waste Manag Assoc. 1998;48:516–26. doi: 10.1080/10473289.1998.10463706. [PubMed] [CrossRef] [Google Scholar]
18. European Commission, Eurostat, author. [Updated on Jan 2020];Renewable energy statistics. https://ec.europa.eu/eurostat/statistics-explained/index.php?title=Renewable_energy_statistics .
19. Molero A, Calabrò M, Vignes M, Gouget B, Gruson D. Sustainability in Healthcare: Perspectives and Reflections Regarding Laboratory Medicine. Ann Lab Med. 2021 Mar 1;41(2):139-144. doi: 10.3343/alm.2021.41.2.139. PMID: 33063675; PMCID: PMC7591295.
20. Shrank WH, Rogstad TL, Parekh N. Waste in the US health care system: estimated costs and potential for savings. JAMA. 2019;322:1501–9. doi: 10.1001/jama.2019.13978. [PubMed] [CrossRef] [Google Scholar]
21. OECD and the Sustainable Development Goals: delivering on universal goals and targets. [Updated on 2019];OECD. http://www.oecd.org/dac/sustainable-development-goals.htm
22. European Commission, Directorate General for Environment, author. Sustainable development 2020. https://ec.europa.eu/environment/sustainabledevelopment/
23. European Commission, author. [Updated on Jan 2020];The European Green Deal Investment Plan and Just Transition Mechanism explained, 2020. https://ec.europa.eu/commission/presscorner/detail/en/qanda_20_24 .
24. European Commission, author. [Updated on Sep 2020];Energy intelligent, energy Europe; towards zero carbon hospitals with renewable energy systems, 2020. https://ec.europa.eu/energy/intelligent/projects/en/projects/res-hospitals .

Conference Proceedings
ICPAE 2023, 24th August – 26th August, Zrenjanin, Serbia
University of Novi Sad, Technical Faculty "Mihajlo Pupin", Zrenjanin

The Impact of Oil Industry on the Environment: Challenges, Consequences, and Possible Steps Toward a Sustainable Future

Milan Marković[1*], Teodora Crvenkov[2], Dejan Bajić[1], Saša Jovanović[1], Luka Đorđević[1], Borivoje Novaković[1], Jasna Tolmač[1], Ognjen Popović[3]

[1]University of Novi Sad, Technical Faculty "Mihajlo Pupin", Djure Djakovića bb, Zrenjanin, Serbia
[2]University Clinical Centre of Serbia, Pasterova 2, Belgrade, Serbia
[3]Mining Institute, Batajnički put 2, Belgrade, Serbia
milanzrmarkovic@gmail.com

Abstract. This paper is a systematic review of the professional literature on the environmental impact of the oil industry. The oil industry has long been a key factor in global energy production, but its activities, such as exploration, exploitation, and processing, produce significant concerns about environmental degradation. This study examines the challenges facing the oil industry, including oil spills, air and water pollution, habitat destruction, and greenhouse gas emissions. The consequences of these ecological impacts have been examined in detail, highlighting negative effects on ecosystems and climate change. Furthermore, this paper considers possible steps toward a more sustainable future, emphasizing the importance of adopting cleaner technologies, promoting renewable energy sources, implementing stricter regulations, and encouraging international cooperation. Synthesizing existing literature, this research provides valuable insights into the complex relationship between the petroleum industry and the environment, providing a basis for informed decision-making and promoting sustainable practices.

Keywords: the oil industry, environment, energy, degradation, pollution, ecosystem, sustainable future, cleaner technology

INTRODUCTION

The petroleum industry, as an essential pillar of modern society, has played an important role in the formation of the modern economic system and global progress. However, this rapid development has not been without environmental consequences. The growth of oil consumption, the exploitation of oil reserves, and the processing, storage, and transportation of oil have led to serious challenges for the conservation and sustainability of natural ecosystems. This paper aims to provide a review of the professional literature on the environmental impact of the oil industry, identify the key consequences that this impact has produced, and present possible steps toward a more sustainable future.

We will consider various aspects of the environmental impact of the oil industry, including greenhouse gas emissions, water pollution, biodiversity loss, and the effects of

climate change. At the same time, we will also analyze the significant economic and societal implications, with a focus on energy security, geopolitical tensions, and social implications.

Further, through a systematic review of the relevant literature, we will explore initiatives and regulations that have been developed to reduce the negative environmental impacts of the oil industry.

We aim to provide a comprehensive overview of the current state of play and an understanding of the challenges facing the oil industry in the context of environmental conservation, based on the expert literature.

MATERIAL AND METHODS

Origin and demand for crude oil and natural gas

About 5000 – 6000 years ago, the ancient Sumerians, Assyrians, and Babylonians used crude oil collected from large seeps at Tuttul on the Euphrates River as medicine for wounds and as oil in lamps to provide light. This represents the earliest recorded use of crude oil. Around the same time in Iran, between 6000 and 2000 years BCE, the first discoveries of natural gas seeps were made. Crude oil and natural gas demand grew with population and on August 27, 1859, Edwin L. Drake struck crude oil at his well near Titusville, Pennsylvania. He found oil underground and devised a way that could pump it to the surface. This became the origin of modern-day crude oil production [1]. Crude oil and natural gas, collectively referred to as petroleum, are considered fossil fuels because it is believed that they were formed from the buried remains of plants and animals that lived and died millions of years ago. They are non-renewable sources of energy and are made up of a mixture of hydrocarbons [1,5]. Crude oil is a naturally occurring complex mixture of hydrocarbon and nonhydrocarbon compounds which at appropriate concentration, possesses a measurable toxicity towards living systems. The toxicity of crude oil or petroleum products varies widely, depending on their composition, concentration, environmental factors, and the biological state of the organisms at the time of the contamination [2]. Crude oil is made up of mostly alkanes, cycloalkanes, and various aromatic hydrocarbons. It also contains other organic compounds like nitrogen, oxygen, sulfur, and trace amounts of metals such as iron, nickel, copper, and vanadium. Crude oil can range from light, volatile oils that are highly fluid to highly viscous oils. Most crude oil is dark brown or black but it could also occur in green, red, or yellow color. On the other hand, natural gas is composed primarily of methane (85 – 95%) but may also contain ethane, propane, and heavier hydrocarbons. Small quantities of nitrogen, oxygen, carbon dioxide, sulfur compounds, and water may also be found in natural gas. Natural gas is a colorless, odorless, tasteless but nontoxic gas that burns with a blue flame. Natural gas exists as either associated gas alongside liquid hydrocarbons (crude oil, condensate) or non-associated gas in dry gas wells that generally produce only natural gas. It could also be found as coal bed methane in coal seams. Given the dearth of infrastructure in most developing countries, the economic advantage of crude oil and natural gas production has always been the focus in these countries leaving the environmental impacts to the background. It is believed that a good review of the economic effects and the environmental impacts of oil and gas production will help inform decision-makers in these countries of the need to formulate and

implement structures geared towards protecting the environment from the negative effects of the processes and products of oil and gas production [1].

The need for oil and gas

The 2016 International Energy Association (IEA) Market Report forecasted worldwide average demand of nearly 96 million barrels of crude oil and liquid fuels daily. In the same vein, global natural gas demand was estimated at just under 3500 billion cubic meters in 2014, and the IEA Medium-Term Gas Market Report 2015 saw an average annual growth rate of 2% from 2014 to 2020. In the United States, crude oil and natural gas account for about 62% of the nation's energy needs. Crude oil and natural gas are among the most important energy sources in the world and are used for many purposes other than fuel for energy and transport. Crude oil is commonly used for the production of gasoline, aviation fuel, diesel, heating oil, asphalt, and propane. It also serves as feedstock for the manufacture of chemicals, synthetic rubber, and plastics. Natural gas is used as domestic cooking and heating gas (CNG), for power generation, production of hydrogen, automobile fuel for transportation, aviation fuel, and as feedstock for the petrochemical industry in the production of fertilizers, fabrics, glass, steel, plastics, paint, and others [1].

However, the process of extraction of these natural resources is very complicated, and most of the time the pollutant products that accompany the process of oil exploration play a vital role to declare an inconsistency in the ecosystem. This means an increase in the probability of environmental risk and as a result a widespread of hazardous material in the aquatic environment, air, soil, and all the living world belonging to these environments [3].

Therefore, with the world's increasing dependency on the production of crude oil products, the crude oil water contamination problem becomes the major factor that can alter the natural consistency of the outstanding life source in a particular environment. Therefore, to decrease or remedied these effects, oil companies must adopt proper measures that are helpful to minimize the contamination rate to the normal wedge. This paper reviewed the impacts caused by crude oil exploration and production on (water, soil, air, plants, and animals) and its implications for human health. Oil is currently the backbone of the economies of many countries [3].

Oil spill sources and spill rates

The movement of petroleum from the oil fields to the consumer involves as many as 10–15 transfers between many different modes of transportation including tankers, pipelines, railcars, and tank trucks [7].

Oil is stored at transfer points, terminals, and refineries along the route. Accidents can happen during any of these exploration, production, and transportation steps or storage times. An important part of protecting the environment is ensuring that there are as few spills as possible. Both government and industry are working to reduce the risk of oil spills, with the introduction of strict new legislation and stringent operating codes. The industry has invoked many operating and maintenance procedures to reduce accidents that could lead to spills. The rate of spillage has decreased in the past 20 years. This is especially true for tanker accidents at sea. Intensive training programs have been developed to reduce the potential for human error. Despite these efforts, spill experts estimate that 30–50% of oil

spills are either directly or indirectly caused by human error, with 20–40% of all spills caused by equipment failure or malfunction [7].

Environmental pollution from exploration and exploitation of crude oil

Environmental pollution due to crude oil exploration occurs due to an increase in global demand [7], uncontrolled exploration practices, poor waste management, etc. Despite its growing importance across the world, crude oil exploration leaves the environment polluted. The impact of environmental pollution across the world, especially in Africa, has far reached worrying proportions. The strides being made in the developing world particularly in Africa through industrialization and economic development have undoubtedly increased exposure to environmental pollution. Pollutants can cause adverse effects on human health from early life and this includes cardiovascular disorders, mental disorders, allergies, and respiratory disorders. Despite the economic benefits of crude oil discovery and exploration in Africa, oil exploration no doubt has far-reaching adverse effects on environmental compartments; air, land, water as well as all living things on earth. Some avoidable occurrences, which are often mismanaged in Africa include oil spillage, gas faring (causing various gas emissions), noise, and improper waste management (wastewater and solid wastes). In the exploration and exploitation of oil and gas, the major environmental pollutants are [4]:

(i) effluent water contaminated with oily effluents (oil & grease), chemicals, and solids from drilling fluid,
(ii) formation water produced along with crude oil, and
(iii) gaseous emissions having CO, SO_2, NOx, hydrocarbons, and fine particulate matter from the gas flare [4].

Environmental impacts of crude oil and natural gas

Environmental impacts that occur during the production of crude oil and natural gas would mostly occur from long-term habitat change within the oil and gas field, production activities (including facility component maintenance or replacement), waste management (e.g produced water), noise (e.g from well operations, compressor or pump stations, flare stack, vehicle and equipment), the presence of workers and potential spills. These activities could potentially impact the resources [1].

Crude oil, a mixture of many thousands of organic compounds, can vary in composition from one source to another. This suggests that the effects of crude oil spills will vary from source to source. However, details of the potential biological damage will depend on the ecosystem where the spill occurred [6].

The contamination of water, soil, and air by oil and gas wastes as well as its associated byproducts is a possibility. Reports by citizens have shown the relative effect of production and drilling activities on the contamination of surface waters, soils surrounding well sites, and water wells; air emissions emanating from wellheads, pipelines, drilling sites, compressor stations, and several other oil and gas field infrastructure have been reported to pose air quality concerns. Other significant environmental threats are those emanating from the dust particles left from drilling which can coat the surrounding areas, as well as fames produced upon combustion of natural gas in the oil fields which are known to cause air pollution. Gaseous emissions include SO_2, CO, hydrocarbons, NOx, and particulate from

the gas fare. In addition, accidents, illegal dumping of oil barrels and produced water, and oil spills also lead to distressing health and ecological consequences that may persist for decades. Several activities in crude oil processing ranging from extraction, refining, transportation, and gas faring introduce greenhouse gases especially carbon dioxide into the atmosphere. The process of burning fossil fuels (coal), oil, and gas leading to the emission of carbon dioxide (a greenhouse gas) has led to global warming raising serious environmental challenges [4].

Water and the aquatic world

An aquatic environment can be considered as one of the environments that are subjected more to contamination by crude oil. This seems to be a big issue due to the spillage of some crude oil into the water. This spillage is due to the leakage which accompanies the process of oil exploration and transportation. As a result, the aquatic environment becomes a contaminated region. This situation is a big threat to the evolution of macrophytes and to the life support balance of living organisms in that environment [3].

Oil spills in the marine environment may affect organisms found therein by direct toxicity or physical smothering. Oil spills generally, can cause various damages to the marsh vegetation. It was found to reduce growth, photosynthetic rate, stem height, density, and above-ground biomass. A crude oil spill at sea forms a surface slick whose components can follow many pathways. Some may pass into the mass of seawater and evidence suggests they may persist for a long time before their degradation by microorganisms in the water. The slick usually becomes more viscous and forms a water-in-oil emulsion. Oil in water causes depletion of dissolved oxygen due to the transformation of the organic component into inorganic compounds, loss of biodiversity through a decrease in the amphipod population that is important in the food chain, and eutrophication. Short-term toxicity in fish includes lymphocytosis, epidermal hyperplasia, and hemorrhagic septicemia. It was estimated that tens of thousands of seabirds were killed as a result of spilled oil in the sea [6].

Air pollution also bears a great concern with crude oil exploration and production and both mentioned reflect serious human health effects at a high rate [3].

About half of the oil in the sea derives from natural sources including the many natural “seeps” or discharges from oil-bearing strata on the ocean floor. About 38% of the oil reaching the sea is the runoff of oil and fuel from land-based sources, mostly from urban areas. A significant amount of lubricating oil finds its way into wastewater, which is often discharged directly into the sea. About 13% of oil reaching the sea comes from the transportation sector, which includes tankers, freighters, barges, and other vessels [7].

The impact of crude oil on the soil

On land, crude oil spills have caused a great negative impact on food productivity. For example, a good percentage of oil spills that occurred on dry land between 1978 and 1979 in Nigeria, affected farmlands in which crops such as rice, maize, yams, and cassava plantain were cultivated. Crude oil affects the germination and growth of some plants. It also affects soil fertility but the scale of impact depends on the quantity and type of oil spilled. A severe crude oil spill in Cross River state, Nigeria, has forced some farmers to migrate out of their traditional homes, especially those that depend solely on agriculture.

This is because petroleum hydrocarbons 'sterilize 'the soil and prevent crop growth and yield for a long period. Crude oil contamination of land affects certain soil parameters such as the mineral and organic matter content, the cation exchange capacity, redox properties, and pH value. As crude oil creates an anaerobic condition in the soil, coupled with water logging and acidic metabolites, the result is a high accumulation of aluminum and manganese ions, which are toxic to plant growth [6].

On the terrestrial environment, oil spills cause extensive damages ranging from the destruction of terrestrial flora and fauna to biomagnifications of the toxic components of the petroleum conversion of arable land to barren soils and the destruction of the aesthetic quality of the environment [2].

Oil spilled on land does not spread quickly unlike on water, and the effects remain localized. Most types of oil will penetrate the soil and contaminate organisms in the soil. A full coating of fresh crude oil or diesel fuel will kill most plants and small trees on contact. Because of the usually limited area of impact, however, the effects of oil on land environments are not as great a concern as for marine environments [7].

Relationship between environmental health and human health

It is conceivable to say that there is a relationship between environmental health and human health. While human health is a deep field of science from the time of old, the concept of 'environmental health 'can be viewed as modern science, which is measured as the viability of the inhabitants of a given ecosystem as affected by ambient environmental factors. Practically, environmental health involves the assessment of the health of individual organisms and correlating observed changes in health with changes in environmental conditions. Some diseases have been diagnosed to be the consequences of crude oil pollution. The health problems associated with oil spills may be through any or combinations of the following routes: contaminated food and/or water, emission, and/or vapors. Toxic components in oil may exert their effects on man through inhibition of protein synthesis, nerve synapse function, disruption in the membrane transport system, and damage to the plasma membrane. Crude oil hydrocarbons can affect the genetic integrity of many organisms, resulting in carcinogenesis, mutagenesis, and impairment of reproductive capacity [6].

RESULTS AND DISCUSSION

Environmental biotechnology for crude oil clean up

Biotechnology is defined as a set of scientific techniques that utilize living organisms or parts of organisms to make, modify or improve products (which could be plants or animals). It is also the development of specific organisms for specific applications or purposes and may include the use of novel technologies such as recombinant DNA, cell fusion, and other new bioprocesses. It is also that aspect of biotechnology, which specifically addresses issues in environmental pollution control and remediation. This goes to say that it involves many disciplines in biology, agriculture, engineering, health care, economics, mathematics, and education [6].

One of the greatest challenges to humanity today is the endangering of biota as a result of environmental pollution from crude oil. To estimate the biological danger of oil after a spill, knowledge of the harmful effects of the components is necessary. In other to obtain or ascertain the effects of such polluting substances, every living being and life function can be considered a potential biomarker or bio-indicator. A biomarker is an organism or part of it, which is used in soliciting the possible harmful effect of a pollutant on the environment or the biota. Biomonitoring or biological monitoring is a promising, reliable means of quantifying the negative effect of an environmental contaminant [6].

Bioremediation technologies for crude oil-contaminated sites

Bioremediation is a technology that exploits the abilities of microorganisms and another natural habitat of the biosphere to improve environmental quality for all species, including man. The development of innovative bioremediation technology as a functional tool in the clean-up of the crude oil-polluted environment has depended so much on the basic knowledge of the physiology and ecology of the natural bacterial populations found in such polluted sites. Compliance analysis requires examination of the contaminated site in light of the governing regulation and the action plan. Examination of the site will lead to its characterization and this is a challenging aspect of bioremediation efforts. Knowledge of soil parameters such as cation exchange capacity, relevant nutrient availability, acidity (soil pH), aeration or oxygen level, hydraulic properties, etc are paramount and this requires the assistance of specialists in these areas [6].

Some necessary process variables involved in the bioremediation of petroleum hydrocarbon-polluted environments that need to be known include the characteristics of the polluting crude oil, its biodegradability, and the characteristics of the polluted site (physical and chemical) [6].

Bioremediation of crude oil contaminated environment may require some engineering process, to facilitate recovery efforts. Engineering may include the construction of booms, trenches, and barriers for contaminant containment, boreholes, bio-cells, and using engineered microbial systems. Increasing the bioavailability of the PHC (Primary Health Care) can be achieved by physically processing the crude oil-polluted soil or sediment by excavation, pulverizing, and mixing. The simplest method of bioremediation of oil-polluted soil is in situ land treatment. This technology utilizes standard farming procedures such as plugging the oil-polluted soil with a tractor, periodical irrigation, and aeration. This technology embraces the use of aerobic microorganisms to degrade the PHC and other derivatives to carbon dioxide and water, or other less toxic intermediates. This technology may involve nutrient enrichment in the form of fertilizer application or further manipulation of site conditions such as inoculations with selected or adopted microbial populations, mixing and aeration of the soil surface, pH adjustment, and irrigation [6].

Biodegradation, especially by microbes, is one of the primary mechanisms of the ultimate removal of petroleum hydrocarbons from polluted environments. The acceleration of this natural process is the objective of bioremediation efforts. Seeding a contaminated environment with strains of bacteria that are tolerant and capable of degrading a high percentage of the contaminating petroleum hydrocarbons, and thus supplementing the natural resident microbial population has proven to be useful in bioremediation. The relative success of such adapted bacteria, when added to crude oil polluted site, will depend on

several factors including competitive interactions with the native bacteria, their rate of growth in the system as well as their tolerance to the physico-chemical environment [6].

CONCLUSION

Through this review of the professional literature on the environmental impact of the oil industry, it is clear that the industry carries with it numerous challenges and has a significant negative impact on natural ecosystems and humanity as a whole. The various phases of the oil cycle, from exploitation and processing to transportation and consumption, generate serious consequences that require urgent attention and action.

We have looked at the various negative impacts of crude oil, the emission of harmful gases and their impact on climate change, water and air pollution, and the loss of biodiversity, which poses threats to many species, humans, and ecosystems. We also recognized that the oil industry has an important impact on the economy and society, including energy security and geopolitical relations.

Yet, analyzing current research and innovation, it is encouraging to see that there are possible steps toward a more sustainable future. The development of new technologies, the use of renewable energy sources, and a move toward more environmentally responsible practices in the oil industry may be key to reducing its negative impact on the environment.

Our literature review also highlighted the importance of cooperation between the academic community, industry, and regulatory bodies. Only through coordinated efforts and knowledge sharing can we make decisive progress toward a more sustainable future.

In the final analysis, the oil industry presents a complex issue that requires a balanced approach. Regardless of its significance in the modern world, we cannot ignore its impact on the environment. By reviewing the literature, we have highlighted that it is possible to take steps toward a more sustainable future through innovation, regulation, and cross-cutting engagement.

In light of rapid changes in technology and society, we call for further research to monitor progress in more sustainable practices and their implementation in the oil industry. Only through continued commitment to these issues, can we hope that the oil industry will become a partner in achieving a sustainable and prosperous future for all of us.

REFERENCES

1. Stanley Ngene, Kiran Tota-Maharaj, Paul Eke, Colin Hills, 2016, Environmental and Economic Impacts of Crude Oil and Natural Gas Production in Developing Countries, *International Journal of Economy, Energy and Environment,* pp 65, 67
2. O. Obire; E. C. Anyanwu, 2009, Impact of various concentrations of crude oil on fungal populations of soil, *Archive of SID,* p 211
3. Simon GARANG KUCH & Jean Pierre BAVUMIRAGIRA, 2019, Impacts of crude oil exploration and production on environment and its implications on human health: South Sudan Review, International Journal of Scientific and Research Publications, Volume 9, Issue 4, April 2019, pp247-248
4. Adedapo O. Adeola, Adedibu S. Akingboye, Odunayo T. Ore, Oladotun A. Oluwajana, Adetola H. Adewole, David B. Olawade, Abimbola C. Ogunyele, 2021, Crude oil exploration in Africa: socio-economic implications, environmental impacts, and mitigation strategies, Environment Systems and Decisions (2022) 42:26–50, pp 41-42

5. Радослав Д. Мићић, 2019, ИСТОРИЈАТ ЕКСПЛОАТАЦИЈЕ НАФТЕ И ГАСА, *Универзитет у Новом Саду Технички факултет „Михајло Пупин" Зрењанин*
6. Onwurah, I. N. E., Ogugua, V. N., Onyike, N. B., Ochonogor, A. E. and Otitoju, O. F., 2007, Crude Oil Spills in the Environment, Effects and Some Innovative Clean-up Biotechnologies, Int. J. Environ. Res., 1(4): 307-320, Autumn 2007, pp 309-314
7. Jacqueline Michel, Merv Fingas, 2016, Oil Spills: Causes, Consequences, Prevention, and Countermeasures, Oil Spills and Response, Article January 2016, pp 159-160, 165, 167

Conference Proceedings
ICPAE 2023, 24th August – 26th August, Zrenjanin, Serbia
University of Novi Sad, Technical Faculty "Mihajlo Pupin", Zrenjanin

Possible Impacts of Surface Limestone Mining on Environment Article

Saša Jovanović[1*], Jasna Tolmač[1], Darko Radovančević[1], Milan Marković[1], Luka Đorđević[1], Ognjen Popović[2], Ljubiša Garić[3]

[1*]*University of Novi Sad, Technical Faculty "Mihajlo Pupin" Zrenjanin, Djure Djakovica bb, Zrenjanin, Serbia*
[2]*Mining institute, Batajnički put 2, Belgrade, Serbia*
[3]*University of Pristina with temporary headquarters in Kosovska Mitrovica, Faculty of Technical Sciences, Kneza Miloša br. 7, Kosovska Mitrovica, Serbia*
sasa.jovanovic@tfzr.rs

Abstract. Limestone is the most excavated building material in the world and one of the most excavated minerals. Huge percentage is excavated on surface, which means that the impact on environment can't be ignored. Like all mining activities, impact has to exist, with a few differences depending on type of excavation and type of excavated mineral. In this paper, those impacts of surface mining will be precisely determined. Also, measures to eliminate or reduce those impacts will be defined.

Keywords: surface mining, limestone, quarry, environmental protection, impacts

INTRODUCTION

After coal, limestone is the most excavated mineral in mining industry. Considering the quantity of building being made in the worlds, it is obvious that the more building materials must be produced to satisfy those needs. As already known, surface mining leaves a lot of scars on the environment during the life time of a mine/quarry. While the mining is vital industry in most of the countries and it contributes greatly to their economics, its impact on the environment shouldn't be neglected. Therefore, the first step is to adequately identify risks and how they impact the environment. After that, some steps are taken to minimize them or to exclude them completely. That being done, monitoring procedures must take place to ensure that environment is not threatened during mining operations [1]. Relation between environment and quarry can be seen in Figure 1.

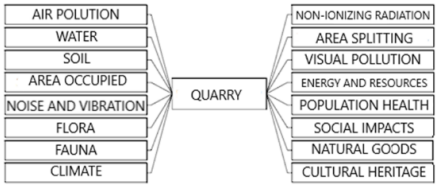

Figure 1. Relation between environment and quarry [2].

POSSIBLE IMPACTS ON THE ENVIRONMENT

Possible impacts can be sorted into several types. The biggest impact is the one on land and soil. The process of mine opening (after obtaining necessary licenses from the government) begins with clearing trees and vegetation in order to prepare that specific region. The topsoil, which is excavated, is the most fertile component of the Earth's crust and it takes a long time to form. For extraction of the limestone itself, multiple layers of materials must be removed to get to the mineral. This layers are called overburden. In most cases, overburden is just waste rock and has to be deposited. Waste rock is dumped on open land and is later used for backfilling of pits. Soil is going to be deteriorated and its properties will be alternated due to prolonged dumping of lime mixed waste rock, Figure 2 [3].

Figure 2. Photographs showing (a) – Loss of forest cover; (b) – Creation of waste land by siltation; (c) - Encroachment of overburden into the forest area; (d) – ASM waste disposal forming a hill of lime waste dumping area; (e) – removal of top soil and landscape deterioration; (f) – encroachment of ASM waste into the nearby local streams; (g) - intrusion of mine waste such as rocks, pebbles and sand into the nearby streams; and (h) - local streams showing high turbidity due to its location near the cement plants; (Lamare & Singh, 2016).

Another very important impact is due to blasting. To excavate mineral material, it has to be removed from the rock mass and that is done with blasting. Large amount of explosives is used to obtain approximate size ruble of limestone. Detonation of explosive releases high amount of energy that displaces rocks from the quarry face while the rest of energy is transmitted in the form of vibrations into the ground and in the air [4]. Vibration induced by blasting can cause fracturing of quarry walls and can increase permeability and drainage towards the quarry face [5]. High noise levels are generated during blasting and by using heavy machineries like excavators, dumpers, loaders and crushing plants. The cumulative impacts of all the noise can affect both humans and environment [6]. Although impact from blasting is not continuous (blasting is done 1-2 times per week), impact on air quality is continuous because the crushing plant is working non-stop. Dust emission are of great concern related to air quality. Mining dust is especially unhealthy and substances can be the size of microns. That means that people can breathe it in and that can have consequences later on. Figure 3 shows chemical composition of limestone rocks at different locations in Meghalaya, India.

Major chemical compounds in %	Jaintia Hills					
	Lakadong	Lumshnong	Nongkhlieh	Nongtalang	Sutnga	Syndai
CaO	42.27-53.89	40.69-54.67	40.46-53.88	46.33	48.75-53.09	42.00-49.60
MgO	1.25-5.58	0.20-11.55	0.36-7.12	3.51	0.72 - 3.41	0.56 - 2.07
SiO_2	0.14-3.12	0.04-17.20	0.16-10.00	-	-	-
Fe_2O_3	0.26-1.59	0.04---3.87	0.07-4.91	-	-	1.73 - 2.31
Al_2O_3	0.22-2.61	0.05-5.71	0.16-6.37	-	-	-
R_2O_3	-	-	-	-	0.48 - 5.40	-
Al	-	-	-	9.07	1.08 - 3.78	6.11-13.90

Figure 3. Chemical composition of limestone rocks at different locations [4].

Total intensity of air pollution is very dependent on meteorological conditions, like rain and wind. That means that the air can be heavily polluted during dry seasons with no wind. This kind of pollution can be empirically calculated. USEPA (U.S. Environmental Protection Agency) database shows emission of dust from working operations, Table 1.

Table 1. Air pollution from different polluters.

Type of polluter	Quantity of dust (per excavated ton or per hour)
One excavator	0,014 kg/t
One dumper	0,4 kg/t
One bulldozer	4 kg/h
Aeolian erosion – wind speed 3 m/s	0,4 kg/ha/h

It is clear that this type of pollution can be very precisely calculated with this type of information. Impacts on water resources are also very important. Mining activities can directly change the course of surface water. Discharging quarry water into nearby streams can increase flood recurrence intervals [7]. The major impact of quarrying on water related to mine dewatering and the associated decline of the water table. For example, to reduce dust, water can be used. That means that there can be huge wastage of water. Within the cone of depression, wells, springs and streams can go dry or have their flows significantly

reduced and the overall direction of groundwater flow may be changed. [8] Figure 4 shows impact of mining activities on water level.

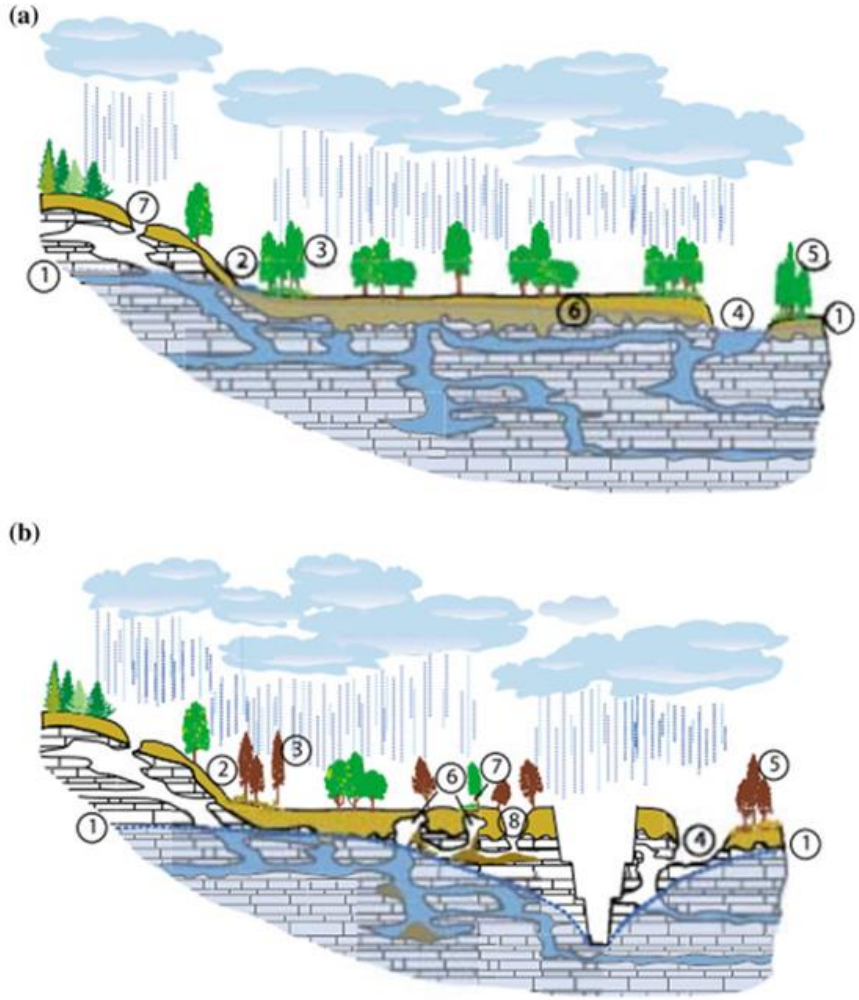

Figure 4. a) Water level prior to quarry development; b) Water level post quarry development (Langer, 2001).

ENVIRONMENT MANAGEMENT PLAN

Environment management plan (EMP) is essential to be made prior mining operations and to be upgraded during mining operations. To leave as less impact on the environment as possible, this plan has to be respected and all activities need to be incorporated. EMP defines mitigation measures for all of the impacts. During mining operations, the fertile

topsoil needs to be stored separately from overburden. It is necessary to reuse the topsoil within the shortest possible time, for plantations. It is necessary that the whole waste rock dump must be stable, with drains around the stockpiles to prevent erosion. Land reclamation activities like backfilling and slope stabilization can be undertaken. Mitigation measures for noise pollution include controlled blasting between favorable hours (avoiding early morning or late night time). Used machinery should be equipped with noise suppression systems. To reduce air pollution, wet drilling should be used and all the dirt roads should be sprayed with water, as well as crushing plant. Greenbelt should be established with the 7,5 m safety zone to capture the particulate matters. Diesel vehicles should be certified in terms of exhaustion gasses. As mine pits are dewatered, that water can be used as technical water and by that reducing freshwater withdrawal. Drains network should be developed to stop the flow of eroded materials to drainage [2-4].

CONCLUSION

In general, every mining activity can cause serious damage on the environment. It takes a lot of work, planning, design and dedication to minimize that damage and to, eventually, exclude it. Effects of mining can be seen after a few years, which means that consequences may not be visible right away and according to that, actions shouldn't wait for consequences to appear, because it may be too late. To reduce impact on the environment, mining companies should carefully follow rules and regulations defined by the government. This field of mining shouldn't have shortcuts, because the consequences can be irreversible.

REFERENCES

1. Gaćina Radmila, Dimitrijević Bojan, 2022, *Reducing environmental impact caused by mining activities in limestone mines,* Underground Mining Engineering 40, pp. 37-44
2. Mining Institute Belgrade, 2020, *Environmental impact study of quarry "Mutalj"*
3. Lamare R. Eugene, Singh Om Prakash, 2017, *Limestone mining and its environmental implications in Meghalaya, India,* ENVIS Bull Himalayan Ecol, pp. 87-100
4. Ganapathi Harsh, Phukan Mayuri, 2020, *Environmental hazards of limestone mining and adaptive practices for environment management plan*, Environmental Processes and Management, pp. 121-135
5. Langer WH, 2001, *Potential environmental impacts of quarrying stone in Karst – a literature review*, U.S. Dept. of the Interior
6. Ahmad Ahanger Faroz, Sharma Harendra K, Ahmad Rather Makhmoor, Rao RJ, 2014, *Impact of mining activities on various environmental attributes with specific reference to health impacts in Shatabdipuram, Gwalior, India,* International Research Journal of Environment Sciences Vol. 3 (6), pp. 81-87
7. Bhatnagar Devanu, Goyal Sandeep, Tignath Sanjay, Deolia D.K., 2014, *Impact of opencast limestone mining on groundwater in Katni river watershed, Madhya, Pradesh, India – A geoinformatics approach,* Journal of Geomatics, Vol. 8 (1), pp. 101-106
8. Hobbs S.L., Gunn J., 1998, *The hydrogeological effect of quarrying karstified limestone: options for prediction and mitigation,* Quarterly Journal of Engineering Geology and Hydrogeology 31 (2), pp. 147-157

Conference Proceedings
ICPAE 2023, 24th August – 26th August, Zrenjanin, Serbia
University of Novi Sad, Technical Faculty "Mihajlo Pupin", Zrenjanin

Influence of Dimensionless Physical Characteristics of Crude Oil in Isothermal Flow Properties

Jasna Tolmac[1*], Slavica Prvulovic[1], Sasa Jovanovic[1], Milan Markovic[1], Darko Radovancevic[1]

[1]University of Novi Sad, Technical faculty "Mihajlo Pupin",
Djure Djakovica bb, 23000 Zrenjanin, Serbia
jasna.tolmac@tfzr.rs

Abstract. The influence of the dimensionless physical characteristics of crude oil in isothermal flow properties was discussed in the paper. Physical quantities that can describe the flow properties of crude oil are: Nusselt number, Reynolds number and Prandtl number. The Nusselt number defines the heat transfer at the fluid-wall interface. The Reynolds number depends on the velocity of the fluid flow, the diameter of the pipeline and the viscosity of the fluid. Prandtl's number depends on the fluid density, viscosity, specific heat capacity and thermal conductivity of the fluid. By increasing the temperature of crude oil, the viscosity decreases, and the Reynolds number and Nusselt number increase. The greatest influence on the value of the Nusselt number, which characterizes the heat transfer at the interface between the fluid and the pipeline wall, is the size of the Reynolds number.

Keywords: temperature, viscosity, Nusselt number, Reynolds number, Prandtl number

INTRODUCTION

The paper presents the results of experimental research on dimensionless parameters of crude oil transport on isothermal flow properties. The scheme of the experimental plant is given in Figure 1. Transport i.e. shipping of oil to the main oil pipeline (5) is carried out from the tank (1). In the section of technological tanks, crude oil is homogenized. Prepared (homogenized) crude oil from the tank (1) is transported using pumps (2) and pipeline (3) to the pump (4). Using the pump (4) and main oil pipeline (5), crude oil is transported to the measuring station (6) and the tank (7).

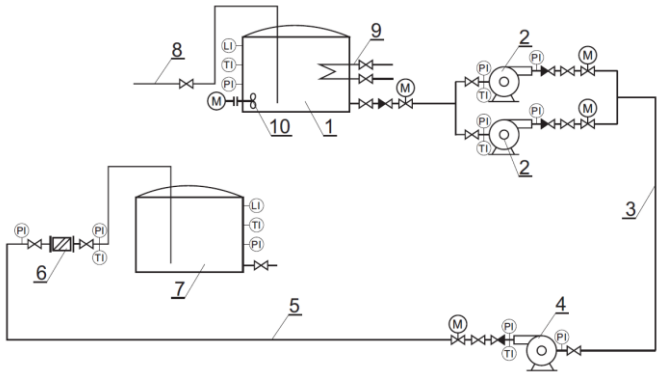

Figure 1. Scheme of the experimental plant, 1-reservoir, 2-centrifugal pump, 3-oil pipeline, 4-centrifugal pump, 5-main oil pipeline, 6-flow measurer, 7-reservoir, 8-crude oil supply, 9-heater, 10-mixer [7]

The results of experimental research are given for the oil pipeline (3). The heating of the oil pipeline (3), with an outer diameter of D_n = 323,9 mm, is done by steam flowing through a pipeline with a diameter of D_p = 25 mm, Figure 2. Both pipelines are laid along the entire length of the oil pipeline. The characteristics of steam are: pressure p = 12 bar, temperature t = 200 °C, heat of evaporation r = 2818 kJ/kg. The oil pipeline is laid above the ground on pillars 0,75 m high.

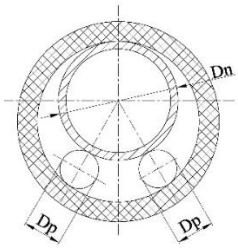

Figure 2. Oil pipeline heating scheme (3), D_n = 323,9 mm using two pipelines D_p = 25 mm [7]

Physical quantities that can describe the flow properties of oil are: Nusselt number, Reynolds number and Prandtl number.

Identification of key research parameters

The Nusselt criterion defines the heat transfer at the fluid-wall interface. By increasing the temperature of crude oil, the viscosity decreases, and the Reynolds number and Nusselt number increase. The Nusselt number depends on heat transfer coefficient from the transported crude oil to the pipeline (α_i) , the heat conduction coefficient of the crude oil (λ_n) and the internal diameter of the pipeline (D_{ci}). The heat transfer coefficient from the transported crude oil to the pipeline (α_i) is a key parameter in the Nusselt criterion.

The Nusselt number is determined using formula (1), [1,2]:

$$Nu = \frac{\alpha_i D_{ci}}{\lambda_n} \tag{1}$$

where is:
Nu – Nusselt number,
α_i (W/m^{2}K) – heat transfer coefficient from the transported crude oil to the pipeline,
D_{ci} (m) – internal diameter of the pipeline,
λ_n (W/mK) – heat conduction coefficient of the crude.

Considering that the pipelines are long, an approximate value of Nu = 3,65 can be taken for laminar flow. The average value of thermal conductivity of oil at standard conditions is λ_n = 0,12 W/mK, [3].

For turbulent flow in hydraulically smooth pipes and for $\delta / D_{ci} << 1$, relation (2) applies [1, 2]:

$$Nu \approx 0{,}116\ (Re^{0,67} - 125)\ Pr^{0,33} \left(\frac{\nu_s}{\nu_c} \right)^{0,14} \tag{2}$$

where is: $\frac{\nu_s}{\nu_c}$ kinematic viscosities of crude oil in the axis of the pipe and near its wall.
Viscosity of oil in the axis of the pipeline and on its wall amounts to $\nu_s / \nu_c = 0{,}9$, [1,4].

The greatest influence on the value of the Nusselt number, which characterizes the heat transfer at the interface between the fluid and the pipeline wall, is the size of the Reynolds number. The Reynolds number depends on the velocity of the fluid flow, the internal diameter of the pipeline and the viscosity of the fluid. The Prandtl number depends on the fluid density, viscosity, specific heat capacity and thermal conductivity of the fluid.

In formula (2), the Reynolds and Prandtl numbers are determined by formulas (3) and (4), [1, 2]:

$$Re = \frac{V \cdot D_{ci}}{\nu} \tag{3}$$

$$Pr = \frac{\rho \nu c_n}{\lambda_n} \tag{4}$$

where is:
ν (m^2/s) – kinematic viscosity,
c_n (J/kgK) – specific heat capacity,
V (m/s) – velocity of the fluid flow,
ρ (kg/m^3) – crude oil density,
D_{ci} (m) – internal diameter of the pipeline.

The average value of the specific heat capacity of oil at standard conditions is c_n = 1885 J/kgK, [3].

Results of experimental research in isothermal flow

For the established values of the flow of crude oil, the sizes of the Reynolds number, the flow velocities were determined and the results are given in Tables 1 to 8. The Reynolds

number is in the range Re = (25625 – 75000), and based on this it can be said that the flow of crude oil through pipeline (3) turbulently, considering that Re > 2320.

The heating of the oil pipeline (3) is carry out on the entire length l = 1550 m, with steam, according to Figure 2. In this way, a constant oil temperature is maintained in the pipeline, so the flow is isothermal. The numerical values of the heat transfer coefficient (α_i) and the Reynolds number (Re) are given in Tables 1 to 8. Results are given for various values of constant oil temperatures of t = (20, 30, 40, 50) ℃, with compatible values of oil viscosity (Tables 1 to 8).

Paraffin-type oils have relatively high flow points, so the crude oil is heated before being introduced into the pipeline, in order to keep the paraffins in a liquid state [2,5].

Table 1. Flow regime, (temperature t = 20 °C, viscosity $v = 23 \cdot 10^{-6}$ m^2/s)

1	Flow Q (m^3/h)	500	560	600	640	700
	Specific flow q (m^3/s)	0,139	0,155	0,167	0,177	0,194
2	Reynolds number Re	25625	28695	30782	32869	35869
3	Flow velocity V (m/s)	1,97	2,20	2,36	2,52	2,75

Table 2. Heat transfer coefficient from the transported crude oil to the pipeline, (temperature t = 20 °C, viscosity $v = 23 \cdot 10^{-6}$ m^2/s.)

1	Flow Q (m^3/h)	500	560	600	640	700
2	Reynolds number Re	25625	28695	30782	32869	35869
3	α_i (W/m^{2}K)	209	229	242	253	271
4	$\alpha_i \cdot D_{ci}$ (W/mK)	63	69	73	76	81

Table 3. Flow regime, (temperature t = 30 °C, viscosity $v = 18 \cdot 10^{-6}$ m^2/s)

1	Flow Q (m^3/h)	500	560	600	640	700
2	Reynolds number Re	32167	36667	39333	42000	45834
	Specific flow q (m^3/s)	0,139	0,155	0,167	0,177	0,194
3	Flow velocity V (m/s)	1,97	2,20	2,36	2,52	2,75

Table 4. Heat transfer coefficient from the transported crude oil to the pipeline, (temperature t = 30 °C, viscosity $v = 18 \cdot 10^{-6}$ m^2/s)

1	Flow Q (m^3/h)	500	560	600	640	700
2	Reynolds number Re	32167	36667	39333	42000	45834
3	α_i (W/m^{2}K)	230	254	269	282	300
4	$\alpha_i \cdot D_{ci}$ (W/mK)	69	76	81	85	90

Table 5. Flow regime, (temperature t = 40 °C, viscosity $v = 15 \cdot 10^{-6}$ m^2/s)

1	Flow Q (m^3/h)	500	560	600	640	700
	Specific flow q (m^3/s)	0,139	0,155	0,167	0,177	0,194
2	Reynolds number Re	39400	44000	47200	50400	55000
3	Flow velocity V (m/s)	1,97	2,20	2,36	2,52	2,75

Table 6. Heat transfer coefficient from the transported crude oil to the pipeline, (temperature t = 40 °C, viscosity $\nu = 15 \cdot 10^{-6}$ m^2/s)

1	Flow Q (m^3/h)	500	560	600	640	700
2	Reynolds number Re	39400	44000	47200	50400	55000
3	α_i (W/m^{2}K)	252	274	288	303	323
4	$\alpha_i \cdot D_{ci}$ (W/mK)	76	82	86	91	97

Table 7. Flow regime, (temperature t = 50 °C, viscosity $\nu = 11 \cdot 10^{-6}$ m^2/s)

1	Flow Q (m^3/h)	500	560	600	640	700
	Specific flow q (m^3/s)	0,139	0,155	0,167	0,177	0,194
2	Reynolds number Re	53727	60000	64363	68727	75000
3	Flow velocity V (m/s)	1,97	2,20	2,36	2,52	2,75

Table 8. Heat transfer coefficient from the transported crude oil to the pipeline, (temperature t = 50 °C, viscosity $\nu = 11 \cdot 10^{-6}$ m^2/s)

1	Flow Q (m^3/h)	500	560	600	640	700
2	Reynolds number Re	53727	60000	64363	68727	75000
3	α_i (W/m^{2}K)	282	310	327	343	365
4	$\alpha_i \cdot D_{ci}$ (W/mK)	85	93	98	103	110

Figure 3 shows the results of the research, which show the dependence of the heat transfer coefficient from the transported crude oil to the pipeline (α_i) on the Reynolds number (Re). The research results are correlated with the experimental equation given in Figure 3.

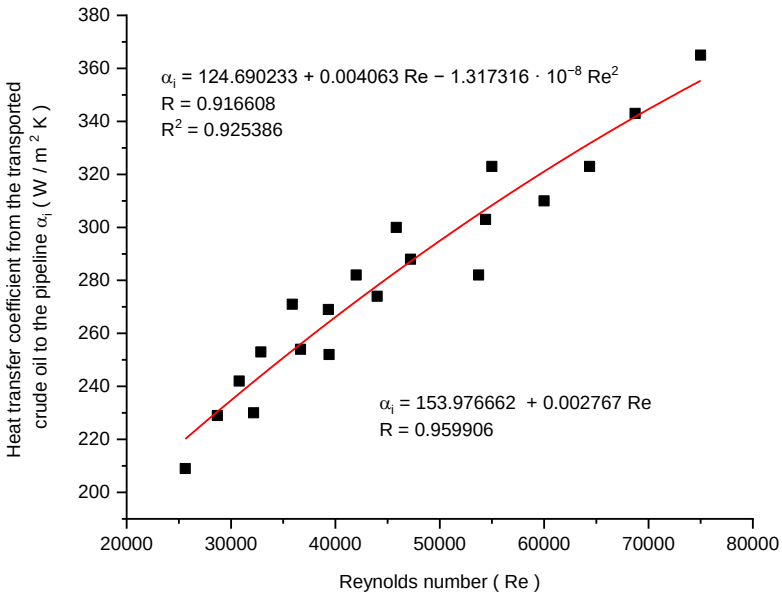

Figure 3. Dependence of the heat transfer coefficient from the transported crude oil to the pipeline (α_i), on the Reynolds number (Re)

When transporting heated oil at a constant temperature t = 20 ℃, for the operating flow mode q = (0,139 – 0,194) m^3/s, the Reynolds number is Re = (25625 – 35869). Based on this, the flow in the oil pipeline (3) is turbulent, given that Re > 2320.

At temperature t = 30 ºC and the given flow regime, the Reynolds number is Re = (32167 – 45834), and the heat transfer coefficient from the transported crude oil to the pipeline is in the range α_i = (230 – 300) W/m^{2}K.

Strujanje kroz naftovod (3) je turbulentno, porastom Rejnoldsovog broja dolazi do porasta koeficijenta prelaza toplote sa sirove nafte na cevovod (α_i). Na osnovu toga pri turbulentnom režimu strujanja dolazi do povećanja koeficijenta prelaza toplote sa sirove nafte na cevovod (α_i).

The flow through the oil pipeline (3) is turbulent. As the Reynolds number increases, the heat transfer coefficient from the crude oil to the pipeline (α_i) increases. Based on this, in the turbulent flow regime, there is an increase in the heat transfer coefficient from the crude oil to the pipeline (α_i).

For the flow range of Q = (500 – 700) m^3/h, the flow velocity was V = (1,97 – 2,75) m/s, and the Reynolds number is in the range Re = (25625 – 75000), for the given values of temperature and viscosity of the transported crude oil (Tables 1 to 8) , so the flow on the given pipeline route is turbulent, i.e. Re > 2320.

As the flow rate increases, the Reynolds number increases too. The viscosity of the crude oil also has an effect on the value of the Reynolds number, as the Reynolds number increases with a decrease in the viscosity of the crude oil and increases with an increase in the heating temperature. The heat transfer coefficient from the transported crude oil to the pipeline (α_i) also increases with the increase in Reynolds number, Figure 3.

Based on the results of the research, the qualitative and quantitative values of the Nusselt number, the Reynolds number and the heat transfer coefficient from the transported crude oil to the pipeline were defined and are given in Tables 9 to 12.

Table 9. Dependence of Nusselt number, Reynolds number and heat transfer coefficient from the transported crude oil to the pipeline, (temperature t = 20 ºC, viscosity $\nu = 23 \cdot 10^{-6}$ m^2/s)

1	Flow Q (m^3/h)	500	560	600	640	700
2	Nusselt number Nu	523	574	605	634	677
3	Reynolds number Re	25625	28695	30782	32869	35870
4	α_i (W/m^{2}K)	209	229	242	253	271

Table 10. Dependence of Nusselt number, Reynolds number and heat transfer coefficient from the transported crude oil to the pipeline, (temperature t = 30 ºC, viscosity $\nu = 18 \cdot 10^{-6}$ m^2/s)

1	Flow Q (m^3/h)	500	560	600	640	700
2	Nusselt number Nu	576	636	672	704	751
3	Reynolds number Re	32167	36667	39333	42000	45834
4	α_i (W/m^{2}K)	230	254	269	282	300

Table 11. Dependence of Nusselt number, Reynolds number and heat transfer coefficient from the transported crude oil to the pipeline, (temperature t = 40 °C, viscosity $\nu = 15 \cdot 10^{-6}$ m^2/s)

1	Flow Q (m^3/h)	500	560	600	640	700
2	Nusselt number Nu	632	685	722	757	807
3	Reynolds number Re	39400	44000	47200	50400	55000
4	α_i (W/m^{2}K)	252	274	288	303	323

Table 12. Dependence of Nusselt number, Reynolds number and heat transfer coefficient from the transported crude oil to the pipeline, (temperature t = 50 °C, viscosity $\nu = 11 \cdot 10^{-6}$ m^2/s)

1	Flow Q (m^3/h)	500	560	600	640	700
2	Nusselt number Nu	717	777	817	857	912
3	Reynolds number Re	53727	60000	64363	68727	75000
4	α_i (W/m^{2}K)	282	310	327	343	365

By increasing the temperature, the viscosity decreases, the Reynolds number, Nusselt number (Nu) and heat transfer coefficient from the transported crude oil to the pipeline (α_i) increase.

In Figure 4, the research results are given, which show the dependence of Nusselt (Nu) and Reynolds number (Re), for the given range of research:

t = 20 °C, $\nu = 23 \cdot 10^{-6}$ m^2/s
t = 30 °C, $\nu = 18 \cdot 10^{-6}$ m^2/s
t = 40 °C, $\nu = 15 \cdot 10^{-6}$ m^2/s
t = 50 °C, $\nu = 11 \cdot 10^{-6}$ m^2/s

The research results are correlated with the experimental equation given in Figure 4.

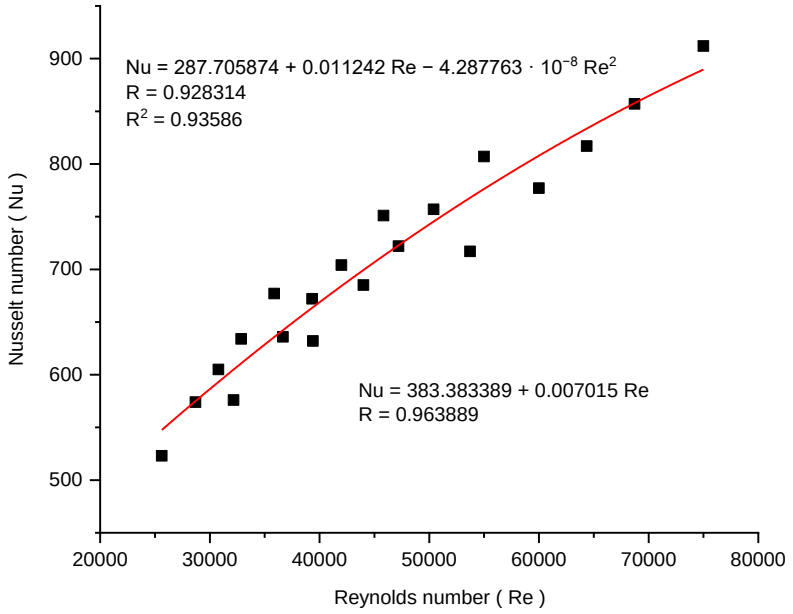

Figure 4. Dependence of Nusselt number (Nu) and Reynolds number (Re)

Numerical values of relevant parameters are given in Tables 9 to 12. For example, for optimal flow values of Q = (560 – 700) m^3/h, the Nusselt number is within limits Nu = (574 – 912), and the Reynolds number is in the range Re = (28695 – 75000) for the given range of research.

At the crude oil heating temperature t = 20 ℃, for the flow rate Q = 700 m^3/h, the Reynolds number is Re = 35870, the Nusselt number is Nu = 677 and the heat transfer coefficient from the transported crude oil to the pipeline is α_i = 271 W/m^{2}K.

At the crude oil heating temperature t = 30 ℃, for the flow rate Q = 700 m^3/h, the Reynolds number is Re = 45834, the Nusselt number is Nu = 751 and the heat transfer coefficient from the transported crude oil to the pipeline is α_i =300 W/m^{2}K.

Based on the research, the values of the Reynolds number Re = (25625 – 75000), and the Nusselt number Nu = (523 – 912) were obtained, Tables 9 to 12. The most influential parameter on the value of the heat transfer coefficient from the transported crude oil to the pipeline (α_i) is the Reynolds number (Re), which characterizes the flow regime. In the turbulent flow regime, the heat transfer coefficient (α_i) increases.

For oil pipelines, the time required to establish a stationary flow of heat in a wider range can be determined by comparing the Nusselt numbers for the stationary flow and the transit state [2].

CONCLUSION

An increase in the heat transfer coefficient from the transported crude oil to the pipeline (α_i) leads to an increase in the Reynolds number, Figure 3. So, for example, for the operational working mode, the value of the Reynolds number is in the range Re = (25625 – 75000) and α_i = (209 – 365) W/m^{2}K is obtained, while the oil flow is turbulent on the entire route of the oil pipeline (3). Based on that, in the turbulent flow regime, higher values are obtained for the coefficient of heat transfer from the transported crude oil to the pipeline (α_i), and therefore the Reynolds number (Re) and the Nusselt number (Nu).

Also, with the increase in flow, the Reynolds number increases, whereby there is an increase in the Nusselt criterion that characterizes the heat transfer at the fluid-wall interface, i.e. the coefficient of heat transfer from the crude oil to the pipeline (α_i).

For the operating flow mode Q = (500 – 700) m^3/h, for the range of constant crude oil heating temperatures t = (20, 30, 40, 50) ℃, the Nusselt number is in the range Nu = (523 – 912), and the Reynolds number is in the range Re = (25625 – 75000), Figure 4 and Tables 9 to 12.

For oil pipelines, the time to establish a stationary flow of heat can be determined by comparing the Nusselt numbers for the stationary flow and the transit state.

Research results and correlation equations can be applied to other pipelines - oil pipelines, under condition that the calculation for dimensionless quantities such as Nusselt (Nu) and Reynolds (Re) number enter the value range of the given research results. Then the correlation equations can be applied to other pipelines.

REFERENCES

1. M. Sasic, Transport of fluids and solid materials by pipes, Science book, Belgrade, 1990.
2. B. Prstojevic, Pipeline transport of oil and gas, Faculty of Mining and Geology, Belgrade, 2012.
3. M. Sasic, Calculation of fluid and solid materials transport by pipes, Science book, Belgrade, 1976.
4. B. Skrbic, Oil and gas transport, Faculty of Technology, Novi Sad, 2006.
5. R. Secerov-Sokolovic, Z. Bjelovic, S. Sokolovic, Influence of solid paraffin content on the rheology of model oil, *Chemical industry*, No. 60, pp.10-14, 2006.
6. P. Tanaskovic, Transportation of Crude Oil and Gas, Part I, II, Faculty of Mining and Geology, Belgrade, 1998.
7. J. Tolmac, Optimization of thermal and hydraulic parameters of crude oil pipeline transport, Ph.D. Thesis, University of Novi Sad, Technical Faculty "Mihajlo Pupin" Zrenjanin, 2020.
8. J. Tolmac, S. Prvulovic, M. Nedic, D. Tolmac, Analysis of the main parameters of crude oil pipeline transport, *Chemical Industry*, Vol. 74, No. 2, pp. 79-90, 2020. ISSN 2217-7426.
9. J. Tolmac, S. Prvulovic, M. Nedić, A. Aleksić, D. Tolmac, Analysis of the influence of physical characteristics of crude oil in pipeline transport, *32th International Congress on Process Industry, PROCESING 2019*, SMEITS Belgrade, Proceedings, pp.105-109, May 30th–31th, 2019, Belgrade, ISBN 978-86-81505-94-6.
10. J. Tolmac, S. Prvulovic, M. Nedić, A. Aleksić, V. Sinik, D. Tolmac, Some Aspects of Crude Oil Pipeline Transport, *9th International Conference Industrial Engineering and Environmental Protection 2019, IIZS 2019*, Proceedings, pp.231-235, October 3rd–4th, 2019, Technical Faculty "Mihajlo Pupin", Zrenjanin, ISBN 978-86-7672-324-9.
11. J. Tolmac, S. Prvulovic, S. Jovanovic, M. Nedic, A. Aleksic, D. Tolmac, Analysis of Crude Oil Transport Parameters in Isothermal Flow, *34th International Congress on Process Industry, PROCESING 2021*, SMEITS Belgrade, Proceedings, pp.157-163, June 03rd – 04th, 2021, Faculty of Technical Science, Novi Sad, ISBN 978-86-85535-08-6.

Conference Proceedings
ICPAE 2023, 24th August – 26th August, Zrenjanin, Serbia
University of Novi Sad, Technical Faculty "Mihajlo Pupin", Zrenjanin

Renewable Energy Sources in Serbia - Electricity Production in the Period 2018 - 2022

Luka Djordjević[1*], Slavica Prvulović[1], Mića Djurdjev[1], Borivoj Novaković[1], Saša Jovanović[1], Milan Marković[1], Dejan Bajić[1]

[1]University of Novi Sad, Technical Faculty "Mihajlo Pupin",
Djure Djakovica bb, Zrenjanin, Serbia
luka.djordjevic@tfzr.rs

Abstract. The utilization of renewable energy sources has gained significant importance worldwide due to their numerous benefits and positive impact on the environment. This study focuses on the status of renewable energy sources and their contribution to electricity production in Serbia over the previous five years. Renewable energy sources play a crucial role in addressing environmental challenges such as climate change and reducing dependence on fossil fuels. In the context of Serbia, there has been a noticeable increase in the utilization of renewable energy sources in recent years. The government has implemented various policies and incentives to promote their development and integration into the national energy mix. This has resulted in a significant expansion of renewable energy capacity, particularly in the areas of wind, solar, and biomass. Despite this progress, the full potential of renewable energy sources in Serbia remains largely untapped.

Keywords: renewable energy sources, electricity production, Serbia, environmental impact, energy transition

INTRODUCTION

Renewable energy sources have emerged as a vital solution to address the challenges of climate change, energy security, and sustainable development worldwide [1]. Their utilization has gained significant momentum in both global and European contexts. This paper explores the status of renewable energy sources and their role in electricity production in Serbia over the previous decade.

In recent years, the importance of renewable energy sources has been widely recognized due to their inherent advantages [2]. Unlike finite fossil fuels, which contribute to greenhouse gas emissions and air pollution, renewable energy sources offer clean, abundant, and sustainable alternatives [3,4]. They include solar power, wind energy, biomass, hydropower, and geothermal energy, among others.

Globally, countries have been actively transitioning to renewable energy sources to reduce their carbon footprint and achieve their climate commitments [5,6]. Europe, in particular, has been at the forefront of this transition, with several countries setting ambitious targets for renewable energy adoption. The European Union (EU) has established binding targets to ensure that 20% of its energy comes from renewable sources by 2020 and

32% by 2030 [7]. This has stimulated significant investment and policy support for renewable energy deployment across the continent.

In the context of Serbia, the utilization of renewable energy sources has experienced noticeable growth in recent years. The country has abundant renewable energy potential, particularly in solar and wind resources. The government has recognized the importance of diversifying the energy mix and reducing dependence on conventional energy sources, primarily coal. Consequently, Serbia has implemented various measures to promote renewable energy development, including adopting supportive policies and establishing feed-in tariffs and incentives [8].

As a result of these efforts, Serbia has witnessed a visible increase in deploying renewable energy projects. The capacity of wind farms, biogas, and biomass plants has expanded significantly, contributing to the overall electricity generation mix. Moreover, the country has also utilized solar and small hydropower resources for electricity production.

Despite progress, the full potential of renewable energy sources in Serbia still needs to be explored. Several challenges and barriers hinder their widespread adoption. Limited investment, inadequate grid infrastructure, complex administrative procedures, and regulatory uncertainties obstruct the further development and utilization of renewable energy resources [9]. Additionally, the dominance of coal-based power generation in Serbia's energy mix remains a significant challenge for transitioning to a cleaner and more sustainable energy system.

Addressing these challenges is crucial to unlocking the benefits of renewable energy sources in Serbia. It requires a comprehensive and coordinated approach that includes strengthening the policy and regulatory framework, enhancing financial mechanisms, improving grid integration, and fostering public-private partnerships [10]. By doing so, Serbia can capitalize on its renewable energy potential, reduce greenhouse gas emissions, improve energy security, and contribute to a sustainable and low-carbon future.

In this paper, we will analyze the progress, challenges, and opportunities associated with renewable energy sources in Serbia over the previous five years. By understanding the current state and exploring potential strategies, we aim to provide insights into maximizing the utilization of renewable energy resources for electricity production and promoting a sustainable energy transition in the country.

MATERIALS AND METHODS

For this research, the authors relied on reports from relevant institutions and agencies in Serbia responsible for monitoring capacity and electricity production. These sources provided valuable data and insights into the status of renewable energy sources and their contribution to electricity generation in the country.

The authors obtained data from reports published by the Energy Agency of Serbia and the Electricity Distribution Company of Serbia to gather information on the current state of renewable energy capacity. These reports presented comprehensive data on the installed capacity of various energy sources, including renewable energy, in Serbia. The data encompassed renewable energy technologies like wind, solar, biomass, and hydropower.

The authors relied on reports published by the Electric Power Industry of Serbia to analyze electricity production from renewable energy sources. These reports provided detailed information on electricity production from different sources, including renewables,

over the past five years. The authors specifically focused on the production data from renewable energy sources to evaluate the trends and changes in the renewable energy sector during the selected period.

The research primarily focused on the previous five years, encompassing 2018 to 2022. This timeframe was selected to capture recent developments and assess the progress of renewable energy production in Serbia. Analyzing this period allowed for a comprehensive understanding of the renewable energy sector's growth rates, trends, and fluctuations.

To ensure the accuracy and reliability of the data, the authors cross-referenced multiple sources and conducted data validation processes.

The collected data were then analyzed using statistical methods and qualitative assessments to evaluate the progress, challenges, and opportunities associated with renewable energy production in Serbia. Key indicators such as installed capacity, electricity generation, growth rates, and the share of renewables in the overall energy mix were analyzed to provide a comprehensive overview of the country's current state of renewable energy.

RESULTS AND DISCUSSION

According to 1, the electricity production capacities comprised 58,1 % of the production from Thermal Power Plants and Combined Heat and Power Plants and 41,9 % from Hydro Power Plants, Wind Power Plants, and other power plants. On the other hand, electricity production has a different distribution. Thermal power plants and Combined Heat and Power Plants make 67,9 % of production, while electricity from renewable energy sources is obtained with a participation of 32,1 %. Table 1 shows the capacities for the production of electricity and the amount of electricity produced in Serbia for the year 2022.

Table 1. Capacities for the production of electricity and the amount of electricity produced in Serbia for the year 2022 [11,12]

	Capacities	Production	Percentage of participation in production capacities	Percentage of participation in electricity production
	[MW]	[GWh]	[%]	[%]
TPP	4,079	21,413	51,9	64,7
CHaPP	297	753	6,2	3,2
HPP	3,015	8,964	34,5	26,9
WPP	373	876	4,4	2,6
OPP	214	871	3	2,6

Table 1 provides additional insights into the capacities for electricity production and the amount of electricity produced in Serbia in 2022. The data shows an imbalance in production capacities and produced electricity. Moreover, even though the production from Thermal Power Plants and Combined Heat and Power Plants participates with 58,1 %, the electricity production is almost 10% higher, i.e., it amounts to 67,9 %. The conventional energy sector's existing production capacities, particularly Thermal Power Plants and Combined Heat and Power Plants, play a substantial role in meeting the electricity demand in Serbia. These facilities contribute a significant portion of the total electricity production

in the country. However, the percentage of electricity production from renewable energy sources remains relatively low.

Table 2 shows data on electricity produced from renewable sources (feed-in tariff) from 2018-2022 [MWh].

Table 2. Electricity produced from renewable sources from 2018-2022 [13]

	2018	2019	2020	2021	2022
Solar energy	10,521	10,941	9,043	10,494	10,899
Hydropower	265,917	230,298	221,283	323,941	299,815
Biomass and biogas energy	95,494	136,070	179,897	244,143	252,699
Wind power	150,419	892,994	835,944	1,070,731	950,210

Based on the data in Table 2, a significant upward trend can be observed in electricity production from various renewable sources in Serbia. Among these sources, Wind Energy experienced the most substantial increase, with a remarkable surge in production from 150,419 MWh in 2018 to 950,210 MWh in 2022. This surge accounts for an impressive growth rate of approximately 632 %. Furthermore, Biomass and biogas energy sources also witnessed a notable rise in production, with an increase from 98,494 MWh in 2018 to 252,699 MWh in 2022, representing a growth rate of approximately 264 % over the course of the previous five years.

Figure 1 provides a visual representation of these data, showing the upward trajectory observed in the electricity production from RES in Serbia over the selected period.

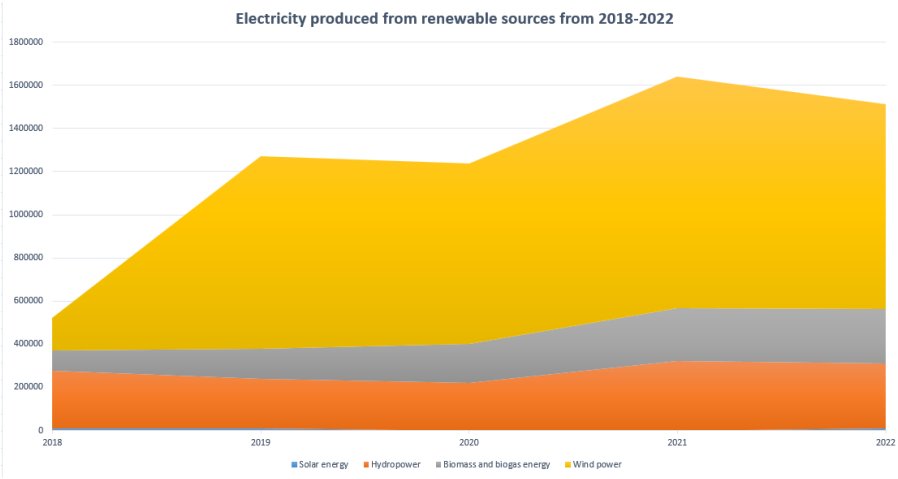

Figure 1. Electricity produced from renewable sources from (feed-in tariff) 2018-2022.

These findings underscore the growing significance of renewable energy sources in Serbia's electricity production landscape. The substantial increase in electricity generation from Wind Energy and the notable growth in Biomass and biogas energy production demonstrates the progress made in utilizing and developing these renewable sources.

Figure 2 shows the feed-in tariff electricity generation structure in Serbia for 2022.

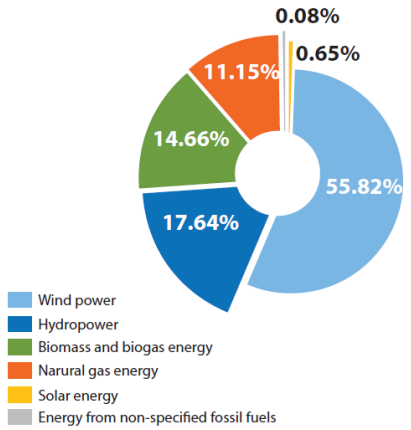

Figure 2. Structure of feed-in tari electricity generation 2022 [12].

In 2022, the feed-in tariff electricity generation structure in Serbia exhibited a diverse mix of renewable energy sources. Wind power held the largest share, contributing approximately 55,82% of the feed-in tariff electricity generation. This indicates the significant role of wind energy in Serbia's renewable energy mix.

Hydropower was the second-largest contributor, accounting for around 17,64% of the feed-in tariff electricity generation. The presence of hydropower highlights its continued importance and utilization as a renewable energy source in Serbia. Biomass and biogas energy sources comprised approximately 14,66% of the feed-in tariff electricity generation. This indicates that using organic materials and waste products to generate renewable energy contributes to Serbia's sustainable energy objectives.

Natural gas energy sources held a share of about 11,15% in the feed-in tariff electricity generation. Although natural gas is not a renewable energy source, its inclusion in the mix may stem from its relatively lower environmental impact than traditional fossil fuels. Solar energy had the smallest share, representing only 0,65% of the feed-in tariff electricity generation. While the contribution is relatively small, it highlights the potential for further development and expansion of solar energy in Serbia.

CONCLUSION

This research is of great importance within the scope of this topic as it provides valuable insights into the status and development of renewable energy sources in Serbia. By utilizing data from authoritative institutions and agencies, the study offers a comprehensive assessment of the country's renewable energy sector's growth and potential. The findings of this research can contribute to a better understanding of the current state of renewable energy production, identify areas for improvement, and inform policymakers and stakeholders in their decision-making processes regarding the promotion and further development of renewable energy sources in Serbia.

ACKNOWLEDGEMENTS

This research was conducted through the project "Creating laboratory conditions for research, development, and education in the field of the use of solar resources in the Internet of Things" at the Technical Faculty, "Mihajlo Pupin", Zrenjanin, financed by the Provincial Secretariat for Higher Education and Scientific Research, Republic of Serbia, Autonomous Province of Vojvodina, Project number 142-451-3118/2022-01.

REFERENCES

1. Hafezi, R.; Alipour, M. Energy Security and Sustainable Development. In *Affordable and Clean Energy*; Encyclopedia of the UN Sustainable Development Goals; Springer International Publishing: Cham, 2020; pp. 1–12 ISBN 978-3-319-71057-0.
2. Javed, M.S.; Ma, T.; Jurasz, J.; Amin, M.Y. Solar and Wind Power Generation Systems with Pumped Hydro Storage: Review and Future Perspectives. *Renewable Energy* **2020**, *148*, 176–192, doi:10.1016/j.renene.2019.11.157.
3. Amin, M.; Shah, H.H.; Fareed, A.G.; Khan, W.U.; Chung, E.; Zia, A.; Rahman Farooqi, Z.U.; Lee, C. Hydrogen Production through Renewable and Non-Renewable Energy Processes and Their Impact on Climate Change. *International Journal of Hydrogen Energy* **2022**, *47*, 33112–33134, doi:10.1016/j.ijhydene.2022.07.172.
4. Mehmood, U. Contribution of Renewable Energy towards Environmental Quality: The Role of Education to Achieve Sustainable Development Goals in G11 Countries. *Renewable Energy* **2021**, *178*, 600–607, doi:10.1016/j.renene.2021.06.118.
5. Yang, H.; Huang, X.; Hu, J.; Thompson, J.R.; Flower, R.J. Achievements, Challenges and Global Implications of China's Carbon Neutral Pledge. *Front. Environ. Sci. Eng.* **2022**, *16*, 111, doi:10.1007/s11783-022-1532-9.
6. Bouyghrissi, S.; Murshed, M.; Jindal, A.; Berjaoui, A.; Mahmood, H.; Khanniba, M. The Importance of Facilitating Renewable Energy Transition for Abating CO2 Emissions in Morocco. *Environ Sci Pollut Res* **2022**, *29*, 20752–20767, doi:10.1007/s11356-021-17179-x.
7. Sikkema, R.; Proskurina, S.; Banja, M.; Vakkilainen, E. How Can Solid Biomass Contribute to the EU's Renewable Energy Targets in 2020, 2030 and What Are the GHG Drivers and Safeguards in Energy- and Forestry Sectors? *Renewable Energy* **2021**, *165*, 758–772, doi:10.1016/j.renene.2020.11.047.
8. Djordjević, L.; Pekez, J.; Novaković, B.; Bakator, M.; Djurdjev, M.; Ćoćkalo, D.; Jovanović, S. Increasing Energy Efficiency of Buildings in Serbia—A Case of an Urban Neighborhood. *Sustainability* **2023**, *15*, 6300, doi:10.3390/su15076300.
9. Prvulovic, S.; Tolmac, D.; Matic, M.; Radovanovic, L.; Lambic, M. Some Aspects of the Use of Solar Energy in Serbia. *Energy Sources, Part B: Economics, Planning, and Policy* **2018**, *13*, 237–245, doi:10.1080/15567249.2012.714842.
10. Loncar, D.; Milovanovic, I.; Rakic, B.; Radjenovic, T. Compound Real Options Valuation of Renewable Energy Projects: The Case of a Wind Farm in Serbia. *Renewable and Sustainable Energy Reviews* **2017**, *75*, 354–367, doi:10.1016/j.rser.2016.11.001.
11. Energy agency of the Republic of Serbia Energy Agency Annual report 2022 Available online: https://shorturl.at/rBMR2 (accessed on 1 July 2023).
12. Electricity Power indusrty of Serbia Technical Report 2022 Available online: https://www.eps.rs/eng/Pages/Technical-reports.aspx (accessed on 7 July 2023).
13. Joint stock company Elektroprivreda Srbije Annual Reports 2018-2022 Available online: https://www.eps.rs/lat/Stranice/tehnicki-izvestaji.aspx (accessed on 7 July 2023).

Conference Proceedings
ICPAE 2023, 24th August – 26th August, Zrenjanin, Serbia
University of Novi Sad, Technical Faculty "Mihajlo Pupin", Zrenjanin

Environmental Impact of Block Caving Mining Method

Ognjen Popović [1*], Saša Jovanović[2], Darko Radovančević[2], Milan Marković[2]

[1*]*Mining institute, Batajnički put 2, Belgrade, Serbia*
[2] *University of Novi Sad, Technical Faculty "Mihajlo Pupin" Zrenjanin, Djure Djakovica bb, Zrenjanin, Serbia*
ognjen.popovic@ribeograd.ac.rs

Abstract. Block caving is a mining method which is more and more popular in underground mines. The reason of its popularity is the biggest capacity of all underground mining methods. Also, its impact on the environment is unavoidable and it can be measured as one of the biggest impacts of all underground mining operations. In this paper, environmental protection from surface subsidence will be discussed. Also, paper will contain current mining projects that are using this method and the future ones.

Keywords: underground mining, block caving, surface subsidence, environmental protection

INTRODUCTION

In the last couple of decades, demand for raw mineral materials increased dramatically. Because of that, mining as an industry, has to provide more quantity of mineral materials. It is already known that the bigger percentage of mineral materials are excavated on the surface. However, some technological boundaries can't be crossed, which limit possible capacity of surface mining. Because of that, some underground mining methods are being upgraded to have bigger capacities, so that they can fulfill those conditions. Block caving mining method has one of the biggest capacities out of all underground mining methods and can go up to 100000 t per day. The use of this method is recommended when the ore body is weak, with steep angle and thick [1]. The first block caving method was used in 1895. in iron mine called Pewabic [2]. The biggest percentage of mined material using this method is copper (Figure 1).

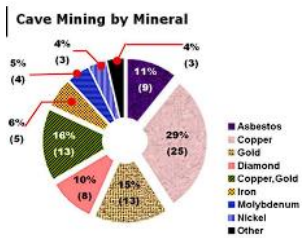

Figure 1. Cave mining by mineral (Woo et al, 2009).

BLOCK CAVING MINING METHOD

Generally, all mining methods that are based on caving have same characteristics: high production rates, low operative costs, high mineral loses and high percentage of waste rock included in mineral excavation. These methods are used for excavating not so rich ore bodies, so those conditions are understandable. Block caving mining method is used in such a way, where the ore body is defined as a block of certain dimensions and the mineral is collected at the bottom of that block. The main condition is that the ore has high cavability. Caving can be done naturally, by influence of rock stress or it can be forced by blasting. Another condition is that the ore shouldn't be adhesive and prone to oxidation (Figure 2).

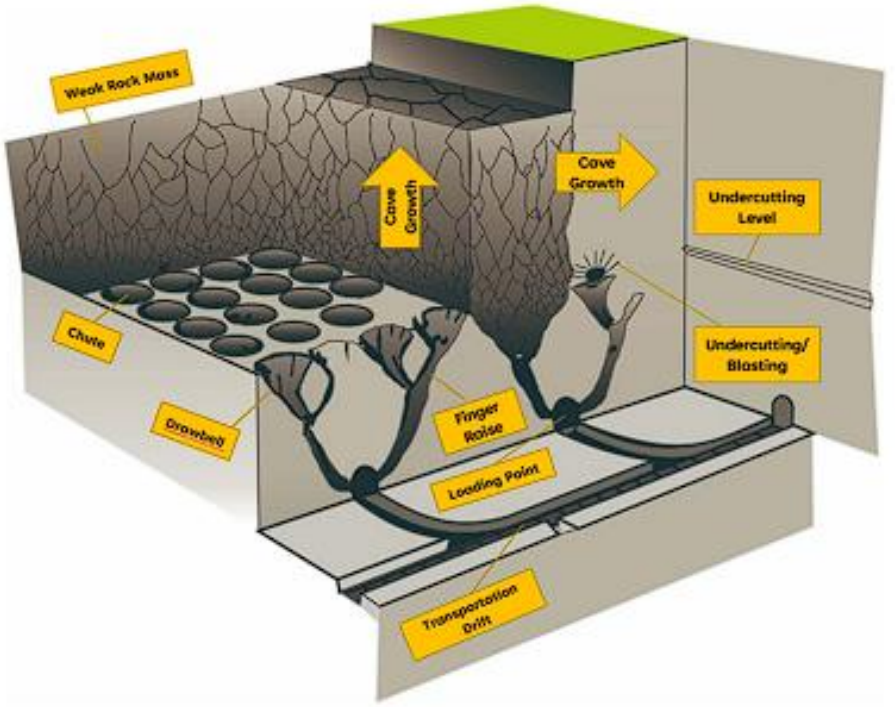

Figure 2. Block caving mining method (Torbica & Lapčević, 2020).

The point of block caving is to excavate part of the rock mass that is big enough to cause instability of the rock mass above it, so that it can start caving on its own. The surface causing instability is the minimal surface of a mining block and it represents characteric of a rock mass. Below undercut level is loading level. Between these levels, draw bells are made where the ore body is going to be drawn. The material is naturally granulated by friction inside a draw bell. The biggest production is achieved by using loaders as a primary transportation system. The transportation can be continued with conveyors to maximize capacity. Block caving has big capital expenses because some time must pass until the production phase begins. In that period, all levels must be made and all of the infrastructure, not to mention that the infrastructure must be at the bottom of ore body, which can be very

deep. That being said, operative costs are very small (1 – 2,5 $/t) and the capacity varies between 10000 and 100000 t/day (El Teniente mine in Chile). Modern mines use this method for ore bodies with thickness 200-800 m, with block height of over 400 m. Rock mass has compression strength of 6 – 60 MPa. As blocks got higher over time, undercut levels also grew and today some undercut levels can be as big as 35280 m^2 (Northparkes mine). Draw rates vary from mine to mine, with average of 0,2 meters a day (Figure 3) [1-3].

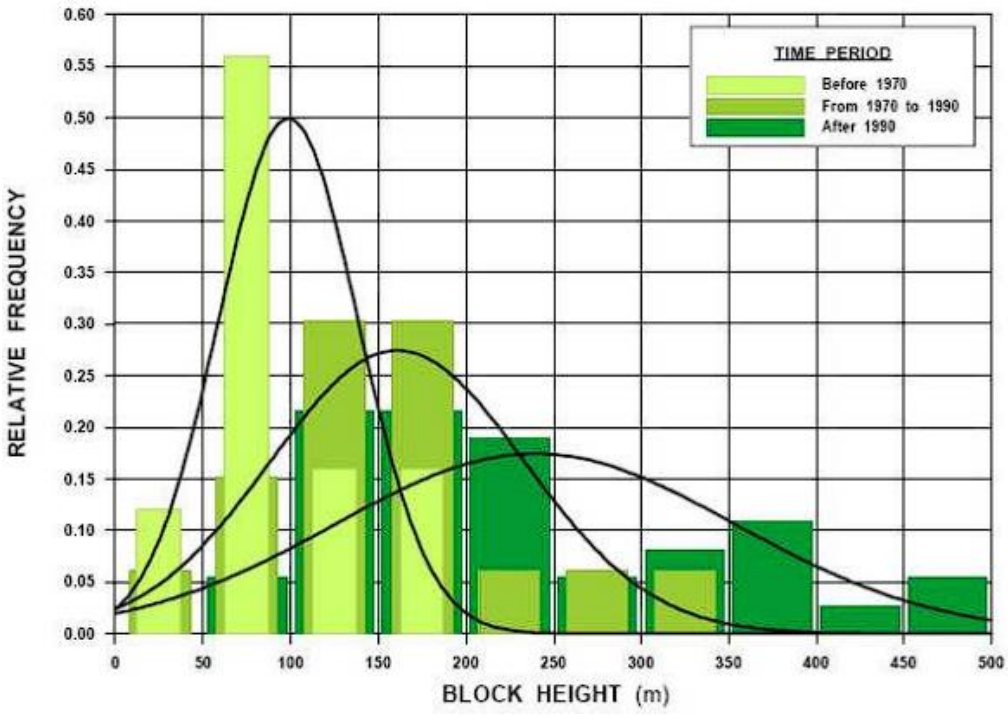

Figure 3. Frequency of a certain block heights over time (Woo et al, 2009).

IMPACT ON ENVIRONMENT

There are three clear impacts on environment, one connected with the whole mining industry and two specifically connected to caving mining methods. The first one is obvious and it is waste rock management. Considering the capacity of this method, huge quantity of waste rock must be managed in a life time of a mine. This means that a mine with a capacity of 100000 t/day, must manage almost 100000 t of waste rock. This is calling for attention on a projected waste rock dump and its stability, so the risks can be minimal [2]. Second impact can have pretty serious consequences and it is defines as impact on underground water. During caving, natural state of a rock mass is disturbed and the whole rock mass is caving. If the ore body is in a water rich area, level of underground water can be disturbed and that can have an impact on a bigger water reserves (rivers, lakes etc.). Also,

underground water can be polluted by oxidized mineral or by residue from blasting. That water can again pollute rivers and others water sources on its way.

The highest and most obvious impact on environment is subsidence. Due to massive quantities of rock mass excavated, subsidence will be huge and it will be show on a surface. That means that there cannot be any objects where the subsidence is projected (houses, rivers, national parks etc.). It is essential to direct attention to risk assessment from this impact, by calculating the area which will be affected by this method. Factors which influence terrain subsidence and their importance are represented in Figure 4.

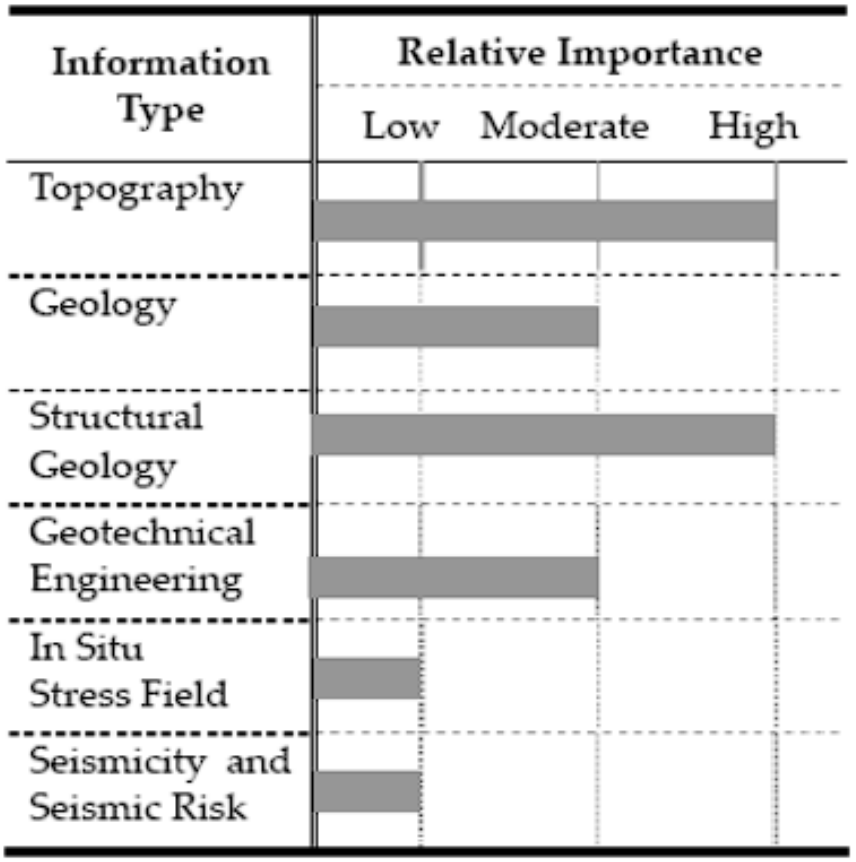

Figure 4. Factors affecting block caving subsidence and their relative importance.

Key factor that impacts subsidence area is are of undercut. If the undercut area is known, subsidence can be predicted based on quality of rock mass and depth of undercut level. Figure 5 shows subsidence scheme [4].

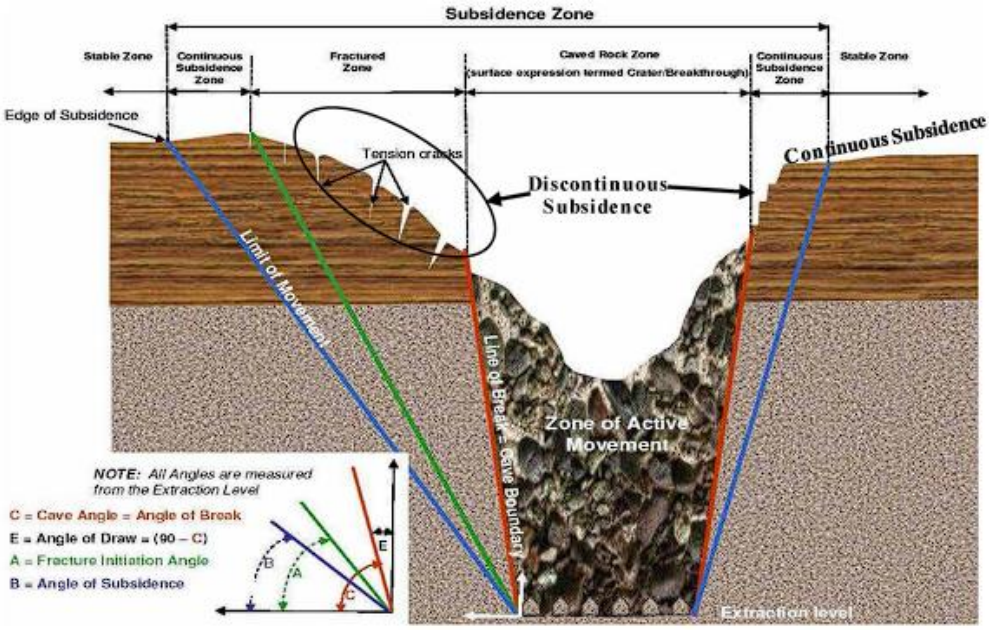

Figure 5. Subsidence zones (Parmar et al, 2019).

It can be seen that the angles of subsidence don't have to be symmetrical on both sides. This is heavily dependent on geology of the area. Different types of rock mass with different strength can change the angles of subsidence. It is important to make a geological model with enough information about surrounding rock types (Figure 6) [5].

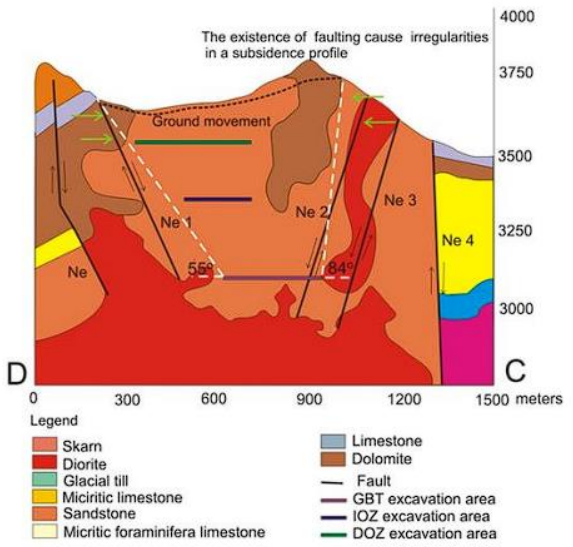

Figure 6. Geological impact on deformation angles (Esaki et al, 2009).

Macro deformations zone represents zone where deformations can be seen with naked eye. Micro deformations zone is a zone where subsidence has its impact, even if it is not seen by the naked eye. Shape of macro deformations zone depends on rock mass characteristics, Figure 7.

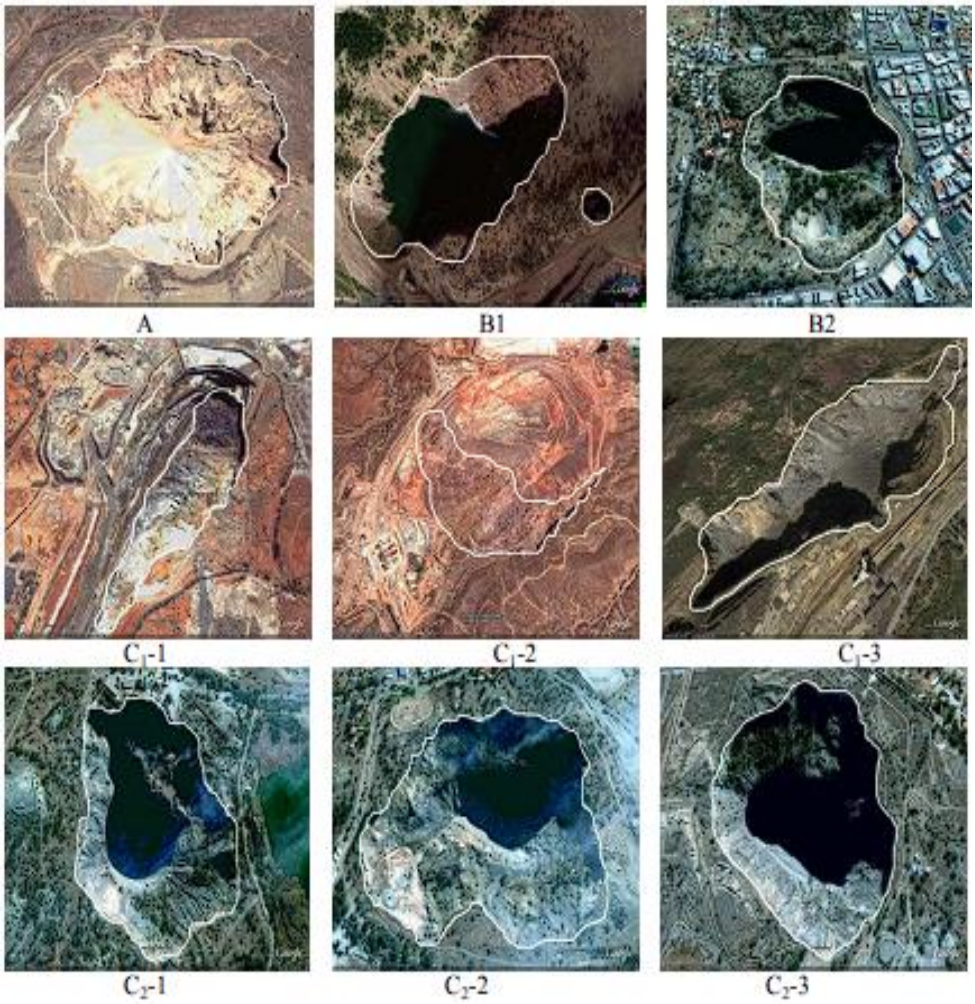

Figure 7. Macro deformation patterns: Type A – circular, Type B – elliptical, Type C_1 – irregular with scarps, Type C_2 – irregular with a distinct collapse structure/glory hole (Woo et al, 2009).

There are mathematical ways to estimate deformation zones. The biggest problem is that there is a lot of variables that can't be mathematically represented (like geology). In that case, empirical analysis of working mines can be helpful. In Table 1, dimensions of deformation zones in existing mines are given, compared to their undercut areas [3].

Table 1. Deformation zones dimensions in mines using block caving method (Woo et al, 2009.)

Mine (State)	Mineral	Undercut area (m^2)	Deformation length (m)	Deformation width (m)
Northparkes (Australia)	Copper, gold	35280	359	299,2
Sunrise (USA)	Iron	5000	587,1	362,5
Kimberly (RSA)	Diamond	1688	397,7	364,9
Wesselton (RSA)	Diamond	4320	484,6	464,9
Cullinan (RSA)	Diamond	3600	806,4	359,1
Ray (USA)	Copper	1855	678,9	232,5
Koffiefontein (RSA)	Diamond	4320	402,5	389,1
Finsch (RSA)	Diamond	5500	367,9	316
Salvador (Chile)	Copper	11440	2064	1345,5

CONCLUSION

With higher demand for mineral materials, mining industry is moving towards underground mining with high capacities. With higher capacities, mines are bigger, everything magnifies, including impacts on environment. Method that is used for high capacities is block caving method. This method includes caving of upper rock mass, which means even more impact on environment that conventional methods. These impacts aren't small, but with careful planning and assessment, they can be projected very well and the risks can be lowered or even removed. Not to mention, with more mines that are using this method, more experience is gained and more data is collected. All of that can be used to put these impacts on environment under control.

REFERENCES

1. Torbica Slavko, Lapčević Veljko, 2020, *Методе подземног откопавања*, pp. 556-578
2. Melati Sari, Wattimena Ridha Kresna, Sahara David Prambudi, Syafrizal, Simangunsong Ganda Marihot, Hidayat Wahyu, Riyanto Erwin, Felisia Raden Roro Shinta, 2022, *Block Caving Mining Method: Transformation and Its Potency in Indonesia*, Energies 16 (1)
3. Woo Kyu-Seok, Eberhardt Erik, Van As Andre, 2009, *Characterization and empirical analysis of block caving induced surface subsidence and macro deformations*, Conference: 3rd Canada-US Rock Mechanics Symposium and 20th Canadian Rock Mechanics Symposium
4. Parmar Hadi, Bafghi Alireza Yarahmadi, Najafi Mehdi, 2019, *Impact of ground surface subsidence due to underground mining on surface infrastructure: the case of Anomaly No. 12 Sechahun, Iran*, Environmental Earth Sciences 78

5. Esaki Tetsuro, Setianto Agung, Mitani Yasuhiro, Djamaluddin Ibrahim, Ikemi Hiro, 2009, *Influence of geological condition study on development of surface subsidence associated with block caving mining using GIS analysis*, International Journal of the JCRM Vol. 5 (2), pp. 87-93

Conference Proceedings
ICPAE 2023, 24th August – 26th August, Zrenjanin, Serbia
University of Novi Sad, Technical Faculty "Mihajlo Pupin", Zrenjanin

The Role of Green Human Resource Management in SMEs

Stefan Ugrinov[1*], Verica Gluvakov[1], Mila Kavalić[1], Sanja Stanisavljev[1], Dragana Kovač[1], Dejan Bajić[1]

[1]*University of Novi Sad, Technical Faculty "Mihajlo Pupin", Djure Djakovica bb, 23000 Zrenjanin, Serbia*

stefanugrinov1@gmail.com

Abstract. Small and Medium-sized Enterprises (SMEs) play a pivotal role in economies, and their engagement with Green Human Resource Management (GHRM) holds substantial environmental and business implications. This abstract explores how GHRM, a strategic integration of sustainability principles into HR practices, is uniquely relevant to SMEs. SMEs possess the agility to swiftly adopt sustainable initiatives, aligning with GHRM's principles. This paper highlights the benefits, such as cost savings and enhanced employee engagement, that SMEs can reap from GHRM. Challenges, including resource constraints, are acknowledged alongside strategies like targeted recruitment and flexible work arrangements to overcome them.

Keywords: green human resource management, sustainability, small and medium-sized enterprises, eco-consciousness, employee engagement, environmental impact

INTRODUCTION

Organizations are currently shifting their strategies and goals to be more environmentally conscious as the significant literature focused on larger firms rather than SMEs despite SMEs highly impacting the environment due to their commercial activities [1]. As engines of innovation, employment, and economic growth, SMEs wield considerable influence in shaping societal and environmental outcomes. In response to the imperatives of sustainability, the convergence of SMEs with Green Human Resource Management (GHRM) presents an essential avenue for aligning organizational practices with ecological responsibility. Accordingly, the top management of SMEs reconsiders their objectives and broadens the scope of their operations by including green HRM practices to improve environmental performance [2]. Organizations and employees both benefit from the adoption of GHRM practices because it boosts employee morale and productivity [3]. As the world confronts pressing challenges like climate change and resource depletion, SMEs embracing GHRM hold the potential to lead by example. By fostering employee engagement, optimizing resource utilization, and positioning themselves as eco-conscious entities, SMEs can not only mitigate their environmental footprint but also elevate their competitive standing in an increasingly sustainability-conscious market.

GHRM PRACTICES

GHRM involves practices such as green recruitment and selection (GRS), green training (GT), and green pay and reward (GPR) to increase green employee performance [4]. GHRM in the organizational setting can improve green performance (GP) by recruiting environmentally concerned employees, providing green training, encouraging employees to be involved in green activities by establishing green reward structures, and creating a platform where employees can engage in green initiatives. Aim of green training as a process is to help employees better understand environmental awareness, sustainable practices, green technologies, corporate social responsibility and sustainable.

Circular economy also plays big role in GHRM. It's core concept is based on reducing waste and maximizing resource efficiency. In addition, a green work climate (GWC) is essential for increasing greenwork engagement (GWE) and performance [5]. GWC, GWE, and green employee behavior(GEB) are among the significant constructs in enhancing GP [6].

The relationship between GHRM practices, GWC, GWE, GEB, and GP has been builton the basis of abilities, motivation, and opportunities (AMO) theory [7]. According to AMO theory, HRM is carried out by increasing employee ability by motivating employees to become high-performers and boosting employee performance by providing them with a platform through which they can avail opportunities and become more productive. Based on the grounds of AMO theory, the objective of green performance can be achieved if employees are provided with GHRM practices such as GT, are recruited on the basis of green values, and are rewarded conditionally by carrying out an effective performance management system [8].

GREEN WORK CLIMATE

Improving environmental performance requires maximizing the incorporation of training, teamwork, monetary and non-monetary rewards, and sustainable goals [9]. It encompasses the collective efforts, values, and norms within an organization that prioritize environmental responsibility and contribute to a greener and more sustainable workplace. Creating a green work climate requires a holistic approach that involves leadership commitment, employee engagement, and ongoing efforts to integrate sustainability into various aspects of the organization's operations and culture.

GHRM involves the policies and practices that motivate employees to participate in activities that promote socially responsible green behavior to create an environmentally conscious and resource-efficient organization [10]. In line with this, several studies have found a positive relationship between GRS and GWC. GRS has been recognized as a key constituent of GHRM practices. Some authors outlined GRS in three parts: employees' green awareness, green employer branding, and green criteria to attract candidates [11]. Firstly, the most crucial part of GRS is employees' green awareness, and it includes personality qualities such as green conscientiousness awareness and agreeableness that allow sustainable goals to be met [12]. Employees who value a green environment have been discovered to have an active improvement in their environmental knowledge, hence providing a GWC [13].

GREEN EMPLOYEE BEHAVIOR

GEB involves both in-role and extra-role green behavior [14]. Green employee behavior can manifest in various ways, such as reducing energy consumption, minimizing waste generation, using eco-friendly products, promoting recycling, and participating in conservation programs. These are the kinds of activities that would be expected of an employee and, as a result, are part of a person's formal work responsibilities [15]. According to HRM behavioral research, a green organizational climate influences employee work attitudes and behavior [16]. Employee outcomes of green behavior are highly dependent on a green work climate, according to HRM behavioral research [17].

Promoting green employee behavior requires a supportive organizational culture, leadership commitment, and ongoing efforts to make environmentally friendly practices convenient and accessible for employees. Encouraging green behavior not only benefits the environment but also fosters employee engagement, collaboration, and a sense of purpose in contributing to a better world.

Work engagement, for example, has been found to improve employees' GP by helping them better understand GHRM principles and giving them the power to apply positive environmental solutions [18]. Employees propagate proactive environmental measures when they are incorporated into their day-to-day roles [19]. As a result, creating an engaging atmosphere has a positive impact on employee performance, allowing employees to focus on improvement projects such as eliminating inefficient tasks [20]. Therefore, minimizing and reusing raw materials improves recycling, reduces resource consumption, lowers prices, and improves overall GP [21]. Employees are encouraged to actively engage in eco-friendly initiatives, such as participating in tree planting drives, waste reduction campaigns, and energy-saving challenges. Green employee behavior involves a shift in everyday practices, such as using reusable water bottles, reducing paper usage by opting for digital documents, and turning off lights and electronic devices when not in use.

CONCLUSION

As SMEs embrace green HRM, they navigate a transformative journey that converges human potential and environmental consciousness. The evolving landscape underscores the importance of leadership commitment, employee engagement, and the seamless integration of green initiatives across HR functions. By fostering an environment of continuous learning, innovation, and collaboration, SMEs can harness the collective power of their workforce to drive tangible sustainability outcomes. In the years to come, the success of SMEs will be indelibly intertwined with their ability to champion green human resource management. The trajectory of sustainable development hinges upon their capacity to integrate eco-centric values into organizational DNA, inspire green employee behavior, and pioneer resilient practices that endure beyond profitability. As SMEs embark on this odyssey, they wield the potential to not only enhance their competitive edge but also contribute to a healthier, more harmonious planet for generations to come.

REFERENCES

1. Song, W.; Yu, H.; Xu, H. Effects of green human resource management and managerial environmental concern on green innovation. Eur. J. Innov. Manag. 2020, 24, 951–967
2. Shafaei, A.; Nejati, M.; Yusoff, Y.M. Green human resource management. Int. J. Manpow. 2020, 41, 1041–1060
3. Roscoe, S.; Subramanian, N.; Jabbour, C.J.; Chong, T. Green human resource management and the enablers of green organizational culture: Enhancing a firm's environmental performance for sustainable development. Bus. Strategy Environ. 2019, 28, 737–749
4. Pham, N.T.; Tučková, Z.; Jabbour, C.J.C. Greening the hospitality industry: How do green human resource management practices influence organizational citizenship behavior in hotels? A mixed-methods study. Tour. Manag. 2019, 72, 386–399
5. Graves, L.M.; Sarkis, J.; Gold, N. Employee pro-environmental behavior in Russia: The roles of top management commitment, managerial leadership, and employee motives. Resour. Conserv. Recycl. 2019, 140, 54–64.
6. Chen, S.; Jiang, W.; Li, X.; Gao, H. Effect of Employees' Perceived Green HRM on Their Workplace Green Behaviors in Oil and Mining Industries: Based on Cognitive-Affective System Theory. Int. J. Environ. Res. Public Health 2021, 18, 4056
7. Renwick, D.W.; Redman, T.; Maguire, S. Green human resource management: A review and research agenda. Int. J. Manag. Rev. 2013, 15, 1–14
8. Iftikar, T.; Hussain, S.; Malik, M.I.; Hyder, S.; Kaleem, M.; Saqib, A. Green human resource management and pro-environmental behavior nexus with the lens of AMO theory. Cogent Bus. Manag. 2022, 9, 2124603
9. Pham, N.T.; Thanh, T.V.; Tučková, Z.; Thuy, V.T.N. The role of green human resource management in driving hotel's environmental performance: Interaction and mediation analysis. Int. J. Hosp. Manag. 2020, 88, 102392
10. Pham, N.T.; Tučková, Z.; Jabbour, C.J.C. Greening the hospitality industry: How do green human resource management practices influence organizational citizenship behavior in hotels? A mixed-methods study. Tour. Manag. 2019, 72, 386–399
11. Muisyo, P.K.; Qin, S. Enhancing the FIRM'S green performance through green HRM: The moderating role of green innovation culture. J. Clean. Prod. 2021, 289, 125720.
12. Yong, J.Y.; Yusliza, M.Y.; Ramayah, T.; Fawehinmi, O. Nexus between green intellectual capital and green human resource management. J. Clean. Prod. 2019, 215, 364–374.
13. .Islam, T.; Khan, M.M.; Ahmed, I.; Mahmood, K. Promoting in-role and extra-role green behavior through ethical leadership: Mediating role of green HRM and moderating role of individual green values. Int. J. Manpow. 2020, 42, 1102–1123.
14. Dumont, J.; Shen, J.; Deng, X. Effects of green HRM practices on employee workplace green behavior: The role of psychological green climate and employee green values. Hum. Resour. Manag. 2017, 56, 613–627
15. Chen, S.; Jiang, W.; Li, X.; Gao, H. Effect of Employees' Perceived Green HRM on Their Workplace Green Behaviors in Oil and Mining Industries: Based on Cognitive-Affective System Theory. Int. J. Environ. Res. Public Health 2021, 18, 4056.
16. .Bhutto, T.A.; Farooq, R.; Talwar, S.; Awan, U.; Dhir, A. Green inclusive leadership and green creativity in the tourism and hospitality sector: Serial mediation of green psychological climate and work engagement. J. Sustain. Tour. 2021, 29, 1716–1737.
17. Shoaib, M.; Abbas, Z.; Yousaf, M.; Záme˘cník, R.; Ahmed, J.; Saqib, S. The role of GHRM practices towards organizational commitment: A mediation analysis of green human capital. Cogent Bus. Manag. 2021, 8, 1870798.
18. Ari, E.; Karatepe, O.M.; Rezapouraghdam, H.; Avci, T. A Conceptual Model for Green Human Resource Management: Indicators, Differential Pathways, and Multiple Pro-Environmental Outcomes. Sustainability 2020, 12, 7089.
19. Tian, Q.; Robertson, J.L. How and When Does Perceived CSR Affect Employees' Engagement in Voluntary Pro-environmental Behavior? J. Bus. Ethics 2017, 155, 399–412

20. Su, X.; Xu, A.; Lin, W.; Chen, Y.; Liu, S.; Xu, W. Environmental leadership, green innovation practices, environmental knowledge learning, and firm performance. Sage Open 2020, 10, 2158244020922909
21. Ren, S.; Tang, G.; Jackson, S.E. Effects of Green HRM and CEO ethical leadership on organizations' environmental performance. Int. J. Manpow. 2020, 42, 961–983

Conference Proceedings
ICPAE 2023, 24th August – 26th August, Zrenjanin, Serbia
University of Novi Sad, Technical Faculty "Mihajlo Pupin", Zrenjanin

Green Marketing: Navigating the Intersection of Business and Environmental Sustainability

Stefan Ugrinov[1*], Verica Gluvakov[1], Mila Kavalić[1], Sanja Stanisavljev[1], Maja Gaborov[1], Dejan Bajić[1]

[1]*University of Novi Sad, Technical Faculty "Mihajlo Pupin", Djure Djakovica bb, 23000 Zrenjanin, Serbia*
stefanugrinov1@gmail.com

Abstract. In today's dynamic business landscape, the imperative to address environmental concerns while pursuing profitability has led to the emergence of green marketing as a pivotal strategy. The paper investigates the challenges and opportunities that arise at the intersection of business and environmental sustainability, shedding light on the ethical dimensions and consumer expectations involved. Additionally, it examines the potential pitfalls and risks of greenwashing, where superficial eco-friendly claims can mislead consumers. Through a comprehensive review of existing literature, this paper presents a nuanced understanding of green marketing's evolution, its impact on consumer behavior, and its potential to drive positive change. Ultimately, it underscores the importance of authentically aligning business goals with environmental protection for long-term success in an increasingly conscious market.

Keywords: green marketing, greenwashing, environmental sustainability, products and services

INTRODUCTION

In an era marked by growing environmental consciousness and the urgent need for sustainable practices, the convergence of business objectives and ecological considerations has given rise to a transformative concept: green marketing. Green marketing is a management process that can make a company more profitable and contribute to the company's long-term viability through sustainable practices [1]. The landscape of modern business is evolving, spurred by a shifting global mindset that demands conscientious consumption and corporate responsibility. Against this backdrop, green marketing stands as a linchpin, embodying the synergy between economic aspirations and environmental stewardship. According to the theory of consumption decision mechanism, consumption intention comes before consumption behavior, and consumer purchase behavior can be effectively reflected through purchase intention, that is, consumers who implement green purchase behavior in real life generally have strong green consumption intention [2].

Many firms are considering environmental protection as their social responsibility because of climate change and environmental risks are now becoming challenging. The reason is that people are not showing responsibility and are not more concerned about environmental risks. In general, people are also unable to realize how their attitudes and behaviours lead to environmental problems [3]. To deal with the growing environmental

concerns it is very significant for marketers to investigate the aspects that influence consumer views and purchase decisions regarding a company's offerings [4].

GREEN MARKETING MIX STRATEGIES

When talking about different green marketing strategies there are certain terms that need to be understood. First would be Green Price . It presents prices for green products, which can be higher compared to conventional non-green products due to the usage of dearer raw materials to maintain good quality, usage of substitutes for chemicals and other toxic substances, and enhanced cost of production due to increased restrictions [5]. The phrase "premium price" is commonly employed in green product research to describe the elevated costs associated with producing, consuming, and disposing of environmentally conscious products. This arises from the increased expenses incurred in adopting green practices throughout the production cycle, leading to higher production costs compared to conventional non-green products. Moreover, the inclusion of policy-driven environmental measures further contributes to production costs, consequently elevating the retail price of green products.

It's impossible to talk about green marketing strategies without mentioning a Green Product. Green products pose no threats to the well-being of both humans and the environment. These items neither contribute to air pollution nor hinder the potential for recycling. Moreover, they facilitate the preservation of precious natural resources, ensuring their availability for generations to come. The most relevant definition of green products says that green products' environmental and societal staging is better than traditional non-green products in all stages, i.e., production, consumption, and disposal [6].

Green promotional tactics are crucial in driving the successful acceptance of green products among consumers. This acceptance hinges on marketers' adept use of appropriate communication approaches. Consequently, effective communication stands as a fundamental element of achieving excellence in green marketing. Advertising and sales promotion have undergone significant modifications due to environmental changes in raw materials, production processes, and distribution strategies [7].

Green place manages reverse logistics to reduce carbon footprint by bringing down transportation emissions [8]. The approaches employed by marketers to ensure the timely availability, appropriate quantity, and suitable distribution of green products are denoted as the "green place" element within the framework of green marketing mix. Green place encompasses improved inventory control, lowered inventory expenditures, efficiency gains in both cost and time, and an elevated level of consumer service. The distributors must formulate an eco-friendly distribution strategy to maintain the sustainability aspect of marketing and benefit from a competitive edge over competitors [9].

ENVIRONMENTAL ATTITUDES OF CONSUMERS AND THEIR INTENTIONS FOR GREEN PURCHASING

The constituents of consumers' environmental attitudes comprise environmental concern, recognition of environmental challenges, mindfulness of environmental issues and remedies, comprehension of environment-related matters, and engagement in environmental activism. Three kinds of environmental attitudes predict the ecological

behavior of a person: attitude towards the environment, which is referred to as an environmental concern (deteriorating quality of air due to pollution); attitude towards ecological behavior (recycling and energy-saving behavior); and the NEP (New Environmental Paradigm) [10].

The impact of pricing on intention was significantly shaped by their environmental stance. Numerous studies conducted across different cultural settings have affirmed the effect of consumers' environmental attitudes on the influence of green marketing strategies on purchasing intention . Environmental knowledge is considered a vital factor that impacts the information-gathering activity of consumers: environmental knowledge and pro-environmental consciousness Environmental attitude, consciousness, and social phenomena strongly impact consumers' ecological consumption, shaping green marketing strategies.

DEMOGRAPHIC FACTORS OF CONSUMERS AND THEIR INTENTIONS FOR GREEN PURCHASING

There are six different categories we have to take into account when talking about consumers in relation to green purchasing. They are : gender, age, income, educational background, profession, and type of educational institution attended.

The review of past studies revealed that consumers' environmental knowledge is significantly influenced by gender [11]. Females have a more eco-friendly attitude than their male counterparts, and males engage less in green buying than females [12]. The existing literature proves that consumers' academic qualifications are more consistently attached to ecologically conscious consumer intention [13].

The previous literature reported mixed results regarding the connection between occupation and the ecological intention of consumers. In addition, buyers' income was found to be a significant predictor of the green buying intentions of consumers, corroborating the positive connection between the two [14].

CONCLUSION

In the ever-evolving landscape of business and environmental consciousness, the exploration of green marketing unveils a powerful bridge between profit and planet. The convergence of economic objectives and ecological imperatives has underscored the vital role of businesses in fostering sustainability through innovative marketing strategies. Through this journey, we have delved into the multifaceted realm where responsible practices and consumer demand intersect.

However, challenges linger, particularly the menace of greenwashing and the demand for authenticity. The path to success in green marketing lies in transparent communication, credible claims, and genuine commitment to environmental betterment. As green marketing forges ahead, it has the power to inspire collective change and drive industries toward more sustainable practices.

In conclusion, the symbiotic relationship between business growth and environmental stewardship is a beacon for future progress. As we navigate the intricate space of green marketing, let us recognize that its impact transcends profits—it encompasses a legacy of responsible consumption, preservation, and a shared commitment to a greener world.

REFERENCES

1. Peattie, K.; Crane, A. Green marketing: Legend, myth, farce or prophesy? Qual. Mark. Res. 2005, 8, 357–370
2. Ramayah, T.; Ahmad, N.H.; Lo, M.-C. The role of quality factors in intention to continue using an e-learning system in Malaysia. Procedia-Soc. Behav. Sci. 2010, 2, 5422–5426.
3. Leiserowitz, A.A.; Kates, R.W.; Parris, T.M. Do Global Attitudes and Behaviors Support Sustainable Development? Environ. Sci. Policy Sustain. Dev. 2005, 47, 22–38.
4. Kalafatis, S.P.; Pollard, M.; East, R.; Tsogas, M.H. Green Marketing and Ajzen's Theory of Planned Behaviour: A Cross-Market Examination. J. Consum. Mark. 1999, 16, 441–460.
5. Peattie, K. Green Marketing; Pearson Higher Education: London, UK, 1993.
6. Dangelico, R.M.; Pontrandolfo, P. From green product definitions and classifications to the Green Option Matrix. J. Clean. Prod. 2010, 18, 1608–1628.
7. Testa, F.; Iraldo, F.; Tessitore, S.; Frey, M. Strategies and approaches green advertising: An empirical analysis of the Italian context. Int. J. Environ. Sustain. Dev. 2011, 10, 375–395.
8. Shil, P. Evolution and future of environmental marketing. Asia Pac. J. Mark. Manag. Rev. 2012, 1, 74–81.
9. .Boztepe, A. Green marketing and its impact on consumer buying behavior. Eur. J. Econ. Political Stud. 2012, 5, 5–21.
10. Kaiser, F.G.; Wölfing, S.; Fuhrer, U. Environmental attitude and ecological behaviour. J. Environ. Psychol. 1999, 19, 1–19.
11. .Meffert, H.; Bruhn, M. The environmental awareness of consumers. Die Betriebswirtsch. 1996, 56, 621–658.
12. Ngo, A.-T.; West, G.E.; Calkins, P.H. Determinants of environmentally responsible behaviors for greenhouse gas reduction. Int. J. Consum. Stud. 2009, 33, 151–161.
13. .Patel, J.; Modi, A.; Paul, J. Pro-environmental behavior and socio-demographic factors in an emerging market. Asian J. Bus. Ethics 2017, 6, 189–214.
14. Evanschitzky, H.; Wunderlich, M. An Examination of Moderator Effects in the Four-Stage Loyalty Model. J. Serv. Res. 2006, 8, 330–345

Conference Proceedings
ICPAE 2022, March 31st – 2nd April, Zrenjanin, Serbia
University of Novi Sad, Technical Faculty "Mihajlo Pupin", Zrenjanin

Winter Measurements of Radon Concentration at TCAS

Iris Borjanović[1*], Milica Rajačić[2], Ivana Vukanac[2]

[1]Technical College of Applied Sciences in Zrenjanin, Đ. Stratimirovića 23, 23000 Zrenjanin, Serbia*
[2]Vinča Institute of Nuclear Sciences, Institute of national importance for the Republic of Serbia, University of Belgrade, M.P.Alasa 12-14, 11351 Vinča, Beograd, Serbia
iris@ipb.ac.rs

Abstract. Radon is a radioactive gas and the dominant natural source of radiation. It is the second leading cause, after smoking, of lung cancer in the world. At Technical College of Applied Sciences in Zrenjanin we did safety checks of radon ^{222}Rn level. These studies were supported by the Provincial Secretariat for Higher Education and Scientific Research ("Radon Level Measurement" project). The article shows results of parallel winter measurements performed by using open charcoal canisters (that were later measured by means of NaI gamma spectrometer) and by using Airthings radon detectors. Measurements were performed in eight rooms. The obtained results were compared and discussed.

Keywords: indoor radon measurements, charcoal canister, environmental radiation

INTRODUCTION

Radon is a naturally occurring noble radioactive gas that is odorless, colorless and tasteless. The biggest part of radiation from natural sources originates from radon [1]. It is produced by the decay of radium. Radium is formed by the decay of uranium and thorium and is present in soil and rocks in minor quantities. Radon can leak out from the soil and rock. In the atmosphere, closer to the ground radon is present in very low concentrations. Radon can enter houses, dominantly from the earth via cracks and holes. Sometimes it can also originate from building materials that dwellings are made of and rarely from the water or a natural gas. Thus, radon can occasionally be accumulated in larger concentration in closed spaces with poor ventilation. When inhaled or ingested radon and radon decay products present risk for human health. Radon is the main cause of the lung cancer among the nonsmokers.

Regular checks of radon level (^{222}Rn and rarely ^{220}Rn) in the houses and buildings are always welcomed. At Technical College of Applied Sciences in Zrenjanin (TCAS) we did radon level measurements in order to establish its concentration level and to contribute the database of indoor radon mesurement results in Serbia. This work was supported by the Provincial Secretariat for Higher Education and Scientific Research (Project "Radon Level Measurement"). This article describes parallel winter measurements of ^{222}Rn

performed by means of charcoal filters and by use of active type radon detectors (brand Airthings).

METHOD EPA 520

Open charcoal canisters [2], are often used for ^{222}Rn screening. They consist of a closed cylindrical metal canister (height 3,4 cm, radius 10,4 cm and mass of about 160 g) filled with activated charcoal. At the beginning of the measurement the canister is open. Radon and some of its decay products attach to the charcoal surface. The time of exposure of a canister can be from 48 h up to 6 days. At the end of the measurement the canisters are sealed and then sent to the certificated laboratory where they are measured by means of scintilation NaI gamma spectrometer. This method is known as EPA 520. On Figure 1, open charcoal canister can be seen. This is a passive type detector. The application of EPA 520 method is convenient because it is cheap as the same canisters can be used many times. Another advantage of it is that exposure of canisters can be performed by untrained persons just by following written instructions.

Figure 1. Photo of Charcoal Canister.

AIRTHINGS DETECTORS

The authors used also Airthings active type radon detectors [3], (Correntium Home Radon Detector and View Plus Radon Detector) for radon measurements. These instruments monitor radon by detecting alpha particles from radon decay [4]. A photodiode inside detector is a digital version of the film that can be used to reconstruct radon events. Special algorithm is made that remove “noise” events. Detector can measure radon continuously up to one year. At 200 Bq/m^3 detector accuracy is 10% (5%) for seven days (two months) long measurements. View Plus model is a “smart” type detector, so the radon graphs can be monitored online via mobile or PC and it also measures also other air quality parameters.

MEASUREMENT RESULTS

Winter radon level measurements at TCAS by using charcoal filters are done in collaboration with the Department of Radiation and Environmental Protection, Vinča Institute of Nuclear Sciences (VINČA). At the same time parallel measurements were performed with Airthings radon detectors. It is also expected that the highest radon concentration during the year should be in the coldest months of winter. Two-day long measurements are done in eight rooms in the basement and ground floor level where radon gas is dominantly expected to be present. During the measurements rooms were completely closed with no ventilation at all. Charcoal canisters and Airthings detectors were placed one near the other, at height of about 1 m above the floor and also far from doors, windows and heating bodies. At least twelve hours before the measurement no one was entering the rooms. The obtained results with associated uncertainties at 95% confidence level (k=2) are shown in Table 1. The authors estimated Airthings detector accuracy for these measurements to be 30%. The maximum measured winter radon concentration level was 97 Bq/m^3 (charcoal canisters) and 78 Bq/m^3 (Airthings). In order to evaluate the statistical difference between individual measurement results obtained with different types of detectors Z – test was used. This test takes into account the measurement uncertainties of the obtained results. Z was calculated using the equation (1)

$$Z = \frac{C_{EPA520} - C_{Airthings}}{\sqrt{u^2_{C_{EPA520}} + u^2_{C_{Airtings}}}}\ , \qquad (1)$$

where C_{EPA520} and $C_{Airthings}$ denote radon concentration measured by charcoal canisters and Airthings detector, respectively, while u denotes the uncertainty of a corresponding measured concentration. Confidence interval of $\alpha = 0{,}05$ (Critical value $|Z_{0,05}| < 1{,}96$) was applied [5].

Table 1. Radon concentration level measured with charcoal canisters (EPA520) and with Airthings radon detectors during winter at TCAS in Zrenjanin.

Room	Radon Concentration (Bq/m^3)		Z-score
	EPA520	Airthings	
Printing press office (basement)	33(6)	19(6)	1,65
Storage for technical equipment (basement)	72(8)	57(19)	0,73
Lab. for welding (basement)	12(7)	10(3)	0,26
Lab. for hybrid engines and vehicles (basement)	12(7)	9(3)	0,39
CIRT (ground floor)	53(6)	39(13)	0,98
Creativity studio (ground floor)	97(8)	78(26)	0,70
Classroom 111 (ground floor)	24(6)	17(6)	0,82
Library (ground floor)	29(5)	24(8)	0,53

For all measurements calculated Z values are below 1,96 (Table 1) and it could be said that there is a good agreement between the two set of values obtained with charcoal canisters and Airthings detectors. Also, as expected winter measurements also show higher values of radon concentration compared to spring [6], summer [7,8] and autumn [8], measurements.

CONCLUSION

Intervention levels of radon concentration given in our legislation [9], are 1000 Bq/m^3 for working places, 200 Bq/m^3 for new and 400 Bq/m^3 for old dwellings. These values should be harmonized with the international recommendations given in the European Union regulations [10], which require less than 300 Bq/m^3 for work and living spaces. World Health Organization proposes even more severe recommended reference limit of less than 100 Bq/m^3 in residental dwellings and gives the recommendation that national reference level should not exceed 300 Bq/m^3 [11].

In the presented study the maximum radon concentration during winter measured with both active type Airthings radon detectors and passive type detectors (charcoal canisters) is below the national intervention levels. We can conclude that it is safe to stay at TCAS for both students and employees. There is no reason to do any space remedies at TCAS building, apart from regular ventilations. Also, obtained result showed the good agreement between results obtained with two detector types.

REFERENCES

1. Sources and effects of ionizing radiation, Annrx B, UNSCEAR 2008 Report to the General Assembly with Scientific annexes, United Nations, New York, USA, 2010.
2. M. Živanivić, Optimization of indoor radon concentration measurement by using the carbon filter method, doctoral dissertation, UDC number: 544.58, Faculty of Physical Chemistry, University of Belgrade, 2017 (in Serbian).
3. https://www.airthings.com/manuals
4. https://www.airthings.com/resources/radon-detector
5. Kanji K. Gopal, 2006. 100 statistical tests, third edition. Sage Publications, London, Thousand Oaks, New Delhi.
6. I. Borjanovic, L. Manojlovic, M. Kovacevic, Seasonal measurements of radon concentration level in the period of spring at Technical College of Applied Sciences in Zrenjanin, Book of Abstracts, 10th Jubilee International Conference on Radiation in Various Fields of Research RAD2022-summer edition, pp 124, RAD Centre Niš, 2022.
7. I. Borjanovic, A. Rajic, Z. Eremic, Seasonal Measurements of Indoor Radon Concentration Level in the Period of Summer at Technical College of Applied Sciences in Zrenjanin, The 11th International Conference of the Balkan Physical Union (BPU11), Proceedings of Science, PoS(BPU11)025, 2023. (to be published)
8. I. Borjanović, M. Rajačić, I. Vukanac, Jesenja merenja nivoa radona na Visokoj tehničkoj školi strukovni studija u Zrenjaninu, DIT, 2023. (to be published)
9. Rulebook on Limits of Exposure to Ionizing Radiation and Measurements for Assessment of the Exposure Levels (Official Gazette RS 86/11 and Official Gazette RS 50/18).
10. EU, Council Directive 2013/59/Euratom, 2014 laying down basic safety standards for protection against the danger arising from exposure to ionizing radiation, and repealing Directives 89/618, 90/641, 96/29,97/43 and 2003/122/Euratom, Official Journal of the European Union.

11. WHO handbook on indoor radon: a public health perspective / edited by Hajo Zeeb, and Ferid Shannoun, World Health Organizatio, 2009, ISBN 978 92 4 154767 3.

Conference Proceedings
ICPAE 2023, 24th – 26th August, Zrenjanin, Serbia
University of Novi Sad, Technical Faculty "Mihajlo Pupin", Zrenjanin

Seasonal Measurements of Radon Concentration at the Technical Faculty ''Mihajlo Pupin'' Zrenjanin

Darko Radovančević[1], Iris Borjanović[2*], Jasna Tolmač[1]

[1]University of Novi Sad, Technical Faculty "Mihajlo Pupin", Đure Đakovića bb, 23 000 Zrenjanin, Serbia
[2]Technical College of Applied Sciences in Zrenjanin, Đorđa Stratimirovića 23, 23000 Zrenjanin, Serbia*
iris@ipb.ac.rs

Abstract. This paper presents the results of the radon concentration measurements at Technical Faculty "Mihajlo Pupin" in Zrenjanin (Serbia). Radon concentration measurements were done during spring 2023. at the basement and groundfloor levels with offices, labs and classrooms situated there. Airthings Correntium Home Radon Detector (active type detector) was used for the measurements. It is capable of performing both short-term and long-term measurements and is based on alpha spectrometry. We did short-term two-day-long (48 h) measurements in rooms with no ventilation and the doors and windows were closed. These rooms were also not ventilated for at least 12 h before the measurements. Radon concentrations ranged from 13 to 140 $Bq \cdot m^{-3}$ and were within safe limits according to our National Reference Level.

Keywords: radon, environmental radiation protection

INTRODUCTION

Radiation is all around us and comes from different natural and artificial sources. It comes from outer space, from the ground, from within the human body, from X-rays. More than half of the total amount of radiation from the natural sources originates from radon [1]. Radon (Rn) is a noble gas without color, smell and taste. In nature it is produced by the decay of uranium's decay products, like radium ^{226}Ra. All radon isotopes are radioactive. Only ^{222}Rn and ^{220}Rn, which comes from uranium and thorium series respectively, are important [1]. Radon dominantly diffuses through soil and rocks and enters the houses through cracks and holes. It can also be found in building materials. Uranium found in soil worldwide is varying in concentration. The same is the case with radon in the building materials. Therefore, the dose of radon in indoor spaces varies from place to place. Radon's daughters can be attached to aerosol particles in the air and then can be inhaled by humans. Its effects on humans' health are hazardous as radon is the second leading cause of the lung cancer. Its effects multiplicate if the person is a smoker.

There is no danger of radon on open spaces. However, radon can accumulate in indoor spaces in large amount. It is important to check indoor radon levels everywhere. It can also vary from room to room inside the same apartment. We performed measurements of

indoor radon concentration (activity per cube meter [2]) at Technical Faculty "Mihajlo Pupin" Zrenjanin (TFZR) during spring 2023. As the amount of ^{220}Rn in the environment is much less (apart from some specific cases) than that of ^{222}Rn, our studies refers to ^{222}Rn.

DETECTORS

We used Correntium Home Radon Detector [3] produced by Airthings. It is active type radon detector, presented on Figure 1.

Figure 1. Photo of Correntium Home Radon Detector by Airthings.

This detector uses alpha spectrometry [4], to measure radon concentration level. Inside detector there is a passive diffusion chamber which allows air to enter into it. Inside the chamber, a photo diode counts the number of radon daughter particles in the air. Fresh air (25 cm^3) flows into the chamber every half an hour. Chrome is used inside the chamber as a kind of cage which prevents unwanted particles to enter. The Airthings team developed special algorithm that can make a difference between radon and noise events. The detectors work continuously and every hour they make a data point that contributes to the average result. It can provide an average radon concentration after 24 h, 48 h or larger number of days (up to one year). Detector precision at 200 Bq/m^3 is 10 % for short-term (seven-days-long) measurements and 5 % for two-months-long measurements. Correntium Home Detector's range is from 0 Bq/m^3 to 9999 Bq/m^3. It operate on temperatures between 4 ^{0}C and 40 ^{0}C and at relative humidity levels below 85 %.

MEASUREMENTS AND RESULTS

In houses and buildings radon usually accumulates in lower spaces like basements and ground floor levels because of its high density. The indoor radon concentration level varies daily and seasonally as the weather affects it [2]. In ideal case radon measurement should last one year. In order to get fast insights into radon levels, we did few days long measurements. If high radon levels would have been found in some of the rooms, then long-term (few months long) measurements would be done in those places.

We choose 4 rooms in the ground floor and 4 rooms in the first floor at TFZR to do the measurements. The total surface of the ground and first floor spaces is about 1300 m^2. There are offices, labs, classrooms. We performed two-day-long measurements in rooms with closed doors and windows all the time. Detectors were put at fixed place, 1 m above the floor, far from doors and windows. The heating system was not in use. Rooms were not ventilated for at least 12 h before the start of the measurement. The obtained data of radon concentration levels are summarized in Table 1. The estimated error for this measurements is shown, too.

Table 1. Radon concentration levels measured at TFZR.

Measurement location/office number	Radon concentration (Bq/m^3)
First floor, office number 22	13(4)
First floor, physics laboratory	46(15)
First floor, office number 23	41(14)
First floor, office number 30a	39(10)
Ground floor, office number 5	127(20)
Ground floor, old library room	140(22)
Ground floor, office number 1	109(20)
Ground floor, office number 2	43(11)

The maximum value of radon concentration measurement is 140 Bq/m^3, while the minimum value is 13 Bq/m^3.

CONCLUSION

Most countries, Serbia as well [5], have adopted a radon concentration of 400 Bq/m^3 for old buildings (200 Bq/m^3 for new ones) for indoor air as an Action or Reference

Level. The World Health Organization (WHO) recommends for these spaces to keep radon concentration below 100 Bq/m^3.

Frequent daily ventilations are always recommended for closed spaces. For high radon indoor levels there are also measures of mitigation of radon that can be performed in homes in order to significantly reduce the presence of radon.

Radon concentration level measured at TFZR during spring 2023. are below National Reference Level. It is safe to stay and work there. There is no need to do any remedies at the TFZR. We also plan to repeat these measurements during colder months.

REFERENCES

1. Sources and effects of ionizing radiation, Annex B, UNSCEAR 2008 report to the General Assembly with Scientific annexes, UNSCEAR, New York (NY), USA, 2010. http://www.unscear.org/docs/reports/2008/09-86753_Report_2008_Annex_B.pdf
2. Sources and effects of ionizing radiation, vol. 1, UNSCEAR Report (A/55/46), UNSCEAR, New York (NY), USA, 2000.
   http://www.unscear.org/docs/publications/2000/UNSCEAR_2000_Report_Vol.I.pdf
3. Correntium Home Radon Detector User Manual, Airthings, Oslo, Norway. https://cdn2.hubspot.net/hubfs/4406702/Website/Manuals/Home/1-043-Corentium-Home-manual-60x77.pdf
4. How we make the Correntium Home Radon Detectors, Airthings, Oslo, Norway. https://www.airthings.com/resources/radon-detector
5. Rulebook on Limits of Exposure to Ionizing Radiation and Measurements for Assessment of the Exposure Levels (Official Gazette RS 86/11 and Official Gazette RS 50/18).

Conference Proceedings
ICPAE 2023, 24th August – 26th August, Zrenjanin, Serbia
University of Novi Sad, Technical Faculty "Mihajlo Pupin", Zrenjanin

Prediction of SOx Emissions Using ANN

Lidija Stamenković[1*], Ivana Krulj[1], Ljiljana Đorđević[1], Tijana Milanović[1]

[1]The Academy of Applied Technical and Preschool Studies,*
Filipa Filipovića 20, Vranje, Serbia,
lidija.stamenkovic@akademijanis.edu.rs

Abstract. Sulphur oxides are air pollutants that have multiple negative effects on the environment. The subject of this paper is the prediction of sulphur oxides emissions at the national level using artificial neural networks (ANN). Industrial, economic and traffic indicators were used as input parameters for the development of the ANN model, as the sectors that were assumed to contribute the most to the emissions of sulphur oxides. Prediction of emissions of sulphur oxides by the ANN model showed very good results with the value of the model performance indicator R^2-0,976. In order to compare the results of the ANN model, a multiple linear regression (MLR) model was developed with the same data. The predictions of the MLR model are worse with a value of R^2-0,95.

Keywords: sulphur oxides, air pollution, ANN, MLP, MLR

INTRODUCTION

Sulfate acid deposition due to the emission of anthropogenic pollutants, primarily the emission of sulpfur oxides, is a subject of global concern [1,2]. The Paris Agreement, signed by more than 195 countries in 2016 and the Convention on Long-Range Transboundary Air Pollution entered into force on March 16, 1983 are global efforts to reduce the emission of air pollutants. Due to the negative effects on the environment and human health, the monitoring of SOx emissions is very important both at the global and local levels. In order to monitor the emissions of pollutants into the air, according to the assumed international obligations, states are obliged to submit annual reports on the inventory of pollutant emissions. One of the pollutants whose emissions are evaluated is SOx. The assessment of national emissions of air pollutants is prepared according to the methodology EMEP/EEA Air Pollutant Emissions Inventory Guidebook. According to this methodology, emission sources are classified into 12 sectors and emissions are estimated using emission factors and activity rates [3].

The existence of alternative models for estimating SOx emissions is important in order to make the estimated emissions as accurate as possible. As one of the alternative models for estimating SOx emissions at the national level, this paper proposes the application of artificial neural networks (ANN). According to literature data, prediction of SOx emissions using ANN was mainly performed for a specific sectors [4–6]. The literature data results show a very good performance of the ANN models. In this paper, the ANN model was

applied to predict SOx emissions at the national level using industrial, economic and traffic indicators.

ANN MODEL DEVELOPMENT

Artificial neural networks are mathematical models that imitate the functioning of the biological nervous system in a simplified way. Information processing in artificial neural networks is performed with the help of a parallel distributed architecture composed of several simple processors (artificial neurons) that are connected to each other. An artificial neural network is formed by connecting a number of independent neurons in layers. ANNs observe a relationship between a given number of solved examples of the problem they are solving. The ANN structure is divided into three main layers: input, hidden and output. The training process is an extremely important segment in building ANN-based models. The training process is based on the input and output data being given to the network, whereby the network tends to obtain the corresponding output value, i.e. a value that approximates the expected value. In order to obtain the desired output during training, the weighting coefficients are changed through the training algorithm, until the network learns to function appropriately [7]. More information on the functioning of neural networks can be found in the relevant literature [8–10].

One of the most important steps in ANN model developing is the selection of appropriate input parameters. In this sense, in this paper, those input parameters that were assumed to contribute the most to the SOx emissions were used. It turned out that the sector of electricity and heat production, industry, individual combustion plants and in a slightly smaller percentage other sectors contribute the most to the emissions of SOx in the air. In this paper, seven input parameters from the industry, economy and traffic sectors were selected for the ANN model development: Energy productivity (EP), Final energy consumption-total (FEC), Final energy consumption - transport sector (FECT), Final energy consumption in households (FECH), Modal split of passenger transport (PT), Primary energy consumption (PEC) and Gross domestic product (GDP). Available data for 22 European countries for the period from 2010 to 2019 were used for the development of the ANN model. The input and output data for every European country included into this study has been published by Eurostat and OECD [11,12].

After selecting the input parameters, the selection of neural network parameters was applied: architecture, number of hidden layers of neurons, activation functions. The standard three-layer neural network (multilayer perceptron-MLP) was used. During the development of the ANN model, 68.6% of the data was used for training the network, while 31.4% of the data was used for testing the network. Standardized rescaling method for inputs and output was used. *Hyperbolic tangent* activation function for hidden layer and *Identity* activation function for output layer was used. Number of hidden layer was one and the number of neurons in hidden layer was 4.

In order to compare the results of the ANN model, a multiple linear regression (MLR) model was developed. A regression MLR model was developed with the same data that was used in the development of the ANN, with the aim of comparing the results. ANN and MLR models were created using IBM SPSS 19 Statistics software.

$$\text{SOx emissions} = 2.048 + 3.491\text{EP} - 11.647\text{FEC} - 42.948\text{FECT} - 0.035\text{FECH} - 0.055\text{PT} + 20.460\text{PEC} - 0.001\text{GDP} \quad (1)$$

The obtained MLR coefficients are represented by Equation 1.

To evaluate the performance of the created models, a statistical indicator of model performance, the coefficient of determination (R^2), was used. The values of the coefficient of determination range from 0 to 1, and the higher the value of the coefficient of determination, closer to 1, the better the results of the created model.

$$R^2 = \frac{[\sum(C_p - \bar{C}_p)(C_o - \bar{C}_o)]}{\sum(C_o - \bar{C}_o)^2 \sum(C_p - \bar{C}_p)^2} \quad (2)$$

The value of this indicator is determined according to Equation 2, where c_p represents the value predicted by the model, while c_o represents the measured value of the observed variable.

RESULTS AND DISCUSSION

Figure 1 shows a comparison between actual and ANN model predicted values of SOx emissions for training dataset. While the results of the created MLR model are shown in Table 1. Based on the results shown in Figure 1 and Table 1, obtained by the created models in the training phase, it can be seen that the ANN model showed better prediction results compared to the regression MLR model with values of the coefficient of determination ANN-0.976 and MLR-0.950. Therefore, it can be said based on the results, that the ANN based model shows very good results.

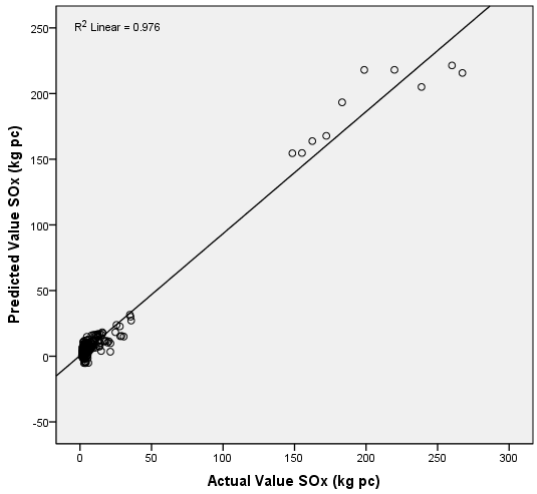

Figure 1. Comparison of actual and ANN model predicted SOx emissions for the training dataset

Table 1. The results of the created MLR model

Model	R	R^2	Adjusted R Square	Std. Error of the Estimate
MLR	0.975	0.950	0.949	9.324

In order to test the capabilities of the created ANN model, new data were presented to the network. The capacity of the ANN model for one-year forecasting of SOx emissions for each country is presented in Figure 2. As can be seen, the ANN model gave very good forecasting results. Somewhat larger deviations between the measured and model-predicted emissions values for individual countries can be attributed to the fact that the values of some input parameters were estimated as well as a break in the time series data.

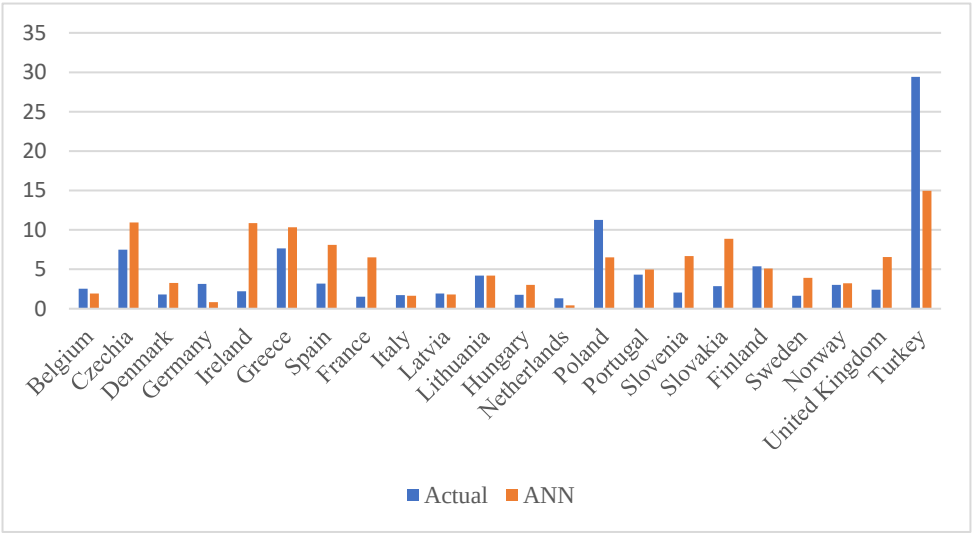

Figure 2. Comparison of actual and ANN model predicted SOx emissions for the test dataset

CONCLUSION

The main goal of the research in this paper was the development of a model for predicting SOx emissions into the air. The developed model is based on artificial neural networks (ANN) and the application of available industrial, economic and traffic indicators as input variables for model development. Since the model based on the ANN approach showed very good results in predicting the SOx emissions, a regression (MLR) model was also developed to compare the results. The prediction results showed that the ANN model gives significantly better prediction results compared to the MLR model. Based on the obtained results and in comparison with existing models, it can be concluded that the created ANN model provides good and reliable predictions of SOx emissions.

REFERENCES

1. McLinden CA, Fioletov V, Shephard MW, et al, 2016, Space-based detection of missing sulfur dioxide sources of global air pollution. *Nat. Geosci*. vol.9, pp 496–500
2. Zhong Z, Zhang X, Bao Z, 2019, Spatial characteristics and driving factors of global energy-related sulfur oxides emissions transferring via international trade. *J. Environ. Manage.* vol.249, pp 109370
3. EMEP/EEA air pollutant emission inventory guidebook — European Environment Agency. https://www.eea.europa.eu/themes/air/air-pollution-sources-1/emep-eea-air-pollutant-emission-inventory-guidebook. Accessed 23 Jun 2023
4. Adams D, Oh D-H, Kim D-W, et al, 2020, Prediction of SOx–NOx emission from a coal-fired CFB power plant with machine learning: Plant data learned by deep neural network and least square support vector machine. *J. Clean. Prod.* vol.270, pp 122310
5. Antanasijević D, Pocajt V, Perić-Grujić A, Ristić M, 2018, Multiple-input–multiple-output general regression neural networks model for the simultaneous estimation of traffic-related air pollutant emissions. *Atmospheric. Pollut. Res.* vol.9, pp 388–397
6. Park M-H, Hur J-J, Lee W-J, 2022, Prediction of oil-fired boiler emissions with ensemble methods considering variable combustion air conditions. *J. Clean. Prod.* vol.375, pp 134094
7. Wagh V, Panaskar D, Muley A, et al, 2018, Neural network modelling for nitrate concentration in groundwater of Kadava River basin, Nashik, Maharashtra, India. *Groundw. Sustain. Dev*. vol.7, pp 436–445
8. Stamenković LJ, Antanasijević DZ, Ristić MĐ, et al, 2017, Prediction of nitrogen oxides emissions at the national level based on optimized artificial neural network model. *Air Qual. Atmosphere. Health.* vol.10, pp 15–23
9. Stamenković LJ, Antanasijević DZ, Ristić MĐ, et al, 2016, Estimation of NMVOC emissions using artificial neural networks and economical and sustainability indicators as inputs. *Environ. Sci. Pollut. Res.* vol.23, pp 10753–10762
10. Sobri NM, Yaacob WFW, Ismail NA, et al, 2021, Predicting Particulate Matter (PM2.5) in Malaysia using Multiple Linear Regression and Artificial Neural Network. *J. Phys. Conf. Ser*. vol.2084, pp 012010
11. Environment - OECD Data. In: theOECD. http://data.oecd.org/environment.htm. Accessed 26 Jun 2023
12. Database - Eurostat. https://ec.europa.eu/eurostat/data/database. Accessed 18 Nov 2022

Conference Proceedings
ICPAE 2023, 24th August – 26th August, Zrenjanin, Serbia
University of Novi Sad, Technical Faculty "Mihajlo Pupin", Zrenjanin

Correction of the Barometric Formula at Low Altitudes Due to a Non-Zero Temperature Gradient

Darko Radovancevic[1*], Ljubisa Nesic[2], Sasa Jovanovic[1], Anita Milosavljevic[1], Ognjen Popovic[3], Teodora Crvenkov[4]

[1]University of Novi Sad, Tehnical Faculty "Mihajlo Pupin", Djure Djakovica bb, 23000 Zrenjanin, Serbia
[2]University of Nis, Faculty of Sciences and Mathematics, Visegradska 33, Nis, Serbia
[3]Mining Institute, Batajnicki put 2, 11080 Belgrade, Zemun, Serbia
[4]University Clinical Centre of Serbia, Pasterova 2, Belgrade, Serbia
darko.radovancevic@tfzr.rs

Abstract. The dependence of atmospheric pressure P on altitude z (barometric formula) $P \propto e^{-const \cdot z}$ is derived from the static equilibrium condition in the atmosphere. In this derivation, it is assumed that the atmosphere is isothermal and the Earth's gravitational field is homogeneous. Both of these assumptions are approximations. The non-zero vertical temperature gradient of the atmosphere is the main criterion for introducing and separately considering different layers of the atmosphere. Thus, at low altitudes, the temperature gradient is constant and negative in its lowest layer – the troposphere, which contains approximately 80% of the atmospheric mass. The paper first presents how the temperature gradient is obtained and then uses it to derive the barometric formula for a non-isothermal troposphere.

Keywords: barometric formula, troposphere

INTRODUCTION

Barometric formula

$$P(z) = P(0)e^{-\frac{m_{av}gz}{k_BT}}, \tag{1}$$

shows the dependency of atmospheric pressure P on the altitude z. In this case, g represents the acceleration due to Earth's gravity, T is the air temperature, k_B is the Boltzmann constant, m_{av} is the average molecular mass of the air (considering that Earth's atmosphere consists of different molecules). Having in mind that k_B can be represented as the quotient of the universal gas constant R and Avogadro's number N_A, the barometric formula can be given in the following way

$$P(z) = P(0)e^{-\frac{M_{av}gz}{RT}}, \tag{2}$$

where M_{av} is the average molar mass of air.

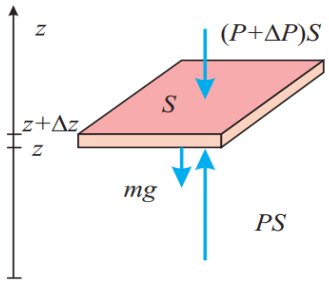

Figure 1. An equilibrium layer of air [2].

This relationship is typically derived [1,2] based on the vertical equilibrium of air layers (Figure 1), leading to the following

$$dP = -\frac{P}{RT} M_{av} g dz \tag{3}$$

from which, by integration, equation (2) is obtained.

Before the time of GPS, the barometric formula was used to determine the aircraft's altitude. A barometer scale can be calibrated to display the altitude immediately at which a given pressure is measured. Instruments designed to measure altitude are called altimeters.

Another method for deriving the barometric formula is based on the Boltzmann distribution and the ideal gas law equation (known as the Mendeleev-Clapeyron equation). According to the Boltzmann distribution, air concentration decreases with altitude according to the following expression

$$n(z) = n(0) e^{-\frac{mgz}{k_B T}} = n(0) e^{-\frac{M_{av} g z}{RT}}. \tag{4}$$

By substituting the expression (4) into the ideal gas law equation , $P = n k_B T$, the barometric formula (1), that is, (2), is obtained.[1]

In both derivation methods, it is assumed that the air temperature is constant, the atmosphere is in an ideal gas state and has a homogeneous composition, and the Earth's gravitational field is homogeneous. None of these assumptions are entirely accurate, with the most significant error being introduced by assuming atmospheric isothermality.

It is commonly considered that the atmosphere is "composed" of the following layers: troposphere (first 10 km), stratosphere (10–50 km), mesosphere (50–85 km), thermosphere (85–500 km), and exosphere (500–1000 km). The main criterion for this division of the atmosphere is the trend of temperature change with altitude, as depicted in Figure 2.

[1]Due to paper length limitations, the intriguing analysis of the origin of atmospheric pressure will not be addressed here.

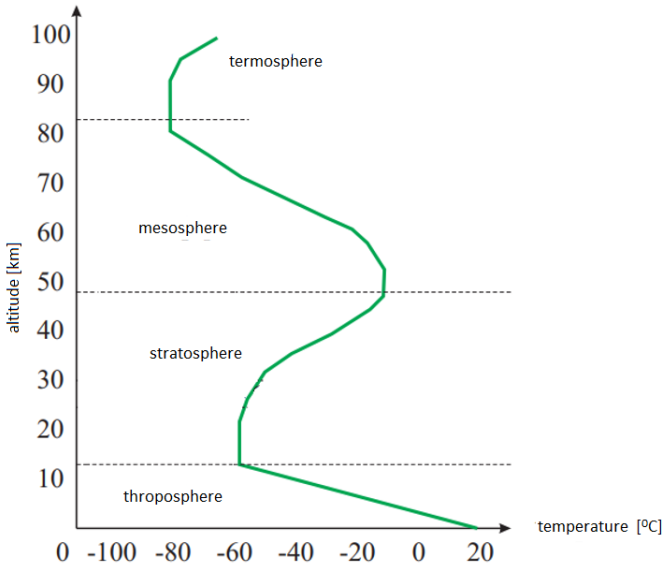

Figure 2. Variations in atmospheric temperature with altitude [2].

It can be observed that the temperature is not only constant, but it also changes through the layers of the atmosphere in very different ways. At this point, it is significant to consider only the troposphere for at least two reasons:

- people live within that layer of the atmosphere and move through it (excluding space travel), and
- about 80% of the total mass of the atmosphere is located within the troposphere.

TEMPERATURE GRADIENT IN THE TROPOSPHERE

Air in the atmosphere, at low altitudes, i.e., in the troposphere, is primarily heated from below, meaning from the Earth's surface. To get an expression describing the vertical temperature gradient, a parcel of dry air[2] that rises convectively will be considered, expanding and cooling in the process. Since the speed of the observed convection is of the order of decimeters per second [3], the heating of the air parcel due to solar radiation can be neglected. Furthermore, since air is a poor conductor of heat, the thermodynamic processes that occur with the parcel will be considered adiabatic.

[2] The influence of water vapour in the air will be considered later.

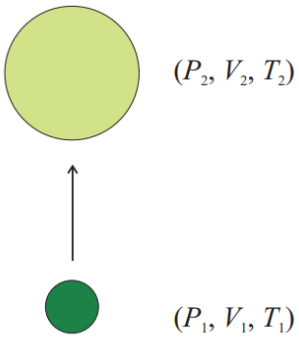

Figure 3. Air parcel convective movement [2].

According to the first law of thermodynamics, the amount of heat ΔQ exchanged between the system and the surroundings is related to the change in its internal energy ΔU and the action ΔA as follows

$$\Delta Q = \Delta U + \Delta A \tag{5}$$

The change in internal energy of an air parcel is given by $\Delta U = mC_V\Delta T$, where m is the mass of the parcel, and C_V is its specific heat capacity at constant volume. The work done by the system is $\Delta A = P\Delta V$. As for adiabatic processes $\Delta Q = 0$, the equation (5) becomes

$$mC_V\Delta T = -P\Delta V \tag{6}$$

or in the differential form $mC_V dT = -PdV$. By differentiating the adiabatic equation, $P \cdot V^\gamma = const, \gamma = \frac{C_P}{C_V}$, one gets $PdV = -VdP/\gamma$, which, upon substitution into equation (6), gives

$$mC_V dT = \frac{VdP}{\gamma} \tag{7}$$

Since the pressure gradient is $\nabla P = -\rho g\vec{e}_z$, the pressure differential is $dP = -\rho g dz$. As a result, the relation (7) transforms into

$$mC_V dT = -\frac{C_V}{C_P} V\rho g dz. \tag{8}$$

After simplifying the expression, one gets

$$\frac{dT}{dz} = -\frac{g}{C_P}. \tag{9}$$

Where the required temperature gradient is

$$\nabla T = -\frac{g}{C_P}\vec{e}_z. \tag{10}$$

The ratio $\frac{g}{C_P} = \Gamma_d$ is called the adiabatic temperature gradient of a dry atmosphere. Based on the values $g = 9{,}81\ \frac{\mathrm{m}}{\mathrm{s}^2}$ and $C_p = 1{,}0035\ \frac{\mathrm{kJ}}{\mathrm{kgK}}$, one gets $\Gamma_d = 9{,}78\frac{\mathrm{K}}{\mathrm{km}} \approx 10\frac{\mathrm{K}}{\mathrm{km}}$. If the temperature were to decrease at this rate, at an altitude of about 10 km (top of the troposphere), the temperature would be around 100 K lower. However, the actual temperature decrease at this altitude is about 50–60 K. This difference results from water vapour in the atmosphere, which releases latent heat that warms the air upon cooling and condensation.

BAROMETRIC FORMULA FOR NON-ISOTHERMAL TROPOSPHERE

Integrating (9), one gets

$$T(z) = T_0 - \Gamma_d z. \tag{11}$$

It can be observed that the temperature of the troposphere decreases linearly with altitude. After substituting (11) into (3) and performing integration, the barometric formula is obtained

$$P(z) = P_0 \left(1 - \frac{\Gamma_d}{T_0} z\right)^{\frac{C_P}{C_P - C_V}}, \tag{12}$$

derived under the condition of a linear temperature gradient.

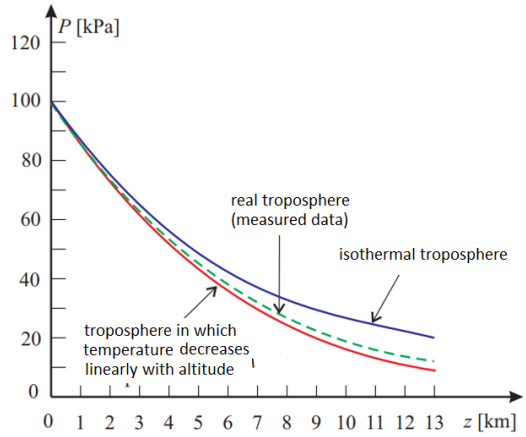

Figure 4. Comparison of two models and measured data [2].

Figure 4 depicts graphs of the barometric formula's dependency for the isothermal and non-isothermal troposphere with solid lines, while the measured pressure values are shown with a dashed line. Since the dashed line is between the solid lines, neither model is entirely accurate. However, given that the dashed line is closer to the line corresponding to the non-isothermal troposphere model, it can be concluded that this model better describes the real situation.

CONCLUSION

Starting with the assumption of a homogeneous gravitational field of the Earth and considering the existence of a vertical temperature gradient in the troposphere, the barometric formula (12) is derived in the study. Measurements show deviations from (12) that result from other effects not considered here (such as the presence of water vapour in the atmosphere, non-homogeneity of the Earth's gravitational field, non-inertial reference frame, variation of the mean molar mass of the atmosphere with altitude...) which forms the basis for considering more accurate theoretical models.

ACKNOWLEDGEMENT

This work is supported by the Ministry of Education, Science, and Technological Development of the Republic of Serbia, contract number 451-03-47/2023-01/200124.

REFERENCES

1. В. Вучић, Д. Ивановић, 1990, *Физика 1*, Научна књига, Београд (in Serbian)
2. Љ. Нешић, Д. Димитријевић, 2013, *Увод у физику околине,* Природно-математички факултет у Нишу (in Serbian)
3. Penn State, College of Earth and Mineral Sciences, DEPARTMENT OF METEOROLOGY AND ATMOSPHERIC SCIENCE, *Introductory Meteorology: The Ups and Downs of Air Parcels*. https://www.e-education.psu.edu/meteo3/node/2230 (January 20, 2023).

Conference Proceedings
ICPAE 2023, 24th August – 26th August, Zrenjanin, Serbia
University of Novi Sad, Technical Faculty "Mihajlo Pupin", Zrenjanin

Enviromental Issuses Hidden Beneath the Equations in High School Mathematics

Đorđe Vučković[1]

[1]*University of Novi Sad, Technical Faculty „Mihajlo Pupin“Zrenjanin, Đure Đakovića BB, 23000 Zrenjanin*
djordje.vuckovic@tfzr.rs

Abstract. Teaching high-school mathematics could be a challenging experience (both for teachers and students) due to lack of real-world problems in mathematical curricula. In this paper we give an example of one teaching topic in high-school mathematics were the environmental issues could be brought into students' attention. Namely, we give an alternative scenario where students learn about the concept of mathematical modelling that bridges the gap between the abstract realm of mathematics and environmental considerations in the real world, empowering their mathematical knowledge and illustrating them how the environmental issues are important in this vibrant world.

Keywords: teaching high-school mathematics, enviromental

INTRODUCTION

The fact that the environment secured its place in the highest legal act of the Republic of Serbia speaks most profoundly about its significance for the whole society. In the Constitution of the Republic of Serbia, there is an Article 74 dedicated to the healthy environment. More precisely, it stipulates that "Everyone shall have the right to healthy environment and the right to timely and full information about the state of the environment" [1]. In this way, problems involving environmental issues were moved from faculties and laboratories, being now problems for the state and society as well. In the National Environmenal Protection Program, problems that contribute to the environmental degradation were identified. Among others, there were "inadequate formal educaton in environmental sciences", as well as "insufficient informal education regarding environmental issuses, as a consequence of the limited access to the appropriate information" [2].

Pieces of information from the media dealing with environmental issues tucked in headlines if these issues are "not so bad". On the other hand, news regarding environmental issues appearing on cover pages or headlines are apocalyptic ones, where there is too late for prevention. Moreover, in public discourse there are so many buzzwords related to environmental problems, e.g. "*greenhouse effect*" of "*global warming*" floating without meaning. Our aim is to present a scenario were students learn about the environmental issuses during the mathematic classes. The purpose of this short paper is to illustrate, through the example, how the importance of environmental conservation could be brought closer to high school students, particularly within the context of mathematics education in

gymnasium, and how it could help fighting two causes of environmental degradation listed in the National Environmental Protection Program.

IS THERE A PLACE FOR NATURE IN THE HIGHSCHOOL MATHEMATCS ?

The implicit answer to the question posted in the (sub)title will be provided by the Mathematics Curriculum for high school [3]. Namely, students should develop "*abstract and critical thinking*", "the ability to communicate in *mathematical language*", as well as "to apply acquired knowledge" and "to solve *real-life problems*" (emphasized by Đ.V.). On the other hand, the language of the curriculum goals significantly differs from the language of the teaching topics and teaching units that are fragmented in the teaching program. The program only provides guidelines and outlines for the lesson, without entering into every classroom. Therefore, the teacher is not merely an administrator who studies one set of tables to fill in another - teachers have the freedom (but also the responsibility!) to, in accordance with their own experience, personal sensibilities, and awareness of the social responsibility, choose topics of significance for the broader community (and the topic of a healthy environment, woven into the Constitution of this country, certainly merits this), and present them in mathematics classes, establishing their importance for society.

The earliest example of "solving *real-life* problems" that a student encounters in mathematics education are known from elementary school, where the problem is first formulated in mathematical language (often as an equation), then solved in a calm environment without the hustle and bustle of *real life,* and, finally, the result from the abstract world of mathematics is translated into real world. Further education will bring changes - more complex problems requires more complex equations, so these simple problems eventually lead to the concept of mathematical modeling.

In the sequel, we will find a place for topics related to students' awareness of a healthy environment that surround us, in high school mathematics education, in the second year of gymnasium.

TEMPERATURE RISES

The content in the second year of high school in mathematics is quite demanding; students acquire concepts they have not encountered before. During just one year, they will systematically study elementary functions: powers, exponential, logarithmic, trigonometry. The laws and rules that govern these elementary functions (many of which appear unnatural to students and are often memorized by heart) will be practiced through complex identities, equations, and inequalities. In this dense *forest* of non-intuitive rules, it is difficult to see *trees*. All these functions have their place in STEM curricula, where the idea of functional dependency is crucial. Hence, it is important to grasp the significance of elementary functions property. For this purpose, it is best to start from the simplest ones.

In Figure 1, taken from [4], the dependency of the change in the average annual Earth's temperature before 1960 is shown, depending of the year of measurement.

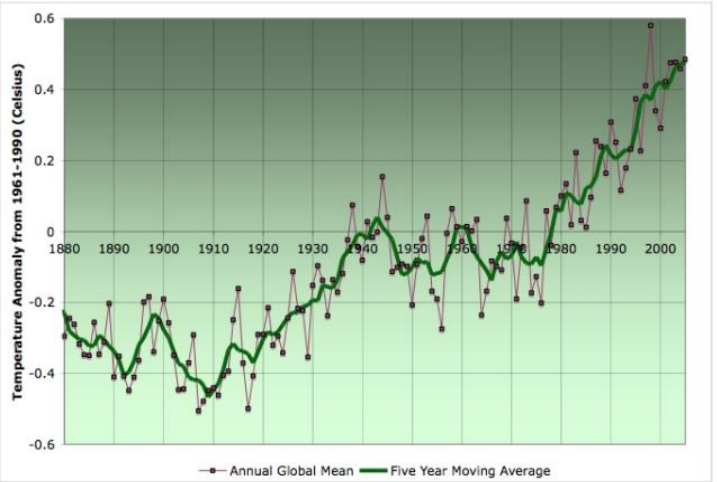

Figure 1. Earth temperature rises

In mathematics education, students generally find the coordinate system as an abstract framework where depended and independent variables are dimensionless or, in the case of physics, relationships like distance vs. speed. In the given example, students have the opportunity to attempt to interpret functional dependency; it is evident that the temperature increases with the year of observation. If we simply the problem and look at the dependence of the average annual temperature with respect to a decade, we get a curve that *resembles* a line. The approximate dependence is

$$t(x) = 0.1\,x + 0.05 \tag{1}$$

In the given equation, t is the temperature in degrees Celsius (℃), and x is the number of decades after 1960, e.g., for the period 1960–1970, x = 0. Students are certainly familiar with the linear function $y = kx + n$; it is necessary to discuss what $n = 0.05$ represents in this specific example. How much temperature change during 'our' decade does this model predict? It is also crucial to explain to students what the coefficient of slope k represents, prompting them to precisely formulate that such a slope means that the Earth's temperature will increase on average by 0.1 degree over a decade. If we ask ourselves what happens if we use Kelvin or Fahrenheit (℉) instead of Celsius, how this unit change would affect the coefficients? There are just a few of the numerous questions that guide students on how to approach a model *in front of them*.

Gifted students could be provided with an outline of the method that calculates the mentioned coefficients; *the least squares method* is a powerful tool of mathematical modeling and, as such, at least a flavor of it deserves a place in high school mathematics.

WHY THE TEMPERATURE RISES

During the second year of mathematical education, new elementary functions will be introduced, along with a new opportunity to delve into the previously mentioned problem. Students will encounter themselves with Arrhenius' law [5]

$$\Delta F = \alpha \ln \frac{C}{C_0} \tag{2}$$

In the latter, ΔF suggests temperature change, α is the constant, while C и C_0 are concentration CO_2 in the atmosphere at the observation moment and "time zero", respectively (such unconventional symbols for dependent and independent variables might confuse students, but they need to be directed to expect such surprises when delving into science). Logarithms are often abstract to students, so it's possible to provide a numerical value for: $\Delta F = \alpha \ln C - \alpha \ln C_0$; on the other hand, change from base *e* ("*why we choose this complicated number as the base of logarithm*?" - students might inquire) to the base 10 could be done. Then the most important question can be posed - if the concentration of CO_2 doubles, how much does the Earth's temperature change?

This problem, without numerical values, demands new variables C_1 and $C_2 = 2C_1$

Now we have

$$\Delta F_1 = \alpha \ln \frac{C_1}{C_0}, \Delta F_2 = \alpha \ln \frac{C_2}{C_0} \tag{3}$$

and therefore

$$\Delta F_2 - \Delta F_1 = \alpha \ln \frac{C_2}{C_0} - \alpha \ln \frac{C_1}{C_0} = \alpha \ln \frac{\frac{C_2}{C_0}}{\frac{C_1}{C_0}} \tag{4}$$

meaning

$$\Delta F_2 - \Delta F_1 = \alpha \ln 2 \tag{5}$$

Therefore the model suggest that the case of doubling the concentration of carbon dioxide will result in increasing ΔF for the value of $\alpha \ln 2$. The graph of the mentioned law could be presented; students should compare logarithmic and linear growth. Moreover, increase in carbon dioxide concentration in the atmosphere is significant, data from [6], could be presented.

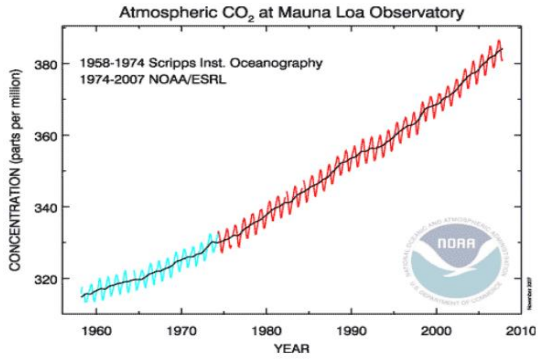

Figure 1. Increase in carbon dioxide concentration in the atmosphere

CONCLUSION

Provided examples, which would not occupy more than two teaching unit, aligned with the spirit of the curriculum and the topics that are about to be learned, help students developing conceptual understanding of a function whose model is obtained. Then, in a unique visa-free regime, the transition occurs from mathematics to a natural phenomenon that is modeled and vice versa. In the first example, a student gains insight into the rise of Earth's temperature, while in the second one, such an increase is connected to the concentration of carbon dioxide in the atmosphere. In this way, student learns about the elementary function whose properties are far from intuitive and may not be entirely natural for the average student. Finally, the student is given the opportunity to explore the rise of carbon dioxide in the atmosphere, based on data. Despite the fact that delving into the physical aspects of greenhouse effect is not possible (nor necessary) during math classes, much is achieved – mathematical knowledge is deepened, mathematical modeling is practices through a very illustrative example, the model of one complicated process is interpreted, and the Constitution says it affects the entire society. Is there much more than that?

REFERENCES

1. The Constitution of the Republic of Serbia, https://www.paragraf.rs/propisi/ustav_republike_srbije.html
2. National Environmenal Protection Program, https://www.zzps.rs/wp/pdf/Nacionalni_program_zastite_%20zs.pdf
3. Curriculum for mathematics in high-school education, https://zuov.gov.rs/wp-content/uploads/2020/08/pravilnik-gimnazija.pdf
4. https://spacemath.gsfc.nasa.gov/Modules/6Mod10Prob1.pdf
5. Martin Walther, Mathematics for the Environment, CRC Press, 2011.
6. https://spacemath.gsfc.nasa.gov/Modules/6Mod10Prob2.pdf
7. https://spacemath.gsfc.nasa.gov/Modules/6Mod10Prob2.pdf

Conference Proceedings
ICPAE 2023, 24th August – 26th August, Zrenjanin, Serbia
University of Novi Sad, Technical Faculty "Mihajlo Pupin", Zrenjanin

Elemental Analysis of Particulate Matter in the Vicinity of an Oil Refinery

Mattea Mačkić Jovanović[1]*, Marija Čargonja[1], Darko Mekterović[1]

[1]*University of Rijeka, Faculty of Physics, Ulica Radmile Matejčić 2, Rijeka, Croatia*
mattea.mackic@gmail.com

Abstract. One of the most important air pollutants is particulate matter, small particles suspended in the air. Industrial production plays a major role in air pollution, and therefore it is important to understand its impact on air quality. $PM_{2.5}$ (particulate matter with an aerodynamic diameter smaller than 2.5 μm) samples were collected in the vicinity of an oil refinery during the period from December 1, 2017 to December 11, 2019. Sampling was performed with two cyclone samplers on thin polytetrafluoroethylene filters and was conducted every other day for 24 hours. Using the XRF (X-Ray Fluorescence) technique, samples were analyzed to obtain concentrations of 17 elements from Na to Pb. Concentration of $PM_{2.5}$ was determined from gravimetric analysis, and the average $PM_{2,5}$ concentration was 11.2 μg/m^3.

Keywords: particulate matter, XRF, oil refinery

INTRODUCTION

Particulate matter (PM) is a mixture of solid and liquid particles suspended in the atmosphere. These particles are usually divided into coarse particles with an aerodynamic diameter greater than 2.5 μm and fine particles with an aerodynamic diameter less than 2.5 μm. The source of coarse particles is mostly natural substances such as sea salt, volcanoes, and plant particles. Fine particulate matter, on the other hand, is mainly anthropogenic, i.e., it is produced by industry, fuel combustion, and wood burning.

Why are particulate matter so important to human health? Because of their size, they can enter the human respiratory system and affect human health, especially the respiratory and cardiovascular systems [1].

Fine particulate matter ($PM_{2.5}$) has been monitored for several years in the city of Rijeka, Croatia, where an overall characterization of urban pollution was assessed. The main pollution sources such as traffic and secondary sulfates were identified at this site [2]. However, in order to characterize some specific pollution sources such as certain industries, metal processing technologies, or waste disposal, pollution should be monitored in the immediate proximity of the source. For this purpose, $PM_{2.5}$ sampling in the vicinity of an oil refinery started in 2016 and some of the results were summarized in [3].

The aim of this study was to extend the sampling and characterization of $PM_{2.5}$ by elemental characterization using the X-Ray Fluorescence (XRF) technique.

EXPERIMENTAL

$PM_{2.5}$ sampling was performed using a homemade cyclone sampler based on the ANSTO APS sampler [4]. With this sampler, particles with an aerodynamic diameter less than 2,5 μm are captured on thin stretched polytetrafluoroethylene membrane filters (d = 25 mm). At the same time, the air flow is measured. The average air flow was 18,98 L/min and the average filtered air volume was 27,33 m^3.

Samples were collected every other day for 24 hours. Sampling started on December 1, 2017 and ended on December 11, 2019. Due to some technical problems, there were several pauses in sampling, so we collected a total of 199 $PM_{2.5}$ samples.

To determine the total $PM_{2.5}$ concentrations, each filter was weighed before and after sampling. Gravimetric analysis was performed at the Laboratory for Macromolecular Research at the Centre for Micro and Nano Sciences and Technologies, University of Rijeka. It is very important to minimize the influence of humidity, so, for this reason, the filters were stored for at least 24 hours under stable conditions of 22 °C and 20% relative humidity before weighing with the Mettler Toledo XA105 Dual range balance (readability 10 μg).

Besides the total $PM_{2.5}$ concentrations, elemental analysis of the samples was done by means of X-Ray Fluorescence technique (XRF) at the Laboratory for Elemental Microanalysis at the Faculty of Physics, University of Rijeka. For this purpose, a low-power Rh X-ray tube was used for excitation at 50 kV and 1 mA. The beam collimated to a diameter of 2 mm was directed perpendicular to the sample. A silicon drift detector was used to detect the characteristic radiation, placed at an angle of 45° to the sample. In this way, each sample was scanned with 7×7 pixels, giving an area of about 8 mm^2. The sum spectrum for each sample was then used for analysis. Scanning was performed in air.

The spectra were analyzed using QXAS software [5], which uses the Voigt profile to fit a spectral line. K-alpha lines were used for quantitative analysis of all elements except for Pb, for which L-lines were used. System efficiencies for each energy were determined using mono- and poly-elemental thin standards. With the given setup, we were able to determine the concentrations of the following elements: S, K, Ca, Ti, V, Cr, Mn, Fe, Ni, Cu, Zn, and Pb.

RESULTS

The sampling site near a refinery (approx.100 m) is in an area with low population density, relatively low traffic, and no other significant local pollution sources. The total $PM_{2.5}$ and elemental concentrations determined with XRF are very similar to those measured at an urban site in the city of Rijeka [2,3]. Nevertheless, the concentrations of some elements such as sulfur, vanadium, and nickel were higher than the usual levels measured in the near urban site.

An example of a time series of elemental concentrations can be seen on Figure 1, which shows sulfur concentrations during the sampling period.

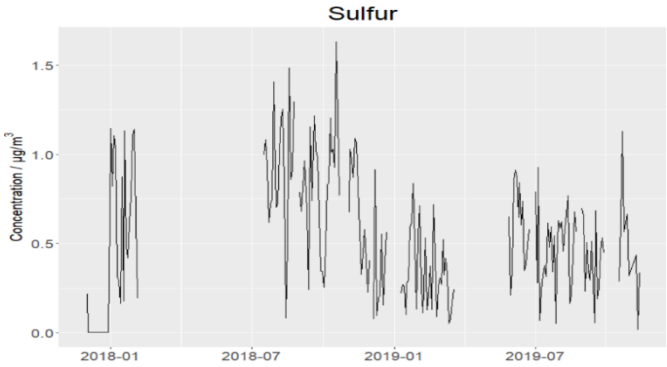

Figure 1. Time series of sulfur concentrations measured in the vicinity of an oil refinery.

CONCLUSION

During the period from December 1, 2017 to December 11, 2019, a sampling campaign of fine particulate matter was conducted near the oil refinery to estimate the concentration of S, K, Ca, Ti, V, Cr, Mn, Fe, Ni, Cu, Zn, and Pb. The concentrations of the observed elements are comparable to the concentrations in the city of Rijeka, but some elements are measured in higher concentrations. Additional statistical analysis should be performed to estimate the extent of the oil refinery's impact on overall air quality at this location.

ACKNOWLEDGEMENTS

This work was supported in part by the University of Rijeka under the project number uniri-prirod-18-232. The authors are grateful to the Municipality of Kostrena for the financial support during the sampling campaign. Gravimetric measurements were done at the Laboratory for Macromolecular Research for which we are grateful to Prof Srećko Valić from the Centre for Micro and Nano Sciences and Technologies.

REFERENCES

1. C. A. Pope III, D. W.Dockery, 2006, Health Effects of Fine Particulate Air Pollution: Lines that Connect, *J. Air. Waste. Manage*, vol. 56, pp 709–742
2. T. Ivošević, I. Orlić, I. Bogdanović Radović, M. Čargonja, E. Stelcer, 2017, Composition and source apportionment of fine particulate matter during extended calm periods in the city of Rijeka, Croatia, *Nucl. Instrum. Meth. B*, vol. 406, pp 82–86
3. M. Čargonja, D. Mekterović, D. Mance, G. Žauhar, I. Bogdanović Radović, I. Zamboni, 2019, Characteristics of aerosol pollution in the vicinity of an oil refinery near Rijeka, Croatia, *X-Ray Spectrom*, vol. 48, pp 561–568
4. D. D. Cohen, E. Stelcer, D. Garton, J. Crawford, 2011, *Atmos. Pollut. Res*, vol. 10, pp 295–305
   P. Van Espen, K. Janssens, J. Nobels, 1986, AXIL-PC, software for the analysis of complex X-ray spectra, *Chemometr. Intell. Lab*, vol. 1, pp 109–114

Conference Proceedings
ICPAE 2023, 24th August – 26th August, Zrenjanin, Serbia
University of Novi Sad, Technical Faculty "Mihajlo Pupin", Zrenjanin

Unveiling the influence of CO_2 on Global Warming: A Pedagogical Model

Lazar Radenković[1*], Ljubiša Nešić[1]

[1]*University of Niš, Faculty of Sciences and Mathematics, Višegradska 33, Niš, Serbia*
lazar.radenkovic@pmf.edu.rs

Abstract. In this paper, we present a simple experiment illustrating the influence of carbon dioxide (CO_2) on the greenhouse effect and its role in global warming. By employing a simple and engaging activity using two glass jars – one filled with regular air and the other with air containing an increased level of CO_2 – we aim to enhance children's understanding of the greenhouse effect and its role in climate change. Using experiments like this could lead to increased environmental awareness and improve children's understanding of this complex phenomenon.

Keywords: CO_2, global warming, greenhouse effect, climate change, environmental education

INTRODUCTION

Global warming and climate change are pressing issues that require comprehensive understanding and collective action. Educating children about these topics is crucial for developing awareness of these issues. A key factor in global warming is the presence of carbon dioxide (CO_2) in the atmosphere. This paper presents a pedagogical experiment designed to illustrate the influence of CO_2 on global temperatures.

The greenhouse effect is a natural process that enables life to thrive on Earth by trapping the heat from the sun within the atmosphere. This process involves the interaction of various greenhouse gases, including CO_2. Carbon dioxide, although present in trace amounts, plays a vital role in the greenhouse effect due to its ability to absorb and re-emit thermal radiation. However, human activities, such as burning fossil fuels and deforestation, have significantly increased the concentration of CO_2 in the atmosphere, leading to an enhanced greenhouse effect and subsequent global warming.

THE PEDAGOGICAL EXPERIMENT

The experiment demonstrates the impact of CO_2 on global warming by comparing the temperature changes in two identical glass jars – one filled with regular air and the other with air containing increased levels of CO_2. The origins of this experiment go back as far as 50 years [1]. Some of the experiment variations used open [2,3] or closed containers [4,5]. However, using open containers had been criticized [6–8] because the temperature change can be explained by reduced convection (since CO_2 is denser than air), and not by

the greenhouse effect of CO_2. We used both approaches because it can be argued that the atmosphere can be modelled as both an open and a closed system.

In our experiment, the CO_2 was produced by mixing vinegar and baking soda in a small bottle and capturing the vapor with a rubber balloon. Both jars were placed next to each other in a location exposed to the sun. The temperature rise of the air inside the jars was monitored with an affordable XK-W1088 digital dual thermometer. The digital thermometer had been previously calibrated using a Roth analogue thermometer with 0.1 ℃ precision.

The experiment setup is shown in *Figure 1*.

Figure 1. Two identical jars were put in the sun (left), one containing regular air, and the other containing increased CO_2 levels. The experiment had two variations – the jars were open and closed. The picture on the right shows a close-up of the thermometer probes.

MEASUREMENT RESULTS

To verify that the measurement conditions were identical, we placed two jars in the sun and measured the temperatures in thermal equilibrium. Because of the constantly changing atmospheric conditions, we considered the temperature to be established if it remained constant for two minutes.

In our initial tests, the two seemingly identical jars were in fact different. The probes in the two jars registered different temperatures of 46.3 ℃ and 45.6 ℃. When the jars were closed, the temperature was different again – 52.7 ℃ and 51.6 ℃. This led us to suspect that the two jars were made of different glass.

After repeating the tests with a new pair of jars, we have obtained equal temperatures of 48.3 ℃ for both probes with open lids. Thus, we could examine the effects of CO_2, since the jars were identical.

We have first injected CO_2 into one of the jars, while leaving the jars open. The results are shown in *Figure 2*. At that time, the atmosphere temperature was dropping, so both jars were cooling off. However, the cooling effect was more noticeable in the jar with plain air. With time, probably due to concentration gradient, the CO_2 escaped the enriched jar, with temperatures levelling.

After this, we tested the closed jar model of the atmosphere. The results are shown in *Figure 3*. At this time, the jar temperature was rising. As expected, the rise was steeper in a CO_2 enriched jar, and the final temperature was higher.

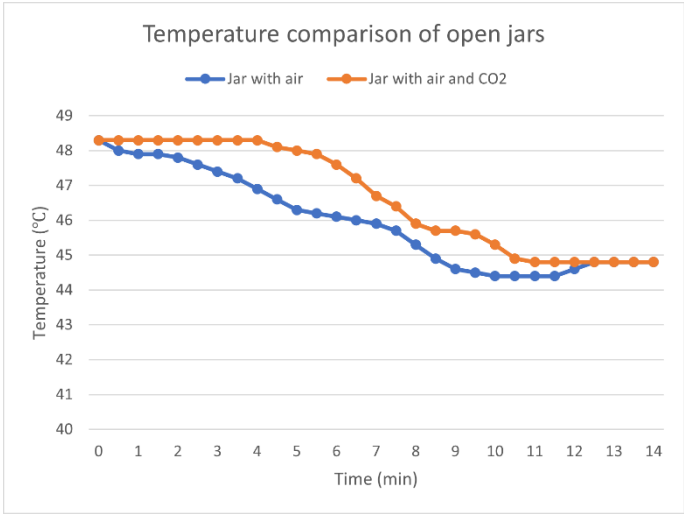

Figure 2. Temperature comparison of two identical open jars. One jar contained air, and the other one contained air with increased levels of CO_2.

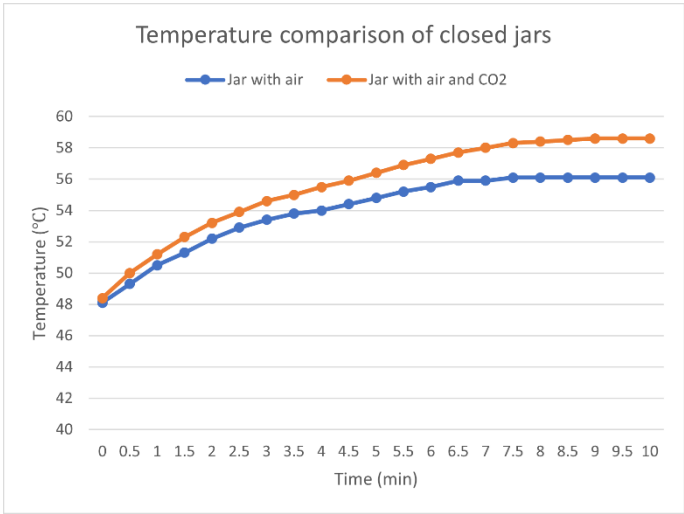

Figure 3. Temperature comparison of two identical closed jars. One jar contained air, and the other one contained air with increased levels of CO_2.

DISCUSSION

Based on the observations and results, the students can be involved in a discussion about the role of CO_2 in trapping sunlight heat and causing the greenhouse effect. Implications of global warming, such as rising sea levels, extreme weather events, and the impact on

ecosystems and human societies could further be discussed. The children can reflect on their individual and collective behaviour and its contributing to the CO_2 emission.

Similarly, the students can be involved in a discussion about subtleties of temperature measurements. The probe temperature was affected by atmospheric conditions, shadows (even the slightest ones), jar orientation towards the sun, jar positioning (horizontal, vertical), our distance from the jars, etc. All these phenomena can be used to illustrate physics of heat transfer.

CONCLUSION

The pedagogical experiment presented in this paper offers an engaging method to educate children about the influence of CO_2 on global warming. It is simple, affordable, and relatively quick. By providing obvious and tangible evidence, this experiment enhances children's comprehension of the greenhouse effect and fosters environmental awareness.

ACKNOWLEDGMENTS

This work is supported by the Ministry of Science, Technological Development, and Innovation of the Republic under Contract No. 451-03-47/2023-01/200124.

REFERENCES

1. Fuller R M, 1973, Greenhouse Effect Study Apparatus, *Am. J. Phys.* **41** 443–443
2. Lueddecke S B, Pinter N and McManus S A, 2001, Greenhouse Effect in the Classroom: A Project- and Laboratory-Based Curriculum, *J. Geosci. Educ.* **49** 274–9
3. Besson U, De Ambrosis A and Mascheretti P, 2010, Studying the physical basis of global warming: thermal effects of the interaction between radiation and matter and greenhouse effect, *Eur. J. Phys.* **31** 375–88
4. Keating C F, 2007, A Simple Experiment to Demonstrate the Effects of Greenhouse Gases, *Phys. Teach.* **45** 376–8
5. Sieg P G, Berner W, Harnish P K and Nelson P C, 2019, A Demonstration of the Infrared Activity of Carbon Dioxide, *Phys. Teach.* **57** 246–9
6. Wagoner P, Liu C and Tobin R G, 2010, Climate change in a shoebox: Right result, wrong physics, *Am. J. Phys.* **78** 536–40
7. Bertò M, Della Volpe C and Gratton L M, 2014, 'Climate change in a shoebox': a critical review, *Eur. J. Phys.* **35** 025016
8. Buxton G A, 2014, The physics behind a simple demonstration of the greenhouse effect, *Phys. Educ.* **49** 171–5

Conference Proceedings
ICPAE 2023, 24th August – 26th August, Zrenjanin, Serbia
University of Novi Sad, Technical Faculty "Mihajlo Pupin", Zrenjanin

The Oil and Gas Industry, Possible Solutions for a Sustainable Future

Dejan Bajić[1*], Milan Marković[1], Valentina Bozoki[1], Verica Gluvakov[1], Stefan Ugrinov[1], Luka Đorđević[1]

[1]*University of Novi Sad, Technical faculty "Mihajlo Pupin", Zrenjanin, Serbia*
bajicdejan.98@hotmail.com

Abstract. The oil and gas industry faces challenges of low carbon and net-zero future. Combustion of fossil fuels negatively affects the environment. It is evident that humanity still needs oil and gas as one of the main sources of energy, but can they be sustainable? In this paper the global demand for energy will be presented. Moreover, alternatives and possible solutions to reducing emissions of carbon-dioxide will be discussed.

Keywords: energy, carbon-dioxide, sustainable development, net-zero, oil and gas

INTRODUCTION

Achieving a net-zero future is a highly challenging task, especially in the modern world where the main sources of energy are still fossil fuels. During the past several decades the oil and gas industry has had the biggest impact on meeting the global energy demand [1]. Global warming, rising of the sea level and climate change are tightly connected with anthropogenic greenhouse gases emissions. The combustion of fossil fuels accelerates these processes, which can provoke a lack of food and fresh water and more frequent natural hazards [2]. On average, the sea level rises around 3,2 mm annually, but according to the National Oceanic and Atmospheric Administration, the sea level rising is dramatically accelerating and it is estimated to rise by 350 mm by 2050 [3,4]. The consequences of the rising of the sea level can have a vast impact on the entire planet and on humans all over the world [5]. Humanity needs to make great changes in the habits of energy consumption and transition to achieve the net-zero concept. This paper aims to explore the general demand for energy, as well as potential solutions for a sustainable future in the oil and gas industry.

Energy demand, consumption and efficiency

The global energy demand is rising rapidly all over the world [6]. It is estimated that the global energy consumption will be around 53% higher in the next 10 years [7]. Taking this information into consideration, it is evident that humanity needs a new approach to the energy management. On the other hand, the global oil production has been increasing monthly in 2023. According to [8], the world crude oil production was 82,30 M in February 2023, while in January 2023 it was 80,74 M. The production is getting higher,

but one of the future's challenges will be the limitation of fossil fuels supplies [9]. The energy efficiency means minimizing the waste of energy. In other words, a process/machine that uses less energy has higher energy efficiency than the one that consumes more energy to perform the same task [10].

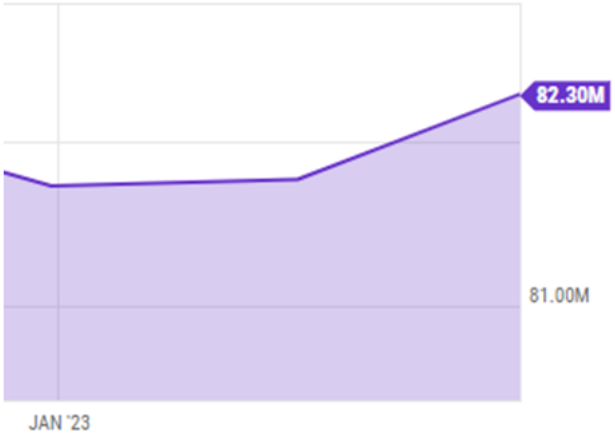

Figure 1. Diagram that shows the oil production difference between January and February 2023 [9].

Geological storing of carbon-dioxide

Carbon capture and storage can be a good transition option when it comes to mitigating carbon dioxide emissions from the processes of combustion of oil and gas. This process consists of several complex operations. The CO_2 can be captured directly in industrial facilities or from the atmosphere. In both cases, when captured, it is being compressed [11]. Compressed CO_2 takes up less volume than the non-compressed, making it more suitable for transportation. The methods of transportation can vary and depend on the specific needs. Transportation can be done by pipeline, rail, ship, etc. When the compressed CO_2 is transported to the location of the injection (which can include deep coal layers, salt-water aquifers or depleted oil and gas fields), the process can begin [12]. Injecting carbon dioxide into underground sites can significantly reduce its concentration in the atmosphere. This technology could play a notable role in terms of global energy and climate change [11].

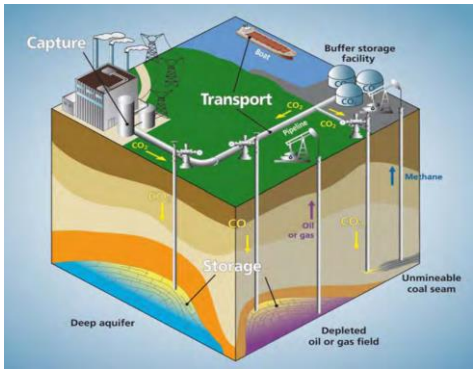

Figure 2. Process of geological storing of CO_2 [12].

CONCLUSION

The oil and gas industry needs to find its way to a sustainable future. This paper presents two possible solutions to solve the problem of the excessive carbon dioxide production when it comes to the usage of fossil fuels (oil and gas). The first one is the energy efficiency, which is the key to sustainable development in terms of the oil and gas industry. This could be achieved by using more efficient machines, industrial processes, devices, vehicles etc., that produce less greenhouse gases. The second one is CCUS (Carbon Capture, Utilization and Storage). If we use less efficient devices that produce more carbon dioxide, we can employ modern technologies to capture and store CO_2 in underground storages and prevent their emissions into the atmosphere. The best solution would be to combine these two approaches, and by implementing them, we will be a step closer to accomplishing the net-zero concept.

REFERENCES

1. H. Sutoyo, G. Angga, H. Schümann, C. Berg, 2023, Energy efficiency of oil and gas production plant operations, *Geoenergy Science and Engineering*, Volume 226
2. A. Bricout, R. Slade, I. Staffell, K. Halttunen, 2022, From the geopolitics of oil and gas to the geopolitics of the energy transition: Is there a role for European supermajors?, *Energy Research & Social Science*, Volume 88
3. https://www.noaa.gov/news-release/us-coastline-to-see-up-to-foot-of-sea-level-rise-by-2050, 18/7/2023
4. C. Nunez et all., 2023, Sea levels are rising at an extraordinary pace. Here's what to know. *National Geographic*
5. Meredith M., M. Sommerkorn, S. Cassotta, C. Derksen, A. Ekaykin, A. Hollowed, G. Kofinas, A. Mackintosh, J. Melbourne-Thomas, M.M.C. Muelbert, G. Ottersen, H. Pritchard, and E.A.G. Schuur, 2019: Polar Regions. In: IPCC Special Report on the Ocean and Cryosphere in a Changing Climate [H.-O. Pörtner, D.C. Roberts, V. Masson-Delmotte, P. Zhai, M. Tignor, E. Poloczanska, K. Mintenbeck, A. Alegría, M. Nicolai, A. Okem, J. Petzold, B. Rama, N.M.

Weyer (eds.)]. *Cambridge University Press, Cambridge, UK and New York, NY, USA*, pp. 203-320. https://doi.org/10.1017/9781009157964.005.

6. Nadia, M., Lassad, H., Abderrahmen, Z. and Abdelkader, C.: Influence of temperature and irradiance on the different solar PV panel technologies, *International Journal of Energy Sector Management*, Vol. 15 No. 2, pp. 421-430, 2021
7. Song, Q., Jinhui, L., Huabo, D., Danfeng, Y., Zhishi, W.: Towards to Sustainable Energy-Efficient City: A Case Study of Macau, Renew. Sustain. *Energy Rev.*, Vol. 75, Aug., pp. 504-514, 2017
8. https://ycharts.com/indicators/world_crude_oil_production 18/7/2023
9. Rakić, N., Gordić, D., Šušteršič, V., Josijević, M., Babić, M.: Renewable Electricity In Western Balkans, Support Policies and Current State, Department of Energy and Process Engineering, Faculty of Engineering, University of Kragujevac, Kragujevac, Serbia, *Thermal Science*: Vol. 22, No. 6A, pp. 2281-2296, 2018
10. https://www.eesi.org/topics/energy-efficiency/description, 18/7/2023
11. https://www.iea.org/reports/about-ccus, 19/7/2023
12. R. Arts, et all., 2012, Šta zaista znači geološko skladištenje CO_2, Association of Geophysicists and Environmentalists of Serbia

Conference Proceedings
ICPAE 2023, 24th August – 26th August, Zrenjanin, Serbia
University of Novi Sad, Technical Faculty "Mihajlo Pupin", Zrenjanin

Crude Oil Demand and the Challenges of Global Warming

Dejan Bajić[1*], Luka Đorđević[1], Valentina Bozoki[1], Stefan Ugrinov[1], Verica Gluvakov[1], Borivoj Novaković[1]

[1]*University of Novi Sad, Technical faculty "Mihajlo Pupin", Zrenjanin, Serbia*
bajicdejan.98@hotmail.com

Abstract. Current global demand for the crude oil will be presented in this paper. Moreover, the consequences of the oil combustion for the environment will be discussed, particularly the release of greenhouse gases. Paper also emphasizes the impacts of global warming on the environment and populated coastal areas.

Keywords: crude oil, demand, global warming, environment, CO_2

INTRODUCTION

Planet's ice-covered regions are in danger. Glaciers, permafrost and high mountain peaks are facing meltdown that is accelerating from year to year. The consequences of these geographically partial changes have far-reaching impacts, affecting the entire planet, as well as people in numerous ways [1]. According to the National Oceanic and Atmospheric Administration, it is estimated that the sea level will rise by up to 35 centimeters during the next 3 decades [3]. Humanity needs energy more than ever, so the energy consumption and demand are getting higher annually. This paper gives a brief analysis of the current situation in the sphere of oil production and climate change, focusing on the impact of the oil and gas industry on global warming.

World's Oil Production

The oil and gas industry has experienced fluctuations throughout history. Important factors that affect production are demand, prices, politics etc. On the other hand, oil as one of the most important energy resources has a great impact on various sectors, economies and geopolitics. Historical chart of crude oil production over the last 15 years is shown in the Figure 1. If we exclude the global Covid-19 lockdown period that started at the beginning of 2020, where the demand was very low, it can clearly be seen that the oil production, as well as demand, was rising through the years, with small oscillations that occured due to different global or local events that negatively affected the oil industry. The rising trend in oil production is confirmed by the fact that the oil production in February 2023 was higher up to 1.93% compared to the average oil production in the previous year [2].

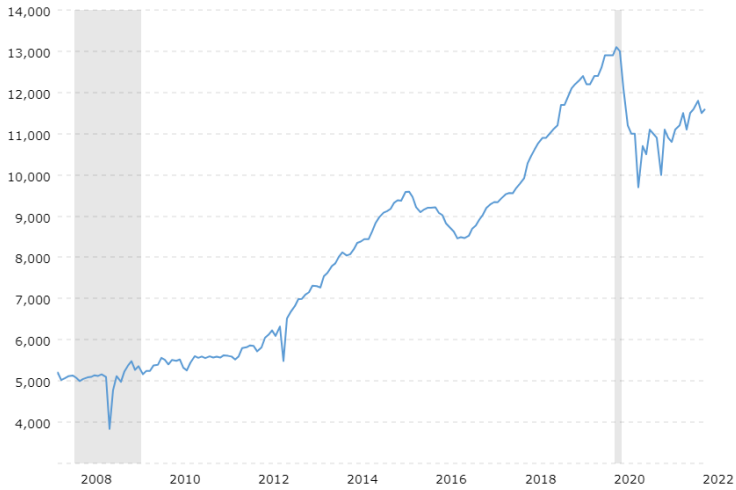

Figure 1. Crude oil production chart [3].

Oil and Carbon

When we talk about pollution and greenhouse gas emissions, it can be said that the oil and gas industry is one of the main contributors to such a high concentration of CO_2 in the atmosphere [4]. On average, crude oil contains between 82 and 87 percent of carbon [5]. When the oil is burning, carbon from the oil combines with the oxygen from the air, which forms molecules of CO_2. This way combustion of the oil releases carbon dioxide and many other greenhouse gases into the atmosphere. These gases provoke the phenomenon known as the greenhouse effect. Basically, gases accumulate in the atmosphere and act like a blanket that traps the heat and does not allow it to return to space and thus overheating of the Earth happens (Figure 2). According to [6], emissions of CO_2 from oil in 2022 grew by 2.5%, comparing to the emissions in 2021.

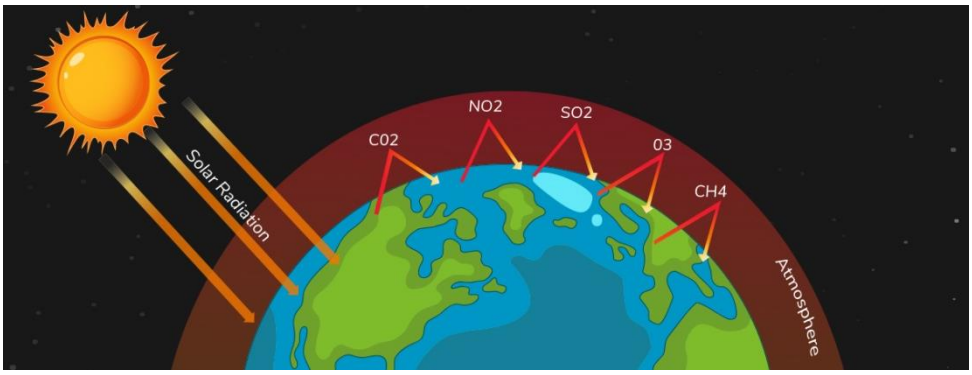

Figure 2. Greenhouse effect [7].

Coastal areas affected by global warming

It is a widely known fact that global warming causes rising of the sea level, as well as the fact that the coastal areas are the most endangered regions when it comes to rising of the sea level. Global warming dramatically accelerates melting of the polar ice, which provokes rising of the sea level. According to NASA, the sea level has risen by 98.5 milimeters in the last thirty years [8]. Considering the fact that extra 20 centimeters of the sea level can lead to significant hazards if a hurricane happens (the water can flood several kilometers of land more than it would flood if the sea level was normal), it can be concluded that coastal areas are in danger.

CONCLUSION

This paper has explored the relationship between crude oil demand, combustion and global warming. The increased demand contributes to global warming via the more intensive production of greenhouse gases. This does not affect just the environment, but also the people who inhabit coastal areas. If the rise of the sea level continues, the near-coast settlements, as well as the big coastal cities, will be flooded forever.

REFERENCES

1. Meredith, M., M. Sommerkorn, S. Cassotta, C. Derksen, A. Ekaykin, A. Hollowed, G. Kofinas, A. Mackintosh, J. Melbourne-Thomas, M.M.C. Muelbert, G. Ottersen, H. Pritchard, and E.A.G. Schuur, 2019: Polar Regions. In: IPCC Special Report on the Ocean and Cryosphere in a Changing Climate [H.-O. Pörtner, D.C. Roberts, V. Masson-Delmotte, P. Zhai, M. Tignor, E. Poloczanska, K. Mintenbeck, A. Alegría, M. Nicolai, A. Okem, J. Petzold, B. Rama, N.M. Weyer (eds.)]. Cambridge University Press, Cambridge, UK and New York, NY, USA, pp. 203-320. https://doi.org/10.1017/9781009157964.005.
2. https://ycharts.com/indicators/world_crude_oil_production 18/7/2023
3. Source
4. Greene S., Jia H., Rubio-Domingo G., 2020, Well-to-tank carbon emissions from crude oil maritime transportation, Transportation Research Part D: Transport and Environment Volume 88
5. https://www.britannica.com/science/crude-oil
6. https://www.iea.org/reports/co2-emissions-in-2022
7. https://www.pranaair.com/blog/what-is-greenhouse-effect-its-gases-causes-solution/
8. https://climate.nasa.gov/vital-signs/sea-level/
9. https://nationalgeographic.rs/zivotna-sredina/a19944/zastrasujuci-uticaj-klimatskih-promena-kako-se-koral-bori-s-visokim-temperaturama-video.html